Investigation of the role of the GGMP motif of *Plasmodium falciparum* Hsp70-1 on the chaperone function of the protein and its interaction with a co-chaperone, PfHop

by

Stanley Makumire

submitted in fulfilment of the requirements for the degree of

Doctor of Philosophy

in the subject of Biochemistry

at

the University of Venda

Promoter: Prof. A. Shonhai

Co-promoter: Dr. T. Zininga

Submitted on 15 March 2019

Investigation of the role of GGMP motif of *Plasmodium falciparum* Hsp70-1 on the chaperone function of the protein and its interaction with a co-chaperone, PfHop

Abstract

The main malaria agent, *Plasmodium falciparum* expresses an Hsp70 (PfHsp70-1) which plays a significant role in parasite survival. PfHsp70-1 is distinct in that it possesses glycine-glycine-methionine-proline (GGMP) tetrapeptide repeats in its C-terminal domain. To date, the GGMP motif of PfHsp70-1 has not been studied. The motif is positioned within the C-terminal lid segment of PfHsp70-1. The motif is also about seven residues upstream the terminal EEVD residues that are responsible for the interaction of PfHsp70-1 with its functional regulators (co-chaperones). *P. falciparum* Hsp70/Hsp90 organizing protein (PfHop) constitutes one of the functional regulators of PfHsp70-1. PfHop allows PfHsp70-1 and its chaperone partner, PfHsp90 to form a functional partnership. Given the proximity of the GGMP repeats to the C-terminus of PfHsp70-1, it was postulated in this study that the GGMP repeat residues may regulate attachment of PfHop to PfHsp70-1. Hence, this study hypothesized that the GGMP repeat motif is important for the interaction between PfHop and PfHsp70-1 as well as the chaperone activity of PfHsp70-1.

Two variants in which the N-terminal and the C-terminal GGMP repeats were conservatively substituted were generated. *E. coli* Hsp70 (DnaK) lacks a GGMP motif. Thus, the GGMP motif of PfHsp70-1 was introduced into *E. coli* DnaK in order to generate a third GGMP variant. Recombinant forms of PfHsp70-1, DnaK, and their GGMP variants were heterologously expressed in *E. coli* XL1 Blue cells. The proteins were purified to homogeneity by using a combination of Ni-NTA affinity chromatography, ion exchange, and size exclusion chromatography. Purified proteins were then biophysically characterized using CD spectroscopy and tryptophan fluorescence. Findings from this study revealed that there were minimal secondary structural differences between PfHsp70-1, DnaK and their GGMP variants. In order to investigate the chaperone function of PfHsp70-1, DnaK and the GGMP variants, a complementation assay in *E. coli dnak756* cells whose Hsp70 is functionally compromised was conducted. The PfHsp70-1 GGMP variants were able to suppress the thermosensitivity of the *E. coli* cells. However, the

Investigation of the role of GGMP motif of *Plasmodium falciparum* Hsp70-1 on the chaperone function of the protein and its interaction with a co-chaperone, PfHop

DnaK-G variant failed to confer cytoprotection to the *E. coli dnak756* cells. To further validate the findings from the complementation assay, the ability of the recombinant proteins to suppress aggregation of heat stressed Malate dehydrogenase (MDH) was elucidated. PfHsp70-1 had better MDH aggregation suppression capabilities than its GGMP variants. Overall, findings from the MDH aggregation suppression assay suggest that the GGMP repeats may contribute towards substrate binding. Substrate binding might be dependent on the specific positioning of a particular repeat in the GGMP motif of PfHsp70-1. Furthermore, the ATPase activity of PfHsp70-G632 and PfHsp70-G648 was significantly reduced compared to PfHsp70-1 (wild type). However, PfHsp70-G632 had the lowest ATPase activity. Interestingly, the ATPase activity of PfHsp70-G632 was enhanced in the presence of synthetic Hsp70 model peptide substrates. Slot blot and ELISA approaches confirmed that the GGMP mutations partially abrogated the interaction of PfHsp70-1 with PfHop. Altogether, the findings suggest that the GGMP motif of PfHsp70-1 has marginal effects on the structure of PfHsp70-1. In conclusion, this study provides the first direct evidence that the GGMP motif is important for the chaperone function of PfHsp70-1 as well as its interaction with PfHop.

Key words: Malaria, *Plasmodium falciparum*, chaperone, GGMP motif, Hsp70, Hop.

Investigation of the role of GGMP motif of *Plasmodium falciparum* Hsp70-1 on the chaperone function of the protein and its interaction with a co-chaperone, PfHop

Declaration

I, Makumire Stanley hereby declare that the thesis for the Doctor of Philosophy in Biochemistry degree at the University of Venda, hereby submitted by me, has not previously been submitted for a degree at this or any other university, and that it is my own work in design and execution and that all reference material contained therein has been duly acknowledged.

Signature……Date…….

Dedication

I dedicate this thesis to my wife Vuyelwa, our daughters Ruvarashe Endinaye and Makanaka Sithenkosi and to our late son Anotidaishe Uthunathi Makumire (MHSRIP).

Preface

This thesis is comprised of seven chapters. The outlines for each chapter are provided below.

Chapter 1: This is a general introduction encompassing all the background to the suggested broad aim and specific objectives. It also highlights the broad problem statement and spells out the study hypothesis.

Chapter 2: This chapter represents the bioinformatics analyses conducted in order to elucidate the role of the GGMP motif of PfHsp70-1.

Chapter 3: This chapter represents the recombinant production of PfHsp70-1, DnaK, and their GGMP variant proteins. In this chapter, the proteins are also biophysically characterized to determine the secondary and tertiary structural features.

Chapter 4: This chapter reports on the investigation of the chaperone function of PfHsp70-1 and DnaK versus their GGMP variants *in vitro.*

Chapter 5: This chapter analyzes the structure-function features of PfHop.

Chapter 6: This chapter encompasses the evaluation of the association of PfHsp70-1, DnaK-G, and their GGMP variants with PfHop.

Chapter 7. This chapter covers conclusive remarks and future perspectives.

Acknowledgments

I wish to thank the Almighty God for with him nothing is impossible. I wish to thank my promoter Prof. A. Shonhai, and co-promoter, Dr. T. Zininga for all the support, motivation and guidance throughout the duration of the project.

I also wish to acknowledge the following people for the technical support and for hosting me during research visits:

1. Dr. E. Prinsloo; Biotechnology Innovation Centre, Rhodes University, South Africa
2. Dr. I. Achilonu and Prof. H. Dirr; Protein Structure-Function Research Unit, University of Witwatersrand, South Africa.
3. Prof. I. Kursula and Dr. J. Vahokoski; University of Bergen, Norway.
4. Dr. G. Owen; HIV Pathogenesis Research Unit, University of Witwatersrand, South Africa.
5. Dr. O.J. Pooe; Council for Scientific and Industrial Research, South Africa.

I wish to extend further acknowledgments to the:

1. Deutsche Forschungsgemeinschaft and National Research Foundation for funding the project and study bursary
2. University of Venda Research Committee (South Africa) for student research funding

I would also like to express my gratitude to Dr. A. Burger, (University of Venda, South Africa) for proof-reading my thesis.

Finally, special thanks go to all the members of the ProBioM research team (University of Venda), all of whom have been a part of my daily life over the duration of the project. Many thanks to Ms. F.S. Monyai for going out of her way to provide technical support.

Biochemistry technicians, Mr. C. Ndou and Miss D. C Mboyi were very helpful in many ways.

Table of Contents

List of Figures

List of Tables

List of Symbols

Abbreviations of units Symbol	Interpretation
%	percent
µl	microlitre
A320	absorbance at 320 nanometres
A360	absorbance at 360 nanometres
A595	absorbance at 595 nanometres
A600	absorbance at 600 nanometres
bp	base pair
kDa	kilodalton
µM	micromolar
pM	picomolar
°C	degree celsius
µl	microlitre
ml	millilitre
l	litres
w/v	weight per volume
v/v	volume per volume
µg	microgram
g	gram
α	alpha
β	beta

List of Outputs

Journal articles

1. Makumire, S., Gitau, G.W., Zininga, T., Vahokoski, J., Kursula, K., Shonhai, A. (2019) Expression analysis and biophysical characterization of *Plasmodium falciparum* Hsp70-Hsp90 organizing protein (PfHop). (Manuscript in Preparation).

2. Mabate, B. Zininga, T., Makumire, S., Achilonu, I., Dirr, H., Shonhai, A. (2018). Structural and biochemical characterization of *Plasmodium falciparum* Hsp70-x reveals functional versatility of its C-terminal EEVN motif. PROTEINS: Structure, Function, and Bioinformatics, (11): 1189-1201. doi: 10.1002/prot.25600.

3. Zininga, T., Makumire, S., Gitau, G.W., Njunge, J.M., Pooe, O.J., Klimek, H., Scheurr, R., Raifer, R., Prinsloo, E., Przyborski, J.M., Hoppe, H., Shonhai, A (2015). *Plasmodium falciparum* Hop (PfHop) interacts with the Hsp70 chaperone in a nucleotide-dependent fashion and exhibits ligand selectivity. PLoS ONE 10(8): e0135326. doi: 10.1371/journal.pone.0135326.

Conference/Workshop Proceedings

1. Makumire, S., Zininga, T., Shonhai, A. Investigation of the effect of the GGMP repeat motif of *Plasmodium falciparum* Hsp70 on its chaperone function and its interaction with a co-chaperone, PfHop. Biophysics and Structural Biology at Synchrotrons Workshop. 16 -24 Jan 2019. University of Cape Town (South Africa).

2. Makumire, S., Zininga, T., Prinsloo, E., Shonhai, A. Evidence for the direct interaction between *Plasmodium falciparum* Heat shock organizing protein (PfHop) and PfHsp70-1. University of Venda Research Open Day. 3 March 2015.

3. Makumire, S., Shonhai, A. Characterization of the interaction between *Plasmodium falciparum* Heat shock organizing protein (PfHop) and *Plasmodium falciparum* heat shock protein 90 (PfHsp90) towards assays in protein-protein interaction. EMBO Practical Course on Computational analysis of protein-protein interactions: From Sequences to networks: 28 September - 3 October 2014, University of Cape Town (South Africa).

Chapter 1

Literature Review

Chapter 1

Literature Review

1.1 Malaria

Malaria is a disease responsible for deaths averaging around 435 000 in 2017; (WHO, 2018). According to the World Health Organization (WHO), there has been an increase in malaria cases over the years reaching an estimated 219 million in 2017 (WHO, 2018). Africa remains the worst affected region accounting for 92 % of the cases. In South Africa, malaria is endemic in low altitude border regions of Limpopo, Mpumalanga and KwaZulu-Natal Provinces. In these regions, active malaria transmission is experienced during summer (November to April). In 2018, about 18 638 malaria cases and 120 deaths were reported in South Africa (Dahan-Moss *et al*., 2018).

The World Health Organization lists children under the age of 5 years, pregnant woman, HIV/AIDS patients and non-immune travelers/mobile populations as being at high risk of contracting malaria. Although children and pregnant women are the most affected, malaria mortality rates in children under the age of 5 years have since decreased from 440 000 in 2010 to 266 000 in 2017 (WHO, 2018). This could be attributed to the seasonal malaria chemo-preventative strategies that reduce fatalities in children and pregnant women which were implemented by WHO in 2012. Despite efforts to prevent and reduce malaria transmission, the estimated numbers of malaria cases continue to vary over the years (WHO, 2018). This suggests that malaria is still a major health burden in developing countries.

Malaria is caused by a *Plasmodium* protozoan parasite belonging to the phylum *Apicomplexa* (Levine, 1988; Cowman *et al*., 2006). Members of the *Plasmodium* genus are eukaryotic, intracellular, unicellular organisms with a characteristic apical complex at the anterior end (Lim and McFadden, 2010). Five species of *Plasmodium* cause malaria in humans. These are: *P. vivax, P. falciparum, P. knowlesi, P. malariae* and *P. ovale* (Vythilingam *et al*., 2006, Tuteja, 2007). *P. falciparum* is the most prevalent species in Africa and causes cerebral malaria, the most lethal form of the disease (Haldar and Mohandas, 2009). According to the WHO (2018), *P. falciparum* is responsible for most malaria cases worldwide (estimated 99.7 % in 2017). *Plasmodium*

parasites are transmitted to humans by female vector mosquitoes belonging to the *Anopheles* genus (Kamareddine, 2012).

1.2 *Plasmodium falciparum* life cycle

P. falciparum undergoes a complex life cycle that spans two organisms, an invertebrate mosquito vector and a vertebrate (human) host (Figure 1.1).

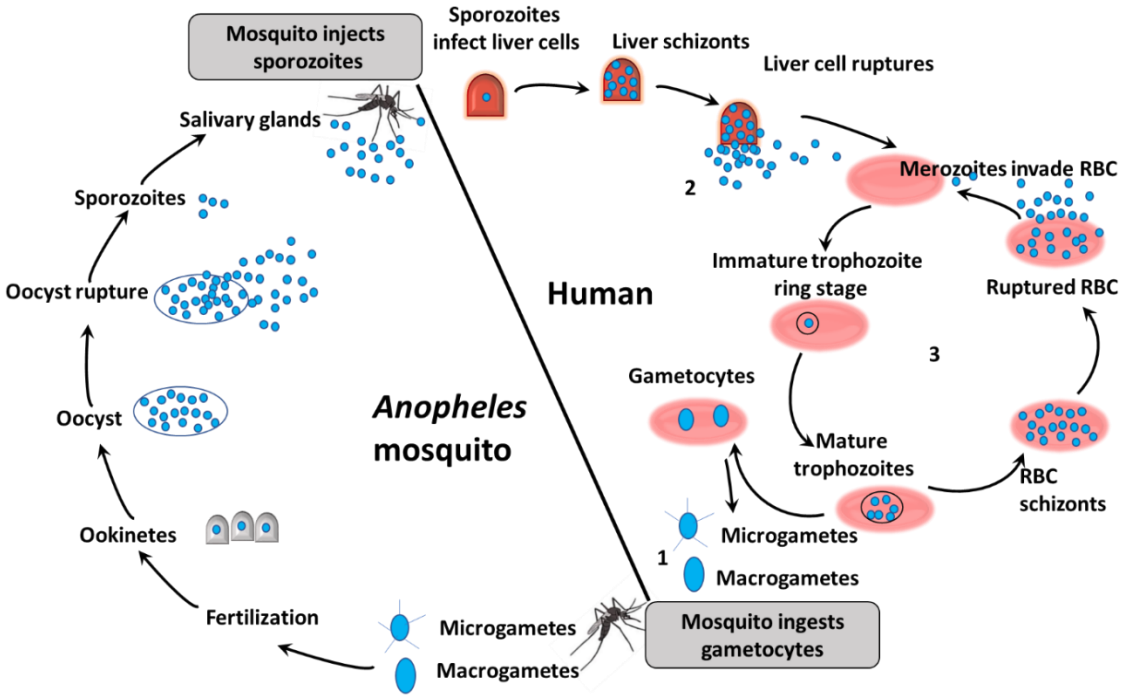

Figure 1. 1: Life cycle of *P. falciparum*
The schematic represents the stages of the life cycle which include: **1**. Gametocytes are ingested by the mosquito during a blood meal. The gametocytes develop into sporozoites, which are then injected into a human host during feeding. **2**. In the liver, sporozoites develop into schizonts. Upon reaching maturity, the schizonts rupture releasing merozoites. **3**. The merozoites invade erythrocytes, develop into trophozoites and finally form schizonts. More merozoites are released into the bloodstream upon rupture of the schizonts. Some invade new erythrocytes while others develop into gametocytes that are readily taken up during a blood meal, adapted from Scherf *et al*. (2008).

Within the human host, the parasite undergoes asexual reproduction which is divided into the pre-erythrocytic stage (exoerythrocytic), the erythrocytic (intra-erythrocyte) stage and the

gametocyte stage. The pre-erythrocytic stage occurs in the hepatocytes and at this stage, the parasites replicate by asexual reproduction. Sporozoites, resident in the salivary glands of the mosquito, are injected into the human host suspended in the mosquito saliva while the mosquito is feeding on blood marking the beginning of the pre-erythrocytic stage. The sporozoites circulate in the bloodstream and subsequently invade hepatocytes and develop into merozoites (Arama and Troye-Blomberg, 2014). A single sporozoite can produce as many as 20 000 merozoites (Fujioka and Aikawa, 2002). The schizonts rupture releasing merozoites into the bloodstream. The merozoites then infect erythrocytes marking the beginning of the erythrocytic cycle and a continuous asexual cycle (Schuster, 2002). Most of the clinical symptoms associated with malaria manifest at this stage.

In the erythrocytes, the parasite develops from a ring to a trophozoite in about 24-32 hours and finally to schizont. A parasite at the schizont stage gives rise to approximately 16-32 merozoites (Arama and Troye-Blomberg, 2014). The merozoites are released into the bloodstream upon erythrocyte rupture (schizont stage) and infect uninfected erythrocytes. At the erythrocytic stage, some parasites differentiate into male (micro-gametes) and female (macro-gametes) forms, which are taken up by the mosquito as it draws its blood meal (Fujioka and Aikawa, 2002). In the midgut of the mosquito, sexual reproduction occurs through fertilization of the macro-gametes by micro-gametes to form a zygote which then develops into a motile ookinete (Bennik *et al*., 2016). Ookinetes invade and reside in midgut epithelial subsequently forming oocyst. The oocysts undergo asexual development resulting in thousands of sporozoites that invade the salivary glands of the mosquito. The sporozoites are then released into the bloodstream and the cycle continues (Bennik *et al*., 2016).

1.3 The erythrocyte as the host cell for malaria parasites

The human erythrocyte functions as the main oxygen carrier in the body. Structurally, the mature erythrocyte lacks a nucleus, intracellular organelles (Bull and Hermamen, 2010) and a *de novo*-protein biosynthesis pathway. The parasite obtains a greater proportion of its nutrition from the

extracellular milieu for it to survive and develop (Desai, 2014). In the initial stages of development (ring stage), the parasite takes up some of the erythrocyte cytoplasm in large vacuoles via a process referred to as the "big gulp" (Elliott *et al*., 2007; Wendt *et al.,* 2016). Trophozoite stage parasites acquire hemoglobin by endocytosis through cytosomes. Cytosomes are small endocytic structures bound by parasite outer membranes. Late stage parasites acquire hemoglobin via an actin-independent process called phagotrophy (Pishchany and Skaar, 2012). The hemoglobin-containing cytosomes then transport the hemoglobin to and fuse with, the parasite's digestive vacuole (Milani *et al*., 2015). Proteases in the parasite's acidic digestive vacuole digest hemoglobin releasing heme and amino acids (Goldberg, 2005). The amino acids are then utilized for parasite protein synthesis (Abu Bakar *et al*., 2010). Heme is toxic to both the parasite and the erythrocyte. Therefore, it is converted to hemozoin (heme dimer crystals; Rinehart *et al*., 2016). In this way, its toxicity is alleviated. However, hemoglobin degradation provides limited nutrition for parasite growth as some amino acids (e.g isoleucine, glutamate, methionine, cysteine and proline) are not derived from hemoglobin as a nitrogen source (reviewed by Mbengue *et al*., 2012). Hence, there is a need for nutrient supply from the extracellular environment. Consequently, the parasite modifies the erythrocyte membrane increasing permeability to various solutes including some anions, cations sodium (Na^+) and potassium (K^+), and organic solutes which are important for parasite survival (Desai, 2014; Soni *et al*., 2016).

1.4 Host cell remodeling by *Plasmodium falciparum*

The parasite merozoite invades the host cells by adhering to the surface receptors on the erythrocyte (Cowman *et al*., 2012; Weiss *et al*., 2015). This process is followed by the irreversible attachment of the parasite. An electron-dense junction between the host cell (erythrocyte) and the apical prominence of the parasite is generated (Cowman *et al*., 2012; Weiss *et al*., 2015). The tight junction moves from the apical to the posterior end of the merozoite. This movement is driven by the parasite actin motor which mediates entry into the erythrocyte. This event is followed by the erythrocyte undergoing echinocytosis (morphological spiking of the cell) due to loss of chloride and potassium ions (Cowman *et al*., 2012). This facilitates internalization of the

parasite. At this stage, the parasite is in a membrane-enclosed compartment called the parasitophorous vacuole (PV, Lingelbach and Joiner, 1998) as represented in Figure 1.2.

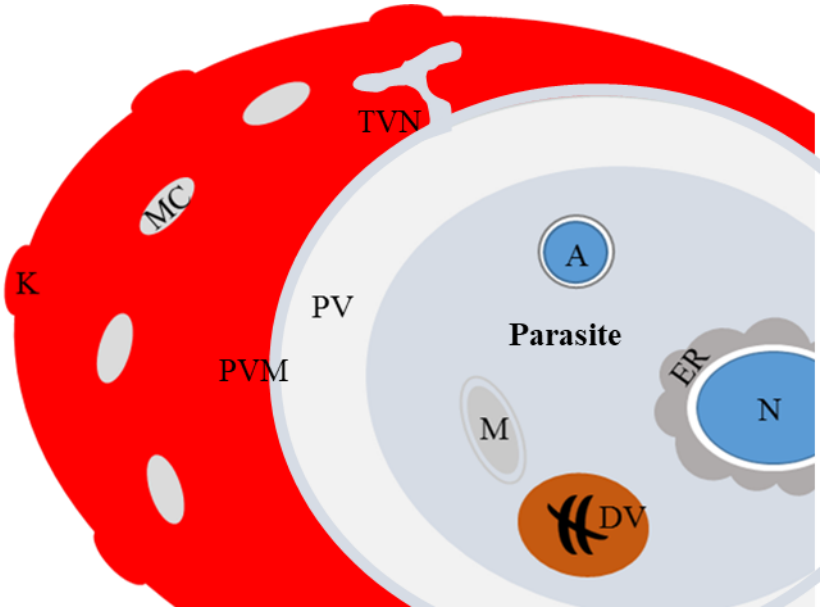

Figure 1. 2: Subcellular organelles implicated in protein traffic in *P. falciparum*-infected erythrocyte
Representation of a trophozoite stage infected erythrocyte: A, apicoplast; DV, digestive vacuole containing hemozoin; ER, endoplasmic reticulum; M, mitochondrion; MC, Maurer's clefts; N, nucleus; PV, parasitophorous vacuole; K, knob and TVN, tubulovesicular network, adapted from Deponte *et al*. (2012).

The parasite is eventually sealed inside the PV (Cowman *et al*., 2012; Weiss *et al*., 2015). The PV is surrounded by the parasitophorous vacuole membrane (PVM, Figure 1.2). The PVM acts as a structural border separating the parasite from the erythrocyte cytosol and hence is important in survival and multiplication of the parasites (Grüring *et al*., 2012). The PV acts as a transit compartment for proteins intended for the infected erythrocyte cytosol (Nyalwidhe and Lingelbach, 2005; Charpian and Przyborski, 2008). The tubulovesicular network (TVN) protrudes into tubular like membranous structures. The TVN is an extension of the PVM (Dhangadamajhi *et al*., 2010). The TVN extends to the erythrocyte membrane and opens to the exterior of the erythrocyte surface. The TVN is thought to play a role in the import of macromolecules. As the parasite matures, parasite induced secretory organelles, called Maurer's clefts, develop within

the infected erythrocyte cytosol (MC**,** Figure 1.2). In the Maurer's clefts lumen, soluble parasite proteins destined for the membrane accumulate. Hence, Maurer's clefts participate in the sorting of parasite proteins destined for the host erythrocyte (Mundwiler-Pachlatiko and Beck, 2013).

The development of the parasite in the mature erythrocyte comes with several drawbacks that include poor nutritional supply and aggressive host-immune response. The parasite overcomes these challenges by remodeling the erythrocyte intensely (Haldar and Mohandas, 2009; Maier *et al*., 2009). This remodeling is facilitated by *P. falciparum*-encoded proteins exported beyond the parasite's plasma membrane (Mbengue *et al*., 2012; Soni *et al*., 2016). *P. falciparum* is thought to traffic approximately 450 (8 %) of its proteins into the infected erythrocyte (Przyborski *et al*., 2015; Soni *et al*., 2016). In this way, the host cell undergoes numerous changes crucial to the parasite's survival marked by sequestration of infected erythrocytes and inflammation due to the host immune response (Craig and Scherf, 2001). The sequestration occurs as a result of parasite expressed adhesins that are exposed on the surface of the infected erythrocyte. These infected erythrocytes then adhere to human endothelial cells lining blood capillaries (Rowe *et al*., 2009). In this way, the parasite avoids clearance by the spleen (Soni *et al*., 2016).

Most proteins that are exported from the parasite to the erythrocyte possess either a signature pentameric signal sequence (RxLxE/Q) called the *Plasmodium* export element (PEXEL) motif or the vacuole transport signal (VTS) (Hiller *et al*., 2004, Marti *et al*., 2004). For protein export to be efficient, the PEXEL motif is cleaved by plasmepsin V (aspartic protease) and the resultant terminus must be acylated. At the PV, these proteins then interact with the PEXEL-protein translocation machine (PTEX) which then facilitates export to the erythrocyte. This export system does not account for proteins lacking the PEXEL motif, so-called PEXEL Negative Proteins (PNEP; Boddey *et al*, 2016). PNEPs include *P. falciparum* skeleton binding protein 1 (PfSBP1), membrane-associated histidine-rich protein (MAHRP1), *P. falciparum* ring exported protein (PfREX1 and 2). Export of PNEPs is thought to be mediated via a short amino acid sequence (identified in PfSBP1, MAHRP1, and PfREX2), which functions like a recessed signal peptide (Przyborski *et al*., 2016). It

is thought that export occurs in a similar manner as in other translocon systems where proteins destined for transport are maintained in an unfolded state (reviewed by Shonhai, 2014).

Most of the exported proteins that are known to associate with the membrane include ring-infected erythrocyte surface antigen (RESA; Goel *et al*., 2014), mature-parasite-infected erythrocyte surface antigen (MESA; Kilili and LaCount, 2011), *P. falciparum* erythrocyte membrane protein 3 (PfEMP-3), knob-associated histidine-rich protein (KAHRP; Pei *et al*., 2005) and *P. falciparum* erythrocyte membrane protein 1 (PfEMP-1; Weng *et al*., 2014). The KAHRP and PfEMP-1 cluster together forming high-density knobs (K, Figure 1.2) while the rest are evenly distributed around the infected erythrocyte membrane. The clustering of PfEMP-1 and KAHRP at the knobs mediates adherence of the infected erythrocyte to endothelial cells, platelets and other infected or non-infected erythrocytes (Cutts *et al*., 2017). In this way, destruction of the infected erythrocyte is evaded by sequestration of the erythrocyte. Together, PfEMP-1 and KAHRP including PfSBP1 and MAHRP associate with the Maurer's clefts (MC**,** Figure 1.2). The PfSBP1 is essential in protein trafficking and during the assembly of numerous proteins at the infected erythrocyte membrane (Cooke *et al*., 2006, Maier *et al*., 2009). This enhances knob formation and is important for pathogenesis.

During remodeling, some of the exported proteins are known to interact with host proteins on the erythrocyte membrane skeleton. Ring stage expressed RESA (Goel *et al*., 2014) binds to beta-spectrin thereby increasing membrane stability and ensures the structural integrity of the erythrocyte. MESA (Kilili and LaCount, 2011) binds to protein 4.1 in the membrane skeleton ensuring parasite survival. Alterations in the erythrocyte morphology are an important immune evasion mechanism by the parasite. However, during the late stages (after 48 hours) of development, destabilization of the membrane is essential for egress of merozoites from the infected erythrocyte. The PfEMP-3 is known to bind α-spectrin destabilizing the spectrin-actin-protein 4.1 complex thereby compromising the mechanical stability of the erythrocyte membrane (Mohandas and An, 2012). Despite altering the erythrocyte morphology to ensure

immune evasion, trophozoite stage parasites alter the erythrocyte to ensure enough nutrient supplies given the limitations of hemoglobin digestion (Section 1.3). Infection by parasites enhances the permeability of the erythrocyte membrane allowing entry of solutes from the exterior environment, exporting metabolic waste and changing the ionic composition of the erythrocyte cytoplasm (Baumeister *et al*., 2006; Tilley *et al*., 2011). The tubulovesicular membrane network (TVN) provides unlimited access to nutrients as it protrudes from the PV to the erythrocyte periphery (reviewed by Mbengue *et al*., 2012). Taken together, the process of host cell remodeling requires correctly folded proteins which are functional. Therefore, an efficient protein folding machinery is necessary to support these events. Not surprisingly, the parasite genome possesses about 2 % of molecular chaperone encoding genes.

1.5 Molecular chaperones

Molecular chaperones form a group of ubiquitous, structurally diverse and highly conserved proteins that exhibit specialized functions (Bukau *et al*., 2006). Molecular chaperones facilitate the folding of newly-synthesized proteins, their translocation through membranes, maturation and assembly of client proteins, prevention of protein aggregation, and facilitate protein degradation (Hartl *et al*., 2011).

1.5.1 Heat shock proteins as molecular chaperones

Cells that have been exposed to stress stimulate the synthesis of a group of molecular chaperones termed heat shock proteins (Hsps) (Lindquist and Craig, 1988). Hsps are classified according to their molecular mass in kilodaltons (kDa). The major classes are the Hsp100, Hsp90, Hsp70, Hsp60, Hsp40 and small Hsps (sHsps) (Table 1.1). Hsps are involved in maintaining proteostasis thereby ensuring cell survival. They are implicated in the development and pathogenesis of parasites (Shonhai *et al*., 2011). Hsps are also implicated in many human diseases. These include diseases caused by parasites (Kaul and Thippeswamy, 2011); autoimmune diseases (Tsan and

Chapter 1

Literature Review

Gao, 2004; Raska and Weigl, 2005; Keijzer *et al*., 2012; Moudgal *et al*., 2013) and neurodegenerative diseases (Turturici *et al*., 2011; Wyttenbach and Arrigo, 2013, Leak, 2014).

Table 1. 1: Heat shock protein families and their general functions

Protein family (Size; kDa)	Localization	Function	Reference
sHsps (10-40)	cytosol, nucleus	prevent aggregation of unfolded proteins and or accumulation of aggregated proteins	Vos *et al*., 2008 Mchaourab *et al*., 2009
Hsp40 (40-100)	cytosol	binding to non-native proteins, delivery of substrate to Hsp70, regulate Hsp70 activity	Botha *et al*., 2007 Njunge *et al*., 2013
Hsp60 (58-65)	cytosol, mitochondria	protein folding and assembly	Sato and Wilson, 2005 Zhang *et al*., 2010
Hsp70 (66-78)	cytosol, nucleus, mitochondria, endoplasmic reticulum	cytoprotection; protein folding and refolding; protein trafficking and degradation	Hartl and Hayer-Hartl, 2009 Vos *et al*., 2008
Hsp90 (82-96)	cytosol, nucleus, endoplasmic reticulum	protein folding and maturation of regulatory proteins eg. kinases and transcription factors; prevention protein of aggregation; prepares proteins for spontaneous folding	Hahn, 2009 Yang *et al*., 2008 Mora´ n Luengo *et al*., 2018
Hsp100 (80-110)	cytosol, nucleus, chloroplast	facilitate protein folding and degradation	Bosl *et al*., 2006 Barends *et al*., 2010 Nowicki *et al*., 2012
Hsp110 (100-150)	cytosol, endoplasmic reticulum	inhibition of protein unfolding; Hsp70 nucleotide exchange factors	Dragovic *et al*., 2006 Vos *et al*., 2008 Muralidharan, 2012; Zininga *et al*., 2016

As a result, Hsps are a potentially attractive class of drug targets. The rationale being that interference with the function of a single Hsp would likely have far-reaching effects on a biological system (Zininga and Shonhai 2014). Heat shock proteins have been reported to be important for the survival of the malaria parasite (*P. falciparum*) in all its life stages (Shonhai *et al*., 2014). The mechanism of action by certain Hsps is either ATP dependent or independent. Some Hsps require the assistance of partner co-chaperones (reviewed by Mayer and Bukau, 2005) to regulate their function.

1.6 *Plasmodium falciparum* heat shock proteins

Heat shock proteins play an important role in the survival and virulence of malaria parasites (Shonhai, 2014). For these parasites, survival under varying conditions is key given a complicated life cycle within a cold-blooded mosquito vector and warm-blooded human host (Shonhai, 2014). The parasite is exposed to temperature changes from ~ 25 °C in the mosquito to 37 °C in the human host and ~41 °C during fever episodes (Pavithra *et al*., 2004). The temperature changes do not necessarily impair parasite survival but enhance their numbers (Pavithra *et al*., 2004). The parasite not only endures thermally induced physiological changes within the host but is subjected to host immune responses (Moll *et al*., 2015; Gomes *et al*., 2016; Belachew, 2018), and oxidative stress (van Schalkwyk *et al*., 2013; Sussmann *et al*., 2017; Rocamora *et al*., 2018). Interestingly, the parasite survives under such conditions with the help of chaperones and still manages to synthesize correctly folded proteins necessary for survival and development. Two major Hsps implicated in the survival and virulence of the malarial parasite are *P. falciparum* Hsp70 (PfHsp70-1; Shonhai *et al*., 2007; 2008) and *P. falciparum* Hsp90 (PfHsp90; Pavithra *et al*., 2004; Shahinas *et al*., 2013). These two Hsps are important for parasite survival and are potential drug targets.

1.6.1 Heat shock protein 90

Hsp90s consists of three domains which are highly conserved: an N-terminal 25 kDa ATP-binding domain, a middle domain of 35 kDa and a 12 kDa C-terminal domain (Figure 1.3; Terasawa *et al*.,

2005). The N-terminal domain binds and hydrolyzes ATP. It is also implicated in dimerization. The middle domain is responsible for client binding. Hsp90 has a charged linker region between the ATP binding domain and the middle domain (Tsutsumi *et al*., 2012; Penkler *et al*., 2018). This linker is responsible for conferring flexibility between the N-domain and the middle domain as well as enhancing the chaperone function of Hsp90. The C-terminal domain is implicated in the dimerization of Hsp90 (Ciglia *et al*., 2014). Dimerization has been shown to be essential in the *in vivo* function of the chaperone (Wayne and Bolon, 2007).

Figure 1. 3. Domain organization of PfHsp90
PfHsp90 possesses an N-terminal ATPase domain, a linker domain, a middle domain and a C-terminal substrate binding domain comprising a dimerization domain and an EEVD motif. The dimerization domain is responsible for PfHsp90 dimer formation and the EEVD motif is responsible for binding to PfHop TPR domains, adapted from Pavithra *et al*. (2007).

The MEEVD motif at the end of the C-terminus facilitates binding of tetrapeptide repeat (TPR) containing co-chaperones (Hsp70/Hsp90 organizing protein, protein phosphatase PP5, J domain-containing protein TPR2, the myosin folding factor uncoordinated 45 [unc-45] and the peptidyl-prolyl isomerases [PPIases], such as Fk506 binding protein 52 [Fkbp52], Fk506 binding protein 51 [Fkbp51] and cyclophilin P40 [cyp40]) to Hsp90 (reviewed by Li *et al*., 2012). Hsp90 functions as a molecular chaperone and stabilizes proteins implicated in signal transduction pathways (Li *et al*., 2012). Hsp90 targets near-native client proteins downstream of Hsp70 and it is important for their complete folding. Recently, Hsp90 was reported to break the folding blockage inflicted on client proteins by Hsp70 thereby allowing their spontaneous folding (Moràn Luengo *et al*., 2018). Thus, inhibition of Hsp90 function is likely to abrogate protein folding and have far-reaching effects within cells.

Chapter 1

Literature Review

1.6.1.1 *Plasmodium falciparum* Hsp90

The *P. falciparum* genome encodes four PfHsp90 proteins, two cytosolic PfHsp90 (PF3D7_0708400 and PF3D7_1443900), an endoplasmic reticulum PfGrp94 (PF3D7_1222300) and a mitochondrial PfTRAP1 (PF3D7_1118200) (Banumathy *et al*., 2003; Pallavi *et al*., 2010). Of the two cytosolic isoforms, only one PfHsp90 (PF3D7_0708400) possesses the MEEVD motif. It is induced by stress and is expressed during the erythrocytic stage in the parasite life cycle (Banumathy *et al*., 2003). PfHsp90 (PF3D7_0708400) is the most studied. PfHsp90 functions as a dimer (Shahinas *et al*., 2013). Hydrogen bonding plays an important role in the interaction of the two monomeric forms of PfHsp90 (Kumar *et al*., 2007). PfHsp90 plays an essential role at the pre-erythrocytic (Posfai *et al*., 2018) and erythrocytic stages (Pavithra *et al*., 2004; Posfai *et al*., 2018) thus facilitating parasite development and survival. The PfHsp90 function is essential in parasite development during the frequent febrile episodes. PfHsp90 has been presented as a drug target because of this crucial role (reviewed by Ramdhave *et al*., 2013; Wang *et al*., 2016; Posfai et al., 2018). Various studies have identified compounds, that inhibit PfHsp90 resulting in parasite death (Wang *et al*., 2016; Posfai *et al*., 2018).

PfHsp90 also occurs in multi-protein complexes with other parasite Hsps such as *P. falciparum* Heat shock protein 70 (PfHsp70-1; Shonhai *et al*., 2007), *P. falciparum* Heat shock protein 110 (PfHsp70-z; Zininga *et al*., 2016), *P. falciparum* Heat shock protein 40 (PfHsp40; Pavithra *et al*., 2007) and co-chaperones; *P. falciparum* Hsp70/Hsp90 organizing protein (PfHop; Gitau *et al*., 2012), *P. falciparum* Activator of Hsp90 ATPase 1 (PfAha1; Chua *et al*., 2012), *P. falciparum* Hsp90 co-chaperone p23 (Pfp23; Banumathy *et al*., 2003) (Figure 1.4). These complexes play important roles in the survival of *P. falciparum*.

Chapter 1

Literature Review

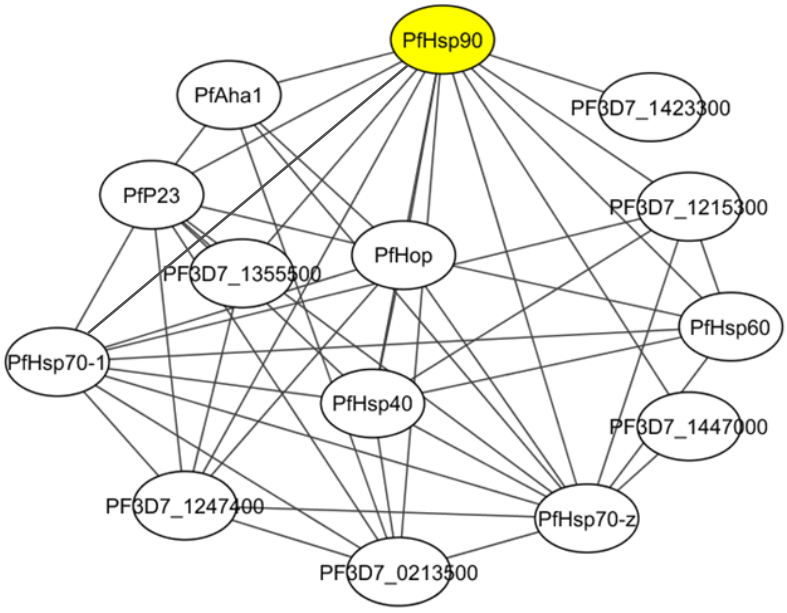

Figure 1. 4. PfHsp90 predicted interaction partners
The predicted interactome of PfHsp90 (yellow) reflects interaction with known molecular chaperones (PfHsp70-z, PfHsp70-1 and co-chaperones (PfHop, Pfp23, PfAha1, PfHsp40) forming functional complexes.

1.6.2 Hsp70-Hsp90 organizing protein

Structurally, Hop is a multi-domain protein made up of three tetratricopeptide repeat (TPR) domains namely TPR1, TPR2A and TPR2B and two aspartic acid-proline domains (DP1 and DP2) (Figure 1.5). Each TPR domain is characterized by three TPR repeat motifs that form superhelical structures giving rise to amphipathic grooves (Morgan *et al*., 2012; Schmid *et al*., 2012). The TPR domains serve as protein-protein interaction modules. TPR domains are made up of tandem repeats of 34 amino acids that form α-helices which are aligned antiparallel to each other (Figure 1.5). The TPR domain surface comprises both concave and convex regions with most interactions occurring on the concave surfaces. The TPR1-DP1 fragment is connected to the TPR2A-TPR2B region by unstructured residues (positions 198-260; Schmid *et al*., 2012; Röhl *et al*. 2015). The DP2 is connected to the TPR2B by unstructured residues (positions 520-526; Schmid *et al*., 2012).

Chapter 1

Literature Review

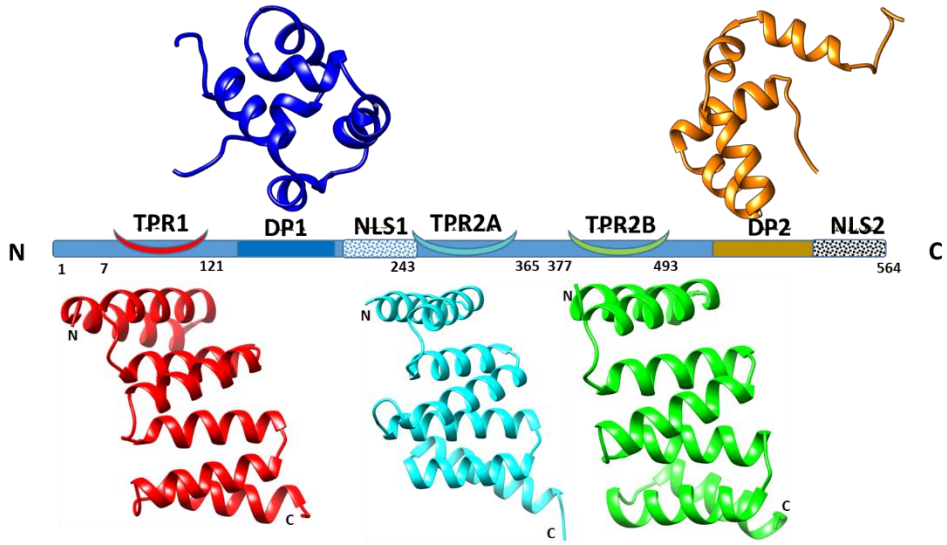

Figure 1. 5. Schematic representation of Hop domains
The positions of the three tetracopeptide repeat domains (TPR), the two dipeptide domains (DP) and the two nuclear localization signals (NLS) are shown. Ribbon representation of the three-dimensional models of TPR1 (1ELW.pdb; Scheufler *et al*., 2000), TPR2A (3ESK.pdb; Kajander *et al*., 2009), TPR2B (3UPV.pdb; Schmid *et al*., 2012), DP1 (c2llvA.pdb; Schmid *et al*., 2012) and DP2 (c2llwA.pdb; Schmid *et al*., 2012) domains are shown.

The TPR1 domain is in the N-terminus region of the protein and is responsible for binding the C-terminally located EEVD motif of Hsp70 (Gitau *et al*., 2012). The middle TPR2A binds the C-terminal MEEVD motif of Hsp90 and the TPR2B, like TPR1, binds to the EEVD motif of Hsp70 (Scheufler *et al*., 2000; Southworth and Agard 2011). The TPR1 and TPR2B preferentially bind PfHsp70-1 compared to PfHsp90 (Zininga *et al*., 2015b), suggesting specificity in the engagement of clients. Although it was initially thought that Hop interacts only with the EEVD/MEEVD of chaperone proteins, some studies suggest the existence of other binding sites on the chaperones (reviewed by Edkins, 2016).

Hop modulates the functional interaction of Hsp70 and Hsp90. Several studies have however shown that the Hsp90/Hsp70 interaction could occur independent of Hop (Nakamoto *et al*., 2014; Kravats *et al*., 2017; 2018). Using Hsp90 and Hsp70 from bacteria and yeast, direct Hsp90/Hsp70 interaction was reported to occur via a region in the middle domain of Hsp90 (Nakamoto *et al*.,

2014; Kravats *et al*., 2017; 2018). Given that there is no Hop homolog in *E. coli*, a direct association between Hsp90 and Hsp70 in *E. coli* is important (Genest *et al*., 2016). The Hop gene is not essential in yeast (Reidy *et al*., 2018), *Trypanosoma cruzi* and *Trypanosoma brucei* (Schmidt *et al*., 2018) although in the absence of Hop certain functions are affected (Lackie *et al*., 2018). This might explain the need for Hsp90/Hsp70 direct interaction (Nakamoto *et al*., 2014). It remains to be investigated whether this direct interaction is conserved among species. Hop has been proposed as a potential drug target (Gitau *et al*., 2012; Zininga *et al*., 2015b). However, this would only apply in cases where Hop is essential for example in cancer (Röhl *et al*., 2014) and Leishmaniasis (Morales *et al*., 2010; Hombach *et al*., 2013).

1.6.2.1 *Plasmodium falciparum* Hsp70/Hsp90 organizing protein

The *P. falciparum* genome encodes a Hop homolog (PfHop; PF3D7_1434300). Cytosolic and nuclear localization of Hop has been reported (Longshaw *et al.,* 2004, Daniel *et al*., 2008; Gitau *et al*., 2012). In these cells, Hop shuttles between the cytosol and the nucleus in response to heat stress (Lässle *et al.,* 1997; Longshaw *et al.,* 2004). Furthermore, the movement of mouse Hop to the nucleus was observed to occur during heat shock (Langer *et al*., 2003; Longshaw *et al*., 2004). Hop contains two nuclear localization signals (NLS) and these are important in the nuclear localization of Hop under heat stress (Longshaw *et al.,* 2004; Daniel *et al*., 2008).

PfHop localizes in the cytosol in a similar pattern with PfHsp70-1 and PfHsp90 suggesting that these proteins may co-operate in a common complex (Gitau *et al*., 2012). Furthermore, like PfHsp70-1, PfHop expression was shown to be upregulated in cells exposed to heat stress (Zininga *et al*., 2015b) signifying its importance during stress. Studies by Zininga and colleagues (2015b) also confirmed a direct association between PfHsp70-1 and PfHop using surface plasmon resonance (SPR).

Hop contact residues important for its interaction with Hsp70 or Hsp90 are conserved among species. Residues lysine (K8), asparagine (N12) in TPR1 and K301, arginine (R305) in TPR2A in

mouse Hop were shown to interact with an aspartic acid (D) residue in the EEVD and MEEVD motifs of Hsp70 and Hsp90 respectively (Odunuga *et al.,* 2004). These charged residues (K; N; R) are surface exposed and protrude in TPR grooves (Odunuga *et al*., 2004). Mutation of these residues disrupted the helical structure of TPRs and inhibited TPR/Hsp70 and TPR/Hsp90 interactions (Odunuga *et al*., 2004; Blundell *et al*., 2017). High conservation of residues implicated in PfHop/PfHsp70-1 interaction has been demonstrated and these are reported to be present in *Plasmodium* Hop. Residues K11, K247, K382 and N15, N251, N386 of PfHop were shown to be conserved within TPR1, TPR2A and TPR2B of yeast, human, mouse and other Plasmodial parasites (Gitau *et al*., 2012). Residues K11 and N15 in PfHop correspond to residues K8 and N12 in mouse Hop. These residues constitute the so-called 'carboxylate clamp' contacting the D residue in the EEVD motif of Hsp70 and Hsp90 (Kumar *et al*., 2017; Adão *et al*., 2018). The interaction between TPR domains and the EEVD motif of chaperones Hsp70 and Hsp90 is conserved although other binding sites outside EEVD have been proposed (Durech *et al*., 2016). However, Batista *et al*. (2016) suggest that there are differences in these co-chaperone residues responsible for binding despite the conservation of structure and function among homologs. Recent insights into these interactions can shed more light towards the design of therapeutics targeting the Hop/Hsp interactions. Interestingly, Hop from *Leishmania major* (LmSTI) has shown potential as an antigen towards the development of a vaccine (Goto *et al*., 2011). Taken together, this has the potential to mitigate diseases in which Hop is implicated for example cancer.

1.6.3 Heat shock protein 70

Heat shock protein 70 (Hsp70) is a ubiquitous and highly conserved family of proteins known to perform a wide range of cellular processes. Some members of the Hsp70 family are constitutively expressed (referred to as heat shock cognate proteins, Hscs) performing general housekeeping functions, while stress-inducible forms are referred to as Hsps (Chiappori *et al*., 2016). Hsp70 (known as DnaK in archaea and eubacteria) is regarded as the most versatile group of molecular chaperones performing a myriad of functions. Hsp70s are capable of folding nascent polypeptides, prevention of aggregation and refolding of misfolded proteins (Zuiderweg *et al*.,

2017). In contrast, a recent report seems to suggest that the binding of Hsp70s blocks the spontaneous folding of client proteins. The study used luciferase, an Hsp70 substrate. Folding only occurs when Hsp90 knocks off the Hsp70 (Moràn Luengo *et al*., 2018). This seems to suggest that Hsp70 is not useful for protein folding at physiological concentrations. However, it is known that Hsp70 is essential at normal temperatures of growth and at high temperatures in different organisms (reviewed by Yu *et al*., 2015). The binding of Hsp70 to hydrophobic patches prevents aggregation of client proteins which is an important function to protein folding (Zylicz and Wawrzynow, 2001; Mayer and Bukau, 2005).

Structurally, Hsp70s consist of two major domains: an N-terminus ATPase (or nucleotide-binding domain; NBD) of 44 kDa and a substrate binding domain (SBD) of 25 kDa (Figure 1.6; Bertelsen *et al*., 2009). On the other hand, Hsp110s exhibit an extended lid segment located in their SBD. Hence, Hsp70s possess a larger SBD. The Hsp70 family of proteins are divided, based on a structural distinction, into canonical Hsp70s and Hsp110s (Easton *et al*., 2000). All DnaK-like Hsp70s are referred to as canonical Hsp70s. Hsp110s act as nucleotide exchange factors (NEFs) for Hsp70s (Dragovic *et al*., 2006) but recent reports suggest that Hsp110s possess independent chaperone activity (Zininga *et al*., 2016).

Chapter 1

Literature Review

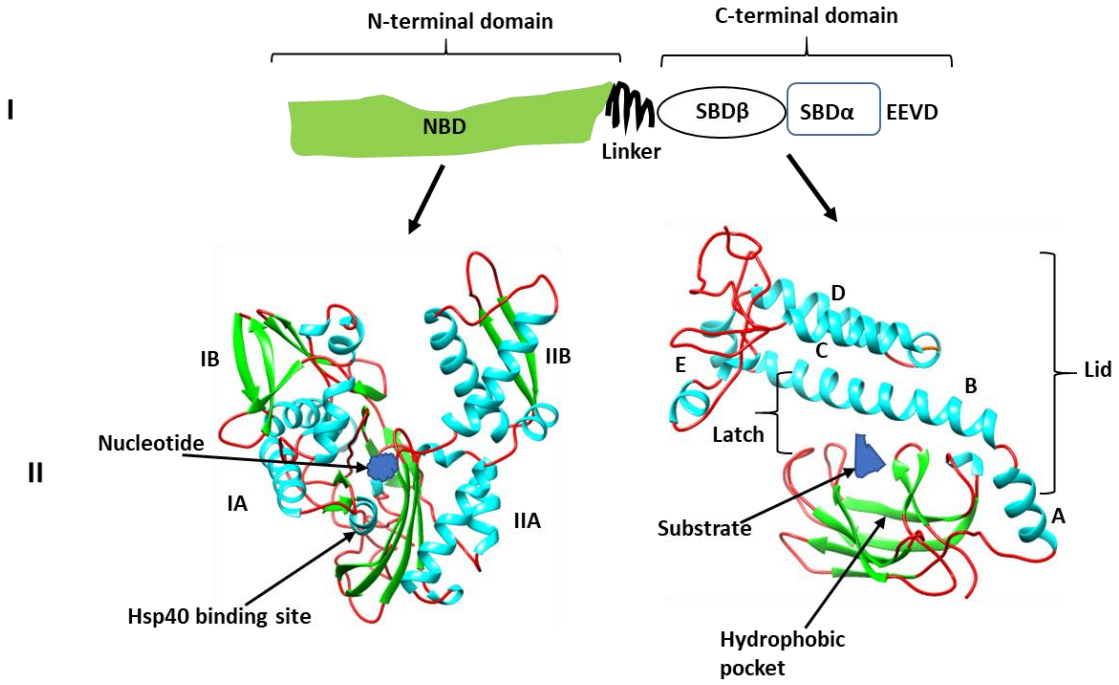

Figure 1. 6. Representation of Hsp70 domains
The domain representation is based on the structure of *E. coli* DnaK. **I**: representation of the basic structure of Hsp70 showing the N-terminal domain, a highly charged linker and a C-terminal domain comprising the EEVD motif. **II**: N-terminal domain (NBD) comprising two domains subdivided into lobes IA, IB, IIA and IIB. Also shown is a bound nucleotide (blue) and the Hsp40 binding site, C-terminal domain (CTD) showing the hydrophobic pocket, a bound substrate and the alpha-helical lid. The lid is made up of helices A, B, C, D and E, adapted from Shonhai (2007).

The two are linked together by a highly charged linker (English *et al*., 2017). The linker is highly conserved and possesses a characteristic D/E-V/I/L-L-L-D-V-*-P hydrophobic sequence (reviewed by Zuiderwig *et al*., 2012). The linker acts to regulate allostery (English *et al*., 2017). In this way, the linker maintains the distance between the NDB and SBD as well as the orientation of the domains. Besides regulating allostery, the linker also modulates ATP hydrolysis (Alderson *et al*., 2014). The linker is reported to bind the NBD and stimulate ATP hydrolysis (Alderson *et al*., 2014). This demonstrates the versatile function of the linker.

The NBD is thought to indirectly regulate the affinity of substrate binding through allostery, while the SBD binds hydrophobic regions of client proteins (Kityk *et al*., 2015). Interdomain

communication (allostery) is crucial for Hsp70 function and occurs via the seven-residue linker (Figure 1.6). The NBD is made up of two linked subdomains I and II, which are in turn subdivided into lobes IA, IB, IIA and IIB (Figure 1.6 B). These are arranged in such a way that there is a crevice with a hydrophilic pocket that only binds adenosine and phosphates on ATP. On the other end, the SBD is composed of two subdomains: the β-sandwich domain and the α-helical lid (Figure 1.6). The double-layered β-sandwich comprises the substrate binding cleft. It is connected to the α-helical subdomain which functions as a flexible lid to cover the SBD cleft (Zhang *et al*., 2014). The terminal region of the SBD is known to be variable between Hsp70s. In most cytosolic Hsp70s this region is glycine/proline (G/P)-rich possessing the terminal EEVD motif responsible for binding co-chaperones and other Hsps (Radons, 2016).

1.6.4 Hsp70 chaperone cycle

The binding of nucleotide to the NBD regulates the activity of Hsp70 function (Figure 1.7). Binding of ATP by the NBD facilitate substrate release from the Hsp70 SBD (section 1.6.2) and conversely, substrate binding to the SBD promotes ATP hydrolysis by the NBD (Zhuraleva and Gierasch, 2015). On the other hand, Hsp70 bound to ADP possesses a high affinity for the substrate. Hsp70 possess low basal ATPase activity, hence it cooperates with Hsp40 co-chaperones (section 1.6.3) which stimulates the ATP hydrolysis (Kityk *et al*., 2012). When Hsp70 binds ATP, lobe I and II of NBD rotate by 25.5° relative to each other concurrently as the SBDβ and SBDα separate to dock on different faces of the NBD. This causes an increase in the substrate on and off rates by two or three orders of magnitude respectively, hence lowering affinity for the substrate by 10-50-fold (Kityk *et al*., 2012; Mayer and Kityk, 2015). Movement in lobe IA and IIA also stimulates ATP hydrolysis resulting in Hsp70 regaining high-affinity state for the substrate in the ADP-bound form (Kityk *et al*., 2015). In this state, the NBD and SBD are further from each other (distances < 16 Å, Kityk *et al*., 2012) but the SBDβ and SBDα dock close to one another resulting in lower on and off rates hence higher affinity for substrate (Kityk *et al*., 2015). On the other hand, Hsp110s have a distinct mechanism of action. In their work, Kumar *et al*. (2017) did not observe changes in the distance between NBD and SBD of Hsp110 (Sse1, in yeast) in the presence of both ATP and ADP.

Hsp110s possess a rigid linker which limits allostery as compared to canonical Hsp70s, hence they are thought not to exhibit inter-domain movement (Stetz and Verkhivker 2015).

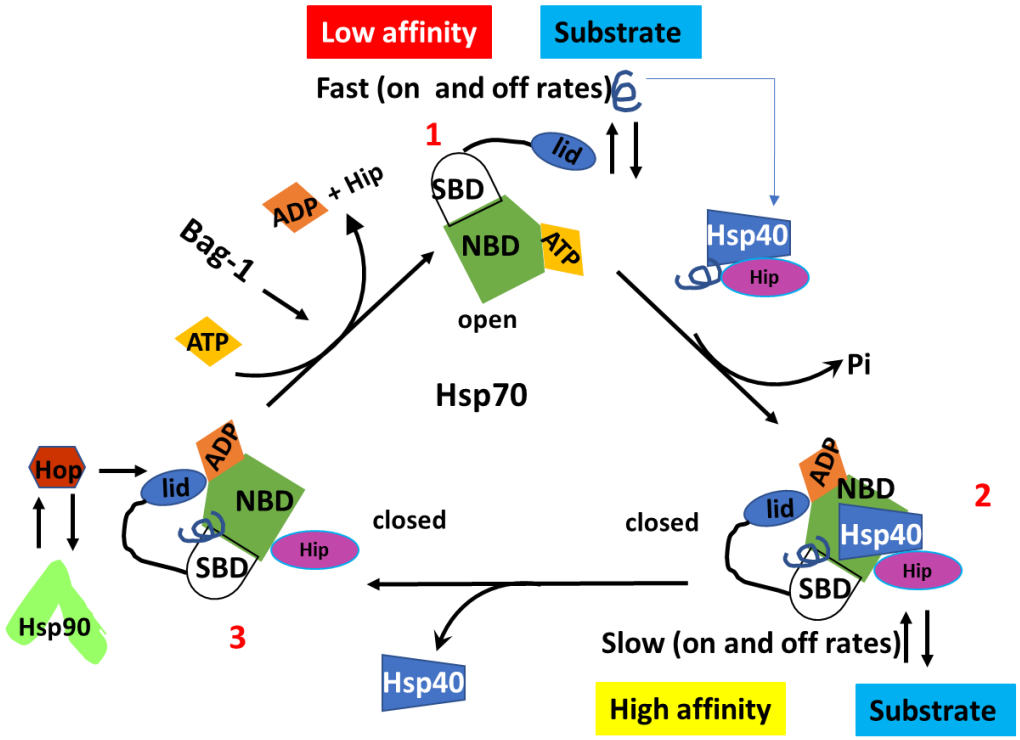

Figure 1. 7. Hsp70 chaperone cycle
Hsp70 assumes different conformations **1**. In its ATP-bound state, there is a low affinity for the substrate. Hsp40 facilitates ATP hydrolysis. **2**. Hsp40 delivers the bound substrate to Hsp70. Hsp40 then interacts with the NBD of Hsp70 thereby facilitating ATP hydrolysis. **3**. ADP-bound state, the binding groove of Hsp70 closes and thus Hsp70 exhibits high affinity for the substrate. Other Hsps amongst them Hsp90 form part of the complex through the mediation of co-chaperones such as Hop (Sti1). ADP exchange is mediated by NEFs. Binding of NEFs to the NBD of Hsp70 causes a conformational change resulting in a low-affinity state. The substrate is released; sketch was adapted from Radons (2016).

1.6.5 The role of co-chaperones in regulating Hsp70 function

Hsp70s mediate a cohort of functions in protein quality control through their co-operation with co-chaperones. Co-chaperones act by either connecting the Hsp70s and substrates or mediating the release of the cargo (Mayer and Bukau, 2005). Prokaryotes and eukaryotes encode different co-chaperones that serve distinct functions (Raviol *et al*., 2006). These co-chaperones are the Hsp40s, Hsp110s, Bcl-2-associated athanogene proteins (Bag), Hsc-70 interacting protein (Hip),

Chapter 1

Literature Review

Hsp70/Hsp90 organizing protein (Hop) and C-terminus of Hsc70-interacting protein (CHIP) (Mayer and Bukau, 2005). It is interesting to note that, although initially considered as NEF, Hsp110s exhibit independent chaperone function (Zininga *et al.,* 2016).

The J-domain (derived from *E. coli* DnaJ) proteins (Hsp40s) serve as targeting factors for Hsp70 clients as they bind to client proteins and hand them to Hsp70 for subsequent folding. Apart from recruiting client substrates, Hsp40s also stimulate the ATPase activity of Hsp70 during the subsequent refolding of substrates or disaggregation of proteins (Torrente and Shorter, 2013). In order to bind to protein aggregates, Hsp70 must first displace the sHsps (section 1.5.1). Small Hsps tend to form a protective shield around protein aggregates (Zwirowski *et al*., 2017). Hsp70 does this by competing with the sHsps for binding to the aggregates (Zwirowski *et al*., 2017). This process is highly dependent on the Hsp70 chaperone. Hence, Hsp70 is activated by Hsp40 and recruited to areas of need. Overall, the role of Hsp40 involves regulating the functional specificity of Hsp70 and also services as the latter's substrate scanner.

Like the Hsp40s, Bag proteins (Takayama *et al*., 1995) in eukaryotes have also been proposed to serve as targeting factors for Hsp70. This family of proteins physically interact with Hsp70 and have also been shown to associate with signaling molecules and some steroid hormone receptors. In eukaryotes, Bag family of proteins, heat shock factor binding protein (HsBP1) and Hsp110 (Dragovic *et al*., 2006) mainly serve as nucleotide exchange factors (NEF), like GrpE in *E. coli*. They bind to the NBD of Hsp70 thereby mediating substrate release (Knapp *et al*., 2014). The hydrolysis of ATP and the exchange of ADP for ATP are essential for the Hsp70 function. NEFs are reported to either positively or negatively modulate Hsp70 chaperone function (Shomura *et al*., 2005; Tzankov *et al*., 2008). Hip also interacts with the NBD of Hsc70. In so doing there is competition between Hip and Bag1 for binding NBD and this inhibits the Bag1 stimulated nucleotide release (Mayer and Bukau, 2005). Nevertheless, Hip plays a role in stabilizing Hsp70-ADP bound state thus preventing the quick release of the client. Another co-chaperone CHIP influences the ATPase activity of Hsp70. It acts by mediating the ubiquitination of Hsc70

substrates for degradation by the proteasome (Edkins, 2015). In protein degradation, co-chaperones Hsp40 and Hip promote binding of client substrate to Hsp70. On the other hand, CHIP and BAG-1 promote substrate release. BAG-1 triggers the exchange of ADP to ATP. CHIP then mediates the ubiquitination of substrate and inhibits ATP hydrolysis. In this way, substrate folding is inhibited as Hsp70 is locked in substrate low-affinity state and the ubiquitinated substrate is shuttled to the proteasome (reviewed by Kriegenburg *et al*., 2011).

1.7 *Plasmodium falciparum* heat shock protein 70

The *P. falciparum* genome encodes six Hsp70s (Table 1.2). The Hsp70s occupy different cellular compartments. Each of the Hsp70s plays important functions in proteostasis in conjunction with partner proteins to ensure parasite survival (Table 1.2; reviewed by Shonhai, 2014). Of the six Hsp70s, more research attention has been given to PfHsp70-1 because it exhibits distinct functional features and plays key cytoprotective roles (section 1.7.1.1). Recently a lot of work has focused on PfHsp70-z as a drug target (Zininga *et al*., 2015a, 2016, 2017a, 2017b) since the protein is essential for parasite viability (Muralidharan *et al*., 2012). Moreover, PfHsp70-z is able to suppress the misfolding of otherwise aggregation-prone asparagine repeat-rich proteins, which make up to 10 % of the *P. falciparum* proteome (Pallarès *et al*., 2018). Zininga and colleagues (2015a) have shown that PfHsp70-z is a thermotolerant molecule with independent chaperone activity. This supports the fact that PfHsp70-z acts to suppress aggregation of asparagine-rich proteins during malarial fever. Recent studies by Pallarès *et al*. (2018) suggest that the presence of such a higher percentage of asparagine-rich proteins in *P. falciparum* is of a functional advantage to the parasite. Long sequences of asparagine or glutamate are implicated in prion-like domains (PrLD). Prion proteins are able to transition between soluble and amyloid conformations, so parasites are thought to utilize this prion-like mechanism to their own benefit (Pallarès *et al*., 2018).

Table 1. 2: Hsp70s from *Plasmodium falciparum*

Name	Location	Expression phase	Function/s	References
PfHsp70-1 (PF3D7_0818900)	nucleus & cytosol	erythrocytic stage	protein folding, translocation, aggregation suppression	Kumar *et al*.,1991 Sharma *et al*., 1992 Shonhai *et al*., 2007 Pesce *et al*., 2008
PfHsp70-2 (PF3D7_0917900)	E.R	erythrocytic stage	protein import and folding in the ER, retrograde translocation of proteins for degradation	Kumar *et al*., 1991 Pavithraa *et al*., 2004 Shonhai *et al*., 2007 Njunge *et al*., 2013 Chen *et al.,* 2018
PfHsp70-x (PF3D7_0831700)	P.V and exported to the erythrocyte	erythrocytic stage	export of specialized virulence proteins and protein folding in the erythrocyte	Shonhai *et al*., 2007 Kulzer *et al*., 2012 Daniyan *et al*., 2016 Charnaud *et al*., 2017 Cobb *et al.,* 2017
PfHsp70-3 (PF3D7_1134000)	mitochondrion	N. E	protein translocation into the mitochondrion	Sharma *et al*., 1992 Shonhai *et al*., 2007 Njunge *et al*., 2013 Nyakundi *et al.,* 2016
PfHsp70-z (PF3D7_0708800)	cytosol	erythrocytic	essential chaperone and proposed NEF for PfHsp70-1; suppression of aggregation of asparagine-rich proteins	Sargeant *et al*., 2006 Shonhai *et al*., 2007 Muralidharan *et al*., 2012 Zininga *et al*., 2015a
PfHsp70-y (PF3D7_1344200)	E.R	N. E	chaperone function and NEF for PfHsp70-2	Sargeant *et al*., 2006 Shonhai *et al*., 2007 Njunge *et al*., 2013

E.R: endoplasmic reticulum; P.V: parasitophorous vacuole; N.E: not elucidated

Most of the prion-like proteins identified in yeast, humans, and plants are involved in diverse functions, mainly gene expression, regulation of either transcription or translation, protein localization and regulation of vehicle mediated transport (King *et al*., 2012; Iglesias *et al*., 2015; Chakrabortee *et al*., 2016). This would be a crucial transport mechanism in *P. falciparum* as about 450 of its proteins are predicted to be exported to the infected erythrocyte (Spielmann and Gilberger, 2015; Przyborski *et al*., 2016).

Chapter 1

Literature Review

PfHsp70-x has been shown to be 74 % identical to PfHsp70-1 (Hatherly *et al*., 2014). PfHsp70-x is exported to the infected erythrocytes (Külzer *et al*., 2012). PfHsp70-x which is regarded as a PEXEL negative protein (PNEP), possesses a 32 amino acid N-terminal secretory signal (MKTKICSYIHYIVLFLIATTTHT**ASNNAEES;** Külzer *et al*., 2012). The 8 amino acids (in bold) referred to as a novel octameric signal (NOES) are thought to remain attached to the NBD of PfHsp70-x after cleavage of the signal sequence. Külzer and colleagues (2012) speculated that the NOES may be responsible for the trafficking of PfHsp70-x into the erythrocyte. However, studies by Rhiel and colleagues (2016), have shown that soluble PfHsp70-x can also be exported via the PTEX translocon despite lack of the PEXEL/HT motif. Recently, using gene knockout and knockdown approaches, PfHps70-x was shown to be dispensable for asexual development of the parasite (Charnaud *et al*., 2017; Cobb *et al*., 2017).

PfHsp70-x was initially thought to play a role in protein transport across the PV (Przyborski *et al*., 2015). However, studies by Cobb and colleagues (2017) suggest that knockout of PfHsp70-x does not abrogate the export of proteins (KAHRP, MAHRP1, PfEMP1, and PfFIKK4.2). Charnaud and co-workers (2017) observed a delayed export of proteins responsible for cytoadherence of erythrocytes infected by parasites void of PfHsp70-x. This suggests that PfHsp70-x only acts to speed up the export of proteins responsible for cytoadherence. Furthermore, PfHsp70-x is also speculated to maintain exported proteins in an unfolded state before transport across the PVM via PTEX. PfHsp70-x is required for the folding and transport of the various proteins to their destinations (Maurer's clefts, or host cell plasma membrane). The fact that PfHsp70-x interacts with an Hsp40 co-chaperone (PFA0660W) implies that PfHsp70-x is involved in the chaperoning of exported parasite proteins (Daniyan *et al*., 2016; Behl *et al*., 2018). Furthermore, studies by Mabate *et al.* (2018) reported that PfHsp70-x interacts with human Hop *in vitro*. It is possible that PfHsp70-x forms functional complexes with proteins of human origin. It is for this reason that PfHsp70-x is implicated in host cell remodeling, infectivity and immune evasion.

The ER-based PfHsp70-2 possesses chaperone properties (Ramya *et al*., 2006). PfHsp70-2 was shown to suppress the aggregation of alcohol dehydrogenase and glutamate dehydrogenase *in vitro*. Together with the translocon machinery (*Plasmodium falciparum* protein transport protein 61; PfSec61 complex), PfHsp70-2 is reported to take part in the secretory pathway as well as the degradation processes within the ER (reviewed in Przyborski *et al*., 2015*)*. PfHsp70-2 is thought to be involved in quality control and is thought to cooperate with *P. falciparum* Hsp40s found in the ER lumen. A second Hsp110 family member, PfHsp70-y acts as a NEF for PfHsp70-2 in the ER (Shonhai, 2014). Recently, PfHsp70-2 was shown to be a viable drug target due to the protein being structurally different from its human orthologue (Chen *et al.,* 2018). The mitochondrial Hsp70, PfHsp70-3 forms part of a motor system which interacts with the pre-protein to facilitate its entry into the matrix.

1.7.1 *Plasmodium falciparum* Hsp70-1

PfHsp70-1 possesses the canonical Hsp70 structure (Figure 1.8). However, PfHsp70-1 possesses seven glycine-glycine-methionine-proline (GGMP) tetrapeptide repeats in the C-terminal lid segment. This stretch of GGMP repeats together with other none-GGMP residues (GAGMPGNAP) is referred to as a GGMP motif. It is located between the SBDα and the terminal EEVD motif (residues 632 to 658; Figure 1.8).

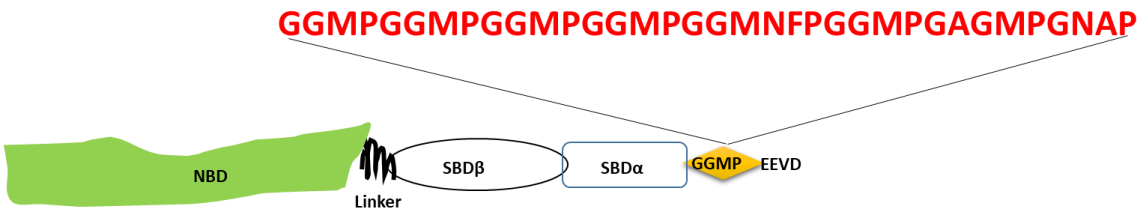

Figure 1. 8. Representation of the structure of PfHsp70-1 showing the N-terminal domain, a highly charged linker domain and a C-terminal domain comprising the GGMP motif and EEVD motif.

PfHsp70-1 is known to be induced by stress and is cytosolic and nuclear-localized (Shonhai *et al*., 2007). It is upregulated in all blood stages of the parasite's life cycle, demonstrating enhanced expression in response to heat shock (Zininga *et al*., 2015b). PfHsp70-1 has been suggested to

facilitate the translocation of proteins destined for the mitochondria (Przyborski *et al*., 2015). Using *in vitro* studies PfHsp70-1 was shown to exhibit ATPase activity and ability to suppress heat-induced protein aggregation (Matambo *et al*., 2004; Shonhai *et al*., 2005; 2008; Ramya *et al*., 2006; Cockburn *et al*., 2011).

PfHsp70-1 is thought to provide cytoprotection to the malaria parasite during stressful events associated with its development in the human host. The cytoprotective role of PfHsp70-1 was previously demonstrated by its ability to complement the DnaK function in *E. coli dnak756* cells whose DnaK was functionally compromised (Shonhai *et al*., 2005). The introduction of PfHsp70-1 conferred thermotolerance to these cells when they were grown at a non-permissive temperature of 43.5 °C (Shonhai *et al*., 2005). Moreover, the introduction of PfHsp70-1 into *E. coli* cells enhanced the heterologous production and quality of recombinant malarial proteins (GTP cyclohydrase 1 and PfAdoMetDC; Stephens *et al*., 2011; Makhoba *et al*., 2016). In addition, the enhanced production of malarial proteins in *E. coli* in the presence of PfHsp70-1 as described above validated that Hsp70 is species-specific in function.

PfHsp70-1 is emerging as a potential drug target (Shonhai, 2010). Recent studies have shown that a lipoprotein, polymyxin B (PMB), binds Hsp70 and inhibits its chaperone activity (Zininga *et al*., 2017a). This was performed based on studies that suggested that cyclic lipopeptides (colistin and PMB) bind and inhibit the chaperone function of Hsp90 (Minagawa *et al*., 2012). PMB inhibited the chaperone activity of two cytosolic Hsp70s in *P. falciparum* (PfHsp70-1 and PfHsp70-z). In addition, PMB abolished the association of PfHsp70-1 with partner proteins PfHop and PfHsp70-z (Zininga *et al*., 2017a). This shows that PMB binds Hsp70 modulating its function. However, PMB only weakly inhibited parasite growth *in vitro*. This is because PMB is largely membrane-bound and does not access the parasite cytosol.

In another study, (-)-Epigallocatechin-3-gallate (EGCG) was shown to bind directly to PfHsp70-1 and PfHsp70-z perturbing the secondary and tertiary structure of the proteins (Zininga *et al*.,

2017b). The ATPase and chaperone functions of both proteins were inhibited by EGCG. Furthermore, like PMB, EGCG also abolished the association of PfHsp70-1 with a partner protein, PfHop (Zininga *et al*., 2017b). Using *P. falciparum* 3D7 parasites maintained in culture, Zininga and colleagues (2017b) demonstrated that EGCG inhibited 50 % of parasite growth at 2.9 µM exhibiting its anti-plasmodial activity. Furthermore, certain plant compounds with antiplasmodial activity were observed to inhibit the ATPase and chaperone activities of the two *P. falciparum* Hsp70s (PfHsp70-1 and PfHsp70-z, Zininga *et al*., 2017c). The plant extracts were obtained from *Pterocarpus angolensis* and *Ziziphus mucronata.* Findings from these studies suggest therapeutic potential involving targeting Hsp70 function. However, there is a need for further studies to assess the effects of these molecules on the Hsps of human origin.

Evidence from recent studies demonstrates that some Hsps are secreted to the extracellular environment as part of the stress response mechanism. These Hsps have been implicated in host immune modulation (Zininga *et al*., 2018). Hsp90, Hsp70, Hsp60, Hsp40 and sHsp families of chaperones are reported to play a role in immunomodulation (reviewed by Zininga *et al*., 2018). PfHsp70-1 possesses a GGMP motif which is thought to be immunogenic (Matambo *et al*., 2004). PfHsp70-1 and PfHsp70-x are thought to play a role in immunomodulation. Antibodies against the two Hsp70s have been reportedly found in sera from patients in areas where malaria is endemic (Cabral *et al*., 2017). In contrast, other findings suggest that PfHsp70-1 lacks immunomodulatory activity (Pooe *et al*., 2017). The above study was based on monitoring the induction of inflammatory cytokines, interleukin 6 (IL-6) and interleukin 8 (IL-8) in immune cells exposed to PfHsp70-1. It is possible other pro-inflammatory cytokines, such as IL-1, IL-12, interferon gamma (IF-gamma) were induced. On the other hand, failure to induce IL-6 and IL-8 could also be due to a poorly post-translationally modified recombinant protein (Tokmakov *et al*., 2012).

1.7.2 The GGMP repeat motif

The motif consists of tandem repeats of glycine-glycine-methionine-proline residues (tetrapeptide) (Figure 1.8). This motif characterizes cytosolic Hsp70s (Shonhai, 2014), including their constitutive isoforms (Hsc70s) (MacFarlane *et al*., 1990, Wu *et al*., 2007; Cui *et al*., 2010). Initially thought to be a characteristic of Hsp70s of parasitic origin, the GGMP repeats have been identified in other protein families as well as homologs from non-parasitic organisms (Table 1.3). The only difference is that parasite Hsp70s seem to have more copies of the GGMP repeats compared to other organisms.

Table 1. 3: The occurrence of the GGMP repeats in various Hsp families

Protein	Organism	No. of GGMP repeats
Hsc70	*Homo sapiens*	2
	Mus musculus	2
	Rattus novergicus	2
Hsp70	*P. falciparum*	5
	P. bergei	9
	P. vivax	9
	Leishmania donovani	2
	Trypanosoma cruzi	4
	Toxoplasma gondii	6
Hsp60	*Saccharomyces cerevisae*	2
Other		
Hip	*Aradiposis thaliana*	10
58 kDa phosphoprotein	*Plasmodium bergei*	9

Probably the enhanced representation in parasite Hsp70 suggest an essential role for them and may contribute towards their virulence (Lyons and Johnson, 1998). There is a paucity of data on the function of the Hsp70 GGMP motif. The location of these highly conserved residues in a less conserved C-terminal region may possibly provide functional versatility to C-terminus of Hsp70. Wu and co-workers (2008) suggest that the GGMP repeats in combination with the EEVD motif and the α-helical subdomain form a structural entity regulating cofactor binding. Gly-met rich

regions tend to be hydrophobic (Tang *et al*., 2006; Gao *et al*., 2015) which may facilitate Hsp70 interaction with substrates. Thus, the GGMP may regulate the chaperone activity of Hsp70.

Miller and colleagues (1999) provided insight that the deletion of one of the GGMP repeats in Hsp70s of virulent and avirulent strains of *T. gondii* affected the synthesis and stability of the molecular chaperone. However, deletion of the GGMP region from Hip (a co-chaperone of Hsp70) did not affect its binding to Hsp70 (Prapapanich *et al*., 1996). Taken together, this suggests that the GGMP motif may be functionally redundant. In light of this, it is important that the function of this motif be elucidated.

1.8 Rationale of the study

1.8.1 Problem statement

Malaria remains a deadly disease accounting for at least 435 000 deaths and most of its victims are young children (under 5 years old) and pregnant women. At least 90% of malaria cases occur in Africa and in South Africa malaria remains a concern in parts of Limpopo, Mpumalanga and KwaZulu Natal provinces (Dahan-Moss *et al*., 2018). *Plasmodium falciparum* is the main causative agent of malaria. Malaria remains a global health burden and this can be attributed to parasite drug resistance among other factors (Carey *et al*., 2017; Haldar *et al*., 2018). Hsps have been implicated in drug resistance and some have been proposed as drug targets (Shonhai *et al*., 2010, Zininga and Shonhai, 2014). PfHsp70-1 plays a major role in the development and pathogenicity of *P. falciparum* (Shonhai 2014). PfHsp70-1 is expressed at all blood stages of the parasite's life cycle (Shonhai, 2014). Increased expression of PfHsp70-1 was observed after heat shock (Zininga *et al*., 2015b) signifying that the protein is important in protecting the parasite against stressful conditions. PfHsp70-1 also occurs in functional multi-protein complexes with other parasitic chaperones and co-chaperones (Banumathy *et al*., 2003) suggesting that it cooperates with functional network partners.

Chapter 1

Literature Review

PfHsp70-1 has been the most studied Hsp70 out of the six Hsp70 isoforms that are encoded by the *P. falciparum* genome (Shonhai, 2014) and is also the only one that possesses GGMP tetrapeptide repeats in the C-terminal domain. Initially, GGMP motifs were thought to be immunogenic (Matambo *et al*., 2004). However, it was recently shown that PfHsp70-1 lacks immunomodulatory activity (Pooe *et al*., 2017). To date, the function of the GGMP motif of PfHsp70-1 has not been ascertained. The GGMP motif is about seven residues upstream of the terminal EEVD residues responsible for the interaction of PfHsp70-1 with its functional regulators such as Hsp40 (Pesce *et al*., 2008; Botha *et al*., 2011; Njunge *et al*., 2015) and Hop (Gitau *et al*., 2012; Zininga *et al*., 2015b). PfHop allows PfHsp70-1 and its chaperone partner, PfHsp90 to form a functional partnership. Given the proximity of the GGMP repeats to the C-terminus of PfHsp70-1, it is possible that these repeats may regulate the direct protein-protein interaction of PfHop to PfHsp70-1. Hence, the current study sought to elucidate the role of the GGMP motif of PfHsp70-1 on its interaction with PfHop. Furthermore, since the GGMP motif is located in the peptide binding domain of PfHsp70-1, it was important to investigate the role of this motif on the chaperone function of PfHsp70-1. The study further explored how the introduction of the PfHsp70-1 GGMP repeats into DnaK would affect the function of the latter.

PfHop plays an important role in the life cycle of *P. falciparum* through facilitating the Hsp70-Hsp90 function. The Hsp70/Hsp90 Hop mediated- interaction has been proposed as a potential drug target. Disruption of the PfHsp70-PfHop-PfHsp90 pathway may possibly result in parasite death. This study sought to further characterize PfHop by using *in vitro* biophysical and biochemical methods to explore structural and functional features of PfHop that endear its interaction with PfHsp70-1.

1.8.2 Hypothesis

Hence, this study hypothesized that the GGMP repeat motif is important for the interaction between PfHsp70-1 and PfHop as well as the chaperone activity of PfHsp70-1.

1.8.3 Main Objective

To characterize the role of the GGMP motif of PfHsp70-1 on function and its effect on the interaction of the chaperone with its co-chaperone, PfHop.

1.8.4 Specific Objectives

1.8.4.1 Design of PfHsp70-1 GGMP variants and prediction of the possible interactors of PfHsp70-1

Approach:

Computational tools were used to predict the association of PfHsp70-1 with functional partners.

(a) Prediction of protein interactors of PfHsp70-1 using STRING (string-db.org);

(b) Comparison of the homology models of the SBDs of PfHsp70-1 and its GGMP variants using Phyre2 (www.sbg.bio.ic.ac.uk/phyre2).

1.8.4.2 Expression and purification of recombinant PfHop, PfHsp70-1, DnaK, and the GGMP variants

Approach:

The recombinant proteins were expressed in *E. coli* and purified in a three-step process: nickel affinity chromatography, ion exchange chromatography (IEC) and gel filtration chromatography (GF) also known as size exclusion chromatography (SEC).

1.8.4.3 Biophysical characterization of PfHsp70-1 and GGMP variant proteins

Approach:

Biophysical analyses of the recombinant proteins were conducted using circular dichroism (CD) spectroscopy and tryptophan fluorescence related assays.

1.8.4.4 Investigation of the role of the GGMP motif of PfHsp70-1 on its chaperone function

Approaches:

(a) The chaperone function of recombinant PfHsp70-1 and its GGMP variants was investigated by analyzing the ability of the proteins to suppress heat-induced aggregation of malate dehydrogenase (MDH) from *porcine* heart (Sigma-Aldrich, USA). The aggregation suppression assay was conducted as previously described (Shonhai *et al*., 2008; Makumire *et al*., 2014; Zininga *et al*., 2016);

(b) ATPase activity assays: The ATPase activity assay was carried out following a previously described approach (Zininga *et al*., 2017b) with slight modifications to include substrate peptides as activators. The amount of phosphate released was quantitated using a colorimetric assay thus determining the ATPase activity and

(c) *In cellula* complementation: The KPf chimeric forms were assessed for their abilities to complement the Hsp70 function using an *E. coli* strain with a deleted *DnaK* gene (Shonhai *et al*., 2005).

1.8.4.5 Investigation of the structure-function features of PfHop

Approaches:

(a) Biophysical characterization was carried out to determine the secondary and tertiary structure of PfHop;

(b) Size exclusion chromatography was carried out to ascertain the dimerization status of PfHop;

(c) Tryptophan fluorescence assay was used to elucidate the structure-function features of PfHop bound to ATP (Zininga *et al*., 2016). The binding kinetics of ATP to PfHop was determined using SPR;

(d) Limited proteolysis was carried out on PfHop to probe conformational changes of the protein in the presence of ATP and ADP (Yamamoto *et al*., 2014) and

(e) ATPase activity assay was also performed to determine the ability of PfHop to hydrolyze ATP (Zininga *et al*., 2016).

1.8.4.6 Investigation of the role of the GGMP motif of PfHsp70-1 on its interaction with PfHop

Approach:

Interaction of the PfHsp70-1 GGMP variants with full-length PfHop was analyzed using enzyme-linked immunosorbent assay (ELISA; Mabate *et al*., 2018) and slot blot as previously described (Zininga *et al*., 2016).

Chapter 2

In silico studies of the GGMP motif of *P. falciparum* Hsp70-1

2.1 Introduction

Protein-protein interaction networks can reveal unknown pathways or complexes a protein is involved in. Numerous databases and online resources dedicated to protein networks are available. These serve as reservoirs for the storage and retrieval, as well as for analysis, visualization, and integration of crucial proteomics data. For example, the STRING database (http://string-db.org/; Szklarczyk *et al*., 2017) collects and integrates information of all functional interactions for different organisms including *P. falciparum*. This is done by combining known and predicted protein-protein associations. Ideally, predictive protein networks act as filters before further studies can be performed because these predictive methods are prone to giving false positives. Some *P. falciparum* proteins predicted to potentially interact with *P. falciparum* Hsp70s were identified using yeast two-hybrid analysis (LaCount *et al*., 2005), validating the predictions. However, a more interactive network for PfHsp70-1 is yet to be elucidated. Predicting the PfHsp70-1 interactions would help unravel the myriad of pathways PfHsp70-1 is involved in given its ubiquitous distribution. Discerning novel interactors of PfHsp70-1 could facilitate drug design (Guney *et al*., 2016). In this case, it is important to predict PfHsp70-1 associates whose interaction with the chaperone may be regulated by its GGMP motif. This study sought to use bioinformatics tools to predict structural differences caused by mutations introduced in the GGMP motif region of PfHsp70-1. The current study also introduced the GGMP repeats of PfHsp70-1 into a non-GGMP containing Hsp70 (*E. coli* DnaK). Structural differences were also predicted for DnaK and its variant. Furthermore, the study elucidated the protein-protein interaction network of PfHsp70-1 using computational predictive tools.

The objectives of this study were to:

i. conduct *in silico* designs of the GGMP variants of PfHsp70-1 and DnaK (a GGMP motif was inserted in DnaK);

ii. generate and compare three-dimensional models of the SBD for PfHsp70-1, DnaK and their GGMP variants; and

iii. predict and construct the protein interactome of PfHsp70-1.

2.2 Experimental procedures

2.2.1 Construction of GGMP variants

To construct PfHsp70-1 GGMP repeat variants, conservative amino acid substitutions were introduced. Residue substitutions (glycine/proline to alanine; methionine to leucine and asparagine to aspartic acid) were carried out based on the similarities in the biochemical properties of the amino acids as outlined in Betts, 2003 (Table 2.1).

Table 2. 1: Properties of residues used for conservative substitutions

Original	Substitute
Glycine (Gly/G) **MW: 75** 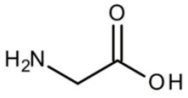 pI: 5.9 Side chain: non-polar and neutral Hydrophobic (score: -0.4)	**Alanine (Ala/A)** MW: 89 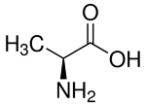 pI: 6 Side chain: non-polar and neutral Hydrophobic (score: 1.8)
Proline (Pro/P) **MW: 115** 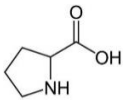 pI: 6.3 Side chain: non-polar and neutral Hydrophilic (score: -1.6)	**Alanine (Ala/A)** MW: 89 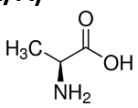 pI: 6 Side chain: non-polar and neutral Hydrophobic (score: 1.8)
Methionine (Met/M) **MW: 149** 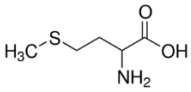 pI: 5.74 Side chain: non-polar and neutral Hydrophobic (Score: 1.9)	**Leucine (Leu/L)** MW: 131 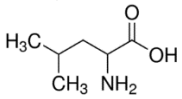 pI: 5.98 Side chain: non-polar and neutral Hydrophobic (Score: 3.8)
Aparagine (Asn/N) **MW: 132** 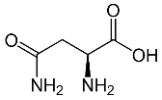 pI: 5.41 Side chain: Polar and neutral Hydrophilic (Score: -3.5)	**Aspartic acid (Asp/D)** MW: 133 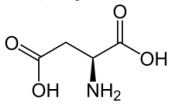 pI: 2.77 Side chain: Polar and negative Hydrophilic (Score: -3.5)

The focus of the mutations was the conserved GGMP repeats (Figure 2.1). The variants were generated by positional targeting of the GGMP repeats. Two variants were constructed

conservatively by substituting the first two N-terminal GGMP repeats (residues 632-639; Figure 2.1A) and last two C-terminal GGMP repeats (residues 648-657; Figure 2.1B). The variants were named PfHsp70-G632 and PfHsp70-G648, respectively. A third mutant named DnaK-G was constructed for *E. coli* DnaK. Using pairwise sequence alignment, aligned residues were substituted with the GGMP repeats of PfHsp70-1, between residues 611-615 of *E. coli* DnaK (Figure 2.1C). The variants were aligned using ClustalW to show the changed residues (Figure 2.1D).

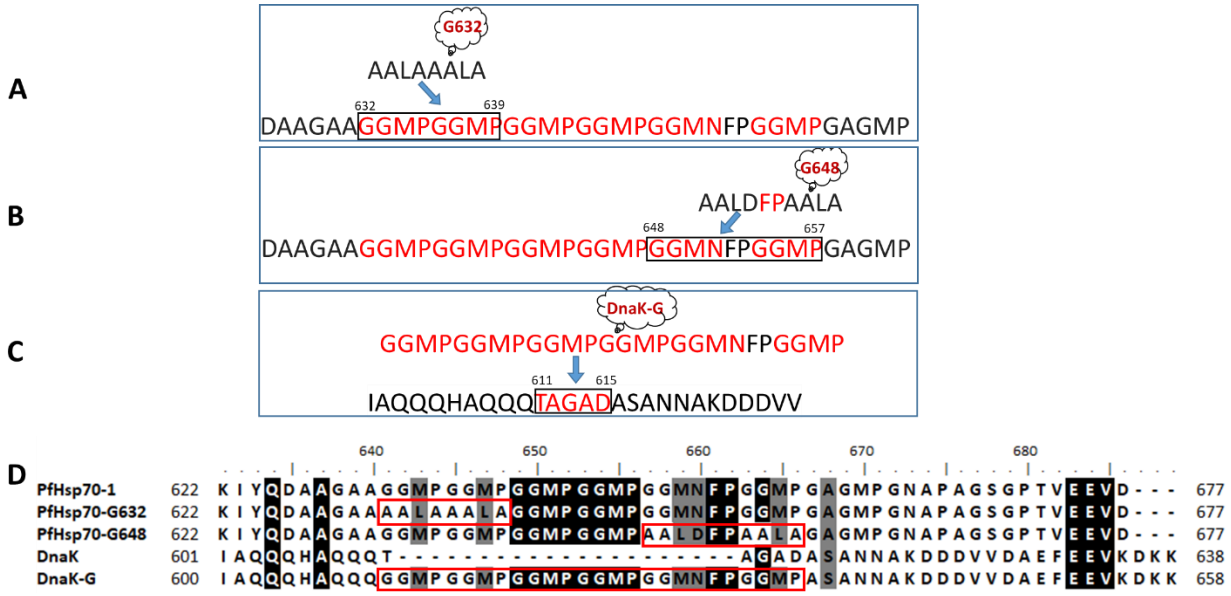

Figure 2. 1. Design of the mutant PfHsp70-1 constructs
Mutations in the GGMP motif region to generate PfHsp70-G632 (**A**), PfHsp70-G648 (**B**) and DnaK-G (**C**) constructs. (**D**) Multiple sequence alignment of the variants showing the mutations. Identical residues are highlighted in black, similar residues in grey. The red boxes highlight mutated residues.

2.2.2 Analysis of the disorder and hydrophobicity of the Hsp70 C-terminal region

The GGMP repeats are in the C-terminal lid region of the protein that is known to be unstructured or disordered (Clerico *et al*., 2015). To ascertain the effects of the mutations on the PfHsp70-1 lid and DnaK lid segment, order-disorder structure predictions were carried out using Predictors of Natural Disordered Regions (PONDR; www.pondr.com; Ruskamo *et al*., 2012). PONDR uses neural networks that consider amino acid composition, hydropathy and net charge to make

predictions. This gives graphical and textual outputs showing disorder along the protein sequence and a charge/hydropathy plot indicating whether a protein is disordered (Dunker et al., 2001). Hydropathy is a measure of the hydrophobic/hydrophilic properties of amino acids. Net charge is the sum of all the charged groups associated with a protein (Gitlin *et al*., 2006). The Hydropathy profiles were conducted using Kyte and Dolittle programme (Kyte and Dolittle, 1982 [http://web.expasy.org/protscale/]). This measures the degree of hydrophobicity or hydrohilicity of a protein based on the amino acid content (Kyte and Dolittle, 1982).

2.2.3 Homology modeling of the SBD of PfHsp70-1, DnaK, and their GGMP mutants

Protein 3D modeling and superpose were utilized to compare structural differences between the proteins. The SBD sequences for PfHsp70-1, DnaK, and their variants were submitted to the Phyre2 server (http://www.sbg.bio.ic.ac.uk/phyre2/; Kelley *et al*., 2015) and were each used to conduct BLAST searches to identify the templates with the highest score of identity/similarity and sequence coverage for homology modeling. These templates are of known crystal structures already present in the protein data bank (PDB, https://www.rcsb.org/). Phyre2 then creates a complete model of the sequence via a combination of multiple template modeling and simplified *ab initio* folding simulation (Kelley *et al*., 2015). A total of 20 templates were initially used to construct a model for the respective proteins. From the 20, a final two best matching templates were used for the final PfHsp70-1 model and three best matching templates were used for the final respective PfHsp70-1 variant models, DnaK and DnaK-G respectively (Appendix B1). To visualize the final output model, Chimera version 1.9 (Pettersen *et al*., 2004) was used. The quality of the final models was validated using Qmean (https://swissmodel.expasy.org/qmean/). To assess any structural differences on the PfHsp70-1 and DnaK C-terminal region due to the GGMP mutations, the SBDs were superposed using SuperPose (http://wishart.biology.ualberta.ca/Superpose/; Maiti *et al*., 2004). SuperPose is capable of superposing two or more structures generating root mean square deviation (RMSD) statistics, and superimposed PDB coordinates together with interactive images of the superimposed

structures. The generated superimposed PDB coordinates were visualized and manipulated using Chimera (http://www.cgl.ucsf.edu/chimera; Pettersen *et al*., 2004).

2.2.4 Construction of the interactome for PfHsp70-1

To construct the interactome for PfHsp70-1, data was downloaded from the STRING 10.5 database (http://string-db.org/, Szklarczyk *et al.,* 2017). The STRING database collects and integrates data from seven evidence channels that include experiments, gene neighborhood, co-expression, databases, text mining, fusion and co-occurrence channels (Jensen *et al*., 2009; Szklarczyk *et al.,* 2017). A total of 100 interacting partners were selected based on the confidence score of 0.7 and these were further screened based on subcellular localization. Confidence scores are estimates of the likelihood that a certain interaction is biologically meaningful, specific and reproducible, based on the supporting evidence (Szklarczyk *et al.,* 2017). The STRING software does not screen for subcellular localization of predicted proteins and hence this was conducted manually to filter only proteins which occur in the same cell compartment as PfHsp70-1. PfHsp70-1 localizes in the cytosol and nucleus and hence only proteins occurring in these two localities were considered. The screened proteins were then grouped according to families or possession of a specific functional domain. Based on data from PlasmoDB (http://plasmodb.org/plasmo/), the interactors were further classified according to predicted or validated biological function.

2.3 Results

2.3.1 Disorder and hydropathy prediction for PfHsp70-1, DnaK, and their variants

Based on a charge/hydropathy plot, PfHsp70-1 is a largely ordered protein (Figure 2.2A). PONDR predicted that PfHsp70-1_{SBD} possesses three disordered regions (Figure 2.2A). Disordered regions have a PONDR score greater than 0.5. One of the regions (residues 623-676), predicted as the longest disordered region contains the stretch of GGMP repeats. The two variants (PfHsp70-G632 and PfHsp70-G648) were observed to possess order-disorder profiles close to that of PfHsp70-1 with minor differences observed in the region of the mutations (Figure 2.2B and C; blue circles). This suggests that mutating the GGMP repeats marginally altered the disorder profile for PfHsp70-1 despite the conservative substitutions. Disordered regions tend to facilitate transient and highly specific interactions (Hsu *et al*., 2012; Dyson and Wright, 2015). Insertion of the GGMP repeats into DnaK also altered its disorder profile based on similar prediction (Figure 2.2D and E). The DnaK-G variant seemed to possess more disorder than DnaK in the C-terminal region. Due to variations in the disorder profiles between the wild type proteins and their GGMP variants, the variants might function poorly.

The hydropathy profiles for PfHsp70-1 and its GGMP variants exhibited variation in the region of the GGMP repeats (Figure 2.2A1, B1 and C1; red rectangle). This region is less hydrophobic in PfHsp70-1 as compared to the variants. This suggests that the substituted residues increased the hydrophobicity in the GGMP repeat region since these residues have higher hydrophobic scores (Table 2.1). In the case of DnaK and DnaK-G, the hydrophobicity profiles possessed more negative peaks, suggesting that DnaK is more hydrophobic than DnaK-G (Figure 2.2D1 and E1, red rectangle). Hydrophobic residues tend to be buried in proteins. Increased hydrophobicity in the GGMP region of the PfHsp70-1 variants might cause this region to be buried within the protein. This may result in the terminal EEVD motif being hidden and will likely affect interaction with Hop.

Chapter 2

In silico studies of the GGMP motif of *P. falciparum* Hsp70-1

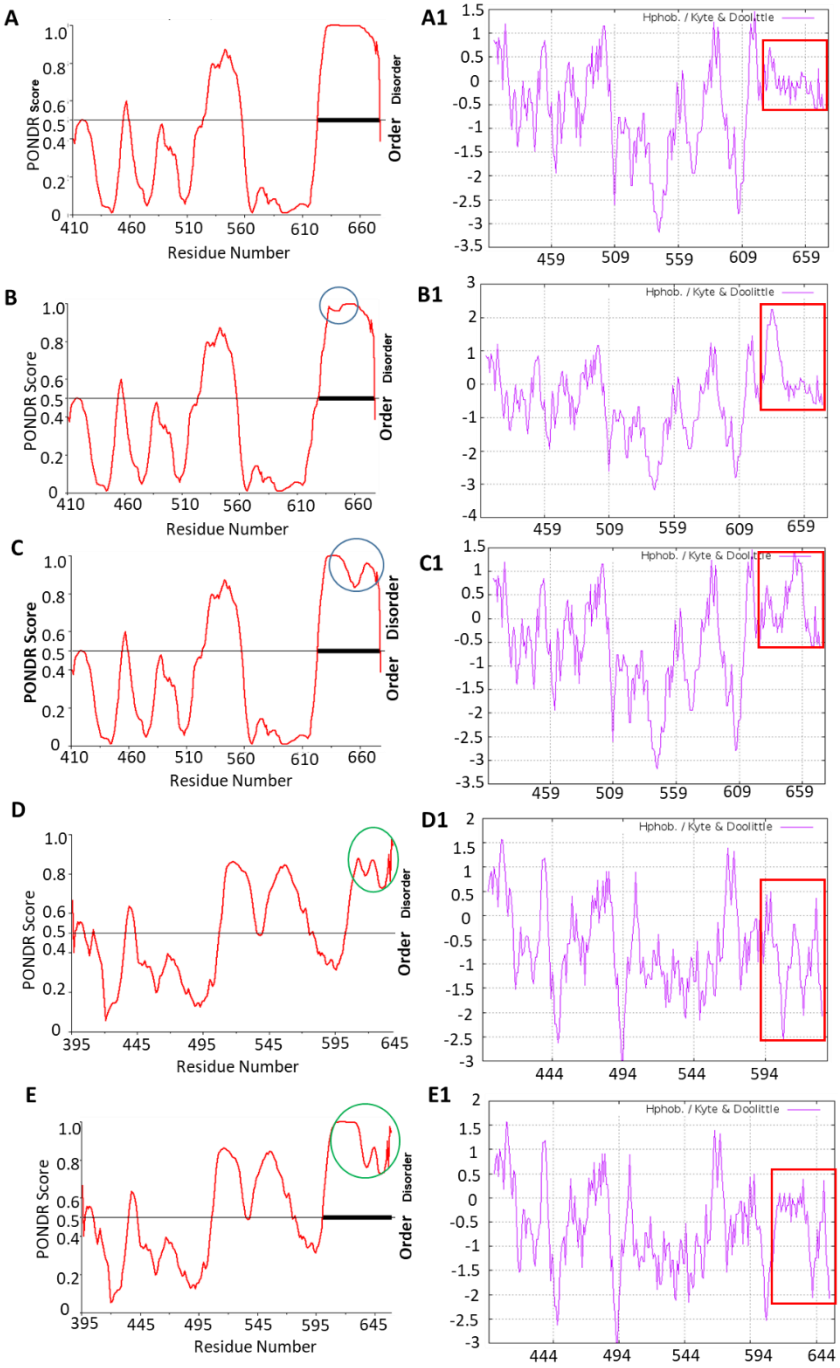

Figure 2. 2. The prediction of order and hydrophobicity in PfHsp70-1 and DnaK versus their variants
PONDR predicts the presence of two major disordered segments in the C-terminal region (black bars) of the PfHsp70-1 (**A);** PfHsp70-G632 (**B**); PfHsp70-G648 (**C**); DnaK (**D**) and DnaK-G (**E**). Differences in the disorder profiles in the C-terminal region of PfHsp70-1 and its GGMP variants are highlighted by blue circles and as green circles for DnaK and DnaK-G. The Kyte and Doolittle hydrophobicity profile analysis of PfHsp70-1 indicates that GGMP region is highly hydrophobic in the variants (**A1**, **B1,** and **C1**; red rectangle). The DnaK-G variant is more hydrophobic in this region compared to DnaK (**D1** and **E1**).

2.3.2 Homology models of PfHsp70-1 and its mutants show minimal structural variations

In silico structural superposition was carried out using PfHsp70-1_{SBD} on the two variants to ascertain the effects of the generated mutations. A similar approach was also carried out for DnaK. The homology models of PfHsp70-1_{SBD}, $DnaK_{SBD}$ and the variants were successfully constructed. The crystal structures of the templates are provided (Table B1; Appendix B). The modeled structures had reasonable QMEAN4 Z-scores of -1.54, -3.20, -1.65, -0.99 and -1.20 for PfHsp70-1, PfHsp70-G632, PfHsp70-G648, DnaK, and DnaK-G respectively (Appendix B2). These values are well within the range (|Z-score|-4 to 0) suggesting the models were of good quality (Benkert *et al*., 2011).

The Superpose server (Maiti *et al*., 2004) was used to assess structural differences due to the mutations on the GGMP motif. This generated RMSD values (Figure 2.3) that were used as a measure of similarity between PfHsp70-1_{SBD}, DnaK and the respective GGMP variant SBDs. Superposing of PfHsp70-1_{SBD} on PfHsp70-$G632_{SBD}$ and PfHsp70-$G648_{SBD}$ generated low RMSD values of 1.52 Å and 2.15 Å respectively (Figure 2.3A and B). Lower RMSD (a value close to zero) implies that the protein structures could be generally identical. Conversely, increases in RMSD imply structural variation (Kufareva and Abagyan, 2012). However, GGMP mutation in PfHsp70-G648 resulted in a short helix region (Figure 2.3B; purple) in place of a coiled region in PfHsp70-1 (Figure 2.3B, yellow rectangle). This would explain the slightly high RMSD value compared to a lower RMSD for PfHsp70-G632. On the other hand, a low RMSD value (1.27 Å) was observed for DnaK and DnaK-G (Figure 2.3C). It was interesting to note that DnaK-G possessed secondary structural changes (Figure 2.3C) as a result of the introduction of the GGMP repeats. These changes are discussed in detail in section 2.3.4. Overall, the low RMSD values suggest that there were no substantial predicted structural variations between the wild type proteins and the GGMP variants. Hence, it remained to be experimentally validated if these structural changes would impact on the chaperone function of the proteins.

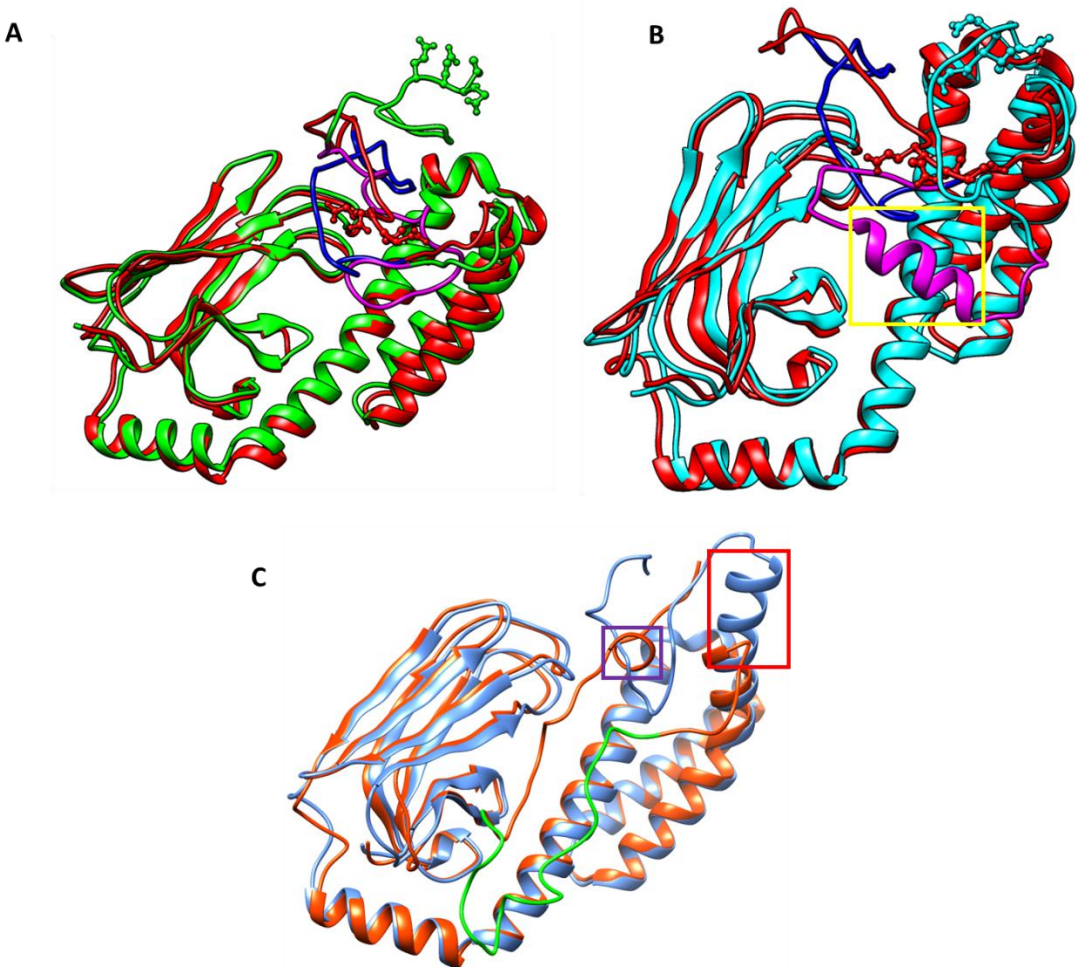

Figure 2. 3. Mutations in the GGMP repeats marginally affected the substrate binding domain of PfHsp70-1 and DnaK

Ribbon images showing the superposed SBDs from PfHsp70-1 (red), PfHsp70-G632 (green, **A**) and PfHsp70-G648 (cyan, **B**) structures. The GGMP motif region is colored blue in PfHsp70-1 and magenta in the mutants. The EEVD motif is represented as ball and stick. (**C**) The superposed SBDs from DnaK (blue) and DnaK-G (brown). Images were rendered on Chimera 1.11. Regions of secondary structural differences between (**B**) PfHsp70-1 and PfHsp70-G648 are indicated by the yellow box; (**C**) between DnaK and DnaK-G by the purple and red boxes.

2.3.3 Structural orientation of the SBD substrate binding cleft and EEVD residues

The GGMP motif region is closer to the SBD and EEVD motif. Given the proximity, it was necessary to ascertain how the substrate binding cleft/arch and EEVD residues are orientated in the variant proteins. The arch and hydrophobic pocket of PfHsp70-1 is made up of residues A419, Y444 and V451 (Shonhai *et al*., 2007). These residues have physical contact with the substrate.

The superposition revealed no significant changes in the structural orientations in the arc residues of PfHsp70-1 as compared to the variants (Figure 2.4). Residues A419 and V451 seem to retain the same orientation in PfHsp70-G632 as in PfHsp70-1 (Figure 2.4A). Similar observations were made for the PfHsp70-G648 variant (Figure 2.4B). In the PfHsp70-1/PfHsp70-G632 superposition, the Y444 residue was observed to lean towards the hydrophobic pocket (Figure 2.4A). In the variant PfHsp70-G648, the Y444 residue seems to retain the same orientation as PfHsp70-1. These predictions suggest there are minor structural orientations in the substrate binding cleft that are due to the GGMP mutations. In DnaK and the DnaK-G variant, no structural changes were observed as well (Figure 2.4C).

The positioning of the EEVD residues in the variants was also elucidated (Figure 2.4). The superposed models of PfHsp70-1 and its GGMP variants show that the EEVD residues are well oriented, in an exposed position. This was observed in PfHsp70-1 and the variants (Figure 2.4; panels A1 and B1). The only visible differences are in the fold of the loop region that contains the GGMP repeats. This loop region is responsible for holding the EEVD motif in an exposed position. The EEVD motif of Hsp70 is responsible for binding the TPR1 and TPR2A domains of Hop. It is possible, as predicted here, that these residues may be hidden due to the GGMP mutations. This might lessen the accessibility of the EEVD residues by PfHop. In all the variants, the EEVD motif is observed to be in an exposed position. On the other hand, there were interesting structural changes in the DnaK-G variant (Figure 2.4C1). DnaK-G possessed a shorter SBDα helix E compared to DnaK (Figure 2.4C1; red rectangle). The loop region preceding the EEVKDKK residues is longer due to the insertion of GGMP repeats. A short helix was also observed a few residues from the C-terminal end (Figure 2.4C1; purple rectangle). These structural changes were due to the GGMP repeats introduced into DnaK. These changes might impact on the function of the lid of DnaK.

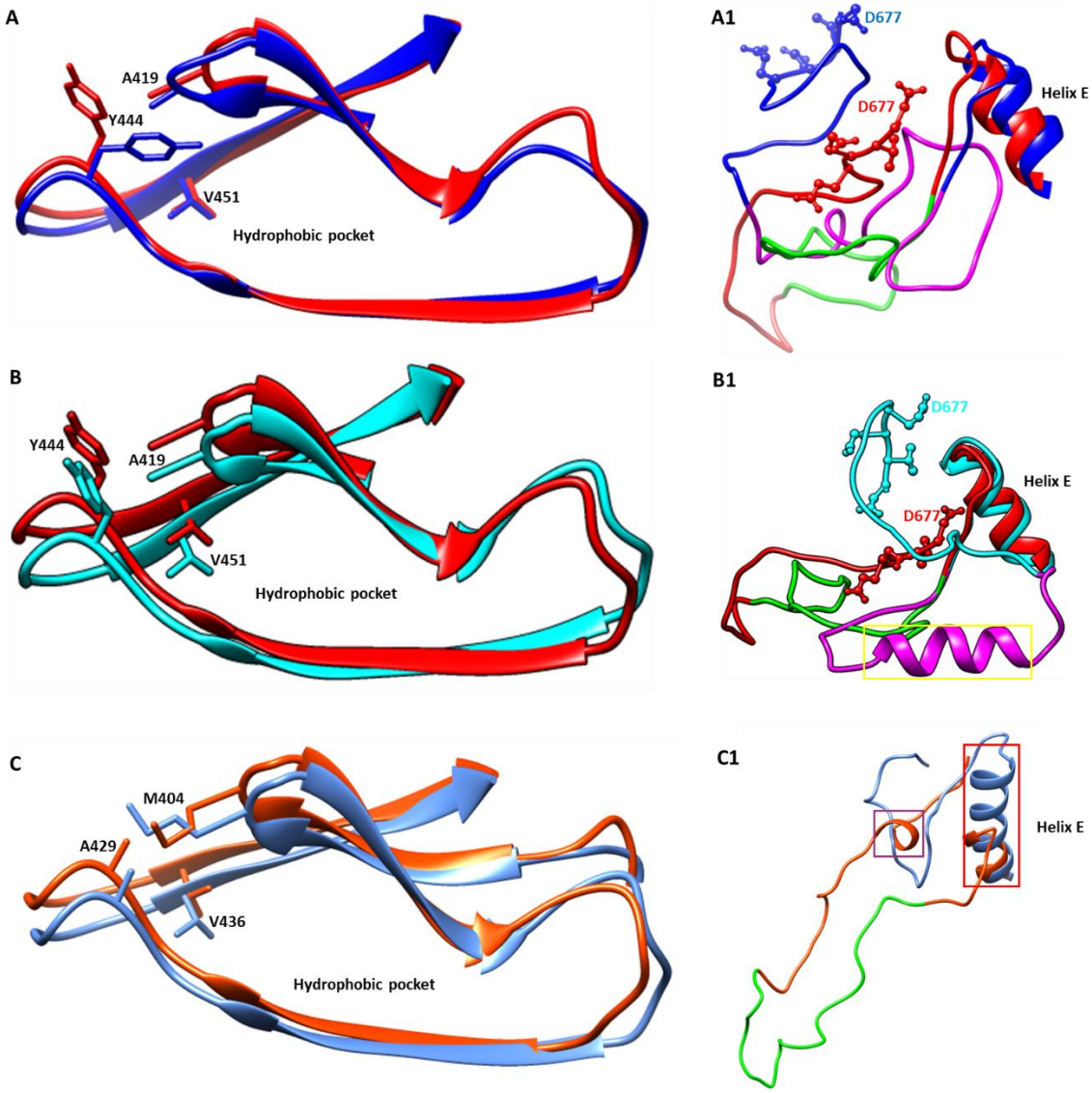

Figure 2. 4. Protein structure superposition

PfHsp70-1 (Red), PfHsp70-G632 (Blue), PfHsp70-G648 (Cyan), DnaK (turquoise) and DnaK-G (brown). The substrate binding cleft of PfHsp70-1 compared to (**A**) PfHsp70-G632 and (**C**) PfHsp70-G648. The substrate binding cleft of DnaK was superposed with that of DnaK-G (**E**). Arch residues represented as sticks. The C-terminal tail of PfHsp70-1 superposed to (**B**) PfHsp70-G632 and (**D**) PfHsp70-G648. The EEVD residues are represented as ball and stick. The GGMP motif region is represented as green in PfHsp70-1 and magenta in the variants. The C-terminal tail of DnaK was also superposed to DnaK-G (**F**). The structures were visualized using Chimera. The boxes indicate the regions in the C-terminal tail where secondary structural differences were observed for the following proteins: PfHsp70-1 versus PfHsp70-G648 (yellow box); DnaK versus DnaK-G (red and purple).

2.3.4 Predicted interaction partners of PfHsp70-1

PfHsp70-1 is a ubiquitous molecule that plays key roles in parasite survival and pathogenesis. It is important to map out the proteins that interact directly with PfHsp70-1 to understand its function. The interactome (Appendix B3 and Appendix B; Table B.1) was centered on PfHsp70-1 (PF3D7_0818900) as identified from STRING (www.string-db.org). It is not surprising that the predicted interactome showed that PfHsp70-1 interacts with a large pool of proteins involved in a wide range of cellular roles (biological processes) given its ubiquitous nature (Figure 2.5). These roles include transcription; translation; protein metabolism; locomotion; DNA metabolism; response to drugs; response to stress; degradation among functions listed as 'other which include membrane organization, cell redox homeostasis, protein targeting and entry into the host cell. It is possible that PfHsp70-1 may be involved in most of these processes.

This analysis revealed the interactors from all major chaperone families [(Hsp40, Hsp60 (chaperonins) and Hsp70; Table B.1)] as previously identified (LaCount *et al*.,2005; Pavithra *et al*., 2007). Also identified were the TPR containing proteins e.g by PfHop and cyclophilin domain containing co-chaperones. Overall, the identification of PfHsp70-z (PF3D7_0708800, Zininga *et al*., 2016), PfHop (PF3D7_1434300; Zininga *et al*., 2015b) and Hsp40s (PF3D7_1211400, Pesce *et al*., 2008; PF3D7_1437900, Botha *et al*., 2011; PF3D7_0213100, Njunge *et al*., 2015) served to validate the predictions. This PfHsp70-1 interactome closely compares with other Hsp70 interactomes (human; Taipale *et al*., 2014 and DnaK; Calloni *et al*., 2012) that have been predicted to interact with a wide variety of chaperones and co-chaperones as well as client proteins.

Chapter 2

In silico studies of the GGMP motif of *P. falciparum* Hsp70-1

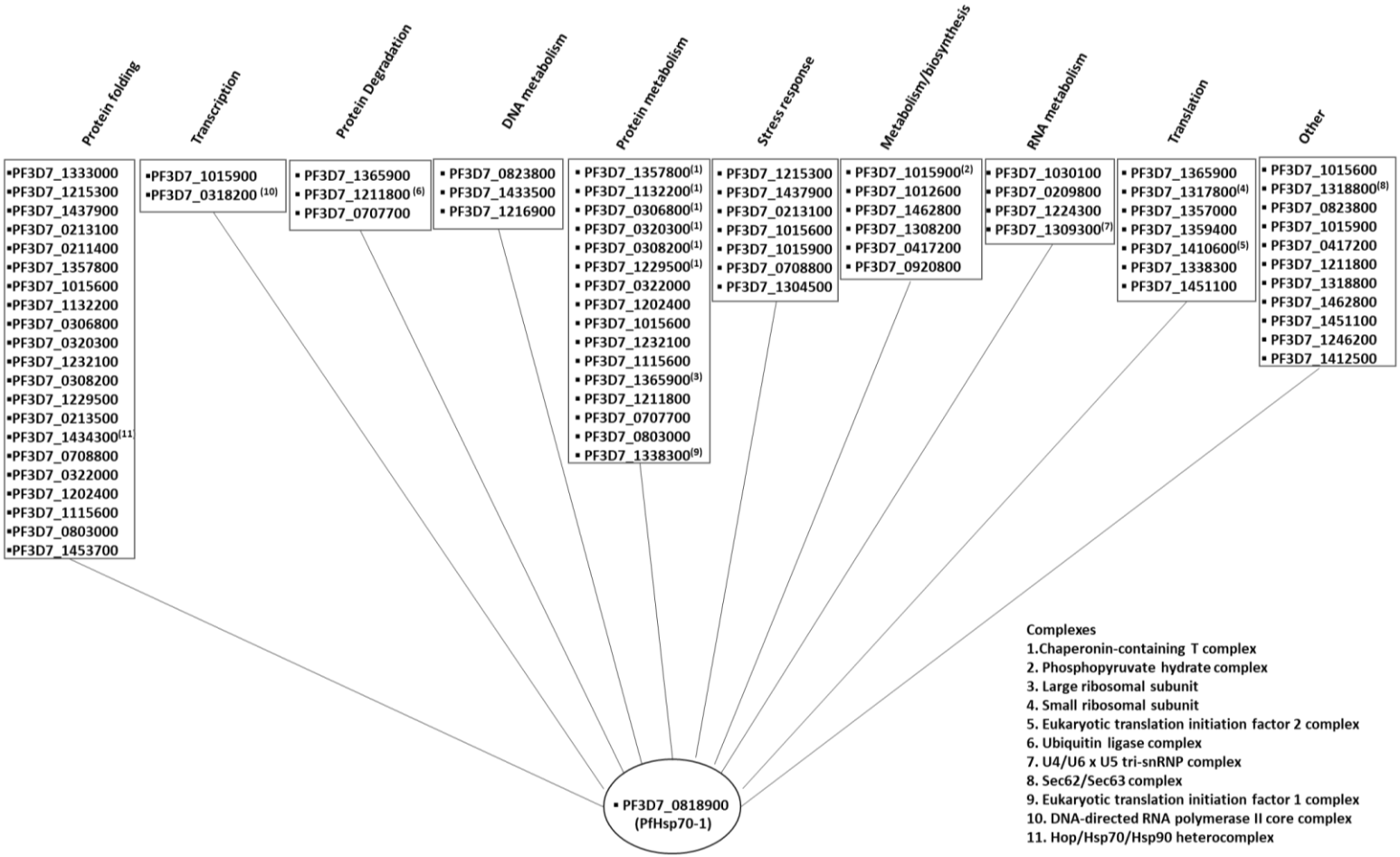

Figure 2. 5. Metabolic pathways for predicted interactors of PfHsp70-1
Interaction partners obtained from STRING are grouped according to their roles based on Gene Ontology categories (The Gene Ontology Consortium, 2000). It is possible PfHsp70-1 may form part of the 11 complexes identified (bottom right).

Some of the interactors were observed to be part of 11 complexes (Figure 2.5). Of interest, were complexes that involve proteins that associate with PfHsp70-1 via its EEVD domain. Only two complexes were identified, and these were the Hop/Hsp70/Hsp90 heterocomplex and the Sec62/Sec63 complex. The two complexes may involve co-chaperones PfHop and PfHsp40 (Gitau *et al*., 2012; Linxweiler *et al*., 2017). The integrity of the two complexes is likely to be affected by mutations in the GGMP motif region of PfHsp70-1. Abrogation of the Hsp70 interaction with the TPR containing proteins or Hsp40s due to mutations in the GGMP motif will likely hinder processes, such as protein folding and degradation that are important to parasite survival (Seo, 2015). However, the effect of the GGMP mutations on the interaction of PfHsp70-1 with PfHop remained to be experimentally ascertained.

2.4 Discussion

The role of the GGMP motif of Hsp70 proteins is not well understood despite its strong representation particularly in proteins of parasitic origin. Mutant forms of PfHsp70-1 with GGMP substitutions, as well as a DnaK GGMP variant, were designed (Figure 2.1). Conserved substitutions were applied to minimize drastic effects on the overall fold of the PfHsp70-1 variants. It is interesting to note that most of the substitutions were made to alanine residues (Figure 2.1). These mutations were predicted to cause only marginal structural differences to PfHsp70-G632 compared to PfHsp70-1. An α-helix developed in PfHsp70-G648 in the mutated region that is usually unordered PfHsp70-1 (Figure 2.4B1). Alanine substitutions are usually referred to as 'neutral' mutations, although they can be detrimental to protein structure or function in some cases (Betts and Russel, 2003). Residues that make up the arch (Shonhai *et al*., 2008) of PfHsp70-1 were observed to retain their orientation in the GGMP variants (Figure 2.4). The DnaK-G variant exhibited structural variation to wild type DnaK in the C-terminal lid. These changes were due to the introduction of the GGMP repeats from PfHsp70-1. This may influence the function of the protein.

On the other hand, this study further sought to map out interactors of PfHsp70-1. The rationale was that some of the associations are likely to be affected by changes in the GGMP motif of PfHsp70-1. Of the 49 interactors predicted for PfHsp70-1, some of these have been experimentally proven (section 2.3.5). Prediction of these known interactions served as a validating measure of the predictions in the network. Of interest to this study were the TPR containing and the Hsp40 proteins (Appendix B, Table B1). PfHsp70-1 associates with TPR containing proteins such as PfHop via the EEVD motif. PfHsp70-1 also interacts with *P. falciparum* Hsp40s via an acidic group within the NBD and the pentapeptide (GPTIEEVD) at the C-terminal end of PfHsp70-1 (Suzuki *et al*., 2010). Mutations in the GGMP motif region are likely to abrogate the EEVD interactions due to the proximity of the GGMP motif to the EEVD motif. Abrogation of the PfHop/PfHsp70-1 and Hsp40/Hsp70 interactions in *P. falciparum* is likely to impact the Hsp90 chaperone pathway and the Sec62/Sec63 complex. The Sec62/Sec63 complex is responsible for

the transport of protein into the ER and is also involved in signal transduction (Linxweiler *et al*., 2017). The Hsp70/Hsp90 chaperone system is central in protein quality control as it prevents protein aggregation and catalyzes the folding of newly synthesized proteins, refolding of aggregated and misfolded proteins, trafficking and promote degradation of denatured proteins (Mayer, 2013). Although Hsp70 is required during the early stages of assisted folding of nascent or denatured proteins, Hsp90 is mainly involved in a later stage of stabilization and activation of many key regulatory proteins involved in signaling pathways, such as kinases and transcription factors hence its importance in aspects such as gene regulation and signal transduction (Makhnevych and Houry, 2012; Taipale *et al*., 2012). Disruption of these complexes through mutations in the GGMP motif will have far-reaching effects on parasite survival, development, and pathogenesis.

Based on the predictive tools used, the mutation in the C-terminal end of the GGMP motif (residues 648-657) of PfHsp70-1 resulted in secondary structural changes. There was a conversion from random coil to α-helix in the mutated GGMP region of PfHsp70-G648. This suggests that the GGMP repeats at position 648-657 might be of structural importance in PfHsp70-1. Again, the introduction of the GGMP repeats in DnaK resulted in structural changes. Part of the random coiled region converted to α-helix in DnaK-G. It was interesting to determine if these structural changes would impact on the function of the chaperones. However, biophysical characterization of the Hsp70s remained to be carried out to ascertain the extent of the structural changes between the wild type proteins and the variants.

Chapter 3

Biophysical characterization of PfHsp70-1, DnaK, and their GGMP variants

3.1 Introduction

PfHsp70-1 has been the most studied Hsp70 of the six homologs that are encoded by the *P. falciparum* genome (Shonhai, 2014). PfHsp70-1 is expressed at all blood stages of the parasite's life cycle. It performs a myriad of functions that are important for the survival of the parasite. On the other hand, the major *E. coli* Hsp70 (DnaK) has also been greatly studied (Kityk *et al*., 2012; 2015). DnaK forms the basis of the so-called canonical Hsp70s (Bertelsen *et al*., 2009).

Following the *in silico* studies on PfHsp70-1, DnaK and their GGMP variants (Chapter 2), it was important to study the biophysical properties of these proteins *in vitro* using CD spectroscopy and tryptophan fluorescence. CD spectroscopy determines the secondary structure of a protein, that is the alpha-helical (α), beta-sheet (β) and unordered (loops/turns) content of a protein (Sreerama *et al*., 1999). On the other hand, tryptophan fluorescence determines the tertiary structure or conformational fold of a protein (Chen and Barkley, 1998). Combined with structure predictions from *in silico* methods, these biophysical characterization methods provide high-resolution protein structural information. Therefore, using the recombinant proteins this study sought to elucidate the role of the GGMP motif on the structure of PfHsp70-1 and DnaK using biophysical techniques.

The objectives of this study were to:

i. heterologously express and purify recombinant PfHsp70-1, DnaK, and the GGMP variants;

ii. determine the secondary and tertiary structures of PfHsp70-1, DnaK, and the GGMP variants and to

iii. assess the effect of the GGMP motif on the heat stability of PfHsp70-1 and DnaK.

3.2 Materials and Methods

3.2.1 Materials

Reagents used in this study are listed in Appendix C. The following antibodies were used: rabbit raised α-PfHsp70-1 antibody as previously described (Gitau *et al*., 2012), α-His antibody and HRP conjugated α-rabbit (Thermo Scientific, USA), mouse raised α-DnaK antibody (Makhoba *et al*., 2016) and HRP conjugated α-mouse secondary antibodies (Enzo Life Sciences, USA) were used to validate the recombinant proteins. The plasmids and strains used for recombinant protein production are listed in Table 3.1.

Table 3. 1: List of plasmids and strains used for protein expression

Strains and plasmids	Description	Supplier/Reference
Plasmids		
pQE30/PfHsp70-1$_{NBD}$	pQE30 encoding the NBD of PfHsp70-1, Amp^R	Zininga *et al*., 2015b
pQE30/PfHsp70-1	pQE30 encoding PfHsp70-1, Amp^R	Matambo *et al*., 2004; Zininga *et al*., 2015b
pQE30/PfHsp70-G632	pQE30 encoding PfHsp70-G632 mutant, Amp^R	This study
pQE30/PfHsp70-G648	pQE30 encoding PfHsp70-G648 mutant, Amp^R	This study
pQE30/DnaK	pQE30 encoding *E. coli* Hsp70 (DnaK), Amp^R	This study
pQE30/DnaK-G	pQE30 encoding *E. coli* DnaK-G variant, Amp^R	This study
Strains for protein expression		
***E. coli* XL1 Blue**	*rec*A1 *end*A1 *gyr*A96 *thi*1 *hsd*R17 supE44 *rel*A1 *lac* (F´proAB lacIqZM15 Tn10 (Tetr)	Thermofischer scientific, (USA)

3.2.2 Construction of plasmids expressing PfHsp70-G632, PfHsp70-G648, and DnaK-G

The GGMP variants were designed (Section 2.2.1). Codon harmonized forms of the genes coding for the variants were synthesized by GenScript (USA). The genes were first cloned into pUC57 with *Bam*HI and *Hind*III restriction sites and then finally into pQE30 making pQE30/PfHsp70-

G632, pQE30/PfHsp70-G648, and pQE30/DnaK-G constructs. PfHsp70-G632 and DnaK-G were custom cloned whereas for PfHsp70-G648, site-directed mutagenesis was carried out and these were verified by DNA sequencing. The constructs were synthesized by GenScript and were verified by restriction digests using *Bam*HI and *Hind*III.

3.2.3 Confirmation of PfHsp70-1 and DnaK DNA constructs

Restriction digests were conducted on pQE30/PfHsp70-1 and pQE30/DnaK plasmid constructs using restriction enzymes, *Bam*HI and *Hind*III (Thermo Scientific, USA) and resolved using 0.8 % agarose gel electrophoresis (Appendices A2 and A3).

3.2.4 Expression of recombinant proteins

E. coli XL1 Blue cells were transformed separately with pQE30/PfHsp70-1, pQE30/DnaK, pQE30/PfHsp70-G632, pQE30/PfHsp70-G648 and pQE30/DnaK-G (Appendix A4). Protein expression was conducted as previously described by Zininga *et al*. (2015b) with slight modifications. Transformed cells were grown in terrific broth (TB, 2.6 % Yeast extract, 1.3 % Tryptone and 0.44 % glycerol) supplemented with TB salts (0.17 M KH_2PO_4 and 0.72 M K_2HPO_4) and 100 µg/ml ampicillin at 37 °C. The terrific broth is an auto-induction broth. Following induction, expression was conducted at 30 °C for 6 hours. Protein expression samples collected at intervals were analyzed using 12 % sodium dodecyl sulfate-polyacrylamide gel electrophoresis (SDS-PAGE) under reducing conditions and visualized by Coomassie blue (Appendix A6).

3.2.5 Purification of recombinant proteins

3.2.5.1 Affinity chromatography using Ni-NTA

Recombinant protein purification followed a previously described method (Zininga *et al*., 2015b). However, the buffers were modified to: lysis buffer (10 mM Tris– HC1, pH 7.5, 300 mM NaCl, 10 mM Imidazole, 1X Sigmafast Protease Inhibitor, 1 mM 2-β-mercaptoethanol and 1 mg/ml lysozyme). The wash buffer (lysis buffer plus 25 mM Imidazole) and elution buffer (lysis buffer plus 500 mM Imidazole). Samples were collected for analysis by SDS-PAGE to assess the purity of

the proteins. Dialysis of the purified recombinant proteins was performed extensively overnight using SnakeSkin dialysis tubing 10 000 MWCO (ThermoScientific) in dialysis buffer (20 mM Tris-HCl, pH 7.5, 10 mM NaCl, 5 % (v/v) glycerol, containing 1 mM 2-β-mercaptoethanol).

3.2.5.2 Ion Exchange Chromatography

As a second purification step to improve the purity of the recombinant proteins, the dialyzed protein was loaded onto a Tricorn Mono Q 4.6/100 P.E column (G.E Healthcare, USA) connected onto an Akta Fast protein liquid chromatography (FPLC; G.E Healthcare USA). Parameters for IEX were set at a flow rate of 2 ml/min and a pressure limit of 4 MPa. The recombinant proteins were separated by increasing the ionic concentration of the mobile phase from buffer A (20 mM Tris-HCl; pH 7.5, 10 mM NaCl containing 0.2 mM Tris-carboxyethyl phosphine [TCEP]) to buffer B (20 mM Tris-HCl; pH 7.5, 1 M NaCl containing 0.2 mM TCEP). Initially, a salt gradient was increased to 0.5 M NaCl (buffer B) over 30 minutes and the NaCl was increased from 0.5 M to 1 M over 10 mins by setting the pumps containing the two buffers appropriately. Fractions were collected in 96 well plates at 1 ml per well. Samples were collected from the eluted fractions corresponding to the main peak and were analyzed by SDS-PAGE. The remainder of the protein was further purified using size exclusion chromatography (SEC).

3.2.5.3 Size Exclusion Chromatography

After ion exchange chromatography, fractions containing each the recombinant PfHsp70-1 and its GGMP variants were separately pooled together and loaded onto either a Superdex^{TM} S200 increase 10/300 GL column connected onto an Akta FPLC system as previously described (Ruskamo *et al*., 2012). The flow rate was set at 0.3 ml/min and a maximum pressure of 1.5 MPa. Recombinant Hsp70 proteins were eluted using buffer C (10 mM Tris-HCl; pH 8, 300 mM NaCl containing 5% Glycerol and 0.2 mM TCEP). Fractions were collected in a 96 well plate at 0.5 ml per well and samples were resolved by SDS-PAGE to determine the purity and homogeneity of the proteins. To confirm the identity and ascertain the purity of PfHsp70-1 and variants, SDS-PAGE analysis was performed. Incised protein bands were sequenced using MALDI-TOF mass

spectrometry at the Biocenter Oulu Proteomics Core Facility, Oulu University, Finland (Ruskamo *et al*., 2012). The proteins were quantified using the Bradford assay and the Christoph-Leidig webtool assay (Appendices A9 and A10).

3.2.6 Secondary structural organization of the GGMP variants

Far-UV circular dichroism (CD) was used to determine secondary structure variations between recombinant PfHsp70-1 and its GGMP variants. This was performed following a method by Zininga *et al*. (2016). The folded state of the proteins at any given temperature was determined as follows: $((\theta)^t - (\theta)^h) / ((\theta)^l - (\theta)^h)$ Equation 1 (Zininga *et al*., 2016)

Where $(\theta)^t$ is the molar ellipticity at any given temperature, $(\theta)^h$ at the highest temperature, and $(\theta)^l$ at the lowest temperature, respectively.

3.2.7 Determination of the tertiary structural organization of the GGMP variants

Tryptophan fluorescence spectroscopy was used to assess the changes in the tertiary structure of PfHsp70-1, DnaK and their GGMP variants, following the secondary structure determinations. This was conducted following the method by Zininga *et al*. (2016) with minor modifications. Recombinant PfHsp70-1, PfHsp70-G632, PfHsp70-G648, DnaK and DnaK-G protein (2 µM) were each incubated in assay buffer F (10 mM Tris-HCl pH 7.5) for 60 minutes at 20 °C in the presence of varying concentrations (0-6 M) of Guanidine hydrochloride (GdHCl) as a denaturant (positive control). The nucleotide-dependent conformational changes of PfHsp70-1, DnaK, and their GGMP variants were then investigated as previously described (Zininga *et al*., 2016). Tertiary structural changes of PfHsp70-1, DnaK, and their GGMP variants were also investigated in the presence of varying concentrations of Hsp70 substrate peptides ALLLMYRR and ANNNMYRR (0-500 nM). The peptide, ALLLMYRR is derived from the precursor of chicken mitochondrial aspartate aminotransferase (Han *et al*., 2004; Goeckeler *et al.,* 2008). ANNNMYRR was designed by substituting asparagine (N) for leucine (L) (Mabate *et al*., 2018). Proteins in *P. falciparum* are asparagine rich and this would act as a suitable substrate. Fluorescence spectra were recorded with initial excitation at 295 nm and emission spectra measured between 300 nm and 400 nm

using a JASCO FP-6300 spectrofluorometer (JASCO, Tokyo, Japan). Data were recorded for three repeats upon subtraction of baseline. Furthermore, to determine the level of hydrophobicity in the proteins, extrinsic ANS fluorescence was carried out as previously described (Achilonu *et al*., 2014). Briefly, 2 µM of recombinant protein (PfHsp70-1 and its GGMP variants) were mixed with 100 mM ANS. The samples were excited at 390 nm and emission was recorded between 400 and 600 nm. To analyze the data, the emission spectrum of free ANS was subtracted from the ANS: protein spectra.

3.3 Results

3.3.1 Confirmation of the various DNA constructs used in this study

The pQE30/PfHsp70-1 plasmid construct was verified by restriction digest (Appendix B4) and DNA sequencing. Restriction digestion of the plasmid with either *Bam*HI or *Hind*III. Plasmid pQE30/PfHsp70-G632 expressed a mutant version of PfHsp70-1 with a GGMP repeat substitution mutation at amino acid position 632-639. The integrity of the pQE30/PfHsp70-G632 plasmid was confirmed by restriction digest using *Bam*HI and *Hind*III (Appendix B5). The plasmid pQE30/PfHsp70-G648 encodes the expression of a mutant version PfHsp70-G648 with a substitution mutation on GGMP repeat at amino-acid position 648-657. Using restriction analysis, the integrity of the pQE30/PfHsp70-G648 plasmid was verified (Appendix B6).In the case of pQE30/PfHsp70-1 and its variants, the size of the cleaved DNA corresponded to the predicted sizes of about 2043 bp for the insert and 3416 bp corresponding to the vector size. Additionally, another mutation was made by inserting the GGMP repeats of PfHsp70-1 into DnaK (position 611-615 after pairwise sequence alignment. The plasmid pQE30/DnaK-G encodes the expression of a DnaK-G mutant. The integrity of both pQE30/DnaK and pQE30/DnaK-G constructs was verified by restriction analysis using enzymes *Bam*HI and *Hind*III. The cleaved insert sizes corresponded to 1989 bp and 2031 bp for pQE30/DnaK and pQE30/DnaK-G (Appendix B7). Since all the PfHsp70 constructs were between *Bam*HI and *Hind*III restriction sites and of similar sizes, they were differentiated by sequencing (Appendix B8-B9).

3.3.2 Expression and purification of recombinant of PfHsp70-1 and its GGMP variants

Recombinant PfHsp70-1 and its GGMP variant proteins were successfully overexpressed in *E. coli* XL1 Blue cells and purified using a 3-step protocol. Successful expression of the proteins was observed on SDS-PAGE analysis as species around 70 kDa (Figure 3.1A-C; lane O/N). The full-length Hsp70 proteins are approximately 74 kDa (Matambo *et al*., 2004). The presence of an N-terminal $(His)_6$ tag facilitated for the native purification of the proteins using Ni-NTA affinity chromatography as the first purification step (Figure 3.1A-C). The proteins were verified by Western blot analysis using α-PfHsp70-1 and α-His antibodies. Notably, the purified proteins

were free of DnaK contamination as confirmed using α-DnaK antibodies (Figure 3.1). DnaK contamination affects downstream applications such as chaperone activity assays.

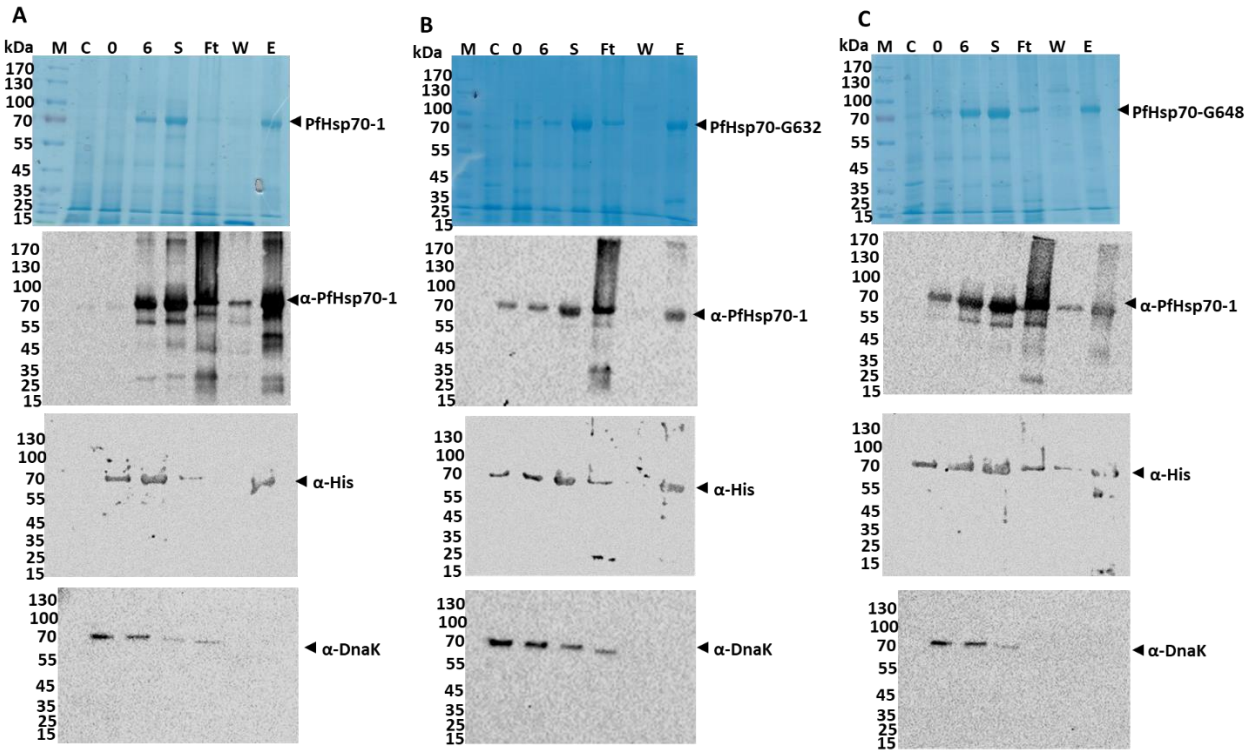

Figure 3. 1: Expression and purification of PfHsp70-1 and its variants
SDS-PAGE analysis for the expression and purification of PfHsp70-1 (**A**); PfHsp70-G632 (**B**) and PfHsp70-G648 (**C**) in *E. coli* XL1 Blue cells. Lane M: molecular weight marker (in kDa); Lane C: the total extract of cells transformed with pQE30 plasmid, Lane 0: represents the total extract of cells transformed with pQE30/PfHsp70-1 plasmid before IPTG induction; lane 6: total extract of cells transformed with pQE30/PfHsp70-1 and it's GGMP variants 6 hr after induction; lane Ft: flow-through, lane W: samples collected after the washing step and lane E: proteins eluted using 500 mM imidazole. Lanes FT, W and E samples were obtained from Ni-NTA affinity matrix. Lower panels: Western blot based on the use of α-PfHsp70-1, α-His antibodies, and α-DnaK antibodies. The SDS-PAGE analysis was performed on 12 % SDS gel under reducing conditions.

PfHsp70-1 and its variants were observed to elute with some contaminants (Figure 3.1A-C; lanes E) and hence the proteins were purified further using ion exchange chromatography (IEC). PfHsp70-1 eluted as peaks 1 and 2 as the salt concentration was increased (Figure 3.2A). The

GGMP variants eluted as a single peak (Figure 3.2B and C). In all, the contaminants eluted separately as witnessed by the numerous smaller peaks as the salt gradient increased.

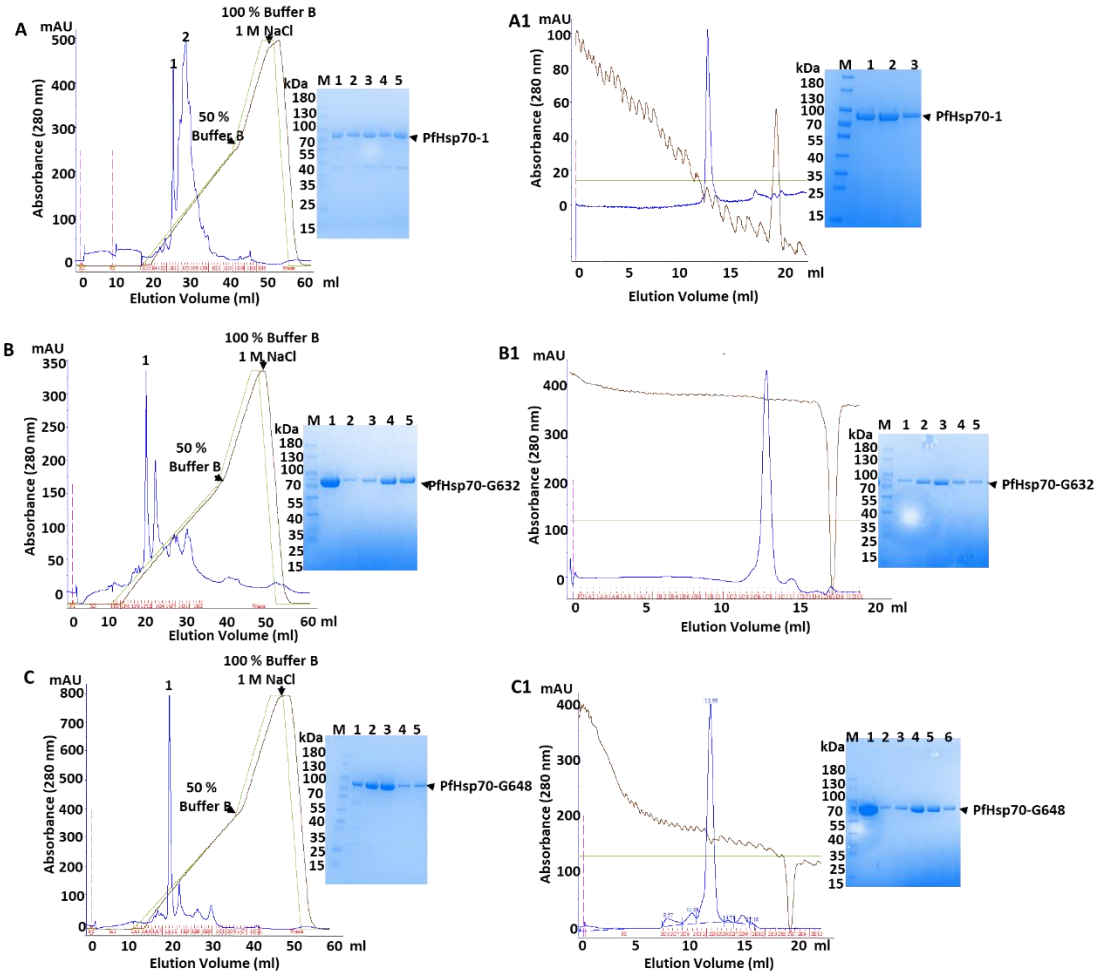

Figure 3. 2. Purification of PfHsp70-1 and its GGMP variants by ion exchange and size exclusion chromatography

Proteins were eluted by increasing the NaCl gradient (brown line) monitored as conductivity (lime green line). Elution profile after ion exchange chromatography monitored with at A280 absorbance (blue line for (**A**) PfHsp70-1, (**B**) PfHsp70-G632 and (**C**) PfHsp70-G648. The SDS-PAGE analysis of fractions from the main peak (**inserts**). Size exclusion chromatography of (**A1**) PfHsp70-1, (**B1**) PfHsp70-G632 and (**C1**) PfHsp70-G648. PfHsp70-1 and its GGMP variants eluted as monomers (inserts; SDS-PAGE of the purified proteins from the peaks after SEC). The lanes represent fractions collected from the respective peaks. The SDS-PAGE analysis was performed on 12 % SDS gel under reducing conditions.

In order to confirm the purity of the proteins from IEC, SDS-PAGE analysis was conducted. Resolution of the fractions from the 2 peaks showed the presence of the PfHsp70-1 protein

(Figure 3.2A; insert lanes 1-2). However, from peak 2, PfHsp70-1 was observed to elute with lower molecular weight fragments (Figure 3.2A; insert lanes 3-5). PfHsp70-1 was probably breaking down into lower molecular weight species. In order to ascertain the oligomeric status and the monodispersed of the protein, the PfHsp70-1 protein from IEC from peak 1 was passed through a Superdex (S200 Increase) SEC column. Recombinant PfHsp70-1 eluted as a monomeric protein (peak 1, Figure 3.2A1). A single band migrating at around 70 kDa was observed upon SDS-PAGE analyses (Figure 3.2A1; insert). All the variants eluted with a single main peak (Figure 3.2B and C) and the proteins seemed pure as the contaminants were undetectable when resolved by coomassie staining. The size exclusion chromatography profile showed that all the variant proteins are monomeric (Figure 3.2B1 and C1). This was further confirmed by SDS-PAGE analysis (Figure 3.2B1 and C1, insert gels). The proteins were confirmed by sequencing with MALDI-TOFF (Appendix B10-13).

3.3.2.1 Recombinant production and purification of DnaK and DnaK-G

Recombinant DnaK and DnaK-G were successfully expressed in *E. coli* XL1 Blue cells. Control *E. coli* cells containing the pQE30 vector plasmid did not express the recombinants proteins as there was no increase in 70 kDa band intensity was observed (Figure 3.3A and B; lane C). Similarly, no bands were observed in the pre-induction samples suggesting that there was no leaky expression (Figure 3.3A and B; Lane 0). Successful expression of DnaK and DnaK-G was observed by the band at approximately 70 kDa after 6 hr post-induction with IPTG (Figure 3.3A and B; lane 6). The soluble fraction from the lysed cells was then loaded onto a Ni-NTA IMAC column, washed and eluted (Figure 3.3A and B; lane E). To verify the purity of the protein, the eluted proteins were analyzed by SDS-PAGE analysis. Single bands of DnaK and DnaK-G were observed as species migrating at 70 kDa (Figure 3.3A and B, lane E). Both DnaK and DnaK-G were confirmed by Western blot analysis using α-DnaK and α-His antibodies (Figure 3.3A and B, lower panels).

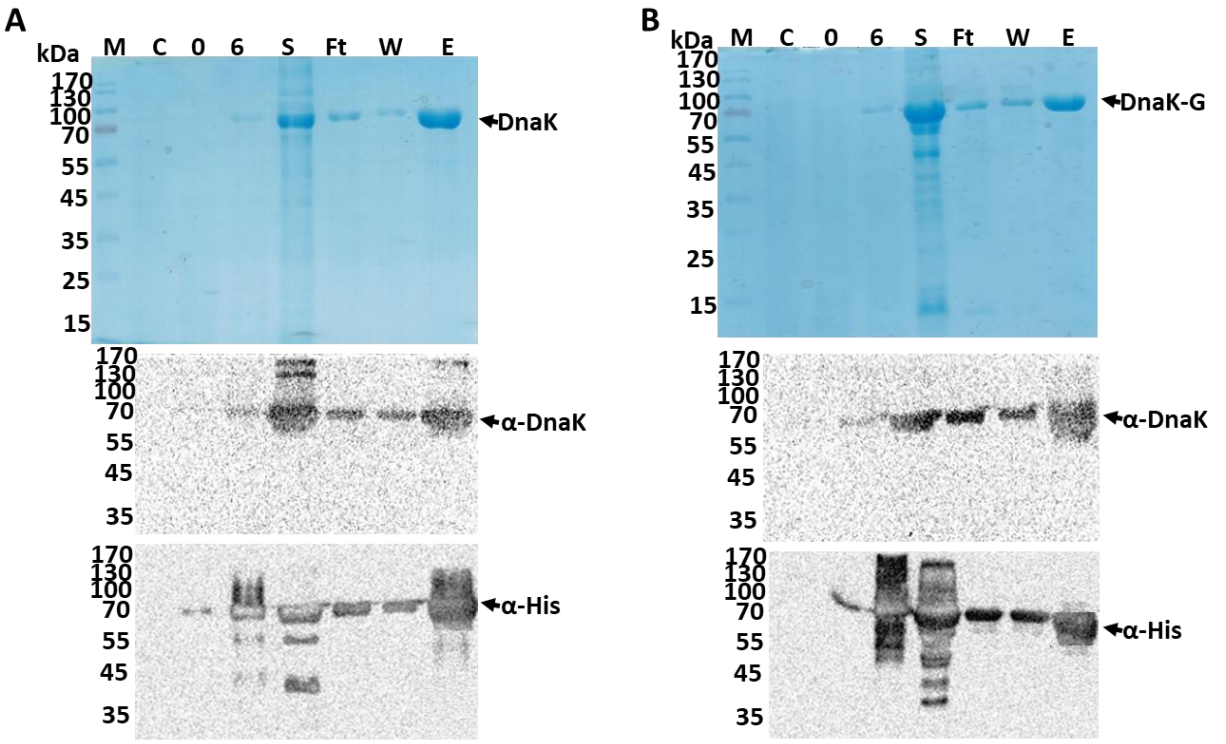

Figure 3. 3. Analysis of the expression and purification of DnaK and DnaK-G in *E. coli* XL1 Blue
Analysis of the expression and purification of (**A**) DnaK and (**B**) DnaK-G by SDS-AGE. Lower panels: Confirmation of the expressed recombinant proteins by Western blot using α-DnaK and α-His antibodies. Lane M: represents molecular weight markers (in kDa); Lane 0: represents the total extract of cells transformed with pQE30/DnaK or DnaK-G plasmid before IPTG induction; lane 6 represents the 6th hour sample after induction; Lane S: the soluble fraction; from Ni-NTA lane Ft: represents flow-through; lane W: represents samples collected after the washing step and lanes E: represent the elution fraction. The SDS-PAGE analysis was performed on 12 % SDS gel under reducing conditions.

3.3.3 Secondary structure determination for PfHsp70-1 and its GGMP variants

The secondary structures of PfHsp70-1 and its GGMP variants were determined using CD spectroscopy by recording signals from 260 nm to 190 nm. CD spectroscopy measures the α-helical, β-sheet, and the coiled (unordered) content of a protein upon deconvolution on Dichroweb. The far UV spectra for PfHsp70-1 exhibited a positive peak at 194 nm and minima at 209 and 220 nm, respectively (Figure 3.4A). The GGMP variants were observed to have a spectrum similar to that observed for PfHsp70-1. These spectra suggest that PfHsp70-1 and its GGMP variants are predominantly α-helical proteins (Whitmore and Wallace, 2008).

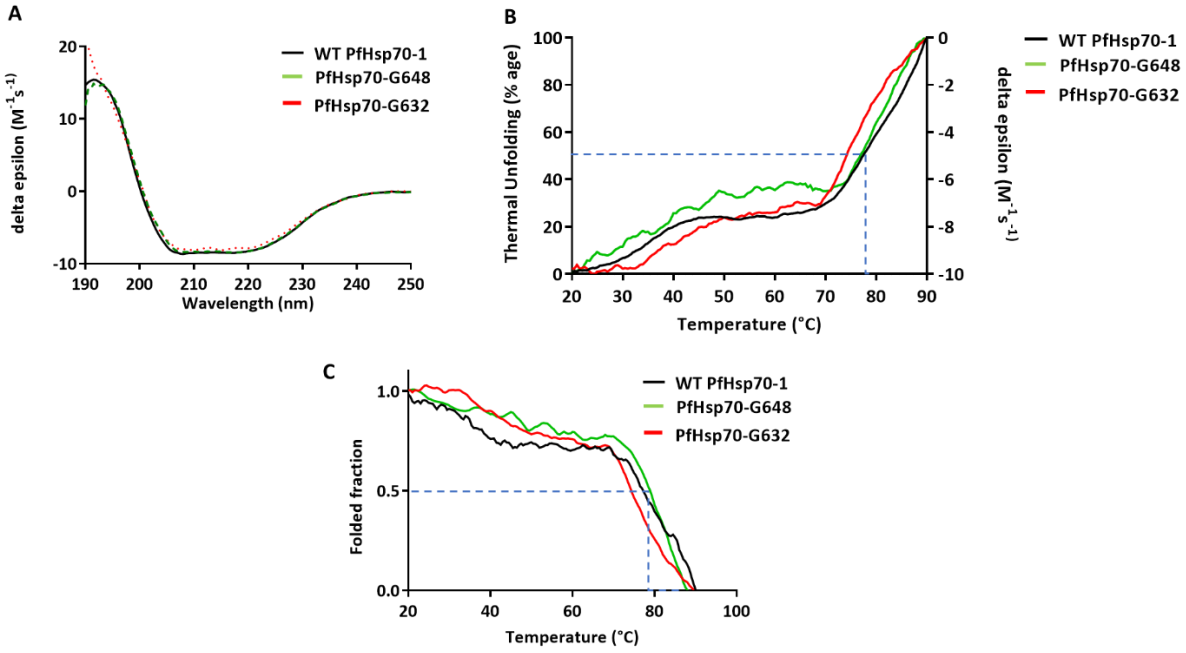

Figure 3. 4. The GGMP substitutions did not compromise the heat stability of PfHsp70-1
(**A**) The CD spectra of native PfHsp70-1, PfHsp70-G632 and PfHs70-G648 were presented as delta epsilon ($M^{-1}s^{-1}$). (**B**) The temperature was raised from 19 °C to 90 °C and ellipticity measured at 222 nm. This permanently abrogated the secondary structure of the proteins. Orange dotted line represents the melting temperature for PfHsp70-1 and variants. Thermal unfolding was represented as a percentage with 100 % being the total unfolded protein at 90 °C. (**C**) The folded fraction of the proteins under varying temperatures. Changes in CD ellipticity at 222 nm measured for PfHsp70-1, PfHsp70-G632, and PfHsp70-G648 in an equimolar ratio. Data were fit into Equation 1: $(\theta)^t - (\theta)^h) / (\theta)^l - (\theta)^h$.

Deconvolution of the spectra for PfHsp70-1 and its variants confirmed that all the proteins are predominantly α-helical (Table 3.2). This agreed with observations made by Misra and Ramachandran, (2009) for PfHsp70-1. However, PfHsp70-G648 had a slightly higher (69 %) α-helical content compared to 62 % and 60 % for PfHsp70-1 and PfHsp70-G632, respectively. This is due to the extra helix observed in the mutated GGMP region during *in silico* studies (section 2.3.3). There were marginal variations in the β-sheet and turn content of PfHsp70-1 and PfHsp70-G648 versus variant PfHsp70-G632 which possessed a higher β-sheet and turn content (Table 3.2; $p<0.001$). β-sheets confer protein secondary structure stability due to the high amount of hydrogen bonding. PfHsp70-1 and PfHsp70-G632 possessed higher percentage content of disorder/unordered (18 % and 17 %) versus PfHsp70-G648 with a lower 12 %.

The thermal stability of the proteins was then analyzed by observing changes in CD molar ellipticity at 222 nm while increasing temperature from 20-90 °C (Figure 3.4B; Table 3.2). Wild type PfHsp70-1 followed a gradual unfolding pattern (gradual loss of molar ellipticity at 222 nm (θ_{222}) from 20 °C onwards (Figure 3.4B). The GGMP variants exhibited a similar pattern as PfHsp70-1(wild type) (Figure 3.4B). Although there were minimal variations in the unfolding patterns, all proteins were thermostable to temperatures above 70 °C. The data showed that 50 % of the PfHsp70-1, PfHsp70-G632 and PfHsp70-G648 remained folded at 76.9 °C, 74.5 °C and 78.9 °C respectively (Figure 3.4C). This suggested that the variants were as heat-stable as the wild type PfHsp70-1.

Table 3. 2: Comparative secondary structure composition of PfHsp70-1 and its GGMP variants

	Helix	Sheet	Turn	Unordered	NMRSD
PfHsp70-1	62	11	6	18	0.007
PfHsp70-G632	60	17	6	17	0.002
PfHsp70-G648	69	11	8	12	0.005

Data are represented as absolute values from the Dichroweb server with CDSSTR reference set 4. Statistical analysis was done using two-way ANOVA *($p<0.001$).*

3.3.4 Tertiary structural organization of PfHsp70-1, DnaK and their GGMP variants

Having determined that GGMP mutations did not affect the α-helical and heat stability of PfHsp70-1, the tertiary structure of PfHsp70-1 relative to its GGMP variants was determined. PfHsp70-1 possesses three tryptophan residues (W32, W101, and W593), two located in the N-terminal ATPase domain and one in the far C-terminus. Despite the differences in fluorescence intensity, PfHsp70-1 and GGMP variants exhibited emission maxima around 340 nm (Appendix B15). The 340 nm maxima observed for PfHs70-1 and the variants suggest that the proteins were properly folded as the tryptophan residues were buried away from the solvent. The emission maxima at 340 nm for PfHsp70-1 agreed with previous reports (Misra and Ramachandran, 2009). In contrast, studies by Zininga and colleagues (2017a, c) showed emission maxima of PfHsp70-1 at 328 nm. However, buried tryptophan residues are known to give emission maxima in the range

of 330-340 nm (Misra and Ramachandran, 2009). Hence, the 328 nm emission maxima observed by Zininga and colleagues might still fall within the lower emission maxima range. In addition, it is also known that experimental conditions such as buffers used (solvent polarity) influence emission maxima observed (Siddiqi *et al*., 2017).

The proteins were analyzed using tryptophan fluorescence in the presence of varying concentrations of GdHCl. Upon incubating all the proteins with GdHCl for 60 min, the fluorescence intensity was observed to decrease consistently with an increase in the concentration of GdHCl (Appendix B16). A red shift in emission maxima was observed with increase in GdHCl concentration (Figure 3.5A). Fluorescence emission maxima at 349, 352 and 349 nm were observed for PfHsp70-1, PfHsp70-G632, and PfHsp70-G648, respectively. Wild type PfHsp70-1 spectrum showed a gradual shift reaching a 349 nm maximum at 6 M GdHCl (Figure 3.5A). In contrast, Misra and Ramachandran (2009) observed a 352 nm maximum at 4.5 M GdHCl. This is probably due to the longer 4 hr incubation they employed compared to the 1 hour used in this study. Overall, the proteins are sensitive to GdHCl induced denaturation which exposes the buried tryptophan residues shifting maxima towards 352 nm. Hence, this validated that the proteins are in a folded (native) state as they were sensitive to GdHCl.

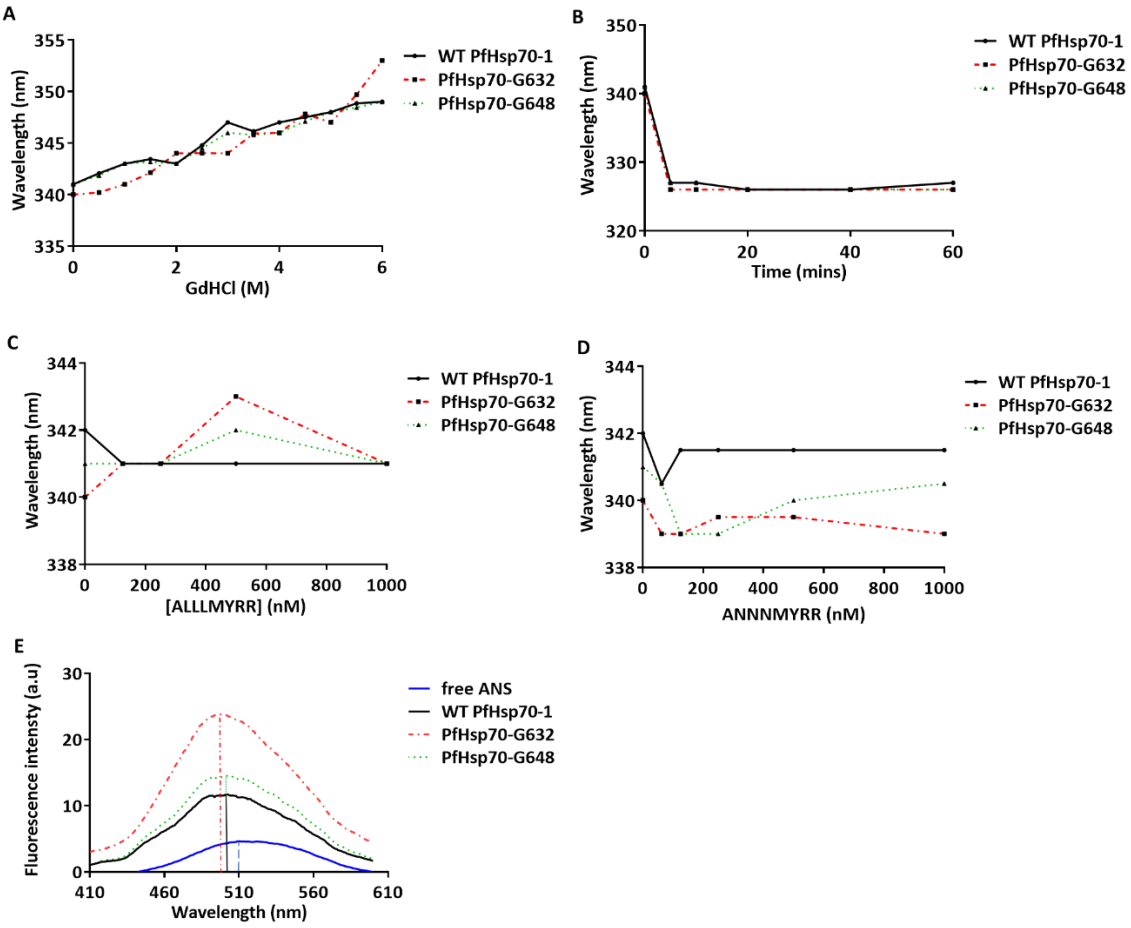

Figure 3. 5. Analysis of the tertiary structure of PfHsp70-1 and it GGMP variants by tryptophan fluorescence

(**A**) GdHCl induced changes in protein structure in the various recombinant proteins. Changes in fluorescence intensity for PfHsp70-1, PfHsp70-G632, and PfHsp70-G648 incubated with 0-6M GdHCl. Red shift in the tryptophan fluorescence emission wavelength of PfHsp70-1 and variants on incubation with increasing concentration of guanidine hydrochloride. Excitation was at 295 nm with the emission measured from 300-400 nm. (**B**) Blue shift in the tryptophan fluorescence emission wavelength of PfHsp70-1 and variants in the presence of 5mM ATP. Fluorescence emission was monitored over time (60 min). Peptide ALLLMYRR (**C**) and ANNNMYRR (**D**) at varying concentrations (0-1000 nM) were incubated with recombinant proteins and the effect on the intrinsic protein tryptophan fluorescence was measured. (**E**) Comparison of the emission spectra of PfHsp70-1, PfHsp70-G632, and PfHsp70-G648. ANS at 100 mM was mixed with proteins (2 µM). Excitation was at 390 nm, and emission was recorded between 400 and 600 nm.

Having determined that the recombinant chaperones were properly folded and responsive to GdHCl treatment, it was important to ascertain the effect of model Hsp70 peptide substrates (Mabate *et al*., 2018) on the structure of PfHsp70-1 and its GGMP variants. In the absence of peptide substrate, PfHsp70-1 exhibits emission maximum at 342 nm (Figure 3.5B). There was a 1 nm decrease in emission maxima of PfHsp70-1 upon addition of 62.5 nM of both peptides ALLLMYRR and ANNNMYRR (Figure 3.5C and D). The emission maxima of PfHsp70-1 were observed to level off at 341 nm with increase in the concentration of peptide ALLLMYRR. The emission maximum for PfHsp70-1 increased by 1 nm in the presence of 125 nM ANNNMYR and then levels off with increased concentration of the peptide. The spectra for the variants follow a similar wild-type-like pattern with minimal shifts (range 0 to ±3 nm) in the emission maxima in the presence of increasing concentrations of both peptides (Figure 3.5C and D). This might suggest that binding occurs with marginal effects on the micro-environment surrounding the tryptophan residues (Li *et al*., 2017). However, the fluorescence intensities of PfHsp70-1 and its GGMP variants show a regular decrease with increasing peptide concentration (Appendix B17). Decreases in the fluorescence intensity are suggestive of quenching. Quenching is described as any process that reduces the fluorescent intensity of a sample and it occurs due to numerous molecular interactions (Siddiqi *et al*., 2017). PfHsp70-G632 was quenched to a higher degree compared to PfHsp70-1 and PfHsp70-G648 (Appendix B17). This suggests that PfHsp70-G632 interacted strongly with the two peptide substrates.

Hsp70s bind nucleotides to assume unique conformation. Additionally, to explore conformational changes in PfHsp70-1 and the mutants in the presence of nucleotides, intrinsic tryptophan fluorescence was measured. The nucleotide-free and ADP-bound forms of PfHsp70-1 assumed closely similar conformational states (Appendix B18). This is in line with a well-established view that the nucleotide-free and ADP bound forms of Hsp70 assume a similarly relaxed conformation (Buchberger *et al*., 1995; Zininga *et al*., 2016). Conversely, the ATP-bound PfHsp70-1 assumed a distinct conformation as evidenced by a blue shift in the spectrum with an emission maximum of 328 nm (Figure 3.5B). This shift in the emission maximum for PfHsp70-1

was observed upon incubation with ATP for 60 minutes. The variants (PfHsp70-G632 and PfHsp70-G648) also assumed similar conformations in nucleotide-free and ADP-bound states. Upon incubation with ATP, they followed a PfHsp70-1 like spectra with the emission maxima observed to drop to around 328 nm (Figure 3.5B). It is plausible that ATP binding and subsequent hydrolysis resulted in the conformational changes of these proteins. Over the 60-min period, the maxima are steadily maintained at 328 nm for all proteins. Interestingly, the proteins bound to ATP were slow to revert to original spectra after 1 hour. This is probably due to the excess ATP (5 mM) used and the fact that ATP hydrolysis is very slow when there is no substrate or a J-domain protein bound to the Hsp70 (Kityk *et al*., 2015).

To probe the presence of hydrophobic patches on PfHsp70-1 and its GGMP variants, ANS binding assay was performed (Figure 3.5E). ANS binds to hydrophobic patches on proteins. ANS emission increases distinctly, coupled with a resultant blue shift in emission maximum when bound to hydrophobic patches upon excitation at 390 nm (Achilonu *et al*., 2014). This can be used as a measure of the level of hydrophobicity in a protein. All the proteins exhibited an increase in the quantum yield upon excitation at 390 nm. PfHsp70-G632 exhibited the highest intensity, followed by PfHsp70-G648 and PfHsp70-1. Additionally, a blue shift in emission maxima was observed, from 510 to 502 nm for PfHsp70-1 and PfHsp70-G648, and 510 to 497 nm for PfHsp70-G632. This implied that PfHsp70-G632 was more hydrophobic than PfHsp70-G648 and PfHsp70-1. This agreed with predictions from hydropathy plots (section 2.1). Hence, PfHsp70-G632 assumed a more unfolded conformation thus exposing hydrophobic patches.

In a separate assay, the tertiary structure of DnaK and its GGMP variant was also determined in the presence of nucleotides and peptide substrates. DnaK possesses one tryptophan residue in the NBD (W102). Initially, GdHCl was used to demonstrate the sensitivity of the proteins to denaturation (Figure 3.6A). Both proteins responded to the denaturation as shown by the red shift in emission maxima from around 335 nm at 0 M to 349 nm at 6 M GdHCl. However, DnaK-G seemed to be more sensitive to GdHCl compared to DnaK. Upon incubating DnaK with

nucleotides, the ADP form exhibited a comparable spectrum as in the absence of nucleotides with no shift in emission maxima (336.5 nm; Figure 3.6B). However, the ATP bound forms exhibited a blue shift spectrum with an emission maximum at 331 nm suggesting changes in the environment around the tryptophan residue. Surprisingly, there was no shift in the emission maxima (330 nm) for the DnaK-G variant in the presence of either ATP or ADP as well as in the absence of nucleotides (Figure 3.6C). This could suggest that the DnaK-G variant was unresponsive to ATP. The peaks in DnaK-G were broad than in DnaK. Also, DnaK exhibited shifted maxima whereas DnaK-G did not. This suggests that the introduced GGMP mutation altered the conformation of the protein.

In the presence of lower concentrations (62.5 and 125 nM) of peptide substrate, ALLLMYRR, the emission maxima of DnaK and its GGMP variant were observed to blue shift by about 2 nm (Figure 3.6D). The emission maxima for DnaK was observed to level off with increases in ALLLMYRR concentrations (250-1000 mM) whereas for DnaK-G there was a slight spike at 250 nM. Although there were decreases in the emission maximum for DnaK in the presence of 125 nM peptide ANNNMYRR, increased concentrations of ANNNMYRR resulted in no change in the maxima (Figure 3.6E). The DnaK-G variant exhibited an almost constant emission maximum around 337 nm. The leveling off emission maxima with increased concentrations of the peptide could imply that the proteins were saturated with substrate. Overall, the GGMP variants of DnaK and PfHsp70-1 behaved in a similar fashion.

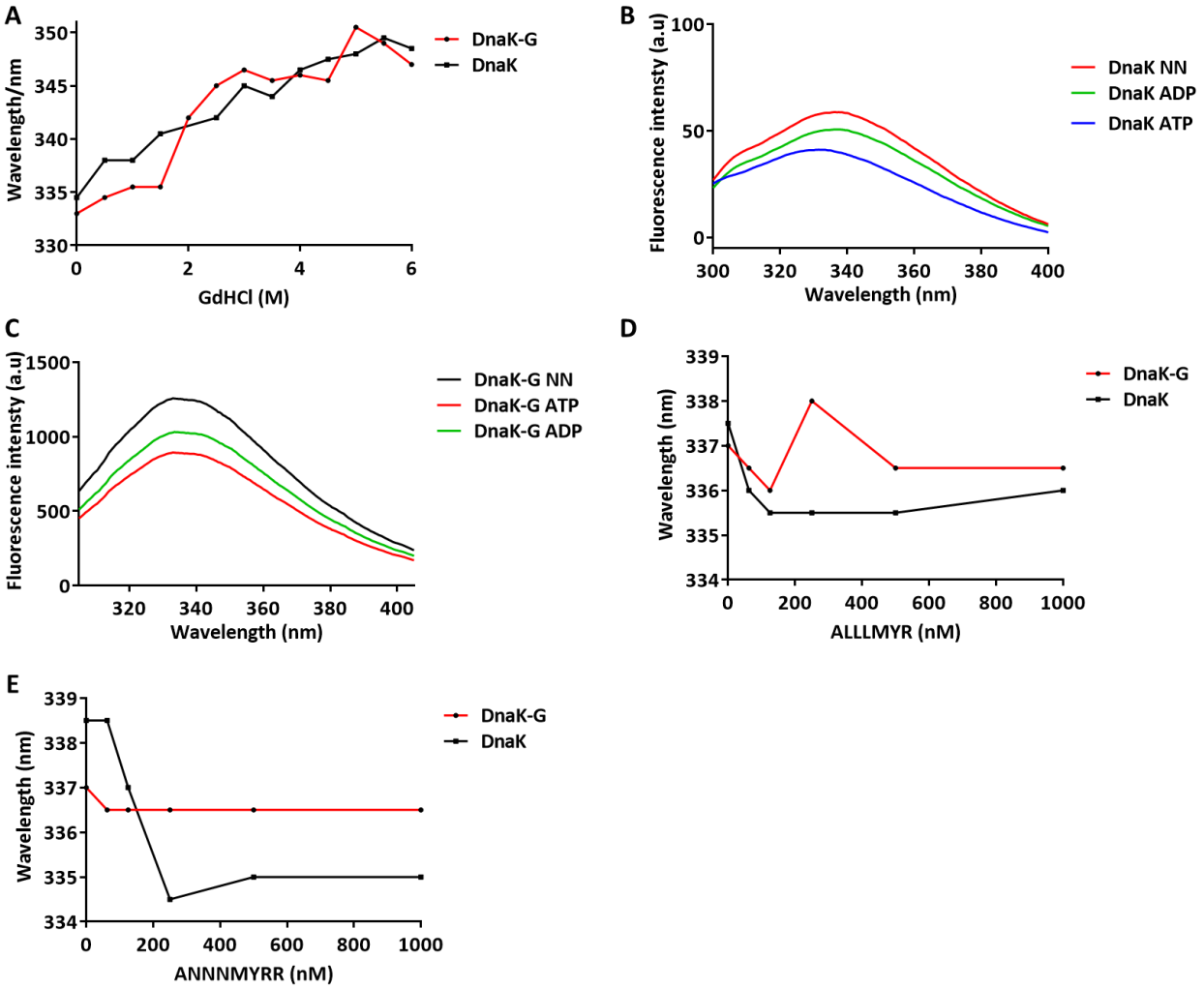

Figure 3. 61. Analysis of the tertiary structure of DnaK and DnaK-G by tryptophan fluorescence
(**A**) GdHCl induced changes in protein structure in the various recombinant proteins. Changes in fluorescence intensity of DnaK and DnaK-G incubated with 0-6 M GdHCl. Red shift in the tryptophan fluorescence emission wavelength of DnaK and DnaK-G on incubation with increasing concentration of guanidine hydrochloride. Excitation was at 295 nm with the emission measured from 300-400 nm. (**B** and **C**) Tryptophan fluorescence signals obtained upon incubating DnaK and DnaK-G in the additional presence of 5 mM of either ATP or ADP. Peptide ALLLMYRR (**D**) and ANNNMYRR (**E**) at varying concentrations (0-1000 nM) were incubated with recombinant proteins and the effect on the intrinsic protein tryptophan fluorescence was measured.

3.4 Discussion

This study employed CD spectroscopy and intrinsic tryptophan fluorescence to gain insights into the secondary and tertiary structures of recombinant PfHsp70-1 in comparison to its GGMP variants. This was extended to DnaK and its GGMP variant. It was also important to ascertain the effects of the GGMP motif introduced into DnaK, on the secondary and tertiary structure of the protein. Initially, all the proteins were overexpressed and purified to homogeneity using a combination of affinity, ion exchange, and size exclusion chromatographic techniques. PfHsp70-1 and its GGMP variants purified from the soluble *E. coli* fraction as monomers based on SEC data (Figure 3.2).

The secondary structure content of PfHsp70-1 and its GGMP variants calculated using Dichroweb (Whitmore and Wallace, 2008) confirmed that the proteins were mainly α-helical comprising of more than 50 % α-helices (Table 3.2). This was in line with previous findings for PfHsp70-1 (Misra and Ramachandran, 2009). Despite the conservative substitutions, secondary structural differences were observed for PfHsp70-1 and its GGMP variants (Table 3.2). PfHsp70-1 and PfHsp70-G632 possessed a significant percentage of unordered regions (Table 3.2). Conversion of a portion of the C-terminal unordered region to α-helix in PfHsp70-G648 resulted in 12 % of the protein's secondary structure being unordered. Unordered regions are responsible for protein-protein interactions (Hsu *et al*., 2012; Dyson and Wright, 2015). The GGMP repeats are in the most unordered region in the extreme C-terminal lid segment of the protein. It is possible GGMP repeats serve as sites for interaction with other proteins.

Findings from this study demonstrated that about 50 % of recombinant PfHsp70-1 and its GGMP variants is thermostable up to 80 °C (Figure 3.3B). PfHsp70-1 has been previously shown to be thermostable (Shonhai *et al*., 2008; Misra and Ramachandran, 2009; Zininga *et al*., 2016). Mutation of the GGMP repeats did not alter the heat stability of variant proteins despite the varying secondary structural composition of the chaperones. Hsp70 is known as a thermosensor due to its ability to regulate the heat shock response (Doberentz *et al*., 2017). This is why

PfHsp70-1 is important for parasite survival during febrile fever episodes. The high heat stability for PfHsp70-1 confirms its role in conferring cytoprotection to the parasite during cellular stress. The heat stability of PfHsp70-1 has been mainly attributed to the role of the C-terminal subdomain of the protein (Misra and Ramachandran, 2009). However, mutation of the GGMP motif is of no consequence to the thermostability of PfHsp70-1 (Figure 3.4B and C).

Hydrolysis of ATP drives the chaperone cycle of Hsp70s. Findings from this study indicated that PfHsp70-1, DnaK and the PfHsp70-1 GGMP variants bind ATP with a characteristic blue shift in emission maxima. Blue shifts are a result of increased hydrophobicity in the micro-environment around W-residues. It is known that upon ATP binding on Hsp70s, substantial conformational changes occur within the NBD and the SBD (Qi *et al*., 2013; Kityk *et al*., 2015). These structural changes could possibly explain the increase in hydrophobicity around the W-residues given that there are two W-residues in the NBD of PfHsp70-1 (W-32 and W-101) and one in the NBD of DnaK (W-102). The emission spectrum of W-102 in DnaK (conserved W-101 in PfHsp70-1) is known to be sensitive to either ATP or ADP binding. Interestingly, the W-32 residue of PfHsp70-1 occurs within one of the motifs (Phosphate 1; Bork *et al*., 1992) that associate with nucleotide. It is possible that the fluorescent properties of the W-32 and W-101 residues are sensitive to ATP binding on the Phosphate 1 motif. This could explain why the emission maxima had a characteristic blue shift. The recent findings agree with previous reports which observed a blue shift in emission maximum upon incubating the *E. coli* Hsp70 (DnaK) with ATP (Qi *et al*., 2013; Kityk *et al*., 2015). This supports both the DnaK and PfHsp70-1 data obtained in this study. Surprisingly, the DnaK-G variant in the presence of ATP behaved in a similar manner as the nucleotide-free and ADP bound forms. It is possible that the protein assumes a similar conformation to ADP and NN forms due to the GGMP insertion.

It was also important to ascertain how the mutations would impact on substrate binding. Peptide substrates ALLLMYRR and ANNNMYRR were observed to bind PfHsp70-1, DnaK and the GGMP variants resulting in quenching of fluorescence (Appendix B18). Peptide ANNNMYRR was

expected to bind to PfHsp70-1 with greater spectral shifts due to the abundance of asparagine (N) residues. However, binding of both peptides resulted in marginal shifts (±3 nm) in the emission maxima for the recombinant proteins. Previous studies have also demonstrated quenching and no shift in emission maxima upon titration of PfHsp70-1 with peptides (Misra and Ramachandran, 2010). There is only 1 W-residue in the SBD of PfHsp70-1 and none in the SBD of DnaK. It is possible that binding of the peptide in the SBD might have caused some structural changes that maintained the hydrophobicity around the W-residues. Interestingly, the binding of ATP in the NDB resulted in major shifts in emission maxima but the binding of substrate to the SBD resulted in minor shifts. This might suggest that structural changes in the NBD contribute more to the fluorescence emission compared to substrate binding in the SBD.

Overall, the positional mutations demonstrated that the GGMP motif is important for the secondary and tertiary structure of PfHsp70-1. The N-terminal GGMP mutation resulted in an increase in the β-sheet content (23 %) in PfHsp70-G648 whereas the C-terminal mutation caused a lower (12 %) unordered secondary structure content in PfHsp70-G632. However, these secondary structural changes did not alter the heat stability of PfHsp70-1 and its GGMP variants. Subsequent to this, the study sought to elucidate the effect of the GGMP mutations on the chaperone activity of PfHsp70-1 and DnaK.

Chapter 4

Analysis of the effect of the GGMP mutations on the chaperone activity of Hsp70

4.1 Introduction

The Hsp70 family of proteins are known to be ubiquitous and conserved molecular chaperones that play important roles in proteostasis under physiological and stressful conditions (Hartl and Hayer-Hartl 2002; Bukau *et al*., 2006). The Hsp70 chaperone activity involves transient interactions between C-terminal SBDβ and hydrophobic patches within substrate polypeptides. The SBDα acts as a lid closing in the substrate (Kityk *et al*., 2015). The chaperone activity of Hsp70 is regulated by nucleotide (ATP and ADP) binding to the NBD. Nucleotide-free and ADP-bound Hsp70s bind substrate with high affinity. This is because, in these two states, the SBDβ and SBDα are closely packed to each other resulting in low 'on' and 'off' rates for substrates (Mayer *et al*., 2000; Clerico *et al*., 2015). The binding of ATP to the NBD causes the SBDβ and SBDα to detach from each other. The SBDβ and SBDα subdomains then dock on either side of the NBD resulting in an increase in the substrate 'on' and 'off' rates by two or three orders of magnitude hence decreased affinity for the substrate by Hsp70 (Kityk *et al*., 2015). Hydrolysis of ATP is essential for the Hsp70 chaperone function. Important for the chaperone function of Hsp70 are co-chaperones, such as Hsp40s and NEFs (section 1.6.5). The binding of Hsp40 to the NBD of Hsp70 stimulates ATP hydrolysis. Exchange of ATP for ADP by NEFs reverts Hsp70 to a high-affinity state (Clerico *et al*., 2015).

The *P. falciparum* genome encodes six Hsp70s. The two cytosolic homologs (PfHsp70-1; PF3D7_0818900 and PfHsp70-z; PF3D7_0708800) and the exported PfHsp70-x (PF3D7_0831700) have been shown to possess chaperone activities (ATPase, protein aggregation suppression; Shonhai *et al*., 2008; Cockburn *et al*., 2011; Zininga *et al*., 2016, 2017; Mabate *et al*., 2018). Although not yet demonstrated to be essential, PfHsp70-1 exhibits distinct functional features and plays key cytoprotective functions. Accordingly, PfHsp70-1 in co-operation with other Hsps and co-chaperones ensures that the parasite survives the physiologically challenging environment in the human host. All these functions of Hsp70s are dependent on key residues located in the different domains or subdomains as well as in motifs. Modulation or alteration of these residues may lead to abrogation of protein function. For example, using mutational analysis

and *in vitro* assays, Shonhai *et al*. (2008) demonstrated that amino acid substitutions (A419Y and Y444A) in the arc of PfHsp70-1 compromised its chaperone function. On the other hand, lidless forms of DnaK have been shown to retain their chaperone activity. A GGMP motif has long been identified in the lid segment of PfHsp70-1 (Matambo *et al*., 2004) but its function is yet to be elucidated. The current study sought to further ascertain how the GGMP motif influences the PfHsp70-1 and DnaK chaperone function.

The objectives of this study were to:

i. determine the ATPase activities of PfHsp70-1, DnaK, and their respective GGMP variants;

ii. investigate the chaperone function of PfHsp70-1 and DnaK relative to their GGMP variants.

4.2 Materials and Methods

4.2.1 Materials

Reagents and materials used in this study are contained in Appendix C1. Peptides (ALLLMYRR, ANNNMYRR, GFTVVLMYRF, and GFTNNNMYRF; Mabate *et al*., 2018) were synthesized by GenScript, USA. The plasmids and strains used for complementation assay are listed in Table 4.1.

Table 4. 1: List of plasmids and strains used for complementation assay

Strains and plasmids	Description	Supplier/Reference
Plasmids		
pQE60	pQE60 vector, Amp^R	Burkholder *et al*., 1994
pQE60/DnaK	pQE60 encoding *E. coli* Hsp70 (DnaK), Amp^R	Burkholder *et al*., 1994
pQE60/KPf	pQE60 encoding DnaK/PfHsp70-1 chimera (KPf), Amp^R	Shonhai *et al*., 2005; Makhoba *et al*., 2016
pQE60/KPf-G633	pQE60 encoding KPf-G633 protein, Amp^R	This study
pQE60/KPf-G617	pQE60 encoding KPf_G617 protein, Amp^R	This study
pQE30/DnaK	pQE30 encoding *E. coli* Hsp70 (DnaK), Amp^R	This study
pQE30/DnaK-G	pQE30 encoding DnaK GGMP mutant (DnaK-G), Amp^R	This study
Strains		
E. coli dnaK756	BB2362 (*dnaK756 recA*: *TcR pDMI,1*)	Gift form Drs. B. Bukau and M. Mayer (University of Heidelberg)

4.2.2 Investigation of the ATPase activity of PfHsp70-1, DnaK, and their GGMP variants

The ATPase assay was carried out following a previously described approach (Zininga *et al*., 2017a) with slight modifications. The assay quantifies the amount of inorganic phosphate released from ATP hydrolysis thus determining the ATPase activity. To determine kinetics for the

ATPase activities of PfHsp70-1, DnaK and their variants, Michaelis–Menten plots were generated using GraphPad Prism 6.05.

To further verify the functionality of the PfHsp70-1 and its variants, the assay was repeated in the presence of typical Hsp70 substrates (ALLLMYRR, ANNNMYRR, GFTVVLMYRF, and GFTNNNMYRF; Mabate *et al*., 2018). These peptides contain stretches of hydrophobic (G, A, V, L, M, and F) and basic (L and R) amino acids which make them suitable Hsp70 substrates (Fourie *et al*., 1994). The two peptides ANNNMYRR and GFTNNNMYRF, each has three asparagine (N) residues representing the asparagine-rich proteome in *P. falciparum.* This also makes them suitable candidates for the assay involving PfHsp70-1. The substrates were titrated at varying concentrations (0-2000 nM). The data were plotted as relative ATPase activity, with the respective basal ATPase activity of each protein being presented as 100 %.

4.2.3 Investigation of the chaperone function of PfHsp70-1, DnaK and their GGMP derivatives using MDH aggregation assay

The chaperone function of recombinant PfHsp70-1, DnaK, and their GGMP variants was investigated by analyzing the ability of the proteins to suppress aggregation of heat-denatured MDH (Sigma-Aldrich, USA). The assay was conducted as previously described (Shonhai *et al*., 2008; Luthuli *et al*., 2013; Makumire *et al*., 2014; Zininga *et al*., 2016). Protein aggregation was monitored at 51 °C for 60 minutes by measuring turbidity at 340 nm at 5 min intervals using the SpectraMax M3 spectrometer (Molecular Devices, USA). Optical densities were converted to aggregation percentages relative to MDH aggregation (set as 100 %) and plotted. To further determine the effect of nucleotides on the chaperone function of the PfHsp70-1 and its GGMP derivatives, the reaction was repeated in the presence of 5 mM ATP/ADP. Additionally, following the ATPase activity assay in the presence of peptides, the aggregation assay was also repeated in the presence of varying concentrations (0-500 nM) of peptide ALLLMYRR for PfHsp70-1 and its GGMP variants. Aggregation was monitored as described above.

4.2.4 Confirmation of KPf-G617 and KPf-G633 DNA constructs

The KPf GGMP variants were generated by conservative substitution as previously described (section 2.2.1). Similar substitutions made in PfHsp70-1 were also made at positions 617 and 633 in KPf, in such a way that PfHsp70-G632 is the GGMP equivalent of KPf-G617 and PfHsp70-G648 of KPf-G633. To confirm the integrity of the pQE60/KPf plasmid constructs (Burkholder *et al*., 1994), the DNA was digested using diagnostic restriction enzymes (Appendix B19). The KPf GGMP variants were synthesized by GenScript, USA. To confirm the integrity of KPf-G617 restriction digest enzymes *Hind*III and *Bam*HI; KPf-G633 restriction digest enzymes *Hind*III and *Xba*I were used. To estimate the size of the fragments, the products were then analyzed by 0.8 % agarose gel electrophoresis (Appendix A.3). The status of the pQE60/DnaK plasmid was confirmed by using the restriction digest enzyme *Nco*I, while for pQE60/KPf the restriction digest enzyme *Kpn*I was used.

4.2.5 Complementation assay

To investigate the *in cellula* functional capabilities of the GGMP variants, a complementation assay was carried out as per procedure by Shonhai *et al*. (2005). This was conducted using an *E. coli dnaK756,* BB2362 (*dnaK756 recA*: *TcR pDMI,1*) strain whose DnaK function is compromised. The *E. coli dnaK756* strain is resistant to bacteriophage lambda (Georgopoulos, 1977), and is unable to grow above 40 °C (Georgopoulos *et al*., 1979; Tilly *et al*., 1983). This strain expresses a DnaK with three amino acid substitutions, one of which reduces its affinity for GrpE, whilst the two other substitutions elevate the basal ATPase activity of DnaK (Buchberger *et al*., 1999).

E. coli dnaK756 cells were transformed using plasmids pQE60, pQE60/KPf, pQE60/KPf-G617, pQE60/KPf-G633, pBB46 (pQE60/DnaK), pQE30/DnaK and pQE30/DnaK-G prior to being subjected to heat stress (Shonhai *et al*., 2005). Freshly transformed cells were grown overnight with shaking at 37 °C in 2xYT supplemented with 10 µg/ml tetracycline and 100 µg/ml ampicillin. Following overnight incubation, the inoculum was transferred into fresh broth and incubated under the same growth conditions. At mid-log phase (OD_{600}=0.6) of growth, cells were induced

with 1 mM IPTG. The cells were grown to OD_{600}=2.0. The cultures were standardized to the same cell density and serial dilutions were made prior to spotting onto agar plates containing the necessary antibiotics and 50 µM IPTG. Plates were incubated overnight at 37 °C and 43.5 °C respectively.

4.2.5.1 Protein production studies

In addition to the thermosensitivity studies, it was necessary to confirm the production of the various proteins. Pre-induction and post-induction samples ($O.D_{600}$=2) were collected for analysis by SDS-PAGE. The production of the various proteins was confirmed by Western blotting analysis (Appendix A7) using primary α-PfHsp70-1 antibodies (Shonhai *et al*., 2008) and monoclonal *α*-DnaK antibodies (Makhoba *et al*., 2016).

4.3 Results

4.3.1 PfHsp70-1 variants exhibit low intrinsic ATPase activity but are capable of suppressing MDH aggregation *in vitro*

Hsp70s bind nucleotides resulting in changes in their structural conformation. The findings from tryptophan fluorescence demonstrated that the conformation of the PfHsp70-1 GGMP variants was also regulated by ATP (section 3.3.7). This was in a similar manner to the wild type proteins PfHsp70-1 and DnaK (section 3.3.7). It was important to assess the ATPase activity of the variants. Their basal ATPase activity was determined by measuring the amount of inorganic phosphate (Pi) released as ATP is hydrolyzed. The Michaelis-Menten curves determined show that PfHsp70-1 exhibits a *Vmax* of 29.93 (nmol/min/mg) and a K_m of 364 µM (Figure 4.1; Table 4.2). This implies high ATP turnover rates and is comparable to what was previously determined by Zininga and colleagues (2017). The variants exhibited higher K_m values; 1,346 mM for PfHsp70-G632 and 929 µM for PfHsp70-G648 compared to PfHsp70-1 (Table 4.1). This suggests that both variants had low turnover rates compared to PfHsp70-1 (Figure 4.1B). The differences in the relative ATPase activity (as K_m) were statistically significant between PfHsp70-1 and variants as well as between PfHsp70-G648 and PfHsp70-G632 based on two-way ANOVA ($p<0.001$) (Figure 4.1 and Table 4.1).

PfHsp70-1 possesses higher intrinsic basal ATPase activity (Matambo *et al*., 2004). It was interesting to assess how the ATPase activity of DnaK would be influenced by introducing the GGMP motif of PfHsp70-1 into DnaK. Using a DnaK variant in which the GGMP motif of PfHsp70-1 was added, this study observed that the variant had higher ATPase activity as compared to DnaK. The kinetics (Table 4.1) determined from Michaelis-Menten plots (Figure 4.3A) suggest that the DnaK-G variant exhibited higher intrinsic ATP turnover rates. The differences in the relative ATPase activity were significant based on Two-way ANOVA (Figure 4.3B; $p<0.001$). This activity was also higher than that for the PfHsp70-1 GGMP variants but still lower than that of PfHsp70-1 (Figure 4.1B). This suggests that the introduction of the GGMP enhanced the ATPase activity of DnaK.

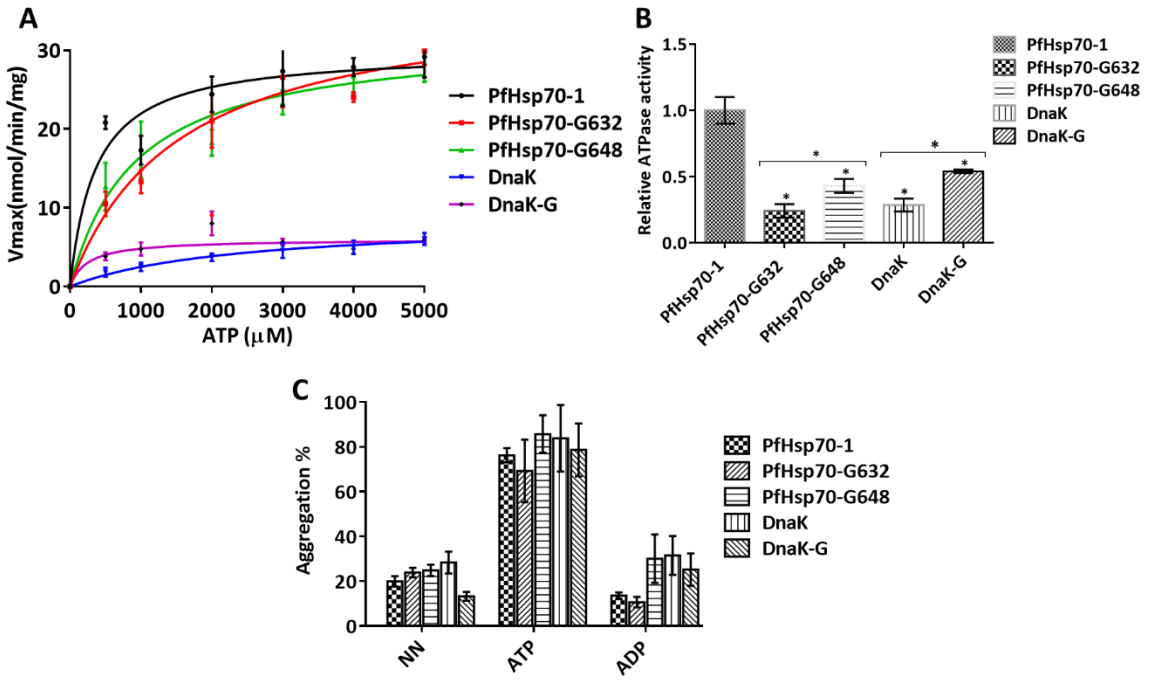

Figure 4. 1. PfHsp70-1 GGMP variants exhibit low intrinsic ATPase activity
Evaluation of the basal ATPase activities of PfHsp70-1, DnaK, and the GGMP variants. The amount of P*i* released was monitored by measuring absorbance at 595 nm using a direct colorimetric assay. (**A**) Michaelis-Menten plot of the ATPase activity. (**B**) ATPase activity of the GGMP variants relative to PfHsp70-1. (**C**) The heat-induced aggregation of malate dehydrogenase was assessed *in vitro* at 51 °C. Statistical analysis was carried out using two-way ANOVA ($p<0.001$). There were no statistically significant differences in the suppression of MDH aggregation by PfHsp70-1, DnaK and the GGMP variants.

Table 4. 2: Kinetics of the ATPase activities of PfHsp70-1 and GGMP variants

	PfHsp70-1	PfHsp70-G632	PfHsp70-G648	DnaK	DnaK-G
V_{max} (nmol/min/mg) [SD]	29.93 [±1.6]	35.72 [±2.9]	31.72 [±2.1]	8.39 [±1.2]	5.997 [±0.4]
K_m (μM) [SD]	364 [±3.5]	1346 [±4.6]	929 [±4.3]	1123.9 [±5.9]	666.0 [±1.8]

Table legends: $\mathbf{V_{max}}$ – the maximum rate of the catalysis reaction; $\mathbf{K_m}$ - is the substrate concentration at which the reaction rate is at half-maximum. At least three independent assays were carried out and results are shown as mean and standard deviations.

The Hsp70 ATPase activity has been previously shown to be enhanced by the binding of Hsp40 as well as the binding of peptide substrates (Kityk *et al*., 2012, 2015). In a separate assay, this study

further sought to investigate whether the ATPase activities of PfHsp70-1 and its GGMP variants was regulated by typical Hsp70 peptide substrates (Mabate *et al*., 2018). Under saturating ATP, there was very low or no stimulation of the ATPase activity of PfHsp70-1 by the peptides at various concentrations (Appendix B20B). Low stimulation of ATPase activity by peptide substrates has been reported for other Hsp70s (Kityk *et al*., 2012, 2015) and this validates these observations made for PfHsp70-1. The PfHsp70-G648 variant responded to stimulation by peptides to a slightly higher extent as compared to PfHsp70-1 (Appendix B20B). The PfHsp70-G632 variant, which initially exhibited the lowest ATPase activity, was highly stimulated by the peptides. Typically, the allosteric function of Hsp70 facilitates stimulation of its ATPase activity by peptides substrates (Vogel *et al*., 2006; Clerico *et al*., 2015; Chiappori *et al*., 2016). It was observed that even though the GGMP variants had low ATP turnover rates, there was minimal stimulation of the ATPase activity by the four peptides used. The minor variations in the stimulation of the ATPase activity of PfHsp70-1 and PfHsp70-G648 by the four peptides were statistically insignificant. Significant differences were observed for PfHsp70-G632 compared to PfHsp70-1 ($p<0.001$).

In order to further ascertain the chaperone activity of the GGMP variants, MDH aggregation suppression assays were conducted. MDH is an aggregation-prone protein when exposed to heat stress (Shonhai *et al*., 2008). However, PfHsp70-1 is known to suppress aggregation of MDH at 48 °C (Luthuli *et al*., 2013, Makumire *et al*., 2014, Zininga *et al*., 2016). This study sought to elucidate how mutations in the GGMP motif would affect the capability of PfHsp70-1 to suppress MDH aggregation. Following the 1:1 chaperone/substrate ratio for PfHsp70-1 determined by Zininga *et al*., 2016, the assay was conducted for the GGMP variants in comparison to PfHsp70-1 and DnaK. As an initial step, the heat stability of the various proteins was established. The recombinant chaperone proteins did not aggregate when exposed to 51 °C for 60 minutes (Appendix B21A). The chaperones are stable to temperatures above 80 °C as shown previously (Figure 3.4). As expected, in the absence of chaperones, MDH aggregated when exposed to heat stress (Appendix B21A). Wild type PfHsp70-1 and DnaK were able to suppress the aggregation of

MDH in the absence of nucleotides (Figure 4.1C). Interestingly, the variants PfHsp70-G648, PfHsp70-G632, and DnaK-G suppressed heat-induced aggregation of MDH (Figure 4.1C). Overall, the chaperones exhibited protein aggregation suppression capabilities in the range of 20-40 % (Figure 4.1C). There were no significant differences in the aggregation suppression capabilities of PfHsp70-1, DnaK and their GGMP variants (Figure 4.1C, $p<0.05$). This could suggest that the GGMP mutations did not compromise the chaperone function of PfHsp70-1 with respect to its role in suppressing MDH aggregation. As expected, there was reduced suppression of aggregation in the presence of ATP for all the recombinant proteins. In the presence of ADP, the level of suppression was similar to NN (Figure 4.1C). These findings are in line with previous reports on PfHsp70-1 showing that PfHsp70-1 equally suppresses MDH aggregation in NN and in the presence of ADP (Shonhai *et al*., 2008; Zininga *et al*., 2016). Furthermore, the introduction of the GGMP motif in DnaK resulted in both DnaK and DnaK-G exhibiting significantly similar abilities to suppress MDH aggregation at equimolar concentrations of MDH to chaperone (Figure 4.1C; $p<0.0$. However, upon titrating DnaK and DnaK-G, the DnaK-G variant was more effective in suppressing MDH aggregation. This was observed at lower concentrations (0.2 μM and 0.4 μM) of the chaperones to 0.8 μM of MDH (Appendix B21B; $p<0.001$). This suggests that the addition of the GGMP repeats to the C-terminal end of DnaK improved its chaperone activity. This seemed to mirror findings from the ATPase activity showing that DnaK-G has higher ATPase activity compared to DnaK. Overall, the data showed that the DnaK-G variant possessed better chaperone activity than DnaK.

Earlier findings showed that the recombinant proteins bind to the model peptide substrate resulting in quenching of intrinsic tryptophan fluorescence (Appendix B18). In line with these findings, the MDH aggregation assay was repeated in the presence of peptide (ALLLMYRR). Peptide ALLLMYR was chosen following preliminary data showing that the peptide binds Hsp70s with high affinity as obtained using SPR (Mabate *et al*., 2018). The MDH aggregation suppression function of PfHsp70-1 and its GGMP variants was reduced as the concentration of the peptide ALLLMYRR increased (Appendix B21C). However, PfHsp70-1 managed to suppress MDH

aggregation (below 40 %) at the highest concentration (500 nM) of peptide used. The variant PfHsp70-G648 was observed to follow a similar aggregation suppression pattern as PfHsp70-1. The aggregation suppression capability of PfHsp70-G632 was greatly reduced as the peptide concentration increased, reaching about 80 % aggregation (Appendix B21C). These findings suggest that the Hsps bind the peptide substrates releasing MDH to aggregate. Variant PfHsp70-G632 seemed to be highly inhibited by peptide ALLLMYRR as its suppression ability was greatly reduced. This seems to agree with the data from the ATPase activities, where PfHsp70-G632 activity was enhanced in the presence of peptide.

4.3.2 Substitutions in the GGMP motif do not abrogate the KPf chaperone function *in cellula*

To further ascertain the chaperone activity of PfHsp70-1, DnaK and their GGMP variants, an *in cellula* system was employed as described previously (Shonhai *et al*., 2005; Makhoba *et al*., 2016). A chimeric Hsp70 comprised of the NBD from DnaK and the SBD from PfHsp70-1 (KPf; Shonhai *et al*., 2005) has previously been shown to reverse thermosensitivity of the *E. coli dnaK756* strain better that PfHsp70-1 (Shonhai *et al*., 2005). KPf is thought to interact with *E. coli* co-chaperones DnaJ and GrpE in the nucleotide exchange function. This chimeric protein of PfHsp70-1 complements for the compromised DnaK in *E. coli dnaK756* cells effectively (Shonhai *et al*., 2005; Makhoba *et al*., 2016). Hence, KPf with GGMP mutations mirroring the PfHsp70-1 GGMP variants was used in the complementation assay. The *E. coli dnaK756* cells transformed with the various plasmids grew at a permissible temperature of 37 °C (Figure 4.2A). These observations suggest that *E. coli dnaK756* growth was not compromised. On the other hand, at an elevated temperature of 43.5 °C, cells transformed with the vector plasmids pQE60 and pQE30 (negative controls) were unable to survive. The cells transformed with pQE60/DnaK and KPf as positive controls grew at 43.5 °C. It is worth noting that KPf conferred cytoprotection better than DnaK. It is known that DnaK is toxic if expressed in excess (Blum *et al*., 1992). Cells transformed with KPf-G617 and KPf-G633 were also able to grow at 43.5 °C. These data suggest that there was no deficiency in the function of the PfHsp70-1 GGMP variants. However, the cells transformed with

the DnaK-G variant failed to grow at 43.5 °C (Figure 4.2A) although the recombinant protein was produced at high levels (Figure 4.2B). This suggests that insertion of GGMP repeat into DnaK led to poor chaperone activity *in cellula.*

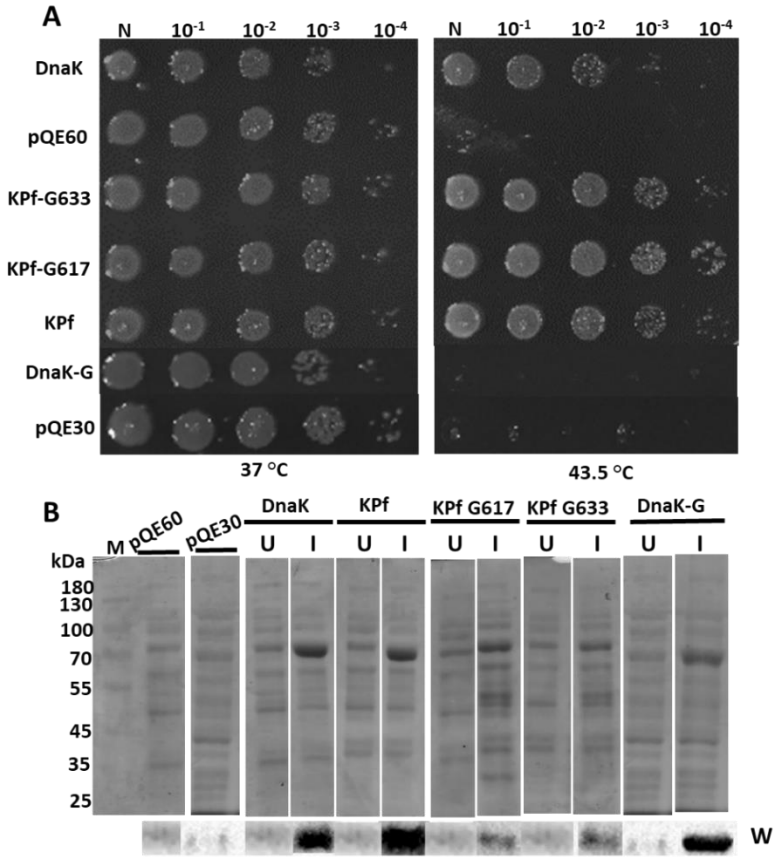

Figure 4. 2. Mutation of part of the GGMP motif did not abrogate the *in cellula* function of KPf
(**A**) *E. coli dnaK756* cells transformed with plasmid constructs expressing KPf and its GGMP repeat mutants were incubated at 37 °C and 43.5 °C. The negative control consisted of cells transformed with pQE60 plasmid vector whilst the positive control was represented by cells transformed with the pQE60/DnaK plasmid. (**B**) SDS-PAGE analysis for the exogenous expression of chimera KPf and its GMMP variants in *E. coli dnaK756* cells. The labels on the top of the gel panels represent the different proteins that were expressed as well as the vector control (pQE60). Lanes **U** and **I** represent the sample that was taken before induction and 5 hours after induction with IPTG, respectively. Molecular weight markers (lane M) in kDa are shown in the extreme left-hand side lane. Western analysis (**W**) of the various proteins was conducted using α-DnaK antibodies. The SDS-PAGE analysis was performed on 12 % SDS gel under reducing conditions.

4.4 Discussion

The GGMP repeats are strongly represented in Hsp70s of parasitic origin in comparison to humans (Table 1.3). To decipher the function of this motif, ATPase activity, MDH aggregation suppression, and complementation assays were conducted. PfHsp70-1 exhibited higher ATPase activity than DnaK and the GGMP variants (Figure 4.1; Table 4.1) in agreement with previous reports showing that PfHsp70-1 possesses higher intrinsic ATPase activity (Matambo *et al*., 2004; Zininga *et al*., 2016). The GGMP variants exhibited significantly lower ATPase activity. The ATPase activity of PfHsp70-G632 was significantly suppressed compared to PfHsp70-G648. The docking of the SBD subdomains on the NBD, upon ATP binding, has an inhibitory effect on the ATPase activity (Kityk *et al*., 2015). It is possible that the introduced mutations in the GGMP motif enhanced SBD docking on NBD thereby furthering the inhibition of the ATPase activity of the PfHsp70-1 variants.

Additionally, the ATPase activity of the GGMP variants of PfHsp70-1 was determined in the presence of a peptide substrate. Peptide substrates are known to regulate the ATPase activity of Hsp70s through allosteric regulation. Peptide substrates were also previously demonstrated to bind the Hsp70s resulting in quenching of fluorescent intensity (Appendix B17). Hence, the study sought to assess the ATPase activity of PfHsp70-1 and its GGMP variants in the presence of peptide substrates. Findings showed that GGMP mutations at both position 632 and 648 lowered the ATPase activity of PfHsp70-1, although PfHsp70-G632 was significantly affected. The ATP hydrolysis rates were observed to be stimulated variably by the different peptide substrates. PfHsp70-1 and PfHsp70-G648 seemed to be marginally stimulated whereas PfHsp70-G632 exhibited a higher degree of stimulation by the peptide substrates. However, the stimulation for PfHsp70-G632 was very low, in the range (0-1.2-fold). This is consistent with reports that the binding of peptide substrate to the SBD stimulates the ATP hydrolysis rates to a less degree (Kityk *et al*, 2012, Kityk *et al*., 2015) than in the presence of both substrate and Hsp40 (Misselwitz *et al*., 1998; Laufen *et al*., 1999; Silberg *et al*., 2004). This study further established that the GGMP insertion enhanced the ATPase activity of DnaK, an Hsp70 that does not natively possess the

GGMP motif. PfHsp70-1 is known to possess significantly high basal ATPase activity compared to other Hsp70s (Shonhai *et al*, 2008; Zininga *et al*., 2016), hence the higher ATPase activity of DnaK-G could be attributed to the presence of GGMP motif of PfHsp70-1. ATP hydrolysis, substrate recognition, and binding are all important functional aspects of Hsp70.

In the current study, PfHsp70-1, DnaK, and their GGMP variants all managed to suppress heat-induced MDH aggregation (Figure 4.1). There were no significant differences in the activity of PfHsp70-1, DnaK and their GGMP variants at equimolar concentrations (0.8 µM) of chaperone to MDH ($p<0.05$). It is interesting to note that the GGMP insertion enhanced the MDH aggregation suppression capability of DnaK-G at lower concentrations of the chaperone (0.2 µM and 0.4 µM). Based on the current findings from the DnaK-G variant, it is possible that the GGMP serves to bind substrate or influences substrate binding. Recent studies have reported that a GGAP motif in yeast Hsp70 is responsible for binding substrates (Gong *et al*., 2018). A similar function could be proposed for the GGMP motif. Additionally, Smock *et al*. (2011) identified a 15-residue motif (**DDVVDAEFEEVKDKK**; position 623-638) that acted as an auxiliary substrate binding site in the lid segment of DnaK. This motif enhanced the chaperone function of DnaK. Such a motif might mirror the GGMP motif in PfHsp70-1 although there is no conservation between the two motifs.

Hsp70s bind to hydrophobic patches of the substrate thus preventing the aggregation of proteins. Suitable Hsp70 peptides substrates possess stretches of hydrophobic and basic amino acids. The current study used synthetic peptides to ascertain the ability of the peptide substrate to influence the chaperone activity of the Hsp70s in the presence of another substrate, MDH. The addition of peptide substrate ALLLMYRR resulted in a general increase in MDH aggregation (Appendix B21). The peptide is mainly comprised of hydrophobic residues hence the Hsp70s might have preferred binding to the peptide ALLLMYRR. Therefore, the peptide inhibited suppression of MDH aggregation. Peptide-induced inhibition of MDH aggregation was most associated with the variant PfHsp70-G632 compared to PfHsp70-1 and PfHsp70-G648. The GGMP mutation at position 632 is closer to the substrate binding cleft than the N-terminal G648 variant. It is possible

the C-terminal GGMP repeats are of importance in substrate binding. Overall, findings from the MDH aggregation suppression assay suggest that the GGMP repeats may contribute towards substrate binding. Substrate binding might be dependent on the specific positioning of a particular repeat in the GGMP motif of PfHsp70-1.

This study further involved analysis of the *in cellula* chaperone function of the GGMP variants using a chimeric Hsp70 (KPf) as a model. KPf is a robust chaperone capable of reversing thermosensitivity of the *E. coli dnaK756* strain (Shonhai *et al*., 2005; Makhoba *et al*., 2016). KPf contains an SBD from PfHsp70-1 hence should recognize *E. coli* proteins and salvage them under cell stress conditions (Makhoba *et al*., 2016). KPf is also able to communicate with *E. coli* co-chaperones that binds in the NDB of DnaK. These co-chaperones regulate the KPf chaperone function. Further complementation studies revealed that GGMP mutant forms of KPf were functional in *cellula* (Figure 4.2). However, KPf-G617 seemed to confer cytoprotection to a slightly higher extent than both KPf and KPf-G633 (Figure 4.2). On the other hand, DnaK-G failed to suppress thermosensitivity. It is also possible that the insertion of the GGMP motif in DnaK caused the protein not to recognize and bind *E. coli* proteins despite the ability of DnaK-G to suppress MDH aggregation *in vitro*. The GGMP motif was inserted eight residues away from the auxiliary binding site for substrates in DnaK. The change in secondary structure, from unordered to a short helix in this region (section 2.3.4), could account for the failure by DnaK-G to bind *E. coli* substrates.

Overall, this study demonstrated that the PfHsp70-1 GGMP variants exhibit low ATPase activity but retain the Hsp70 chaperone function *in vitro*. Using a protein that does not natively possess the GGMP motif, this study also showed that the motif enhanced the chaperone function of DnaK *in vitro*. Chimeric KPf GGMP forms were shown to be functional *in cellula*. Each GGMP repeat in the motif might play a particular function relative to its positioning in the GGMP motif of PfHsp70-1. Findings from this study demonstrated that the C-terminal GGMP repeats are possibly important for substrate binding.

Chapter 5

Structure-function analysis of PfHop

Chapter 5

Structure-function analysis of PfHop

5.1 Introduction

Molecular chaperones are proteins involved in protein quality control and are responsible for maintaining proteostasis. Co-chaperones form a set of proteins that modulate the activities of molecular chaperones. The co-chaperone STI1, also known as Hsp70/Hsp90-organizing protein (Hop), cooperates with Hsp70 and Hsp90 in protein folding and maturation of client proteins. The general structure of Hop comprises three TPR domains and two DP domains (TPR1-DP1-TPR2A-TPR2B-DP2; Odunuga *et al*., 2004). The TPR domains are made up of helix-turn-helix structures while the DP1 and DP2 domains consist of six and five helices, respectively (Blatch and Lassle, 1999; Schmid *et al*., 2012). TPR motifs are protein-protein binding modules (Zeytuni and Zarivach, 2012). Interaction of Hop with Hsp70 is sequential, first through the TPR1 domain and then the TPR2B domain. Sequential binding is important for substrate transfer to Hsp90. Interaction with Hsp90 occurs via the TPR2A domain (Kajander *et al*., 2009, Schmidt *et al*., 2012, Zininga *et al*., 2015b). Binding of the TPR domains of Hop to Hsp70 and Hsp90 facilitates client protein transfer from Hsp70 to Hsp90 (Röhl *et al*., 2015). The chaperone function of both Hsp70 and Hsp90 is regulated by ATP. ATP has an inhibitory effect on the association between Hop with either Hsp70 or Hsp90. When bound to Hsp90, Hop inhibits hydrolysis of ATP by Hsp90 (reviewed in Jackson, 2012). There has been a long-held view that Hop does not bind and hydrolyze ATP, but a recent study suggested that human Hop possesses an ATPase domain (residues 1-359; Yamamoto *et al*., 2014). However, it is not yet clear whether this ATPase domain of Hop shares similarities with other known ATPases.

A *P. falciparum* Hsp70-Hsp90 organizing protein (PfHop) which co-localizes in the parasite cytosol and nucleus has been previously described (Gitau *et al*., 2012). However, there is insufficient biophysical data on PfHop. Using size-exclusion chromatographic analysis, Gitau and colleagues (2012), showed that PfHop exists together in a complex with PfHsp90 and PfHsp70-1 in *P. falciparum* cells. The expression of PfHop is also stress-induced (Gitau *et al*., 2012, Zininga *et al*., 2015b). This suggests that PfHop plays a significant role by modulating the functional partnership between PfHsp70-1 and PfHsp90 particularly under stressful conditions. Conditions such as

periodic fever episodes that characterize clinical malaria are unfavorable to proteostasis. The clients for Hsp90 are mostly receptors and if Hop is inhibited then the cellular signal transduction system and function of kinases is compromised. Therefore, inhibition of PfHop will likely result in the death of the parasite. A fair degree of divergence has been shown to exist between PfHop and *Homo sapien* Hop (Gitau *et al*., 2012; Hatherly *et al*., 2015). There is needed to further investigate the structure and role of PfHop as a possible antimalarial target. This study sought to investigate the biophysical characteristics of PfHop that make it amenable to serve as a module that brings PfHsp70-1 and PfHsp90 into a functional complex.

The specific objectives of this study were to:

i. heterologously express and purify of PfHop;

ii. determine the secondary and tertiary structure of PfHop;

iii. establish the oligomerization status of PfHop;

iv. assess the ability of PfHop to bind nucleotides and hydrolyze ATP, and to

v. probe conformational changes of PfHop in the presence of ATP and ADP.

5.2 Experimental Procedures

5.2.1 Materials

Reagents and materials used in this study are listed in Appendix C1. The strains and plasmids used are listed in table 5.1.

Table 5. 1: Plasmids and strains used for recombinant PfHop production

Strains and plasmids	Description	Supplier/Reference
Plasmids		
pQE30/PfHop	pQE30 encoding PfHop, Amp^R	Gitau *et al*., (2012); Zininga *et al*., (2015b)
Strains		
***E. coli* JM109 DE3**	e14– (McrA–) recA1 endA1 *gyr*A96 thi-1 hsdR17 (rK – mK+) supE44 *rel*A1 Δ(*lac*-proAB) (F´ traD36 proAB *lac*Iq ZΔM15)	Thermofischer Scientific, USA
Antibodies		
α-PfHop	Peptide specific rabbit raised antibody against PfHop	Gitau *et al*., (2012); Zininga *et al*., 2015b)

5.2.2 Confirmation of pQE30/PfHop DNA construct

The plasmid pQE30/PfHop expressing recombinant PfHop was previously described (Gitau *et al*., 2012; Zininga *et al*., 2015b). To confirm the integrity of the plasmid construct encoding the recombinant PfHop protein, restriction digest analysis was performed using enzymes *Xho*I and *Pst*I and this was analyzed by agarose gel electrophoresis (Appendix A.2 and A.3). This was further confirmed through DNA sequencing (Appendix A.5).

5.2.3 Expression and purification of recombinant PfHop protein

The plasmid construct pQE30/PfHop was transformed into *E. coli* JM109 (DE3) cells (Appendix A.4). Expression of recombinant PfHop followed a method previously described (Section 3.2.4). Protein expression samples collected at hourly intervals were analyzed using 12 % SDS-PAGE and visualized using Coomassie (Appendix A.6). Expression of PfHop was confirmed by Western blotting analysis using peptide-specific α-PfHop (Gitau *et al*., 2012) and α-His antibodies (Appendix A.7). Bands were visualized with ECL using a ChemiDoc (BioRad, USA) (Appendix A.8).

Purification of recombinant PfHop was conducted using nickel affinity chromatography as previously described (Gitau *et al*., 2012, Zininga *et al*., 2015b) with slight modifications (Section 3.2.5.1). Samples were collected for analysis by SDS-PAGE to assess the purity of the proteins and confirmation by Western blot using α-PfHop and α-His antibodies. To exclude DnaK contamination in purified PfHop, Western blotting using α-DnaK antibodies (Enzo Life Sciences, Switzerland) was conducted. Dialyses of the purified recombinant protein was carried out extensively overnight using SnakeSkin dialysis tubing 10 000 MWCO (ThermoScientific) in dialysis buffer (20 mM Tris-HCl, pH 7.5, 10 mM NaCl, 5 % (v/v) glycerol, containing 0.2 mM TCEP).

5.2.3.1 Ion Exchange Chromatography

As a second purification step, anion exchange chromatography was carried out as previously described (Section 3.2.5.2). PfHop protein was eluted by applying buffer B (20 mM Tris-HCl; pH 7.5, 1 M NaCl containing 0.2 mM TCEP) to the column in a linear NaCl gradient, initially from 0 to 0.5 M over 30 min and then 0.5 M to 1 M for 10 min. The protein was eluted (1 ml per well) in a 96 well plate and samples from the eluted fractions corresponding to the main peak were analyzed by SDS-PAGE.

5.2.3.2 Size Exclusion Chromatography

Following IEC, protein samples from the collected fractions were resolved by SDS-PAGE. The remaining proteins were pooled together and loaded onto a HiLoad 16/600 Superdex^{TM} 200 pg column connected onto an Akta FPLC system (section 3.2.5.3). The flow rate was set at 0.3 ml/min and a maximum pressure of 0.5 MPa following the manufacturer's instructions (GE Healthcare, USA). The protein was eluted, as 0.5 ml fractions per well in a 96 well plate. Samples were resolved by SDS-PAGE to determine the purity and homogeneity of the PfHop protein. To confirm the identity of PfHop, MALDI-TOF mass spectrometry was applied.

5.2.4 Molecular weight determination of PfHop by multi-angle static light scattering

To determine the molecular weight of recombinant PfHop, analytical SEC was performed on a Superdex S200 increase 10/300 GL column (GE Healthcare, USA) on an Akta FPLC (Amersham Biosciences, UK). The Akta system was coupled to a mini-DAWN TREOS multi-angle static light scattering (MALS) detector (Wyatt, USA) and a RefraMAx520 differential refractometer (Wyatt) for absolute molecular weight determination. This was conducted following a previously described method (Ruskamo *et al*., 2012 and Ignatev *et al*., 2012). Briefly, 100 µg of protein suspended in running buffer C was injected into the column at maximum pressure 4 MPa and the flow rate was 0.5 ml/min. BSA and Ovalbumin were run as molecular weight controls. The molecular weight of PfHop was resolved based on the measured light scattering and refractive index and/or UV absorbance using the ASTRA software (Wyatt, USA).

5.2.5 Secondary structural organization of PfHop

In order to investigate the secondary structure of PfHop, the protein was dialyzed in buffer P (10 mM KH_2PO_4 pH 7.5) with 150 mM NaF. Synchroton radiation circular dichroism (SRCD) spectroscopy measurements were carried out using a UV-CD12 beamline with a temperature-controlled cell holder. Recombinant PfHop (0.5 mg/mL) was suspended in buffer P and analysis was done using a 98.56 µm path length Suprasil round cell cuvette at a constant temperature (10 °C). A total of three spectral scans were recorded and averaged from 280 to 175 nm. The SRCD data was processed and secondary structure deconvolution was performed on the Dichroweb server (Lobley *et al*., 2002), using the CDSSTR algorithm (Compton and Johnson, 1986) and the SP175 reference database.

To investigate the effect of heat on PfHop CD spectral scans were conducted at 192, 193, 210 and 220 nm as the temperature was increased monotonically from 10 to 90 °C in 1 °C per min. This was also repeated using conventional CD spectroscopy on a Jasco J-1500 (JASCO Ltd, UK), in a 2-mm quartz cuvette to validate findings from SRCD. Furthermore, the effects of urea as a denaturant on the stability of PfHop was monitored on a J1500 CD spectrometer (JASCO Ltd, UK). Molar residue ellipticity at 222 nm was assessed in the presence of an increasing concentration

of urea (0-8 M). To calculate the folded fraction of the protein at a given temperature or urea concentration, equation 1 (section 3.2.) was used.

5.2.6 PfHop tertiary structure determination using fluorescence spectroscopy

Using tryptophan fluorescence-based analysis, the effect of nucleotides on the tertiary structure of PfHop was monitored as previously described (Section 3.2.7; Zininga *et al*., 2016). Initially, as controls, tertiary structure perturbation was performed in the presence of varying concentrations of known denaturants, urea (0-8 M) and GdHCl (0-6 M). This was also repeated in the additional presence of nucleotides (5 mM ATP or ADP).

5.2.7 Investigation of nucleotide-dependent conformational changes of PfHop using limited proteolysis

To further ascertain nucleotide-dependent conformational changes on PfHop, partial tryptic digestion of recombinant PfHop was carried out. This was conducted in the buffer (50 mM Tris-HCl, pH 8.0; 5 mM $MgCl_2$) supplemented with 5 mM ATP or ADP as per protocol (Zininga *et al*., 2016). Briefly, recombinant PfHop at 4 µM was digested at 30 °C using 0.25 ng/ml trypsin (Sigma Aldrich, USA) and samples were collected at 0-, 10-, 30- and 60-min intervals and prepared for SDS-PAGE analysis (Appendix A.6). Western blot analysis was used to detect PfHop fragments using α-His (Sigma-Aldrich, U.S.A) and α-PfHop antibodies (Gitau *et al*., 2012) (Appendix A.7).

5.2.8 Assessment of the oligomerization status of PfHop

Previous studies speculated that PfHop may exist in higher-order oligomers (Gitau *et al*., 2012). Additionally, during the early stages of optimizing the purification of PfHop, higher-order species of PfHop were observed (Figure 5.2B) leading to speculation that PfHop may oligomerize as has been previously reported (Zininga *et al*., 2015b). It was necessary to perform follow up studies. To explore the ability of PfHop to self-associate, protein-protein interaction assays were conducted on a Proteon XPR36 surface plasmon resonance (SPR) machine using a GLC sensor chip (BioRad, USA) as described (Zininga *et al*., 2015b).

5.2.9 Investigation of the nucleotide binding affinity of PfHop using SPR

Hop acts as an adaptor molecule bringing together Hsp70 and Hsp90 into a functional complex. Hsp70 and Hsp90 are ATPases whose chaperone function is regulated by nucleotides. It has been proposed that Hop may independently bind to ATP (Yamamoto *et al*., 2014). The current study sought to investigate the ability of PfHop to bind nucleotides. This was analyzed using SPR following the described protocol (Zininga *et al*., 2016).

5.2.10 Investigation of basal ATPase activity of PfHop

Studies by Yamamoto *et al*. (2014) revealed that Hop binds and slowly hydrolyzes ATP. The current study elucidated if PfHop exhibited a similar function. The basal ATPase activity assay was carried out following a previously described approach (Zininga *et al*., 2015b; 2017). Recombinant PfHop (0.4 µM) was incubated for 5 min in HKMD buffer. As a positive control, recombinant PfHsp70-1 was used as it possesses known ATPase activity and the reaction mix with boiled protein was used as a non-enzymatic control. To determine the kinetics for the ATPase activity of PfHop, Michaelis-Menten plots were generated using GraphPad Prism 6.05.

5.3 Results

5.3.1 Confirmation of pQE30/PfHop DNA construct

The identity of the pQE30/PfHop plasmid construct was confirmed by sequencing and restriction digest analyses using *Xho*I and *Pst*I restriction endonucleases (Appendix B22). The size of the cleaved DNA corresponded to the predicted sizes of 1855 bp and 3416 bp representing the insert and vector respectively.

5.3.2 Expression and purification of recombinant PfHop protein

Recombinant PfHop protein was successfully expressed as an N-terminal His fusion protein in *E. coli* JM109 cells (Figure 5.1A).

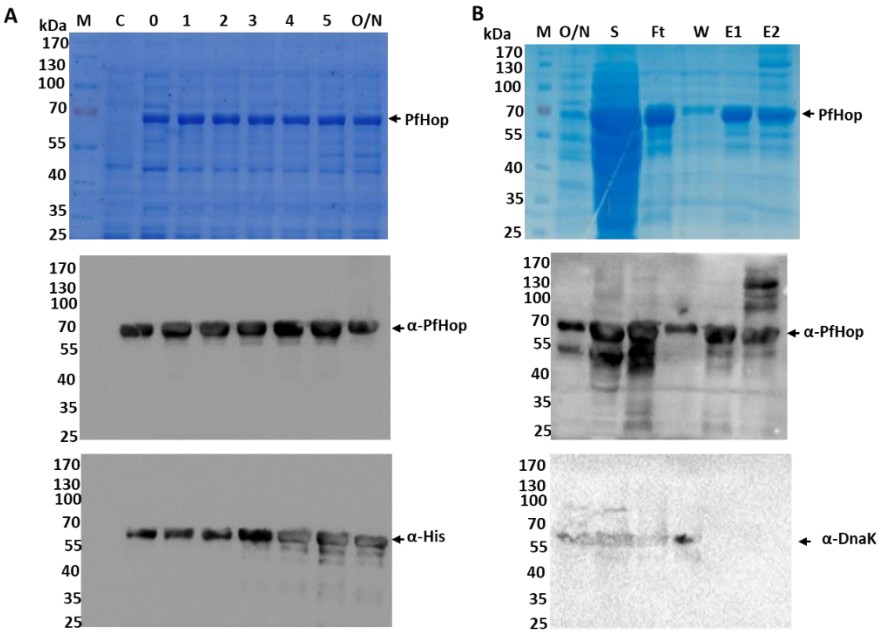

Figure 5.1. Analysis of the expression and purification of PfHop in *E. coli* JM109
(A) Analysis of the expression of PfHop JM109 cells using SDS-AGE. Lane M: represents molecular weight markers (in kDa); Lane 0: represents the total extract of cells transformed with pQE30/PfHop plasmid before IPTG induction; lanes 1-5 represent hourly samples collected and lane O/N: total extract of cells transformed with pQE30/PfHop after induction overnight. (**B**) Ni-NTA Purification of PfHop expressed in JM109 cells. Lane S: the soluble fraction; lane Ft represents the protein that does not bind to the Ni-NTA (flow-through); lane W: represents samples collected after the washing step and lanes E1, E2 represent PfHop elution fractions. Lower panels: Confirmation of the purified PfHop protein by Western blot using α-PfHop. DnaK contamination was also confirmed using α-DnaK. The SDS-PAGE analysis was performed on 12 % SDS gel under reducing conditions.

Chapter 5

Structure-function analysis of PfHop

Previous expressions in *E. coli* XL1 Blue cells showed that PfHop expressed together with a truncated version of PfHop that migrated at 55 kDa (Gitau *et al*., 2012). This truncated 55 kDa version of PfHop was lowly observed in protein expressed in *E. coli* JM109 cells (Figure 5.1A). The protein migrated as a 66 kDa species on SDS-PAGE and was confirmed by Western blot analysis (Figure 5.1, lower panels; Gitau *et al*., 2012; Zininga *et al*., 2015b). The His-tag facilitated the purification of PfHop by Ni-NTA affinity chromatography (Figure 5.1B). A considerable amount of the protein passed through the matrix as flow-through (Figure 5.1B, lane Ft). Most of the protein together with other impurities remained bound during washes (Figure 5.1B, lane W). Some of the impurities (other proteins) co-eluted with PfHop (Figure 5.1B, lanes E1 and E2). In elution three (E2), bands above and below the 66 kDa molecular weight of PfHop were observed during SDS-Page and Western blotting. These were speculated to be either higher-order forms of PfHop that were probably resistant to SDS and heat treatment or fragments of PfHop. It is also possible that these could be other protein contaminants. Western blot analysis using α-DnaK antibodies confirmed the absence of DnaK contamination in the eluted protein (Figure 5.1B, lower panel). This eliminates the effect of DnaK in downstream applications. The PfHop protein eluted with more impurities (proteins of lower and higher molecular weight) compared to observations by Gitau *et al*. (2012).

Subsequent to the Ni-NTA purification of PfHop, ion exchange chromatography (IEC) was performed to further purify PfHop from impurities. (Figure 5.2A). The buffers used for this purification were pH 7.5. PfHop has an isoelectric point of 6.63 and was negatively charged under the assay conditions. This facilitated binding to the positively charged MonoQ column. PfHop was eluted from the column at a low salt concentration (Figure 5.2A; peak 1). Anion exchange chromatography removed most of the protein impurities leaving only PfHop as observed on SDS-PAGE (Figure 5.2A; insert). After IEC, the larger molecular weight bands initially speculated to be SDS or heat resistant PfHop dimers were absent. This could suggest that the large molecular weight species were contaminants that were eliminated by IEC.

Fractions collected from the IEX were pooled for analysis using size exclusion chromatography. The observed elution profile indicates that native PfHop is monomeric in solution (Figure 5.2B). However, a minor peak was also observed just before the main PfHop elution peak. This small peak may be due to PfHop forming higher-order oligomers. However, fractions from the main peak were associated with the presence of a single band with a molecular mass of 66 kDa (Figure 5.2B; insert). The protein was confirmed to be PfHop by sequencing with MALDI-TOFF (Appendix B13).

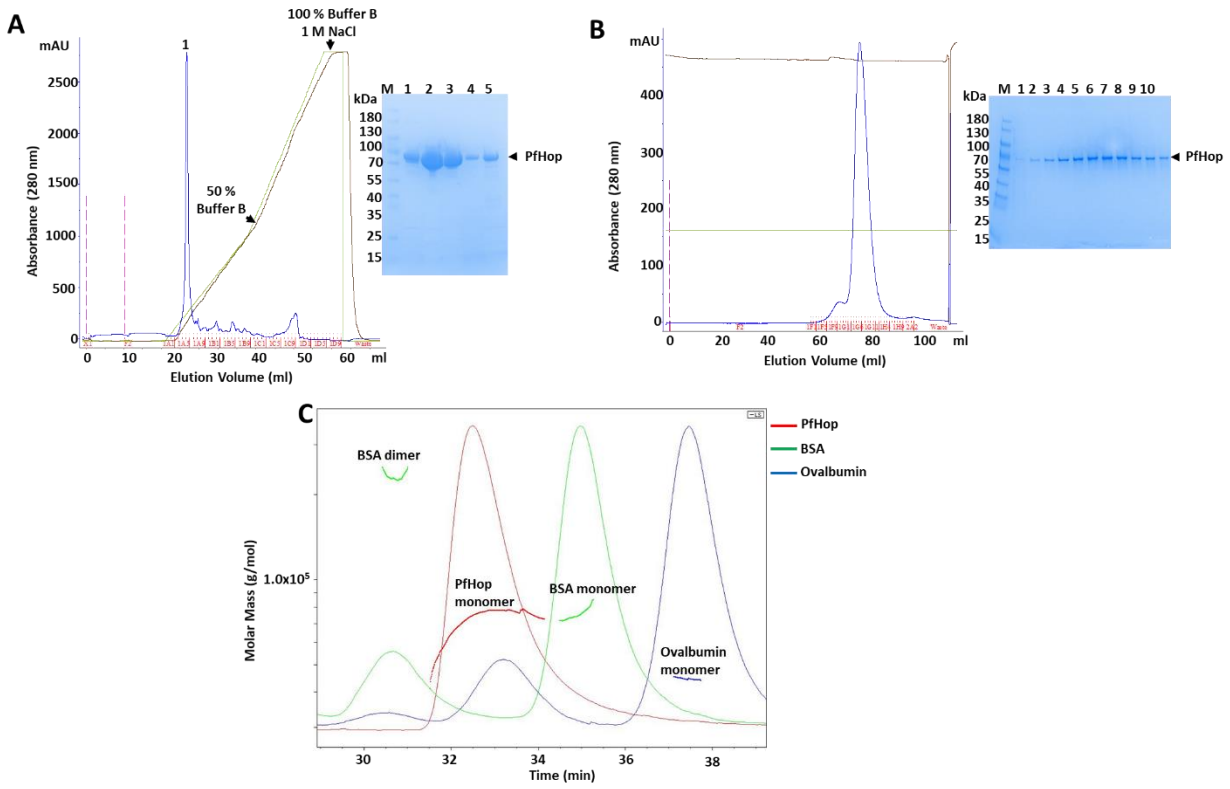

Figure 5.2. Ion exchange chromatography and size exclusion chromatographic analyses of PfHop
(**A**) Protein elution was monitored with an A 280 absorbance trace (blue line). The protein that bound to the column was then eluted by an increasing NaCl gradient (brown line) monitored as conductivity (lime green line). The SDS-PAGE analysis of the protein fractions from peak 1 (insert; lanes 1-5). (**B**) Freshly purified PfHop was analyzed by analytical size exclusion chromatography in 10 mM Tris-HCl, 150 mM NaCl, pH 7.5 using a Superdex Hiload S200 column. Analyses of the purified protein from the main peak after SEC was conducted using 12 % SDS-PAGE under reducing conditions (insert; lanes 1-10). (**C**) SEC-MALS analysis of purified PfHop with BSA and Ovalbumin as controls. The molecular weights are represented as horizontal lines.

SEC coupled with static light scattering (SLS) was conducted to determine the molecular weight and oligomeric status of PfHop in solution (Figure 5.2C). BSA and ovalbumin are standard proteins used for column calibration (Ruskamo *et al*., 2012). Consistent with SEC data, the SLS data also clearly shows PfHop eluting with a single peak, demonstrating that PfHop is indeed monomeric (Figure 5.2C). However, despite having almost similar molar masses, BSA and PfHop elute differently with PfHop eluting first. This implies that PfHop has a relaxed/elongated structure compared to the more compact BSA. SEC-MALS estimates the molecular weight for PfHop as 73 ± 2.96 kDa, which is slightly different from the 66 kDa for the PfHop monomer reported by Gitau *et al*. 2012 or as calculated from the amino acid sequence using the Protparam tool (https://web.expasy.org/protparam/). This could be attributed to the fact that the molar mass distribution of PfHop is uneven (Figure 5.2C) as there is an increase in MW across its elution peak. This observed increase in MW is inconsistent with SEC-MALS theory and was also reported by Zhao *et al.* (2012). Ideally, the MW of a protein is supposed to decrease as the elution time increases. Upward increases in MW distribution have been attributed to changes in the refractive index, the concentration of the protein sample and the solvent (Zhao *et al.,* 2012). This would make the molecular weight average of PfHop estimated to be higher than 66 kDa. A more plausible explanation could be the conformational changes in the protein in the two analyses. The protein behaves differently when denatured and run on an SDS-PAGE gel compared to the passage of the soluble protein through a gel filtration matrix (Hagel, 2001).

5.3.3 PfHop exhibits a strongly helical disposition

Synchrotron radiation circular dichroism (SRCD) spectra were recorded for full-length protein to evaluate the folding state and secondary structure composition of recombinant PfHop. The PfHop spectrum exhibited two negative minima at 222 nm and 208 nm and a positive peak at 194 nm (Figure 5.3A) characteristic of mostly helical proteins (Whitmore and Wallace, 2008). The Dichroweb server was used for deconvolution and PfHop was observed to be mainly α-helical comprising of 50 % α-helices, 16 % β-sheets, 10 % β-turns, and 23 % unordered. The stability of PfHop secondary structure was monitored at 192, 193, 210 and 220 nm, as the temperature was increased to 90 °C (Figure 5.3C). PfHop lost almost 50 % of its folded fraction around 45 °C (Figure

5.3D). Similar results were also observed when using conventional CD spectroscopy (Appendix B23). As a control, urea was used to validate that PfHop undergoes structural perturbation when denatured (Appendix B23D-E). PfHop remained stable in 4 M urea and unfolded beyond this (Appendix B23D). About 50 % of the protein is unfolded at 5 M urea (Appendix B23E). As expected, the unfolding of PfHop was dependent on the urea concentration (Appendix B23E) proving that the protein was sensitive to chemical denaturation.

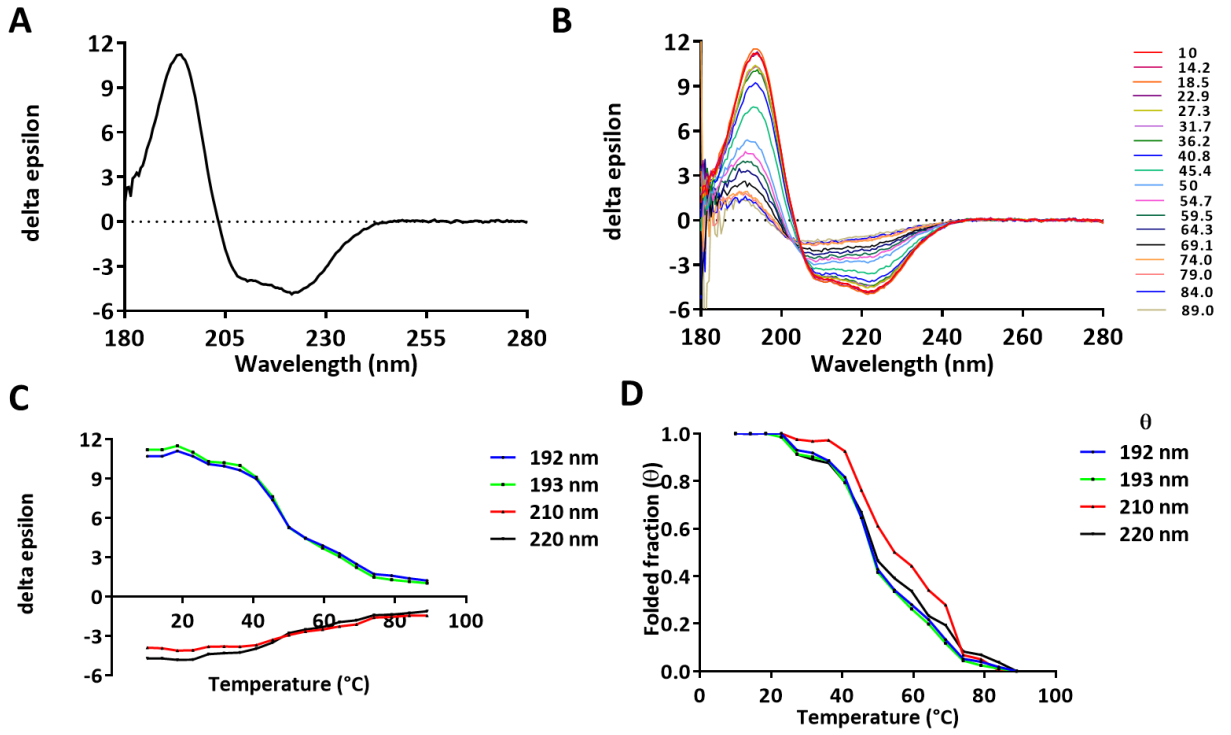

Figure 5.3. Analysis of the secondary structure of PfHop
(**A**) High-resolution SRCD spectrum of full-length PfHop. (**B**) SRCD spectral scans were conducted with an increase in temperature from 10 °C to 90 °C, causing PfHop to unfold. (**C**) Thermal melting of PfHop permanently abrogated the secondary structure. (**D**) The folded fraction of PfHop under varying temperatures as calculated using equation 1 (section 3.2.6.1).

5.3.4 PfHop undergoes conformational changes in the presence of nucleotides

Tryptophan fluorescence was used to investigate the tertiary structural organization of PfHop. PfHop possesses one tryptophan residue at position 74 (W74). Initially, GdHCl and urea were used as chemical denaturants to assess the unfolding of PfHop. The emission maxima red shifted with an increase in GdHCl and urea concentrations (Figure 5.4A). The tryptophan fluorescence

changes revealed red shift emission maxima with peaks at 347 nm and 340.1 nm corresponding to 6 M GdHCl and 8 M urea respectively (Figure 5.4). This shows that PfHop is more sensitive to GdHCl (stronger denaturant than urea), a phenomenon that was previously reported for Hsps of *P. falciparum* origin (Misra and Ramachandran, 2009). The assay was then performed in the presence of either ATP or ADP (Figure 5.4B). Nucleotides were incubated with recombinant PfHop to assess conformational changes in response to their binding. PfHop assumed different conformational states in the absence of nucleotides compared to the presence of ADP or ATP. In the nucleotide-free buffer, the emission maximum for PfHop was 337 nm. This confirmed that PfHop was properly folded. There was a blue shift in emission maxima upon incubation with ATP (330 nm) and ADP (333 nm) (Figure 5.4B). These changes in the tryptophan fluorescence emission maxima confirmed that PfHop assumed unique conformations in all cases (nucleotide-free), the presence of ATP and the presence of ADP (Figure 5.4B).

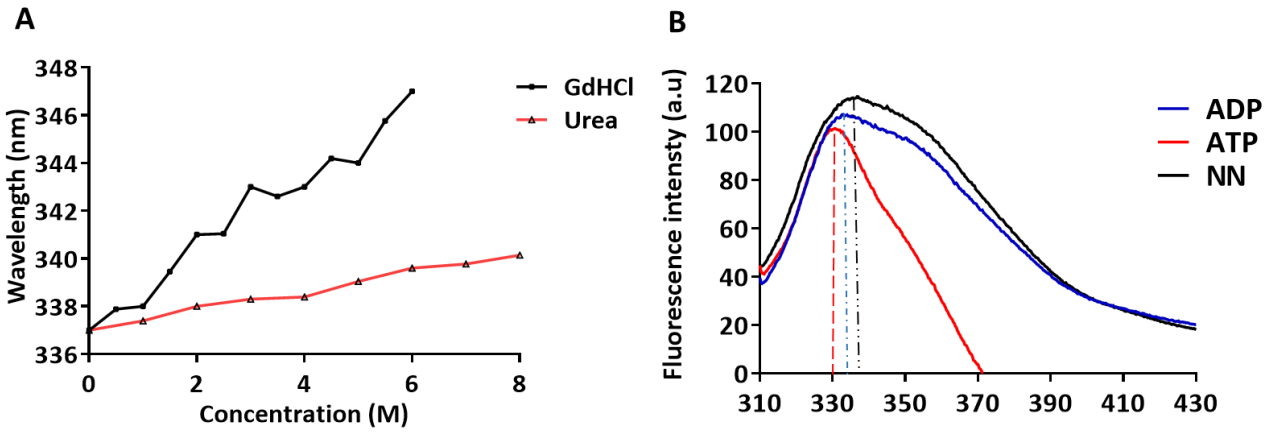

Figure 5.4. Analysis of the tertiary structure of PfHop by tryptophan fluorescence
The fluorescence emission spectra monitored at 300-450 nm after an initial excitation at 295 nm. The recombinant PfHop protein tryptophan fluorescence emission spectra were recorded under (**A**) various concentrations of GdHCl and urea. The red shift in PfHop emission spectra was plotted. (**B**) Tryptophan fluorescence-based spectra for PfHop in the presence of 5 mM ATP and ADP. Dotted lines show variable emission maxima, with respect to color, for PfHop in the presence and absence of ATP and ADP.

The effect of the nucleotides on the conformation of PfHop was further investigated by subjecting the protein to partial trypsin proteolysis in the additional presence of 5 mM ATP or ADP. The profiles of the generated PfHop fragments were analyzed using SDS-PAGE and Western

blot (Figure 5.5). Prior to trypsin digestion, PfHop was stable generating no apparent breakdown products (Figure 5.5, Lane U).

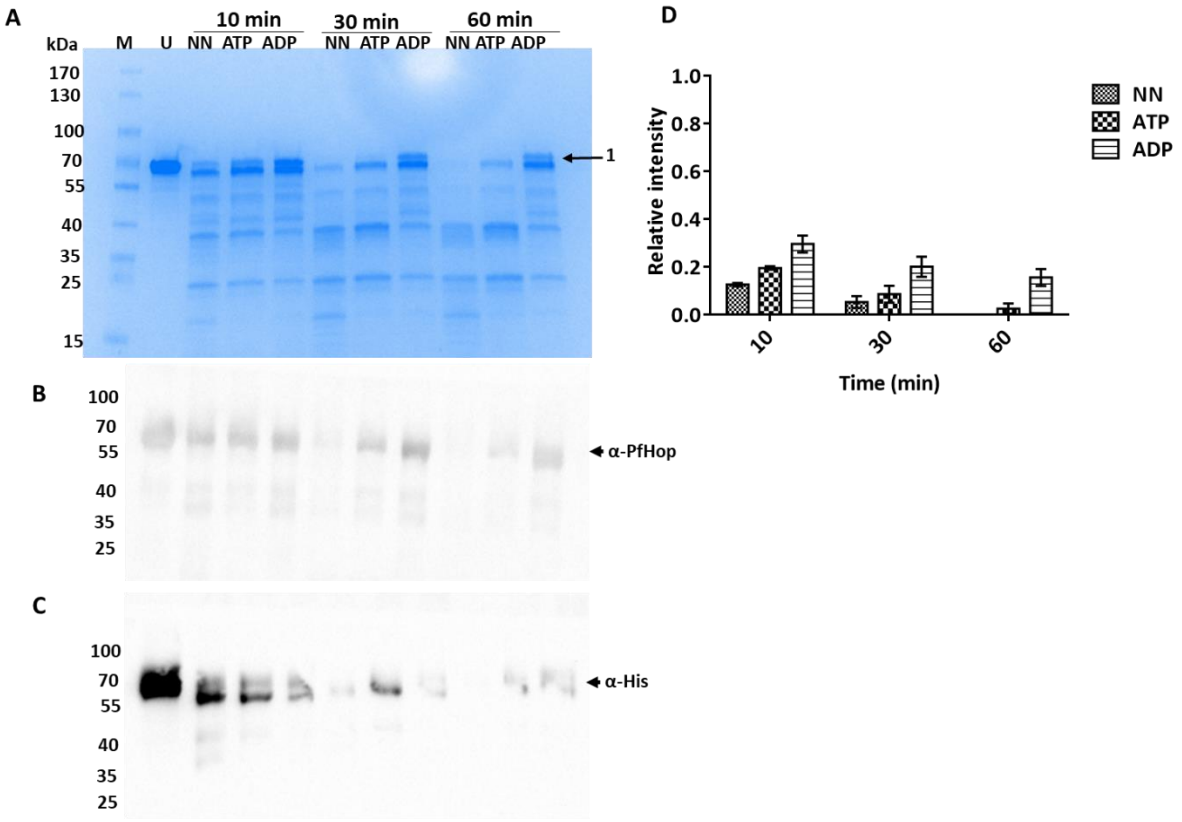

Figure 5.5. Limited proteolysis confirming nucleotide-induced conformational changes in PfHop
(**A**) Coomassie-stained SDS-PAGE gel (12 % gel under reducing conditions) representing the partial tryptic digestion of recombinant PfHop in a nucleotide-free buffer and in the presence of 5 mM ADP or ATP. Western blot representing PfHop fragments that were detected using (**B**) α-PfHop and (**C**) α-His antibodies. PfHop was digested at 30 °C using 0.25 ng/ml trypsin for 60 min. (D) Densitometry analysis based on the full PfHop band (labeled 1) in the SDS-Page gel.

At 10 min post addition of trypsin, various species ranging in size from 66 kDa to 15 kDa were generated in all three reaction mixes (NN, ATP, and ADP). Although the fragment profiles were apparently similar in size, most of the protein remained undigested in the presence of nucleotides. Protein stability to digestion was highest in ADP followed by ATP and lowest in NN (Figure 5.5). This suggests that the protein assumed unique conformations in the absence of nucleotides and in the presence of ATP or ADP as also demonstrated by tryptophan fluorescence

data (Figure 5.4B). After 30 min of incubation PfHop (NN) seemed to be digested to a greater degree when compared to the scenario in which ATP or ADP was present leading to the generation of unique fragments. This suggests that the nucleotide bound PfHop assumed different conformations from the nucleotide-free form and hence digestion occurred differently. These observations were further confirmed at 60 min, as only a few small fragments in the range 10-45 kDa were observed for PfHop (NN). In the absence of nucleotides, PfHop is almost completely digested (Figure 5.5A). Higher-order fragment species were observed mostly in the presence of ADP and ATP at 60 min (Figure 5.5). A fraction of the PfHop protein remained undigested in the presence of ADP after 60 min. Western blot analysis using α-PfHop and α-His confirmed mostly the higher-order fragments (Figure 5.5B and C). Densitometry analysis of the full length PfHop band (marked as 1) showed that PfHop was preserved in the following order: presence of ADP> presence of ATP> absence of nucleotide (Figure 5.5D). Taken together, PfHop undergoes nucleotide-induced conformational changes that slowed the rate of digestion. Conformational changes were also reported for a human Hop homolog although in the previous study ATP was more protective from digestion than ADP (Yamamoto *et al*., 2014). It is possible that the different buffers used in each assay contributed to the observed differences. On the other hand, Yamamoto *et al*. (2014) should have used a densitometry analysis to verify their data.

5.3.5 PfHop forms higher-order oligomers

PfHop was purified and shown to exist as a monomer based on SEC and SLS analyses (Figure 5.2). However, the protein was observed to form species that are higher-order on SDS-PAGE and Western blot analysis at the preliminary purification steps (Figure 5.1B). It was interesting to investigate whether the protein could form higher-order oligomers since Hop homologs are reported to form dimers (Bose *et al*., 1996; Prodromou *et al*., 1999; Hildenbrand *et al*., 2011). Based on SPR generated data, PfHop self-associated in a concentration dependent manner. The self-association of PfHop was also ascertained in the presence of nucleotides. The association was observed to be stable (K_D =1.57 nM) in the absence of nucleotide (NN). Higher affinity is observed in NN in comparison to the presence of either 5 mM ATP or ADP (Table 5.2). This suggests that nucleotides reduced PfHop self-association under the experimental conditions

used. The changes in PfHop conformation in the presence of either ATP or ADP observed during tryptophan fluorescence-based analysis (Figure 5.4B) and limited proteolysis (Figure 5.5) may have accounted for the lower affinities observed during the self-association studies using SPR (Table 5.2).

Table 5. 2: The rate constants for PfHop self-association

Analyte	Ligand	k_a (M-1s-1) (E+03) [SD]	k_d (s^{-1}) (E-05) [SD]	K_D (nM) [SD]	X^2	Reference
PfHop	PfHop	228.0 [±2.0]	3.6 [±0.1]	1.6 [±0.7]	0.89	This study/ Zininga *et al*., (2015b)
PfHop + ATP	PfHop	63.5 [±0.9]	3.3 [±0.08]	5.2 [±0.1]	1.84	This study/ Zininga *et al*., (2015b)
PfHop + ADP	PfHop	59.1 [±0.9]	4.6 [±0.02]	7.9 [±0.5]	2.49	This study/ Zininga *et al*., (2015b)

Table 5.2 legend: ***ka*** association rate constant, ***kd*** dissociation rate constant, K_D equilibrium constant, X^2 correlation for SPR sensorgram fitting to the Langmuir model, **ND** not determined. Standard deviations (**SD**) of at least three independent protein batches are shown in parenthesis.

The generated K_D indicates that PfHop self-associates with affinities in the nanomolar range, comparable to dimerization of human Hsp70 (Marcion *et al*., 2015) and PfHsp70-z (Zininga *et al*., 2016) (Table 5.2). PfHsp70-1 was used as a positive control as it is known to interact with PfHop and $PfHsp701_{NBD}$ served as a negative control. Due to a lack of the EEVD motif, the interaction of $PfHsp701_{NBD}$ with PfHop is thought to be abrogated (Table 5.2; Zininga *et al*., 2015). The EEVN/EEVD motif is important for interaction with TPR containing co-chaperones (Mabate *et al*., 2018). The lack of an EEVN motif in PfHsp70-x abrogated the interaction between PfHsp70-x and human Hop *in vitro* (Mabate *et al*., 2018). Overall this demonstrated the capability of PfHop to self-associate even though it was shown to be monomeric using SEC/SLS (Figure 5.2). The self-association of PfHop could be a transient interaction. SPR is capable of measuring transient interactions which cannot be measured by SEC. This could explain the differences observed between the assays.

5.3.6 PfHop directly binds ATP

Surface plasmon resonance analysis was further carried out to determine the nucleotide binding affinity of PfHop. Equilibrium analysis was conducted on the SPR sensograms to analyze the steady-state ATP binding affinity for recombinant PfHop using variable ATP concentrations as an analyte. PfHsp70-1_{NBD} was included as a positive control since it is known to bind ATP (Zininga *et al*. 2016). PfHop ATP binding affinity (K_D value) was found to be in the same order of magnitude as that of PfHsp70-1_{NBD} and is comparable to that of known nucleotide binding chaperones such as PfHsp70-1 and PfHsp70-z (Table 5.3). Findings from SPR show that PfHop binds to ATP with high affinity (K_D 3.73 µM, Table 5.3). Similarly, a human Hop homolog was observed to also bind ATP with high affinity using proton nuclear magnetic resonance (NMR, Yamamoto *et al*., 2014). These results suggest that Hop possesses a nucleotide binding motif.

Table 5. 3: PfHop affinity for ATP at equilibrium binding phase

Analyte	Ligand	K_D (µM) [SD]	Reference
ATP	PfHop	3.7 [±0.9]	This study
	PfHsp70-1_{NBD}	3.6 [±0.9]	This study
	PfHsp70-1_{NBD}	3.5 [±0.2]	Zininga *et al*. (2016)
	PfHsp70-z	25.3 [± 1.1]	Zininga *et al*. (2016)
	PfHsp70-1	3.5 [± 0.4]	Zininga *et al*. (2016)

The nucleotide binding domain in Hop is speculated to be in the TPR1-TPR2A (1–359) region (Yamamoto *et al*., 2014). Using multiple sequence alignment, the percentage identities of the nucleotide binding domain for the various Hop homologs ranged between 28-98 % (Table 5.4). This suggested that the proposed nucleotide binding domain is conserved among Hop homologs. It is interesting to note that the nucleotide binding domain as elucidated by Yamamoto *et al*. (2014) is practically made up of the conserved TRP1, DP1, and TPR2A domains. This could account for the high percentage sequence identities observed in the putative nucleotide binding domain (Table 5.4).

Table 5. 4: Percentage sequence identities for the nucleotide binding domains of Hop homologs

	hHop	PfHop	LmSTI	LbHop	LdHop	TbHop	TcSTI	TgHop
hHop	-	28.8	36.7	36.2	36.7	40.1	37.2	31
PfHop	28.8	-	30.9	30.6	31.2	32.3	32	40
LmSTI	36.7	30.9	-	91	98	58	57	33
LbHop	36.2	30.6	91	-	92	57	53	32
LdHop	36.7	31.2	98	92	-	59	56	32
TbHop	40.1	32.3	58	57	59	-	77	32
TcSTI	37.2	32	57	53	56	77	-	32
TgHop	31	40	33	32	32	32	32	-

Percentage sequence identities of Hop homologues from *P. falciparum* (PfHop, PF3D7_1434300), *Homo sapiens* (Hop, NCBI accession no. NP_006810.1), *Leishmania major* (LmSTI, NCBI accession no. XP_001681140.1), *Leishmania braziliensis* (LbHop, NCBI accession no. XP_001562145.1), (LdHop, NCBI accession no. XP_003858661.1), *Trypanosoma brucei* (TbHop, NCBI accession no. CBH11274.1), *Trypanosoma cruzi* (TcSTI, NCBI accession no. AAC97378.1) and *Toxoplamsa gondi* (TgHop, NCBI accession no. XP_002369330.1).

5.3.7 PfHop exhibits low ATPase activity

Having observed that PfHop is capable of binding to nucleotides resulting in unique conformational changes, it was important to elucidate whether PfHop hydrolyzed ATP. The kinetic parameters determined using the Michaelis-Menten plots (Figure 5.6A) showed that PfHop has very low ATPase activity as compared to the PfHsp70-1 control (Figure 5.6B). PfHop exhibits a K_m value of 2.53 mM (Table 5.4) suggesting that the co-chaperone requires very high levels of ATP to achieve a V_{max} of 42 nmol/min/mg. This was achievable under saturating ATP concentrations (5 mM). The obtained kinetics signify a low turnover rate for PfHop. This agreed with reports that a human Hop homolog was able to bind and slowly hydrolyze ATP (Yamamoto *et al*., 2014).

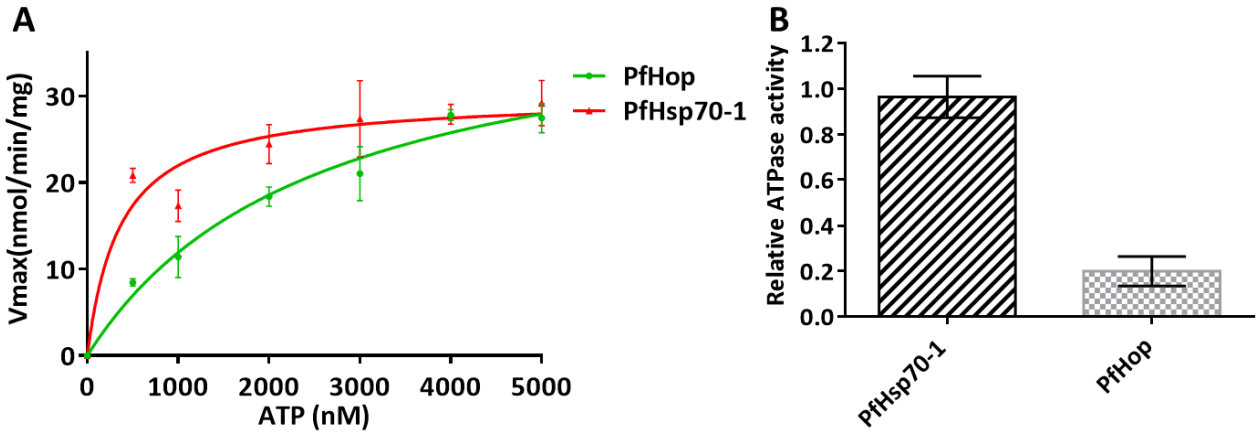

Figure 5.6. PfHop exhibits very low intrinsic ATPase activity

Evaluation of the basal ATPase activities of PfHop. (A) Michaelis Menten plot of the amount of P*i* released. (B) Relative ATPase activity of PfHsp70-1 and PfHop based on the K_m values for PfHsp70-1 and PfHop. The amount of P*i* released was monitored by measuring absorbance at 595 nm using a direct colorimetric assay. The experiment was carried out in the presence of 0.4 µM protein under saturating ATP (5 mM).

Table 5. 5: Data for kinetics of the ATPase activities of PfHop

Protein	*Vmax* (nmol/min/mg) [SD]	K_m (µM) [SD]	Reference
PfHop	42.0 [±3.64]	2534 [±3.1]	This study
PfHsp70-1	29.9 [±1.6]	364.2 [±3.5]	This study
PfHsp70-1	30.5 [±0.9]	384.3 [±0.5]	Zininga *et al*., (2017)

Table 5.5 legend: $\mathbf{V_{max}}$ – the maximum rate of the catalysis reaction; $\mathbf{K_m}$ - is the substrate concentration at which the reaction rate is at half-maximum. At least three independent assays were carried out and standard deviations (SD) are shown.

5.4 Discussion

PfHop has been previously shown to bind both PfHsp70-1 and PfHsp90, thereby modulating the activities of both chaperones (Gitau *et al*., 2012; Zininga *et al*., 2015b). The Hsp70/Hsp90 pathway has been proposed as a drug target as it is responsible for the folding of key proteins such as steroid hormone receptors and kinases (Röhl *et al*., 2015; Gu *et al*., 2016). This study sought to biophysically characterize PfHop and gain more insights into its structure and function. Recombinant PfHop protein purified as a monomer and was monodisperse as observed during SEC and SEC/SLS (Figures 5.3). This agrees with previous studies on human Hop (Yi *et al*., 2010; Li *et al*., 2011; Ebong *et al*., 2011) and *Leishmania braziliensis* Hop (Batista *et al*., 2016). However, a smaller proportion of the PfHop protein was seen to elute as higher-order oligomers (Figure 5.2). It is possible that these could have been dimers that were partially resistant to reducing agent (Grigorian *et al*., 2004), the action of SDS and heat treatment (Gentile *et al*., 2002; Kolodziejski *et al*., 2003; Renwrantz *et al*., 2008). On the other hand, human Hop dimeric forms have been reported (Bose *et al*., 1996; Prodromou *et al*., 1998 and Hilderbrand *et al*., 2011), hence it is possible that PfHop formed weak dimers as reported for human Hop (Southworth and Agard, 2011).

Studies with SPR revealed that PfHop self-associated with high affinities comparable to human Hsp70 (Marcion *et al*., 2014) and PfHsp70-z (Table 5.2, Zininga *et al*., 2015a). Interactions with K_D values in the nanomolar range are considered strong transient to permanent interactions (Ozbabacan *et al*., 2011). Interestingly, if PfHop self-associated with such high affinity, this might naturally impact on its interactions with partner proteins. Hop dimerization influences its interaction with Hsp70 or Hsp90 (Onuoha *et al*., 2008; Alvira *et al*., 2014). The Hop interaction with Hsp70 follows a 1:1 stoichiometry (Scheufler et al., 2000; Ebong *et al*., 2011; Röhl *et al*., 2015). However, Hernandez and co-workers (2002) suggest that a Hop dimer binds two molecules of Hsp70 in the absence of Hsp90. Hsp70 dimerization has been reported (Marcion *et al*., 2015), hence it is possible that a Hop dimer binds an Hsp70 dimer. The Hop: Hsp90 stoichiometry of binding has been reported to be either 1:2 or 2:2 (Ebong *et al*., 2011;

Southworth and Agard, 2011; Alvira *et al*., 2014). A 2:2 stoichiometry was reported to occur in excess of Hop (Ebong *et al*., 2011; Southworth and Agard, 2011; Alvira *et al*., 2014). It is also possible that an Hsp90 dimer binds a single Hop molecule in the presence of another TPR containing co-chaperone, FKBP52 (Hildebrand *et al*., 2011; Ebong *et al*., 2011). Hence, PfHop dimerization might be important for these interactions. Hop alternating between monomer and dimer might be the perfect state for these interactions.

Although PfHop was initially characterized by Gitau and colleagues (2012), its secondary and tertiary structure had not yet been established. This study established that PfHop comprised of approximately 50 % α-helices, 16 % β-sheets, 10 % β-turns and a significant 23 % unordered. This suggests that PfHop was a predominantly α-helical protein. Findings from this study suggest that PfHop was thermally labile as 50 % of the protein unfolded at approximately 45-50 °C (Figure 5.4). PfHop has been previously shown to be heat-labile at 43 °C (Zininga *et al*., 2015b). This is similar to findings from this study.

Using tryptophan fluorescence analysis and tryptic proteolysis it was further confirmed that PfHop undergoes unique conformational changes in the presence of either ATP or ADP. The W-residue of PfHop is more sensitive to the binding of ATP as compared to ADP, hence the greater blue shift in emission maxima. PfHop was shown to be relaxed (elongated) which would explain why the NN form was prone to cleavage by trypsin (Figure 5.6). In the presence of ADP, PfHop possibly assumed a more compact structure than it did in the presence of ATP, hence it showed better resilience to proteolysis than the ATP bound form. Conformational changes in the presence of nucleotides have been reported for other proteins. PfHop conformational changes in the presence of either ATP or ADP followed observations made for Nitrogen fixation specific regulator (NIFA; Money *et al*., 2001) although both proteins are not related. However, for PfHsp70-z and human Hop, the ATP bound forms had the most resilience to proteolysis than the ADP-bound forms (Yamamoto *et al*., 2014; Zininga *et al*., 2016). This suggests that various proteins bind nucleotides to assume unique conformations. Based on the observed

conformational changes in PfHop, it was important to elucidate the capability of PfHop to hydrolyze ATP.

The capability of PfHop to bind ATP was investigated using SPR. The equilibrium analysis showed that PfHop binds ATP with high affinity, comparable to ATPases PfHsp70-1, PfHsp70-z, and PfHsp70-1_{NBD} (Table 5.3). This was in line with findings by Yamamoto and colleagues (2014) which demonstrated that human Hop exhibits high affinity for ATP. Human Hop is reported to possess Walker B motifs (Yamamoto *et al*., 2014). These motifs bind ATP. However, Yamamoto *et al*. (2014) proposed that ATP binding in Hop occurs through non-walker motifs although this is yet to be elucidated. Interestingly, PfHop exhibited very low basal ATPase activity in comparison to PfHsp70-1 (Figure 5.7). A high K_m value obtained from ATPase hydrolysis assays signified that PfHop has low ATP turnover rates (Table 5.5). The K_m value is calculated based on the amount of phosphate (*Pi*) released during ATP hydrolysis. It is possible PfHop had a high affinity for ATP but hydrolyzes it slowly. Hop molecules seem to have low turnover rates, as a low basal ATPase activity was also reported for human Hop (Yamamoto *et al*., 2014). It is possible that the low ATP hydrolysis might be required for substrate transfer from Hsp70 to Hsp90. The TPR1-DP1 of Hop displaces Hsp70 after substrate transfer for the continuation of the chaperone cycle. Hop/Hsp70 interaction is known to be abrogated in the presence of ATP. It is also possible that ATP binding and hydrolysis in the TPR1-DP1 region of Hop is also important for this displacement of Hsp70.

Overall, PfHop is a monomeric protein exhibiting a strongly helical nature. Its high affinity self-association implies it might exist as oligomeric forms. Affinity for the self-association of PfHop was significantly lower in the presence of ATP and ADP. This could be attributed to the nucleotide-induced conformational changes observed by tryptophan fluorescence and by limited proteolysis. Conformational changes in Hop are important during its interactions with Hsp70 and Hsp90.

Chapter 6

Investigation of the role of the GGMP motif of PfHsp70-1 on its association with PfHop

Chapter 6

Investigation of the role of the GGMP motif of PfHsp70-1 on its association with PfHop

6.1 Introduction

Proteins usually do not function as single entities but as a cohort of participants in a dynamic network (Guo and Wan, 2014). Thus, the structure-function features of proteins are regulated by their interactors. Protein-protein interactions are known to form a significant part of many biological processes within living cells (Zeytuni and Zarivach 2012). The current study (section 2.3.4) predicted that PfHsp70-1 interacts with proteins involved in the modulation of numerous molecular pathways. Among the experimentally validated interactors of PfHsp70-1 were PfHsp40 (Botha *et al*., 2011); PfJ1 (Pesce *et al*., 2008); PfHop (Gitau *et al*., 2012) and PfHsp70-z (Zininga *et al*., 2016). The interaction of PfHsp70-1 with PfHop was of interest to this study. The C-terminal EEVD motif of PfHsp70-1 is known to interact with the TPR1 and TPR2B of PfHop (Zininga *et al*., 2015b). However, recent studies suggest that other regions outside the EEVD may regulate the binding of co-chaperones (Durech *et al*., 2016; Gong *et al*., 2018).

The GGMP motif of PfHsp70-1 is located 16 residues upstream of the terminal E-674 residue of the EEVD motif and seven residues away from the lid. Given the proximity of the GGMP repeats to the C-terminal end of PfHsp70-1, it is possible that the GGMP motif may regulate the association of PfHop with PfHsp70-1. Pellegrini (2015) remarked that tandem repeats in proteins serve as binding sites and may have structural roles by giving rigidity, and by exposing domains that are of functional importance such as the EEVD motif. This study elucidated the role of the GGMP motif of PfHsp70-1 on its interaction with PfHop in relation to the EEVD motif.

PfHop modulates the functional partnership between PfHsp70-1 and its chaperone partner, PfHsp90. In contrast, bacteria lack a Hop homolog hence there is direct interaction between *E. coli* Hsp90 and DnaK (Kravats et al., 2017). Using a DnaK GGMP variant, it was interesting to elucidate if insertion of the GGMP repeats from PfHsp70-1 into DnaK would promote the possible association between DnaK and PfHop *in vitro*.

Chapter 6

Investigation of the role of the GGMP motif of PfHsp70-1 on its association with PfHop

The objectives of this study were to:

i. investigate the role of the GGMP motif of PfHsp70-1 in regulating its interaction with PfHop;

and

ii. investigate the role of the GGMP insertion in DnaK on its probable association with PfHop *in vitro*.

6.2 Experimental Procedures

6.2.1 Materials

The materials and reagents used in this study are listed in Appendix C. The plasmids and antibodies are listed in tables 3.1 and 5.1.

6.2.2. Investigation of the effect of the GGMP mutation of PfHsp70-1 on its interaction with PfHop using Enzyme-Linked Immunosorbent Assay

The direct association of PfHop with PfHsp70-1, DnaK, and their respective GGMP variants was determined using an enzyme-linked immunosorbent assay (ELISA). The ELISA was conducted following a previously described protocol (Mabate *et al*., 2018) with minor modifications. Briefly, recombinant PfHsp70-G632, PfHsp70-G648, DnaK and DnaK-G proteins (5 µg/mL) were prepared separately as ligands in buffer T (25 mM Tris-HCl pH 7.4, 140 mM NaCl, and 3.0 mM KCl). PfHsp70-1 was prepared as a positive control since its interaction with PfHop has already been validated (Gitau *et al*., 2012, Zininga *et al*., 2015b). BSA was included as negative control. To immobilize the ligand proteins onto the wells of the microtiter plates, 0.5 µg of the recombinant protein were added into each well. Microtiter plates have adsorption or hydrophilic binding properties that allow protein binding and immobilization overnight at 4 °C. Immediately after emptying the wells, the wells were rapidly washed once to remove any unbound protein using buffer W (25 mM Tris, 140 mM NaCl, 3.0 mM KCl and 0.1 % Tween-20). To block the wells, 150 µL of buffer S (25 mM Tris, 140 mM NaCl, 3.0 mM KCl, 0.1 % Tween-20 and 1 % BSA) was added into each well and incubated at 16 °C for 1 hr. Unless stated, all steps subsequent to blocking were done at 16 °C. Following the blocking, the wells were washed three times (3 min each) with Buffer W. Serial dilutions of recombinant PfHop protein (0-0.5 µg) [analyte] were prepared in buffer (25 mM Tris, 140 mM NaCl, 3.0 mM KCl, 0.1 % Tween-20 and 0.1 % BSA). The analytes were incubated with the ligand Hsp70 proteins for 2 hr followed by washing steps to remove unbound analyte. Rabbit raised peptide-specific α-PfHop primary antibody (1:4000) in buffer (25 mM Tris, 140 mM NaCl, 3.0 mM KCl, 0.1 % Tween-20 and 0.1 % BSA) was added to all the wells and the plate was incubated for 1 hr. After incubation, the wells were washed prior to addition of secondary HRP

conjugated goat raised α-rabbit antibody (1:4000) in buffer (25 mM Tris, 140 mM NaCl, 3.0 mM KCl, 0.1 % Tween-20 and 0.1 % BSA) and the plate was incubated for 45 mins. Excess unbound antibody was washed off three times (3 min each wash) using buffer W prior to detection with TMB substrate solution (Bioo Scientific, USA). For detection, 100 µL/well of 3,3',5,5'-tetramethylbenzidine (TMB) was added and the substrate reaction was incubated for 2 min with 3-sec shaking. Colour development was monitored by measuring absorbance readings at 370 nm using a SpectraMax M3 microplate reader (Molecular Devices, USA) at time intervals (0, 5, 10, 15, 20, 25, and 30 min). The absorbance for each well was plotted against time. From the well showing the highest absorbance (A=2 cutoff), a 5 min time point before a deviation from linear color development was selected for data analysis. In addition, to investigate the effect of nucleotides on the interaction, the assay was repeated in the presence of 5 mM ATP or ADP.

6.2.2.1 Data Analysis

The resultant absorbance values at the highest concentration of PfHop were averaged as the maximum (100%) binding for the protein after background subtraction. A titration curve was plotted against a log scale of the various dilution concentrations using GraphPad Prism 6.05 (GraphPad Software, USA). The comparison of the relative binding affinities between PfHsp70-1 versus PfHop, PfHsp70-G632 versus PfHop and PfHsp70-G648 versus PfHop under different conditions were normalized to the maximum absorbance value obtained at the highest concentration of PfHop used.

6.2.3 Investigation of the direct association of the GGMP variants with PfHop using slot blot analysis

Varying concentrations (1 µg, 2 µg, 4 µg) of recombinant PfHsp70-1, DnaK and the GGMP variants were prepared in buffer T (25 mM Tris-HCl pH 7.4, 140 mM NaCl, and 3.0 mM KCl). BSA as a negative control as it does not associate with PfHop (Zininga *et al*., 2015b). By applying gentle vacuum, the proteins were immobilized onto the nitrocellulose membrane. Blocking was performed using 5 % non-fat milk made in buffer T plus 0.1 % Tween-20. The membrane was

overlaid with 4 µg of purified PfHop protein overnight on ice. The membranes were washed three times (10 min each wash) with buffer T. As a primary antibody, α-PfHop (1:2000, Zininga *et al*., 2015b) was used to detect the PfHop for 1 hr and an HRP conjugated goat raised α-rabbit IgG was used as secondary antibody (1:4000). Detection of protein bands was performed using ECL and visualization was done using the Chemidoc (Bio-Rad). Assays were also repeated in the presence of 5 mM ATP or ADP.

6.3 Results

6.3.1 Analysis of PfHop/PfHsp70-1 interaction using ELISA

Hop associates with Hsp70 via the EEVD motif of the chaperone. PfHop/PfHsp70-1 interaction has been previously demonstrated (Zininga *et al*., 2015b). PfHsp70-1 possesses a GGMP motif which is in close proximity to the EEVD motif of the protein. Hence, this study elucidated how positional (N- and C-terminal) mutations in the GGMP motif would affect PfHsp70-1 interaction with PfHop. Prior to performing the assay, it was also validated that the α-PfHop antibody was specific (Appendix B24) in line with what was observed by Zininga *et al*. (2015b). PfHsp70-1 protein successfully immobilized on the inside of the wells. This was performed to confirm the binding of proteins to the maxisorp plates (Appendix B24). To investigate the interaction of PfHsp70-1 and GGMP variants with PfHop, varying concentrations (0-0.5 μg) of PfHop as analyte were overlaid on the immobilized proteins (PfHsp70-1, DnaK, and their variants). This was followed by probing with an α-PfHop antibody to detect PfHop bound to the immobilized proteins (Appendix B24). Very low signal intensities were observed for the BSA control. This was in line with previous studies by Zininga *et al*. (2015b).

Increase in signal intensities (absorbance) was observed for the binding of PfHop to PfHsp70-1 as the concentration of PfHop was increased (Figure 6.1A). This suggested that PfHop interacted with PfHsp70-1 in a concentration dependent manner. The assay was also conducted in the presence of either ATP or ADP (Figure 6.1B and C). Similar trends of concentration dependent interactions were observed in the presence of nucleotides. ADP had a similar effect on the interaction as was observed in the absence of nucleotide (NN). However, in the presence of ATP, the association of the proteins was less favored (Figure 6.1B). The observations made in this study for the PfHop/PfHsp70-1 interaction were in line with previous observations by Zininga and colleagues (2015b). This served as validation for this assay. Interestingly, the variants interacted lesser with PfHop compared to PfHsp70-1 in NN, ATP, and ADP. PfHsp70-G648 exhibited the lowest interaction. However, the differences exhibited were marginal in NN and ADP (Figure

6.1D). Significant differences were observed in the presence of ATP (Figure 6.1D). Overall, PfHsp70-1 interacted with PfHop exhibiting the highest affinity compared to its GGMP variants. The GGMP variants (PfHsp70-G632 andPfHsp70-G648) interacted with PfHop exhibiting comparable affinities.

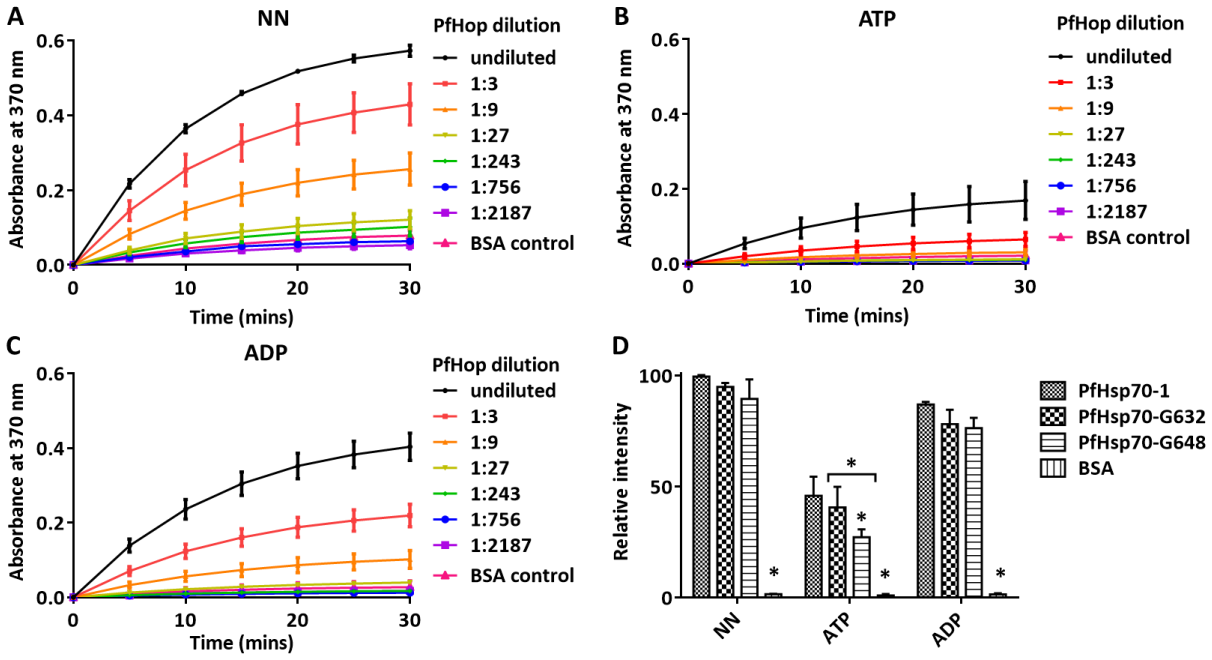

Figure 6. 1. The GGMP motif of PfHsp70-1 is important for PfHop interaction
The ELISA generated representative curves for the interaction of PfHop and PfHsp70-1 GGMP variants (**A**). The assay was repeated in the additional presence of 5 mM ATP (**B**) and 5 mM ADP (**C**). The resultant absorbance values at the highest concentration of PfHop were averaged as the maximum (100%) binding for the protein. The comparison of the relative intensity of binding between PfHsp70-1 and PfHop; PfHsp70-G632 versus PfHop and PfHsp70-G648 versus PfHop under different conditions were normalized (**D**). The standard deviations obtained are represented as error bars for at least three assays conducted using three different batches of purified recombinant protein. Asterisk (*) represent statistical significance ($p<0.001$).

6.3.2 Validating PfHop's interaction with PfHsp70-1 and its GGMP derivatives using slot blot approach

The findings from ELISA were further validated by carrying out protein slot blots. The recombinant proteins were immobilized onto the nitrocellulose membrane. The interaction of

PfHop with PfHsp70-1 was conducted by immunoblotting with α-PfHop antibody (Figure 6.2 and Appendix B25). The detection of bands suggested that PfHop was bound to PfHsp70-1 (Figure 6.2A). This was repeated in the presence of ATP and ADP (Figure 6.2B and C). In agreement with previous ELISA data, ATP inhibited the interaction with PfHop.

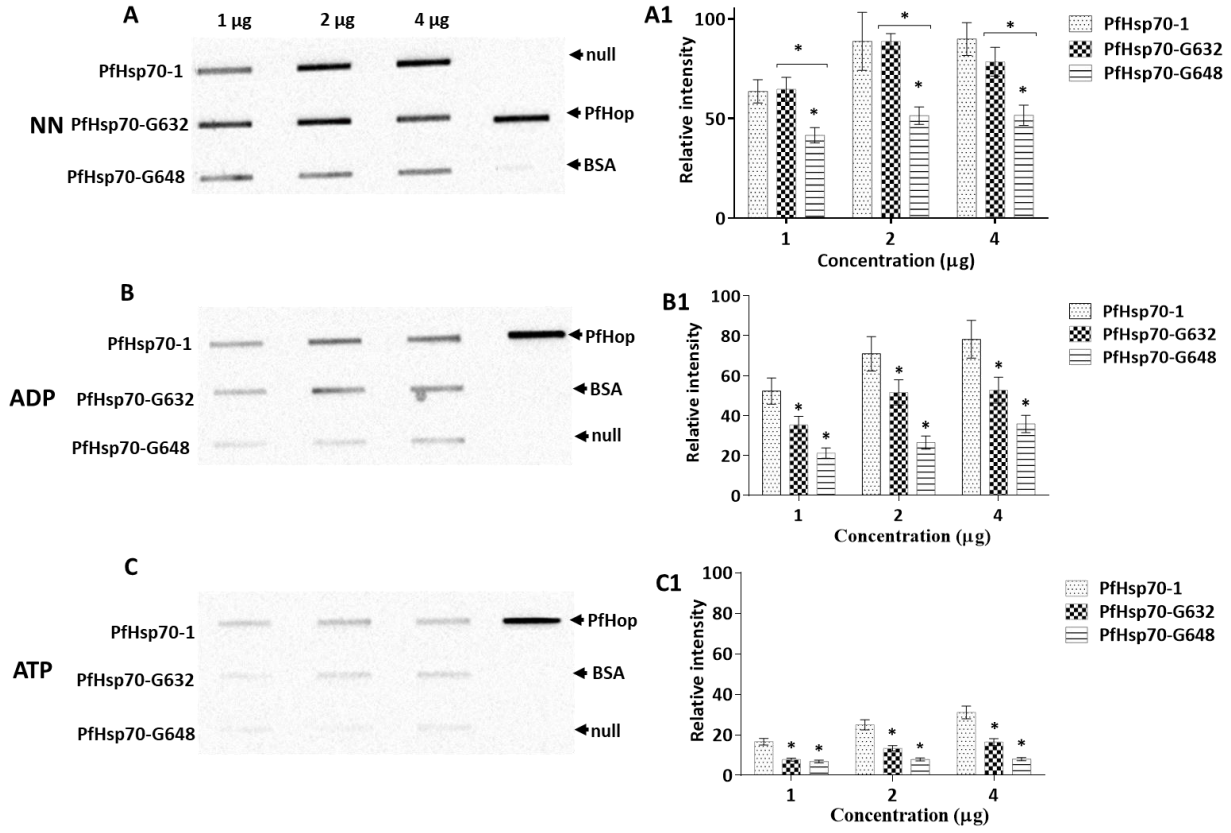

Figure 6. 2. The GGMP motif is necessary for the interaction between PfHsp70-1 and PfHop
Various concentrations of PfHsp70s (1 µg, 2 µg, and 4 µg) were spotted onto nitrocellulose membrane as the prey protein. BSA (4 µg) was used as a negative control. Each respective protein concentration was spotted using a vacuum and overlaid with 4 µg of purified PfHop protein (**A**) and accompanying densitometry analysis (**A1**). The assay was also conducted in the presence of ADP and ATP (**B** and **C**) and accompanying densitometry analysis (**B1** and **C1**). α- PfHop antibody was used to detect the presence of PfHop protein. The data represents at least three independent assays. Standard errors are indicated, and statistical analysis was conducted using two-way ANOVA ($p<0.001$).

Densitometry analysis demonstrated that there were stronger interactions in nucleotide-free and in the presence of ADP (Figure 6.2A1 and B1) compared to the weaker interactions in the

presence of ATP (Figure 6.2C1). ELISA data also showed that the GGMP variants exhibited a weaker association with PfHop compared to PfHsp70-1 in the presence of ATP. Densitometry analysis confirmed that PfHsp70-1 and PfHsp70-G632 exhibited a stronger association with PfHop compared to PfHsp70-G648 in the absence of nucleotide (NN). The interactions were stronger for PfHsp70-1 followed by PfHsp70-G632 and then PfHsp70-G648 in the presence of either ADP or ATP (Figure 6.2A1, B1 and C1). The weaker associations for the variants suggest that the mutations in the GGMP motif abrogated interactions with a co-chaperone, PfHop. This agrees with recent studies in which yeast Hsp70 (Ssa1) GGAP mutants were reported not to interact with yeast co-chaperone Hsp40 (Ydj1) (Gong *et al*., 2018). Given a few inconsistent bands observed in slot blot, it would be more interesting to further ascertain interaction kinetics and affinity of these associations using more definitive assays such as SPR or ITC.

6.3.3 The GGMP motif of PfHsp70-1 does not promote the association of PfHop with DnaK

In a separate experiment, DnaK and DnaK-G were overlaid with PfHop to validate whether the GGMP repeats would promote the interaction between PfHop and a none-EEVD containing Hsp70. Direct interaction between DnaK/DnaK-G with PfHop was carried out using ELISA. Recombinant DnaK and DnaK-G were immobilized onto 96 well plates. PfHsp70-1 and BSA were immobilized as positive and negative controls respectively. Immunoblotting was conducted using α-PfHop antibody. DnaK and DnaK-G associations with higher concentrations (0.02-0.5 µg) of PfHop followed a concentration dependent pattern (Figure 6.3 A and B). At lower concentrations of PfHop, interaction patterns were not concentration dependent. Similar non-concentration dependent interaction patterns were also observed in the presence of ATP (Figure 6.3 D and E) and ADP (Figure 6.3 G and H). Compared to PfHsp70-1, a known PfHop interactor, both DnaK, and DnaK-G did not exhibit significant interaction with PfHop (Figure 6.3 C). This was similarly observed in the presence of ADP and ATP (Figure 6.3 F and I).

Chapter 6

Investigation of the role of the GGMP motif of PfHsp70-1 on its association with PfHop

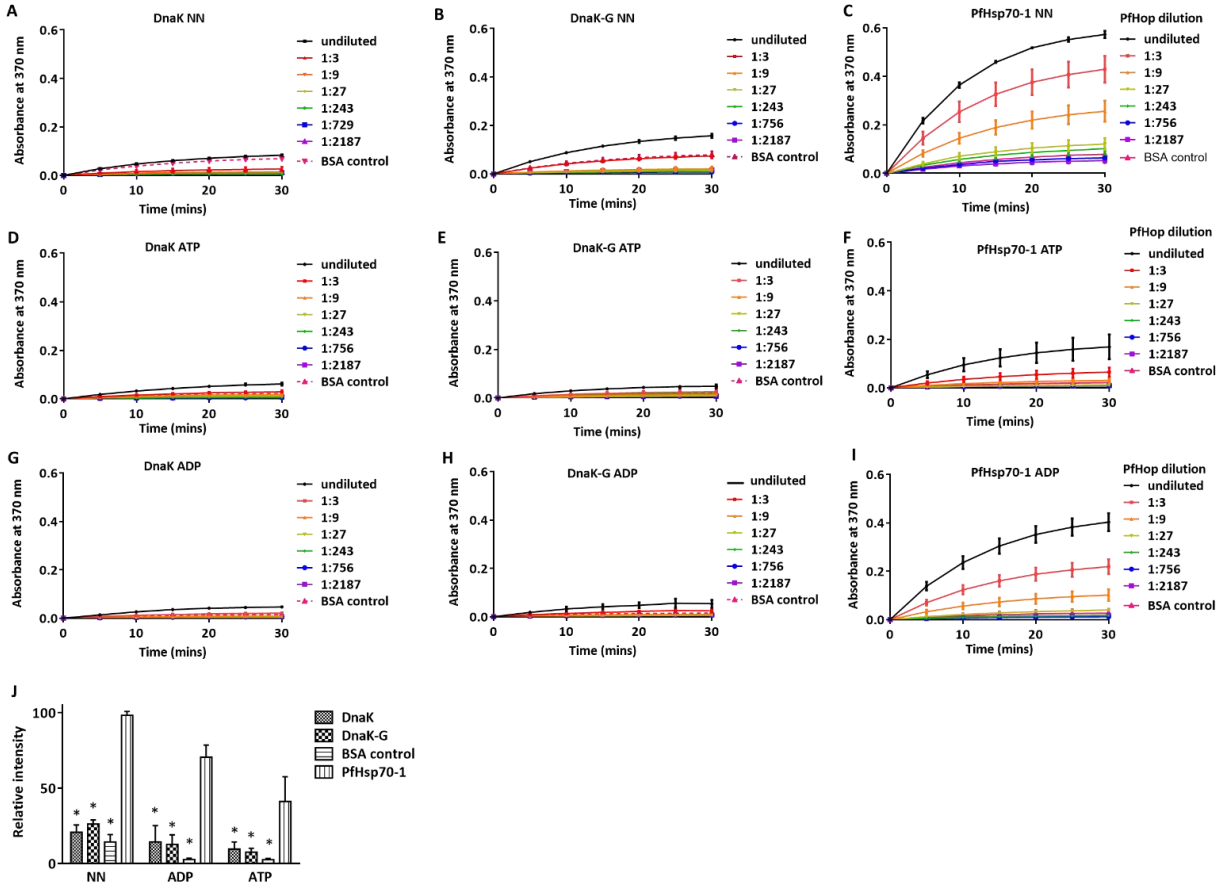

Figure 6. 3. The GGMP motif of PfHsp70 does not promote the association of PfHop with DnaK
ELISA generated interaction curves for the association of PfHop versus DnaK and DnaK-G. PfHsp70-1 was used a positive control and BSA as a negative control. The dose-dependent association between PfHop and the chaperones assay was established in the presence of varying concentrations of PfHop (**A**) DnaK; (**B**) DnaK-G and (**C**) PfHsp70-1. The assay was repeated in presence of 5 mM ATP for DnaK-PfHop (**D**); DnaK-G-PfHop (**E**) and PfHSp70-1-PfHop (**F**) and 5 mM ADP for DnaK-PfHop (**G**); DnaK-G-PfHop association (**H**), and PfHsp70-1-PfHop (**I**). The relative binding affinities under different conditions were normalized to the maximum absorbance value obtained for PfHsp70-1 at the highest concentration of PfHop used (**J**). The standard deviations obtained for at least 3 assays conducted independently are represented as error bars. Statistical analysis was conducted using Two-way ANOVA ($p<0.001$).

Furthermore, there were no statistically significant differences between the BSA-PfHop interaction compared to the DnaK-PfHop and DnaK-G-PfHop interactions (Figure 6.3J, $p<0.001$). Altogether, this shows that there was no interaction between PfHop and either DnaK or DnaK-G. This suggests that in the absence of C-terminal EEVD motif of eukaryotic Hsp70s, the presence of the GGMP is insufficient to facilitate interaction of Hsp70 with Hop.

To further confirm the findings from ELISA, a slot blot assay was performed. Bait proteins DnaK and DnaK-G; positive control (PfHsp70-1); negative control (BSA) and (PfHop) were immobilized onto nitrocellulose membrane respectively. The ligand proteins were overlaid with recombinant PfHop and immunoblotting was conducted using α-PfHop antibody (Figure 6.4A and Appendix B26). The association of PfHsp70-1 associated with PfHop has been previously demonstrated (section 6.3.1). Faint bands were observed for the DnaK-PfHop and DnaK-G-PfHop association. This suggests a lack of association as observed with ELISA (section 6.3.4). Densitometry analysis confirmed that there were no statistically significant differences in the DnaK-PfHop or DnaK-G-PfHop association as compared to the BSA-PfHop associations (Figure 6.4A1; $p <0.001$). The experiment was also repeated in the presence of 5 mM ATP and ADP (Figure 6.4B and C) as nucleotides are known to influence Hop/Hsp70 interactions. Lack of association between DnaK or DnaK-G and PfHop was also observed in the presence of ATP and ADP respectively (Figure 6.4 B1 and C1). The slot blot based data supported the observations from ELISA that the presence of GGMP residues in Hsp70 lacking EEVD residues is insufficient to facilitate its interaction with Hop. DnaK possesses EEVKDK residues in place of the EEVD residues present in cytosolic Hsp70s of eukaryotes. It is possible that the presence of the (K) residue in-between the V and D residues blocks interaction with Hop.

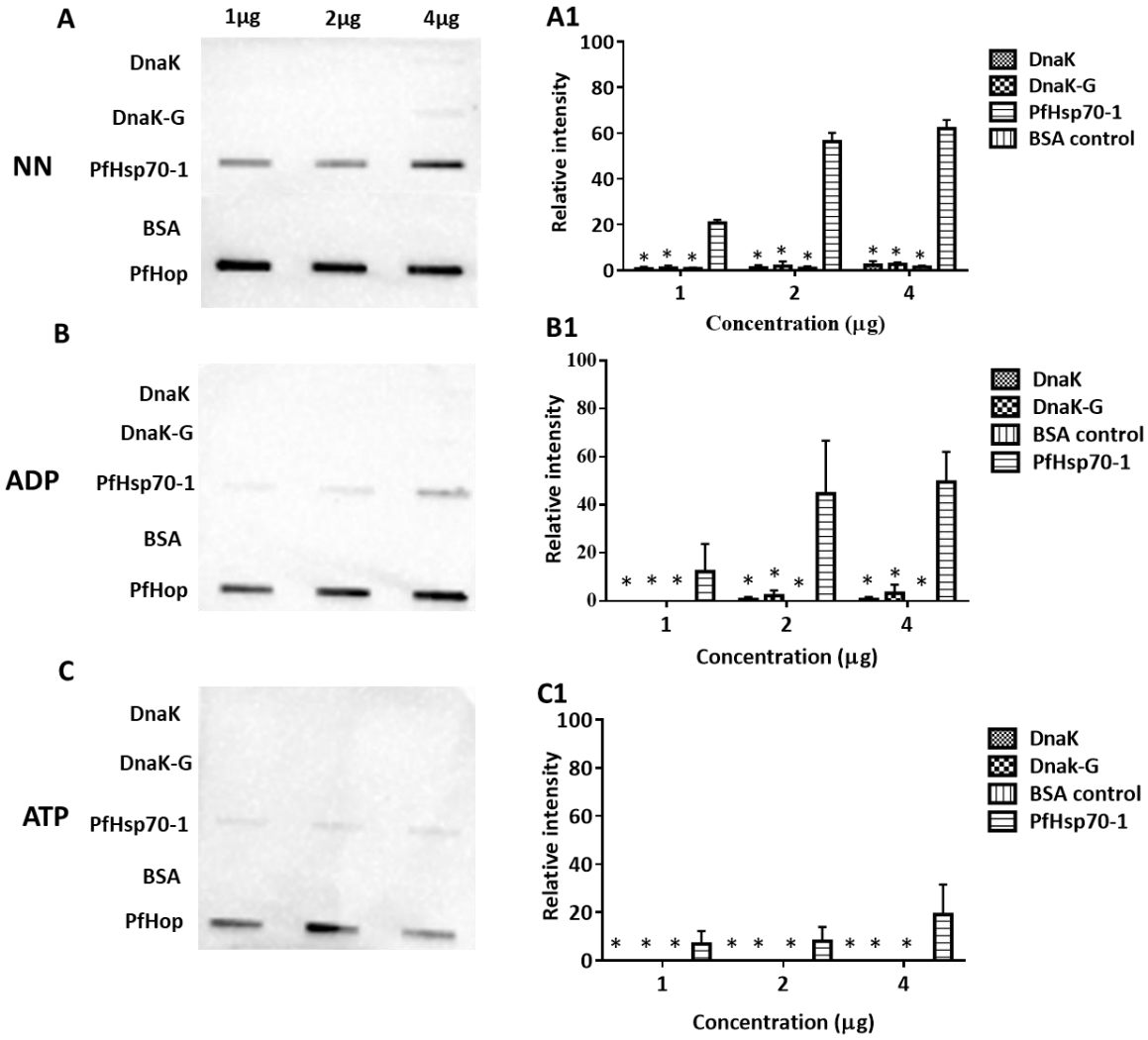

Figure 6. 4. The GGMP motif of PfHsp70-1 is insufficient to promote the association of PfHop with DnaK

Various concentrations of DnaK and DnaK-G (1 µg, 2 µg, and 4 µg) were spotted onto nitrocellulose membrane as the prey protein. PfHsp70-1 and BSA were used as positive and negative controls respectively. PfHop protein was used as an antibody control. The membrane was overlaid with 4 µg of purified PfHop protein (**A**) and accompanying densitometry analysis (**A1**). The assay was also conducted in the presence of ADP and ATP (**B** and **C**) and accompanying densitometry analysis (**B1** and **C1**). α- PfHop antibody was used to detect the presence of PfHop protein. The data represents at least three independent assays. Standard errors are indicated, and statistical analysis was conducted using two-way ANOVA ($p<0.001$).

6.4 Discussion

The association between PfHop and PfHsp70-1 has been previously demonstrated using co-immunoprecipitation assays (Gitau *et al*., 2012) and *in vitro* biochemical assays such as SPR (Zininga *et al*., 2015b). Hop facilitates substrate transfer from Hsp70 to Hsp90 for completion of the folding process. This study investigated the interaction between PfHop and PfHsp70-1 GGMP variants. Using purified recombinant proteins, the association between PfHop and PfHsp70-1 GGMP variants was validated using two independent assays (ELISA and slot blot analysis). The current study provided evidence confirming that the mutation of GGMP residues reduced the affinity of PfHop for PfHsp70-1. As previously reported, the interaction between PfHop and PfHsp70-1, as well as the GGMP variants, occurred strongly in a nucleotide-free medium as well as in the presence of ADP (Figure 6.1 and 6.2). The weaker interactions observed in the presence of ATP, versus nucleotide-free and ADP state, could be a result of the conformational changes that occur in Hsp70 and Hop during ATP binding and hydrolysis. For Hsp70s, the SBDβ and SBDα are reported to separate and dock on either side of the NBD upon ATP binding (Kityk *et al*., 2015). It is possible that these shifts might change the positioning of the EEVD and reduce accessibility by the TPR1 domain of PfHop thereby lowering interaction. The TPR1 domain of Hop responsible for binding Hsp70 lies in the proposed ATP binding domain of Hop (residues 1-359). The binding of ATP probably blocks the binding of the EEVD motif to the TPR1 domain of PfHop hence the low affinities.

In the slot blot assay PfHsp70-1 bound strongly to PfHop compared to its GGMP variants (Figure 6.2). ELISA data showed that PfHsp70-1 and PfHsp70-G632 bind PfHop stronger than PfHsp70-G648. The closeness of the PfHsp70-G648 mutation to the EEVD motif of PfHsp70-1 possibly abrogates the interactions of the variant with PfHop observed with both ELISA and slot blot analysis. However, affinities of the interaction of PfHsp70-1 with PfHop need to be ascertained by employing more sensitive assays such as SPR and isothermal titration calorimetry (ITC). Overall, the findings show that the GGMP motif regulates the interaction of PfHsp70-1 with PfHop. Both the GGMP variants associated weakly with PfHop, although PfHsp70-G648 exhibited

the weakest interactions as defined by ELISA and slot blot assays (Figures 6.1 and 6.2). This suggests that the GGMP motif can be altered thereby abrogating the functional association between PfHsp70-1 and its partner protein PfHop. This is likely to have adverse effects on parasite survival and development. These findings suggest that the GGMP repeats function in Hop binding and they are not redundant or just part of the repetitive low complexity sequences present in most *Plasmodium* proteins (Davies *et al*., 2016). Low-complexity regions are amino acid sequences that possess repeats of single amino acids or short amino acid motifs (Haerty and Golding, 2010; Toll-Riera *et al*., 2012) and are mostly assumed to have no function. The current study demonstrates that the GGMP repeats are important for the functional association between PfHsp70-1 and PfHop. These findings are in line with a recent study which reported that a GGAP motif of yeast Hsp70 (Ssa1) was important for interaction with Hsp40 (Ydj1) (Gong *et al*., 2018). Hsp40s have other binding sites in the Hsp70 NBD besides the EEVD. Findings by Gong *et al*. (2018) suggest that the closely similar motifs probably serve the same function, i.e association with co-chaperones.

Having established that the GGMP repeats play a role in Hop interaction, this study sought to further elucidate these findings using an Hsp70 homolog (DnaK) that lacks both the GGMP and EEVD motifs. The GGMP repeats were introduced into DnaK creating a DnaK-G variant. The DnaK-G variant was then used to elucidate whether this will promote interaction with PfHop. The data generated from both ELISA and slot blot showed that the DnaK-G variant did not associate with PfHop. This might suggest that without the EEVD the GGMP is insufficient to facilitate association between PfHsp70-1 and PfHop. Taken together, findings from the PfHsp70-1 variants suggest that the GGMP repeats regulate the interaction of PfHop with PfHsp70-1. Findings from the DnaK-G variant also highlight the importance of the EEVD motif in Hop interaction. However, there are speculations that suggest that the Hop/Hsp70 interaction occurs through other auxiliary sites outside the EEVD (reviewed by Edkins, 2016). It could also suggest that DnaK lacks residues important for interaction with Hop that may be positioned elsewhere outside the C-terminus.

Chapter 7

Conclusions and future perspectives

7 Conclusion and Future Work

Mutations were made in the GGMP repeat region of PfHsp70-1 as well as in the C-terminal tail of DnaK (Section 2.3.1) and the structural and functional consequence of this motif was elucidated. All the recombinant proteins expressed and purified successfully from *E. coli* cells. Both predictive studies and *in vitro* biophysical studies showed that there were secondary structural differences between the wild type proteins and the GGMP variants despite the conservative substitutions. Additionally, a DnaK-G variant in which the GGMP motif was introduced was also predicted to possess secondary structural differences deviant from the DnaK structure (Figure 3.6). These findings suggest that the changes the GGMP motif is of significance in the secondary structural composition of the C-terminal end of PfHsp70-1. However, it would be interesting to employ more robust structural characterization methods such as SRCD and SAXs in order to get definitive evidence on any minor structural differences.

The GGMP variants studied here exhibited reduced ATPase activity (Figure 7.1A) but retained the capability to suppress aggregation of heat-stressed MDH (Figure 7.1C). However, the PfHsp70-G632 ATPase function was enhanced by peptide substrates. Additionally, the capability of PfHsp70-G632 to suppress MDH aggregation was also abrogated by peptide substrates. On the other hand, the GGMP variants of KPf (KPf-G617 and KPf-G633) conferred thermosensitivity to *E. coli dnaK756* cells grown at 43.5 °C. Again, KPf-G617 (a derivative of the G632 mutation in PfHsp70-1) conferred better cytoprotection over KPf and KPf-G633. Evidently, the GGMP mutation at position 632 had the greatest effect on the chaperone function of the protein. This suggests that the N-terminal positioned GGMP repeats may be important for substrate binding in PfHsp70-1. Also based on the observed effect of peptide ALLLMYRR on PfHsp70-G632, modulation of PfHsp70-1 through the GGMP motif could abrogate the Hsp70 function in the parasite. PfHsp70-1 plays an important role in protein quality control and facilitates protein degradation via the ubiquitin-proteasome. In parasite, PfHsp70-1 is thought to be involved in drug resistance by reversing the oxidative damage exerted on parasite by antimalarial drugs (Akide-Ndunge *et al*. 2009).

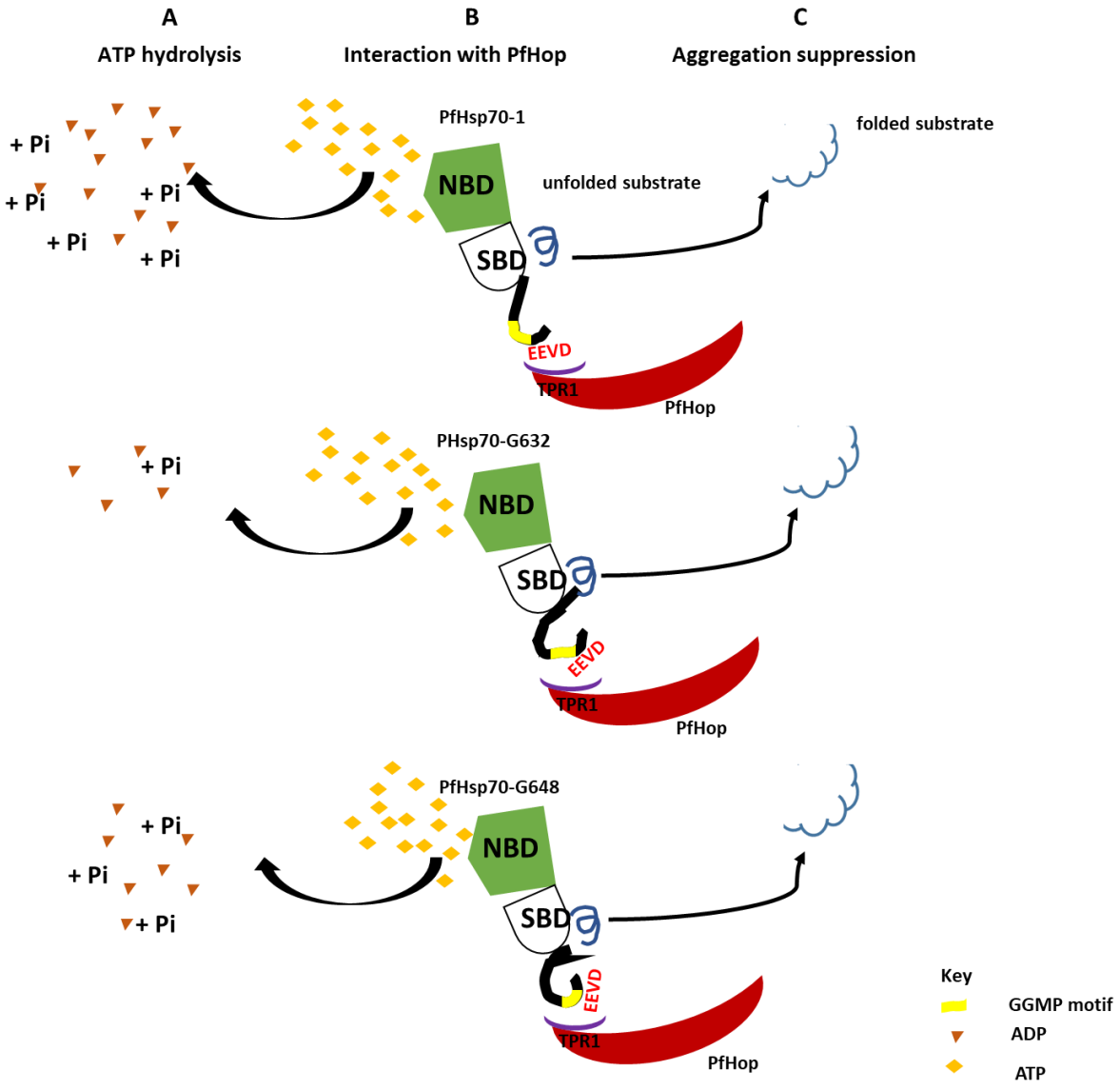

Figure 7.1. Model representing the role of the GGMP motif of PfHsp70-1. The figure highlights the effect of the GGMP motif of PfHsp70-1 on the protein's various functions such as (**A**) ATP hydrolysis. The PfHsp70-1 variants exhibited lower ATPase activity. (**B**) interaction with PfHop. The PfHsp70-1 variants exhibited reduced affinity for PfHop. (**C**) aggregation suppression capability. PfHsp70-1 variants retained the ability to suppress aggregation of heat stressed model substrate, MDH.

Furthermore, the effect of the structural modifications on the interaction of PfHsp70-1 with the co-chaperone, PfHop was evaluated. The PfHop/PfHsp70-1/PfHsp90 interaction has been shown

to be important for cytoprotection in *P. falciparum* (Banumathy *et al*., 2003; Gitau *et al*., 2012). Based on current findings, positional mutations in the GGMP motif influenced the association between PfHsp70-1 and co-chaperones (Figure 7.1B). This will likely affect the heterocomplex mediated by PfHop. However, it is important to further evaluate the role of the GGMP motif of PfHsp70-1 in its interaction with PfHop by using robust methods such as SPR and ITC. Taken together, evidence provided from this study indicates that the GGMP motif of PfHsp70-1 is important for the protein's chaperone function and interaction with PfHop. Interestingly, the inhibition of the variant PfHsp70-G632 by peptide substrates could be used as a model in peptide design towards targeting PfHsp70-1. However, despite their potential as antimalarial drugs, peptides are prone to binding to the plasma membrane and also proteolytic digestion (Vale *et al*., 2014), hence they are not bioavailable. Also, the production of peptide-based drugs is reported to be costly and hence the drugs would be expensive for low-income populations in developing countries that are most affected by malaria.

References

Abu Bakar, N.A., Klonis, N., Hanssen, E., Chan, C., Tilley, L. (2010). Digestive-vacuole genesis and endocytic processes in the early intraerythrocytic stages of *Plasmodium falciparum*. *J Cell Sci*, **123**: 441-50. doi: 10.1242/jcs.061499.

Achilonu, I., Siganunu, T.P., Dirr, H.W. (2014). Purification and characterization of recombinant human eukaryotic elongation factor 1 gamma. *Protein Expr Purif*, **99**: 70-77. doi: 10.1016/j.pep.2014.04.003.

Adão, R., Zanphorlin, L.M., Lima, T.B., Sriranganadane, D., Dahlström, K.M., Pinheiro, G.M.S., Gozzo, F.C., Barbosa, L.R.S., Ramos, C.H.I. (2017). Revealing the interaction mode of the highly flexible Sorghum bicolor Hsp70/Hsp90 organizing protein (Hop): A conserved carboxylate clamp confers high affinity binding to Hsp90. *J Proteomics*, **191**: 191-201. doi. 10.1016/j.jprot.2018.02.007.

Akide-Ndunge, O.B., Tambini, E., Giribaldi, G., McMillan, P.J., Muller, S., Arese, P., Turrini, F. (2009). Co-ordinated stage-dependent enhancement of *Plasmodium falciparum* antioxidant enzymes and heat shock protein expression in parasites growing in oxidatively stressed or G6PD-deficient red blood cells. *Malar J*, **8**: 113. doi: 10.1186/1475-2875-8-113.

Alderson, T.R., Kim, J.H., Cai, K., Frederick, R.O., Tonelli, M., Markley, J.L. (2014). Specialized Hsp70 (HscA) interdomain linker binds to its nucleotide-binding domain and stimulates ATP hydrolysis in both *cis* and *trans* configurations. *Biochemistry,* **53**: 7148-59. doi: 10.1021/bi5010552.

Alvira, S., Cuéllar, J., Röhl, A., Yamamoto, S., Itoh, H., Alfonso, C., Rivas, G., Buchner, J., Valpuesta, J.M. (2014). Structural characterization of the substrate transfer mechanism in Hsp70/Hsp90 folding machinery mediated by Hop. *Nat Commun*, **5**: 5484. doi: 10.1038/ncomms6484.

Arama, C., Troye-Blomberg, M. (2014). The path of malaria vaccine development: challenges and perspectives. *J Intern Med*, **275**: 456-466. doi: 10.1111/joim.12223.

Arteaga, C.L. (2011). Why is this effective Hsp90 inhibitor not being developed in HER2+ breast cancer? *Clin Cancer Res*, **17**: 4919-4921. doi: 10.1158/1078-0432.

Ashburner, M., Ball, C.A., Blake, J.A., Botstein, D., Butler, H., Cherry, J.M., Davis, A.P., Dolinski, K., Dwight, S.S., Eppig, J.T., Harris, M.A., Hill, D.P., Issel-Tarver, L., Kasarskis, A., Lewis, S., Matese, J.C., Richardson, J.E., Ringwald, M., Rubin, G.M., Sherlock, G. (2000). Gene ontology: tool for the unification of biology. The Gene Ontology Consortium. *Nat Genet*, **25**: 25-9. doi: 10.1038/75556.

Bajaj, K., Madhusudhan, M.S., Adkar, B.V., Chakrabarti, P., Ramakrishnan, C., Sali, A., Varadarajan, R. (2007). Stereochemical criteria for prediction of the effects of proline mutations on protein stability. *PLoS Comput Biol*, **3**: e241. doi: 10.1371/journal.pcbi.0030241.

References

Banerji, U., O'Donnell, A., Scurr, M., Pacey, S., Stapleton, S., Asad, Y., Simmons, L., Maloney, A., Raynaud, F., Campbell, M., Walton, M., Lakhani, S., Kaye, S., Workman, P., Judson, I. (2005). Phase I pharmacokinetic and pharmacodynamic study of 17-allylamino, 17-demethoxygeldanamycin in patients with advanced malignancies. *J Clin Oncol,* **23**: 4152-4161. doi: 10.1200/JCO.2005.00.612.

Banumathy, G., Singh, V., Pavithra, S.R., Tatu, U. (2003). Heat shock protein 90 function is essential for *Plasmodium falciparum* growth in human erythrocytes. *J Biol Chem*, **278**: 18336-18345. doi: 10.1074/jbc.M211309200.

Barends, T.R., Werbeck, N.D., Reinstein, J. (2010). Disaggregases in 4 dimensions. *Curr Opin Struct Biol*, **20**: 46-53. doi: 10.1016/j.sbi.2009.12.014.

Batista, F.A.H., Seraphim, T.V., Santos, C.A., Gonzaga, M.R., Barbosa, L.R.S., Ramos, C.H.I., Borges, J.C. (2016). Low sequence identity but high structural and functional conservation: The case of Hsp70/Hsp90 organizing protein (Hop/Sti1) of *Leishmania braziliensis*. *Arch Biochem Biophys*, **600**: 12-22. doi: 10.1016/j.abb.2016.04.008.

Baumeister, S., Winterberg, M., Duranton, C., Huber, S.M., Lang, F., Kirk, K., Lingelbach, K. (2006). Evidence for the involvement of *Plasmodium falciparum* proteins in the formation of new permeability pathways in the erythrocyte membrane. *Mol Microbiol*, **60**: 493-504. doi: 10.1111/j.1365-2958.2006.05112.x.

Behl, A., Mishra, P.C. (2018). Structural insights into the binding mechanism of *Plasmodium falciparum* exported Hsp40-Hsp70 chaperone pair. bioRxiv, doi: 10.1101/311191.

Belachew, E.B. (2018). Immune response and evasion mechanisms of *Plasmodium falciparum* parasites. *J Immunol Res*, 2018: 6529681. doi: 10.1155/2018/6529681.

Benkert, P., Biasini, M., Schwede, T. (2011). Toward the estimation of the absolute quality of individual protein structure models. *Bioinformatics,* **27**: 343-350. doi: 10.1093/bioinformatics/btq662.

Benkert, P., Tosatto, S.C.E., Schomburg, D. (2008). QMEAN: A comprehensive scoring function for model quality assessment. *Proteins*, **71**: 261-277. doi: 10.1002/prot.21715.

Bennink, S., Kiesow, M.J., Pradel, G. (2016). The development of malaria parasites in the mosquito midgut. *Cell Microbiol*, **18**: 905-918. doi: 10.1111/cmi.12604.

Bernado, P., Mylonas, E., Petoukhov, M.V., Blackledge, M., Svergun, D.I. (2007). Structural characterization of flexible proteins using small-angle X-ray scattering. *J Am Chem Soc*, **129**: 5656-5664. doi: 10.1021/ja069124n.

Bertelsen, E.B., Chang, L., Gestwicki, J.E., Zuiderweg, E.R.P. (2009). Solution conformation of wild-type *E. coli*Hsp70 (DnaK) chaperone complexed with ADP and substrate. *Proc Natl Acad Sci USA,* **106**: 8471-8476. doi: 10.1073/pnas.0903503106.

References

Betts, M.J., Russell, R.B. (2003). Amino acid properties and consequences of substitutions. Chapter 4. Bioinformatics for Geneticists. Edited by Michael R. Barnes and Ian C. Gray Copyright John Wiley & Sons, Ltd. ISBN: 0-470-84393-4 (HB); 0-470-84394-2 (PB).

Biesiadecki, B.J., Jin, J-P. (2011). A high-throughput solid-phase microplate protein-binding assay to investigate interactions between myofilament proteins. *J Biomed Biotechnol*, 2011: 421701. doi: 10.1155/2011/421701.

Blatch, G. L., Lässle, M. (1999). The tetratricopeptide repeat: a structural motif mediating protein-protein interactions. *Bioessays*, **21**: 932-939. doi: 10.1002/(SICI)1521-1878(199911)21:11<932::AID-BIES5>3.0.CO;2-N.

Blum, P., Ory, J., Bauernfeind, J., Krska, J. (1992). Physiological consequences of DnaK and DnaJ overproduction in *Escherichia coli*. *J Bacteriol*, **174**: 7436-44. doi: 10.1128/jb.174.22.7436-7444.1992.

Blundell, K.L.I.M., Pal, M., Roe, S.M., Pearl, L.H., Prodromou, C. (2017). The structure of FKBP38 in complex with the MEEVD tetratricopeptide binding-motif of Hsp90. *PLoS ONE*, **12**: e0173543. doi: 10.1371/journal.pone.0173543.

Boddey, J. A., O'Neill, M.T., Lopaticki, S., Carvalho, T.G., Hodder, A.N., Nebl, T., Wawra, S., van West, P., Ebrahimzadeh, Z., Richard, D., Flemming, S., Spielmann, T., Przyborski, J., Jeff J. Babon., Cowman, A.F. (2016). Export of malaria proteins requires co-translational processing of the PEXEL motif independent of phosphatidylinositol-3-phosphate binding. *Nat Commun*, **7**: 10470 doi: 10.1038/ncomms10470.

Bork P., Sander, C., Valencia, A. (1992). An ATPase domain common to prokaryotic cell-cycle proteins, sugar kinases, actin, and Hsp70 heat-shock proteins. *Proc Natl Acad Sci USA*, **89**: 7290-7294. doi: 10.1073/pnas.89.16.7290.

Bose, S., Weikl, T., Bugl, H., Buchner, J. (1996). Chaperone function of Hsp90-associated proteins. *Science*, **274**: 1715-1717. doi: 10.1126/science.274.5293.1715.

Bosl, B., Grimminger, V., Walter, S. (2006). The molecular chaperone Hsp104-a molecular machine for protein disaggregation. *J Struct Biol*, **156**: 139-148. doi: 10.1016/j.jsb.2006.02.004.

Botha, M., Chiang, A.N., Needham, P.G., Stephens, L.L., Hoppe, H.C., Külzer, S., Przyborski, J.M., Lingelbach, K., Wipf, P., Brodsky, J.L., Shonhai, A., Blatch, G.L. (2011). *Plasmodium falciparum* encodes a single cytosolic type I Hsp40 that functionally interacts with Hsp70 and is upregulated by heat shock. *Cell Stress Chaperones*, **16**: 389-401. doi: 10.1007/s12192-010-0250-6.

References

Botha, M., Pesce, E.R., Blatch, G.L. (2007). The Hsp40 proteins of *Plasmodium falciparum* and other apicomplexa: regulating chaperone power in the parasite and the host. *Int J Biochem Cell Biol,* **39**: 1781-1803. doi: 10.1016/j.biocel.2007.02.011.

Buchberger, A., Gassler, C.S., Buttner, M., McMacken, R., Bukau, B. (1999). Functional defects of the *DnaK756*mutant chaperone of *Escherichia coli* indicate distinct roles for amino- and carboxyl-terminal residues in substrate and co-chaperone interaction and interdomain communication. *J Biol Chem*, **274**: 38017-38026. doi: 10.1074/jbc.274.53.38017.

Buchberger, A., Theyssen, H., Schröder, H., McCarty, J.S., Virgallita, G., Milkereit, P., Reinstein, J., Bukau, B. (1995). Nucleotide-induced conformational changes in the ATPase and substrate binding domains of the DnaK chaperone provide evidence for interdomain communication. *J Biol Chem,* **270**: 16903-16910. doi: 10.1074/jbc.270.28.16903.

Buczynski G., Slepenkov S. V., Sehorn M. G., Witt S. N. (2001). Characterization of a lidless form of the molecular chaperone DnaK: deletion of the lid increases peptide on- and off-rate constants. *J Biol Chem*, **276**: 27231-27236. doi: 10.1074/jbc.M100237200.

Bukau, B., Weissman, J., Horwich, A. (2006). Molecular chaperones and protein quality control. *Cell*, **125**: 443-451. doi: 10.1016/j.cell.2006.04.014.

Bull, B.S., Herrmann, P.C. (2010). Morphology of the erythron. Chapter in Hematology**,** edited by Marshall A. Lichtman, Thomas J. Kipps, Uri Seligsohn, Kenneth Kaushansky, Josef T. Prchal. Copyright 2010, by The McGraw-Hill Companies.

Burkholder, W.F., Panagiotidis, C.A., Silverstein, S.J., Cegielska, A., Gottesman, M.E., Gaitanaris, G.A. (1994). Isolation and characterization of an *Escherichia coli* DnaK mutant with impaired ATPase activity. *J Mol Biol*, **242**: 364-377. doi: 10.1006/jmbi.1994.1587.

Cabral, F.J., Vianna, L.G., Medeiros, M.M., Carlos, B.C., Martha, R.D., Silva, N.M., da Silva4, L.H.P., Stabeli, R.G., Wunderlich, G. (2017). Immunoproteomics of *Plasmodium falciparum*-infected red blood cell membrane fractions. *Mem Inst Oswaldo Cruz,* **112**: 850-856. doi: 10.1590/0074-02760170041.

Calloni, G., Chen, T., Schermann, S.M., Chang, H.C., Genevaux, P., Agostini, F., Tartaglia, G.G., Hayer-Hartl, M., Hartl, F.U. (2012). DnaK functions as a central hub in the *E. coli* chaperone network. *Cell Rep*, **1**: 251-264. doi: 10.1016/j.celrep.2011.12.007.

Carey, M.A., Papin, J.A., Guler, J.L. (2017). Novel *Plasmodium falciparum* metabolic network reconstruction identifies shifts associated with clinical antimalarial resistance. *BMC Genomics*, **18**: 543. doi: 10.1186/s12864-017-3905-1.

References

Chakrabortee, S., Kayatekin, C., Newby, G.A., Mendillo, M.L., Lancaster, A., Lindquist, S. (2016). Luminidependens (LD) is an *Arabidopsis* protein with prion behavior. *Proc Natl Acad Sci USA*, **113**: 6065-6070. doi: 10.1073/pnas.1604478113.

Charnaud, S.C., Dixon, M.W.A., Nie, C.Q., Chappell, L., Sanders, P.R., Nebl, T., et al. (2017) The exported chaperone Hsp70-x supports virulence functions for *Plasmodium falciparum* blood-stage parasites. *PLoS ONE,* **12**: e0181656. doi: 10.1371/journal.pone.0181656.

Charpian, S., Przyborski, J.M. (2008). Protein transport across the parasitophorous vacuole of *Plasmodium falciparum*: into the great wide open. *Traffic*, 9: 157-165. doi: 10.1111/j.1600-0854.2007.00648.x.

Chen, S., Smith, D.F. (1998). Hop as an adaptor in the heat shock protein 70 (Hsp70) and Hsp90 chaperone machinery. *J Biol Chem*, **273**: 35194-35200. doi: 10.1074/jbc.273.52.35194.

Chen, Y., Barkley, M.D. (1998). Toward understanding tryptophan fluorescence in proteins. *Biochemistry*, **37**: 9976-9982. doi: 10.1021/bi980274n.

Chen, Y., Murillo-Solano, C., Kirkpatrick, M., Antoshchenko, T., Park, T., Pizarro, J. (2018). Repurposing drugs to target the malaria parasite unfolding protein response. *Sci Rep,* **8**:10333-10350. doi: 10.1038/s41598-018-28608-2.

Chiappori, F., Merelli, I., Milanesi, L., Colombo, G., Morra, G. (2016). An atomistic view of Hsp70 allosteric crosstalk: from the nucleotide to the substrate binding domain and back. *Sci Rep,* **6**, 23474. doi: 10.1038/srep23474.

Chua, C.S., Low, H., Lehming, N., Sim, T.S. (2012). Molecular analysis of *Plasmodium falciparum* co-chaperone Aha1 supports its interaction with and regulation of Hsp90 in the malaria parasite. *Int J Biochem Cell Biol*, **44**: 233-45. doi: 10.1016/j.biocel.2011.10.021.

Cierpicki, T., Bushweller, J.H., Derewenda, Z.S. (2005). Probing the supramodular architecture of a multidomain protein: The structure of syntenin in solution. *Structure*, **13**: 319-327. doi 10.1016/j.str.2004.12.014.

Ciglia, E., Vergin, J., Reimann, S., Smits, S.H.J., Schmitt, L., Groth, G., Holger, G. (2014). Resolving hot spots in the C-terminal dimerization domain that determine the stability of the molecular chaperone Hsp90. *PLoS ONE,* **9**: e96031. doi: 10.1371/journal.pone.0096031.

Clerico, E. M., Tilitsky, J. M., Meng, W., Gierasch, L. M. (2015). How Hsp70 molecular machines interact with their substrates to mediate diverse physiological functions. *J Mol Biol*, **427**: 1575-1588. doi: 10.1016/j.jmb.2015.02.004.

Cobb, D.W., Florentin, A., Fierro, M.A., Krakowiak, M., Moore, J.M., Muralidharan, V. (2017). The exported chaperone PfHsp70x is dispensable for the *Plasmodium falciparum* intraerythrocytic life cycle. *mSphere*, **2**: e00363-17. doi: 10.1128/mSphere.00363-17.

References

Cockburn, I.L., Boshoff, A., Pesce, E.-R., Blatch, G.L. (2014). Selective modulation of Plasmodial Hsp70s by small molecules with antimalarial activity. *Biol Chem*, **395**: 1353-1362. doi: 10.1515/hsz-2014-0138.

Cockburn, I.L., Pesce, E.R., Pryzborski, J.M., DaviesColeman, M.T., Clark, P.G.K., Keyzers, R.A., Stephens, L.L., Blatch, G.L. (2011). Screening for small molecule modulators of Hsp70 chaperone activity using protein aggregation suppression assays: inhibition of the plasmodial chaperone PfHsp70-1. *Biol Chem*, **392**: 431-438. doi: 10.1515/BC.2011.040.

Compton, L.A., Johnson, W.C.J. (1986). Analysis of protein circular dichroism spectra for secondary structure using a simple matrix multiplication. *Anal Biochem*, **155**: 155-167. doi: 10.1016/0003-2697(86)90241-1.

Cooke, B.M., Buckingham, D.W., Glenister, F.K., Fernandez, K.M., Bannister, L.H., Marti, M., Mohandas, N., Coppel, R.L. (2006). A Maurer's cleft-associated protein is essential for expression of the major malaria virulence antigen on the surface of infected red blood cells. *J Cell Biol*, **172**: 899-908. doi: 10.1083/jcb.200509122.

Cowman, A.F., Crabb, B.S. (2006). Invasion of red blood cells by malaria parasites. *Cell*, **124**: 755-66. doi: 10.1016/j.cell.2006.02.006.

Cowman, A.F., Berry, D., Baum, J. (2012). The cellular and molecular basis for malaria parasite invasion of the human red blood cell. *J Cell Bio*, **198**: 961-71. doi: 10.1083/jcb.201206112.

Craig, A., Scherf, A. (2001). Molecules on the surface of the *Plasmodium falciparum* infected erythrocyte and their role in malaria pathogenesis and immune evasion. *Mol Biochem Parasitol*, **115**: 129-43. doi: 10.1016/S0166-6851(01)00275-4.

Cui, Z., Liu, Y., Luan, W., Li, Q., Wu, D., Wang, S. (2010). Molecular cloning and characterization of a heat shock protein 70 gene in swimming crab (*Portunus trituberculatus*). *Fish Shellfish Immun,* **28**: 56-64. doi: 10.1016/j.fsi.2009.09.018.

Cutts, E.E., Laasch, N., Reiter, D.M., Trenker, R., Slater, L.M., Stansfeld, P.J., Vakonakis, I. (2017). Structural analysis of *P. falciparum* KAHRP and *Pf*EMP1 complexes with host erythrocyte spectrin suggests a model for cytoadherent knob protrusions. *PLoS Pathog*, **13**: e1006552. doi: 10.1371/journal.ppat.1006552.

Dahan-Moss, Y., Jamesboy, E., Gilbert, A., Burke, A., Kaiser, M., Mwamba, M., Ekoka, E., Oliver, S., Braack, L., Munhenga, G., Lobb, L., Tshikae, P., Wood, O., Samuel, M., Qwabe, B., Dlamini, D., Mabaso, N., Manyawo, Z., Zhikali, J., Davies, C., Sibambo, S., Nkosi, B., Koekemoer, L., Brooke, B. (2018). Malaria vector surveillance report, South Africa, January – December 2018. The Public Health Surveillance Bulletin, National Institute for Communicable Diseases (NICD) of the National Health Laboratory Service (NHLS).

References

Daniel, S., Bradley, G., Longshaw, V.M., Söti, C., Csermely, P and Blatch, G.L. (2008). Nuclear translocation of the phosphoprotein Hop (Hsp70/Hsp90 organizing protein) occurs under heat shock, and its proposed nuclear localization signal is involved in Hsp90 binding. *Biochimica et Biophysica Acta*, **1783**: 1003-1014. doi: 10.1016/j.bbamcr.2008.01.014.

Daniyan, M., Boshoff, A., Prinsloo, E., Pesce, E.R., Blatch, G.L. (2016). The malarial exported PFA0660w is an Hsp40 co-chaperone of PfHsp70-x. *PLoS ONE,* **11**: e0148517. doi: 10.1371/journal.pone.0148517.

Deponte, M., Hoppe, H.C., Lee, M.C., Maier, A.G., Richard, D., Rug, M., Spielmann, T., Przyborski, J.M. (2012). Wherever I may roam: protein and membrane trafficking in *P. falciparum*-infected red blood cells. *Mol Biochem Parasitol*, **186**: 95-116. doi: 10.1016/j.molbiopara.2012.09.007.

Desai, S.A. (2014). Why do malaria parasites increase host erythrocyte permeability? *Trends Parasitol*, **30**: 151-159. doi: 10.1016/j.pt.2014.01.003.

Dhangadamajhi, G., Shantanu, K.K., Manoranjan, R. (2010). The survival strategies of malaria parasite in the red blood cell and host cell polymorphisms. *Malar Res Treat*, doi: 10.4061/2010/973094.

Doberentz, E., Genneper, L., Wagner, R., Madea, B. (2017). Expression times for hsp27 and hsp70 as an indicator of thermal stress during death due to fire. *Int J Legal Med*, **131**: 1707-1718. doi: 10.1007/s00414-017-1566-x.

Dragovic, Z., Broadley, S.A., Shomura, Y., Bracher, A., Hartl, F.U. (2006). Molecular chaperones of the Hsp110 family act as nucleotide exchange factors of Hsp70s. *EMBO J,* **25**: 2519-2528. doi: 10.1038/sj.emboj.7601138.

Dunker, A.K., Lawson, J.D., Brown, C.J., Williams, R.M., Romero, P., Oh, J.S., Oldfield, C.J., Campen, A.M., Ratliff, C.M., Hipps, K.W., Ausio, J., Nissen, M.S., Reeves, R., Kang, C., Kissinger, C.R., Bailey, R.W., Griswold, M.D., Chiu, W., Garner, E.C., Obradovic, Z. (2001). Intrinsically disordered protein. *J Mol Graph Model*, **19**: 26-59. doi: 10.1016/S1093-3263(00)00138-8.

Durech, M., Trcka, F., Man, P., Blackburn, E.A., Hernychova, L., Dvorakova, P., Coufalova, D., Kavan, D., Vojtesek, B., Muller, P. (2016). Novel entropically driven conformation specific Interactions with Tomm34 protein modulate Hsp70 protein folding and ATPase activities. *Mol Cell Proteomics*, **15**: 1710-27. doi: 10.1074/mcp.M116.058131.

Dyson, H.J., Wright, P.E. (2005). Intrinsically unstructured proteins and their functions. *Nat Rev Mol Cell Biol,* **6**: 197-208. doi: 10.1038/nrm1589.

Easton, D.P., Kaneko, Y., Subjeck, J.R. (2000). The hsp110 and Grp1 70 stress proteins: newly recognized relatives of the Hsp70s. *Cell Stress Chaperones*. **5**:276-90. doi: 10.1379/1466-1268(2000)005<0276:thagsp>2.0.co;2.

References

Ebonga, I., Morgnera, N., Zhoua, M., Saraivab, M.A., Daturpallib, S., Jacksonb, S.E., Robinsona, C.V. (2011). Heterogeneity and dynamics in the assembly of the heat shock protein 90 chaperone complexes. *Proc Natl Acad Sci USA,* **108**: 17939-17944. doi: 10.1073/pnas.1106261108.

Edkins, A.L. (2015). CHIP: a co-chaperone for degradation by the proteasome**.** *Subcell Biochem*, **78**: 219-42. doi: 10.1007/978-3-319-11731-7_11.

Edkins, A.L. (2016). Hsp90 co-chaperones as drug targets in cancer: Current perspectives. *Top Med Chem*, **19**: 21-54. doi: 10.1007/7355_2015_99.

Elliott, D.A., McIntosh, M.T., Hosgood, H.D., Chen, S., Zhang, G., Baevova, P., Joiner, K.A. (2007). Four distinct pathways of hemoglobin uptake in the malaria parasite *Plasmodium falciparum*. *Proc Natl Acad Sci USA*, **105**: 2463-2468. doi: 10.1073pnas.0711067105.

Emmanouilidis, L., Schutz, U., Tripsianes, K., Madl, T., Radke, J., Rucktaeschel, R., Wilmanns, M., Schliebs, W., Erdmann, R., Sattler, M. (2017). Allosteric modulation of peroxisomal membrane protein recognition by farnesylation of the peroxisomal import receptor PEX19. *Nat Commun*, **8**: 14635-14635. doi: 10.1038/ncomms14635.

Fourie, A.M., Sambrook, J.F. and Gething, M.J. (1994). Common and divergent peptide binding specificities of hsp70 molecular chaperones. *J Biol Chem*, **269**: 30470-30478.

Fujioka, H., Aikawa, M. (2002). Structure and life cycle. In Malaria parasites and disease. Perlmann P, Troye-Blomberg M (eds): Malaria Immunology. Chem Immunol. Basel, Karger. 80: 1-26.

Gao, L., Imanaka, T., Fujiwara, S. (2015). A mutant chaperonin that is functional at lower temperatures enables hyperthermophilic archaea to grow under cold-stress conditions. *J Bacteriol,* **197**: 2642-2652. doi: 10.1128/JB.00279-15.

Gao, X.C., Zhou, C.J., Zhou, Z.R., Wu, M., Cao, C.Y., Hu, H.Y. (2012). The C-terminal helices of heat shock protein 70 are essential for J-domain binding and ATPase activation. *J Biol Chem*, **287**: 6044-6052. doi: 10.1074/jbc.M111.294728.

Gautam Kaul, G., Hitesh Thippeswamy, H. (2011). Role of heat shock proteins in diseases and their therapeutic potential. *Indian J Microbiol*, **51**: 124-131. doi: 10.1007/s12088-011-0147-9.

Genest, O., Hoskinsa, J.R., Kravats, A.N., Doylea, S.M., Wickner, S. (2016). Hsp70 and Hsp90 of *E. coli* directly interact for collaboration in protein remodeling. *J Mol Biol*, **427**: 3877-3889. doi: 10.1016/j.jmb.2015.10.010.

Gentile, F., Amodeo, P., Febbraio, F., Picaro, F., Motta, A., Nucci, R. (2002). SDS-resistant, active and thermostable dimers are obtained from the dissociation of homotetrameric β-glycosidase from hyperthermophilic *Sulfolobus solfataricus* in SDS. Stabilizing role of the A-C intermonomeric interface. *J Biol Chem,* **277**: 44050-44060. doi: 10.1074/jbc.M206761200.

References

Georgopoulos, C.P., Lam, B., Lundquist-Heil, A., Rudolph, C.F., Yochem, J., Feiss, M. (1979). Identification of the *E. coli dnaK* (groPC756) gene product. *Mol Gen Genet*, **172**: 143-149. doi: 10.1007/bf00268275.

Gitau, G.W., Mandal, P., Blatch, G.L., Przyborski, J., Shonhai, A. (2012). Characterization of the *Plasmodium falciparum* Hsp70-Hsp90 organizing protein (*Pf*Hop). *Cell Stress Chaperones*, **17**: 191-202. doi: 10.1007/s12192-011-0299-x.

Gitlin, I., Carbeck, J.D., Whitesides, G.M. (2006). Why are proteins charged? Networks of charge-charge interactions in proteins measured by charge ladders and capillary electrophoresis. Angew Chem Int Ed, **45**: 3022-3060. doi: 10.1002/anie.200502530.

Goeckeler, J.L., Petruso, A.P., Aguirre, J., Clement, C.C., Chiosis, G., Brodsky, J.L. (2008). The yeast Hsp110, Sse1p, exhibits high affinity peptide binding. *FEBS Lett*, **582**: 2393-2396. doi: 10.1016/j.febslet.2008.05.047.

Goel, S., Muthusamy, A., Miao, J., Cui, L., Salanti, A., Winzeler, E.A., Gowda, D.C. (2014). Targeted disruption of a ring-infected erythrocyte surface antigen (RESA)-like export protein gene in *Plasmodium falciparum* confers stable chondroitin 4-sulfate cytoadherence capacity. *J Biol Chem*, **289**: 34408-34421. doi: 10.1074/jbc.M114.615393.

Goldberg, D.E. (2005). Hemoglobin degradation. In: Compans R.W. et al. (eds) Malaria: Drugs, disease and post-genomic biology. *Curr Top Microbiol Immunol*, **295**: 275-291. doi: 10.1007/3-540-29088-5_11.

Goldman, A., Harper, S., Speicher, D.W. (2016). Detection of proteins on blot membranes. *Curr Protoc Protein Sci*, **86**: 1-11. doi: 10.1002/cpps.15.

Gomes, P.S, Bhardwaj, J., Rivera-Correa, J., Freire-De-Lima, C.G., Morrot, A. (2016). Immune escape strategies of malaria parasites. *Front Microbiol*, **7**: 1617. doi: 10.3389/fmicb.2016.01617.

Gong, W., Hu, W., Xu, L., Wu, H., Wu, S., Zhang, H., Wang, J., Jones, G.W., Perrett, S. (2018). The C-terminal GGAP motif of Hsp70 mediates substrate recognition and stress response in yeast. *J Biol Chem*, **293**: 17663-17675. doi: 10.1074/jbc.RA118.002691.

Goto, Y., Bhatia, A., Raman, V.S., Liang, H., Mohamath, R., Picone, A.F., Vidal, S.E., Vedvick, T.S., Howard, R.F., Reed, S.G. (2011). KSAC, the first defined polyprotein vaccine candidate for visceral leishmaniasis. *Clin Vaccine Immunol*, **18**: 1118-24. doi: 10.1128/CVI.05024-11.

Griffin, C.E., Hoke, J.M., Samarakoon, U., Duan, J., Mu, J., Ferdig, M.T., Warhurst, D.C., Cooper, R.A. (2012). Mutation in the *Plasmodium falciparum* CRT protein determines the stereospecific activity of antimalarial *Cinchona* alkaloids. *Antimicrob Agents Chemother*, **56**: 5356-5364. doi: 10.1128/AAC.05667-11.

References

Grigorian, A.L., Bustamante, J.J., Hernandez, P., Martinez, A.O., Haro, L.S. (2005). Extraordinarily stable disulfide-linked homodimer of human growth hormone. *Protein Sci*, **14**: 902-913. doi: 10.1110/ps.041048805.

Grüring, C., Heiber, A., Kruse, F., Flemming, S., Franci, G., Colombo, S.F., Fasana, S., Schoeler, H., Borgese, N., Stunnenberg, H.G., Przyborski, J.M., Gilberger, T.W., Spielmann, T. (2012). Uncovering common principles in protein export of malaria parasites. *Cell Host Microbe*, **12**: 717-729. doi: 10.1016/j.chom.2012.09.010.

Grüring, C., Heiber, A., Kruse, F., Spielmann, T. (2012). Uncovering common principles in protein export of malaria parasites. *Cell host microbe* **12**:717-29. doi: 10.1016/j.chom.2012.09.010.

Guney, E., Menche, J., Vidal, M., Bar´abasi, A.L. (2016). Network-based *in silico* drug efficacy screening. *Nat Commun,* **7**:10331-10343. doi: 10.1038/ncomms10331.

Guo, N.L., and Wan, Y.W. (2014). Network-based identification of biomarkers co-expressed with multiple pathways. *Cancer Inform*, **13**: 37-47. doi: 10.4137/CIN.S14054.

Guo, W., Reigan, P., Siegel, D., Zirrolli, J., Gustafson, D., Ross, D. (2006). The bioreduction of a series of benzoquinone ansamycins by NAD(P)H: quinone oxidoreductase 1 to more potent heat shock protein 90 inhibitors, the hydroquinone ansamycins. *Mol Pharmacol,* **70**: 1194-1203. doi: 10.1124/mol.106.025643.

Haerty, W., Golding, G.B. (2010). Low-complexity sequences and single amino acid repeats: not just "junk" peptide sequences. *Genome*, **53**: 753-62. doi: 10.1139/g10-063.

Hagel, L. (2001). Gel-Filtration Chromatography. *Curr Protoc Protein Sci,* doi: 10.1002/0471140864.ps0803s14.

Hahn, J.S. (2009). The Hsp90 chaperone machinery: from structure to drug development. *BMB Rep*, **42**: 623-630. doi: 10.5483/bmbrep.2009.42.10.623.

Haldar, K., Bhattacharjee, S., Safeukui, I. (2018). Drug resistance in *Plasmodium*. *Nat Rev Microbiol*, **16**: 156-170. doi: 10.1038/nrmicro.

Haldar, K., Mohandas, N. (2009). Malaria, erythrocytic infection, and anemia. *Hematology Am Soc Hematol Educ Program*, **2009**: 87-93. doi: 10.1182/asheducation-2009.1.87.

Hartl, F.U. (1996). Molecular chaperones in cellular protein folding. *Nature*, **381**: 571-579. doi: 10.1038/381571a0.

Hartl, F.U., Bracher, A., Hayer-Hartl, M. (2011). Molecular chaperones in protein folding and proteostasis. *Nature*, **475**: 324-32. doi: 10.1038/nature10317.

Hartl, F.U., Hayer-Hartl, M. (2009). Converging concepts of protein folding in vitro and in vivo. *Nat Struct Mol Biol*, **16**: 574-581. doi: 10.1038/nsmb.1591.

References

Hatherley, R., Clitheroe, C.L., Faya, N., Bishop, O.T. (2015). *Plasmodium falciparum* Hop: Detailed analysis of complex formation with Hsp70 and Hsp90. *Biochem Biophys Res Commun*, **456**: 440. doi: 10.1016/j.bbrc.2014.11.103.

Hatherley, R., Blatch, G.L., Bishop, O.T. (2014). *Plasmodium falciparum* Hsp70-x: a heat shock protein at the host-parasite interface. *J Biomol Struct Dyn*, **32**: 1766-79. doi: 10.1080/07391102.2013.834849.

Heiber, A., Kruse, F., Pick, C., Grüring, C., Flemming, S., Oberli, A., Schoeler H., Retzlaff, S., Mesén-Ramírez, P., Hiss, J.A., Kadekoppala, M., Hecht, L., Holder, A.A., Gilberger, T-W., Spielmann, T. (2013). Identification of new PNEPs indicates a substantial non-PEXEL exportome and underpins common features in *Plasmodium falciparum* protein export. *PLoS Pathog*, **9**: e1003546. doi: 10.1371/journal.ppat.1003546.

Hildenbrand, Z. L., Molugu, S. K., Herrera, N., Ramirez, C., Xiao, C., Bernal, R.A. (2011). Hsp90 can accommodate the simultaneous binding of the FKBP52 and HOP proteins. *Oncotarget*, **2**: 45-58. doi:10.18632/oncotarget.225.

Hiller, N.L., Bhattacharjee, S., van Ooij, C., Liolios, K., Harrison, T., Lopez-Estranõ, C., Haldar, K. (2004). A host-targeting signal in virulence proteins reveals a secretome in malarial infection. *Science*, **306**: 1934-1937. doi: 10.1126/science.1102737.

Hombach, A., Ommen, G., Chrobak, M., Clos, J. (2013). The Hsp90–Sti1 interaction is critical for *Leishmania donovani* proliferation in both life cycle stages. *Cell Microbiol*, **15**: 585-600. doi: 10.1111/cmi.12057.

Hsu, W.L., Oldfield, C., Meng, J., Huang, F., Xue, B., Uversky, V.N., Romero, P., Dunker, A.K. (2012). Intrinsic protein disorder and protein-protein interactions. *Pac Symp Biocomput*, **2012**: 116-27.

Iglesias, V., de Groot, N.S., Ventura, S. (2015). Computational analysis of candidate prion-like proteins in bacteria and their role. *Front Microbiol*, **6**: 1123. doi: 10.3389/fmicb.2015.01123.

Ignatev, A., Bhargav, S.P., Vahokoski, J., Kursula, P., Kursula, I. (2012). The Lasso segment is required for functional dimerization of the *Plasmodium* Formin 1 FH2 domain. *PLoS ONE,* **7**: e33586. doi: 10.1371/journal.pone.0033586.

Jhaveri, K., Modi, S. (2015). Ganetespib: research and clinical development. *Onco Targets Ther*, **8**: 1849-1858. doi: 10.2147/OTT.S65804.

Johnson, J.L. (2012). Evolution and function of diverse Hsp90 homologs and cochaperone proteins. *Biochimica et Biophysica Acta (BBA) - Molecular Cell Research*, **3**: 607-613. doi: 10.1016/j.bbamcr.2011.09.020.

References

Jonson, P.H., Petersen, S.B. (2001). A critical view on conservative mutations. *Protein Eng Des Sel,* **14**: 397-402. doi:10.1093/protein/14.6.397.

Kajander T., Sachs J. N., Goldman A., Regan L. (2009). Electrostatic interactions of Hsp-organizing protein tetratricopeptide domains with Hsp70 and Hsp90: computational analysis and protein engineering. *J Biol Chem*, **284**: 25364-25374. doi: 10.1074/jbc.M109.033894.

Kamareddine, L. (2012). The biological control of the malaria vector. *Toxins*, **4**: 748-767. doi: 10.3390/toxins4090748.

Kampinga, H. H., Craig, E. A. (2010). The HSP70 chaperone machinery: J proteins as drivers of functional specificity. *Nat Rev Mol Cell Bio,* **11:** 579-592. doi: 10.1038/nrm2941.

Keijzer, C., Wieten, L., van Herwijnen, M., van der Zee, R., Van Eden, W., Broere, F. (2012). Heat shock proteins are therapeutic targets in autoimmune diseases and other chronic inflammatory conditions. *Expert Opin Ther Targets*, **16**: 849-57. doi: 10.1517/14728222.2012.706605.

Kelley, L.A., Mezulis, S., Yates, C.M., Wass, M.N., Sternberg, M.J. (2015). The Phyre2 web portal for protein modeling, prediction and analysis. *Nat Protoc*, **10**: 845-58. doi: 10.1038/nprot.2015.053.

Kilili, G.K., LaCount, D.J. (2011). An Erythrocyte cytoskeleton-binding motif in exported *Plasmodium falciparum* proteins. *Eukaryotic Cell*, **10**: 1439-1447. doi**:** 10.1128/EC.05180-11.

King, O.D., Gitler, A.D., Shorter, J. (2012). The tip of the iceberg: RNA-binding proteins with prion-like domains in neurodegenerative disease. *Brain Res*, **1462**: 61-80. doi: 10.1016/j.brainres.2012.01.016.

Kityk, R., Kopp, J., Sinning, I., Mayer, M.P. (2012). Structure and dynamics of the ATP-bound open conformation of Hsp70 chaperones. *Mol Cell*, **48**: 863-874. doi: 10.1016/j.molcel.2012.09.023.

Kityk, R., Vogel, M., Schlecht, R., Bukau, B., Mayer, M.P. (2015). Pathways of allosteric regulation in Hsp70 chaperones. *Nat Commun*, **6**: 8308 doi: 10.1038/ncomms9308.

Knapp, R.T., Wong, M.J.H., Kollmannsberger, L.K., Gassen, N.C., Kretzschmar, A., *et al*. (2014). Hsp70 Cochaperones HspBP1 and BAG-1M differentially regulate steroid hormone receptor function. *PLoS ONE,* **9**: e85415. doi: 10.1371/journal.pone.0085415.

Kolodziejski, P.J., Rashid, M.B., Eissa, N.T. (2003). Intracellular formation of ‘‘undisruptable’’ dimers of inducible nitric oxide synthase. *Proc Natl Acad Sci USA*, **100**: 14263-14268. doi: 10.1073/pnas.2435290100.

Konarev, P. V., Petoukhov, M. V., Volkov, V. V., Svergun, D. I. (2006). ATSAS 2.1, a program package for small-angle scattering data analysis. *J Appl Cryst*, **39**: 277-286. doi: 10.1107/S0021889806004699.

References

Kravats, A.N., Doyle, S.M., Hoskins, J.R., Genest, O., Doody, E., Wickner, S. (2017). Interaction of *E. coli* Hsp90 with DnaK involves the DnaJ binding region of DnaK. *J Mol Biol*, **429**: 858-872. doi: 10.1016/j.jmb.2016.12.014.

Kravats, A.N., Hoskins, J., Michael Reidy, M., Johnson, J.L., Doyle, S.M., Genest, O., Masison, D.C., Wickner, S. (2018). Functional and physical interaction between yeast Hsp90 and Hsp70. *Proc Natl Acad Sci USA*, **115**: 2210-2219. doi: 10.1073/pnas.1719969115.

Kriegenburg, F., Ellgaard, L., Hartmann-Petersen, R. (2012). Molecular chaperones in targeting misfolded proteins for ubiquitin-dependent degradation. *FEBS Journal*, **279**: 532-542. doi: 10.1111/j.1742-4658.2011.08456.x.

Kufareva, I., Abagyan, R. (2012). Methods of protein structure comparison. *Methods Mol Biol*, **857**: 231-257. doi: 10.1007/978-1-61779-588-6_1.

Külzer, S., Charnaud, S., Dagan, T., Riedel, J., Mandal, P., Pesce, E.R., Blatch, G.L., Crabb, B.S., Gilson, P.R., Przyborski, J.M. (2012). *Plasmodium falciparum*-encoded exported hsp70/hsp40 chaperone/co-chaperone complexes within the host erythrocyte. *Cell Microbiol*, **11**: 1784-1795. doi: 10.1111/j.1462-5822.2012.01840.x.

Kumar, N., Koski, G., Harada, M., Aikawa, M., Zheng, H. (1991). Induction and localization of *Plasmodium falciparum* stress proteins related to the heat shock protein 70 family. *Mol Biochem Parasitol*, **48**: 47-58. doi: 10.1016/0166-6851(91)90163-Z.

Kumar, R., Moche, M., Winblad, B., Pavlov, P.F. (2017). Combined x-ray crystallography and computational modeling approach to investigate the Hsp90 C-terminal peptide binding to FKBP51. *Sci Rep*, **7**: 14288. doi: 10.1038/s41598-017-14731-z.

Kumar, R., Pavithra, S.R., Tatu, U. (2007). Three-dimensional structure of heat shock protein 90 from *Plasmodium falciparum*: molecular modeling approach to rational drug design against malaria. *J Biosci,* **32**: 531-536. doi: 10.1007/s12038-007-0052-x.

Lackie, R.E., Lopes, M.H., Farhan, S.M.K., Razzaq, A., Moshitzky, G., Prado, M.B., Beraldo, F.H., Maciejewski, A., Gros, R., Fan, J., Choy, W.Y., Greenberg, D.S., Martins, V.R., Duennwald, M.L., Soreq, H., Prado, V.F., Prado, M.A.M. (2018). A hypomorphic Stip1 allele reveals the requirement for chaperone networks in mouse 2 development and aging. *bioRxiv*, doi: 10.1101/258673.

LaCount, D.J., Vignali, M., Chettier, R., Phansalkar, A., Bell, R., Hesselberth, J.R, Schoenfeld, L.W., Ota, I., Sahasrabudhe, S., Kurschner, C., Fields, S., Hughes, R.E. (2005). A protein interaction network of the malaria parasite *Plasmodium falciparum*. *Nature*, **438**: 103-107 doi: 10.1038/nature04104.

References

Langer, T., Rosmus, S., Fasold, H. (2003). Intracellular localization of the 90 kDa heat shock protein (HSP90alpha) determined by expression of a EGFP HSP90 alpha-fusion protein in unstressed and heat-stressed 3T3 cells. *Cell Biol Int,* **27**: 47-52. doi: 10.1016/S1065-6995(02)00256-1.

Lässle, M., Blatch, G.L., Kundra, V., Takatori, T., Zetter, B.R. (1997). Stress-inducible, Murine protein mSTI1. Characterization of binding domains for heat shock proteins and *in vitro* phosphorylation by different kinases. *J Biol Chem*, **272**: 1876-1884. doi: 10.1074/jbc.272.3.1876.

Laufen, T., Mayer, M.P., Beisel, C., Klostermeier, D., Mogk, A., Reinstein, J., Bukau, B. (1999). Mechanism of regulation of Hsp70 chaperones by DnaJ cochaperones. *Proc Natl Acad Sci USA,* **96**: 5452-5457. doi: 10.1073/pnas.96.10.5452.

Leak, R.K. (2014). Heat shock proteins in neurodegenerative disorders and aging. *J Cell Commun Signal*, **8**: 293-310. doi: 10.1007/s12079-014-0243-9**.**

Levine, N.D. (1988). Progress in taxonomy of the apicomplexan protozoa. *J Protozool*, **35**: 518-520. doi: 10.1111/j.1550-7408.1988.tb04141.x.

Li, J., Sun, X., Wang, Z., Chen, L., Li, D., Zhou, J., Liu, M. (2012). Regulation of vascular endothelial cell polarization and migration by Hsp70/Hsp90-organizing protein. *PLoS One,* **7**: e36389. doi: 10.1371/journal.pone.0036389.

Li, J., Soroka, J., Buchner, J. (2012). The Hsp90 chaperone machinery: conformational dynamics and regulation by co-chaperones. *Biochim Biophys Acta*, **1823**: 624-635. doi: 10.1016/j.bbamcr.2011.09.003.

Lide, D.R. (1991). Handbook of Chemistry and Physics, 72nd Edition, CRC Press, Boca Raton, FL. ISBN-13: 978-0849304729.

Lim, L., McFadden, G.I. (2010). The evolution, metabolism and functions of the apicoplast. *Philos Trans R Soc Lond B Biol Sci*, **365**: 749-763. doi: 10.1098/rstb.2009.0273.

Lindquist, S., Craig, E.A. (1988). The heat-shock proteins. *Annu Rev Genet*, **22**: 631-677. doi: 10.1146/annurev.ge.22.120188.003215.

Lingelbach, K., Joiner, K.A. (1998). The parasitophorous vacuole membrane surrounding *Plasmodium* and *Toxoplasma*: an unusual compartment in infected cells. *J Cell Sci*, **111**: 1467-1475.

Linxweiler, M., Schick, B., Zimmermann, R. (2017). Let's talk about Secs: Sec61, Sec62, and Sec63 in signal transduction, oncology, and personalized medicine. *Signal Transduct Target Ther*, **2**: e17002. doi: 10.1038/sigtrans.2017.2.

References

Lobley, A., Whitmore, L., Wallace, B.A. (2002). DICHROWEB: an interactive website for the analysis of protein secondary structure from circular dichroism spectra. *Bioinformatics,* **18**: 211-212. doi: 10.1093/bioinformatics/18.1.211.

Longshaw, V. M., Chapple, J. P., Balda, M. S., Cheetham, M. E., Blatch, G. L. (2004). Nuclear translocation of the Hsp70/Hsp90 organizing protein mSTI1 is regulated by cell cycle kinases. *J Cell Sci*, **117**: 701-710. doi: 10.1242/jcs.00905.

Luthuli, S.D., Chili, M.M., Revaprasadu, N., Shonhai, A. (2013). Cysteine-capped gold nanoparticles suppress aggregation of proteins exposed to heat stress. *IUBMB Life*, **65**: 454-461. doi: 10.1002/iub.1146.

Lyons, R.E., Johnson, A.M. (1998). Gene sequence and transcription differences in 70 kDa heat shock protein correlate with murine virulence of *Toxoplasma gondii. Int J Parasitol*, **28**: 1041-1051.

Mabate, B., Zininga, T., Ramatsui, L., Makumire, S., Achilonu, I., Dirr, H.W., Shonhai, A. (2018). Structural and biochemical characterization of *Plasmodium falciparum* Hsp70-x reveals functional versatility of its C-terminal EEVN motif. *Proteins*, **86**: 1189-1201. doi: 10.1002/prot.25600.

MacFarlane, J., Blaxter, M.L., Bishop, P., Miles, M.A., Kelly, J.M. (1990). Identification and characterization of a *Leishmania donovani* antigen belonging to the 70 kDa heat shock protein family. *Eur J Biochem*, **190**: 377-384. doi: 10.1111/j.1432-1033.1990.tb15586.x.

Maier, A.G., Cooke, B.M., Cowman, A.F., Tilley, L. (2009). Malaria parasite proteins that remodel the host erythrocyte. *Nat Rev Microbiol*, **7**: 341-354. doi: 10.1038/nrmicro2110.

Maiti, M., Van Domselaar, G.H., Zhang, H., Wishart, D.S. (2004). SuperPose: a simple server for sophisticated structural superposition. *Nucleic Acids Res*, **32**: 590-594. doi: 10.1093/nar/gkh477.

Makhnevych, T., Houry, W.A. (2012). The role of Hsp90 in protein complex assembly. *Biochim Biophys Acta*, **1823**: 674-682. doi: 10.1016/j.bbamcr.2011.09.001.

Makhoba, X.H., Burger, A., Coertzen, D., Zininga, T., Birkholtz, L.M., Shonhai, A. (2016). Use of a chimeric Hsp70 to enhance the quality of recombinant *Plasmodium falciparum* S-adenosylmethionine Decarboxylase protein produced in *Escherichia coli*. *PLoS ONE*, **11**: e0152626. doi: 10.1371/journal.pone.0152626.

Makumire, S., Chakravadhanula, V.S.K., Köllische, G., Redel, E., Shonhai, A. (2015). Immunomodulatory activity of zinc peroxide (ZnO_2) and titanium dioxide (TiO_2) nanoparticles and their effects on DNA and protein integrity. *Toxicology Let*, **227**: 56-64. doi:10.1016/j.toxlet.2014.02.027.

References

Marcion, G., Seigneuric, R., Chavanne, E., Artur, Y., Briand, L., Hadi, T., Gobbo, J., Garrido, C., Neiers, F. (2015). C-terminal amino acids are essential for human heat shock protein 70 dimerization. *Cell Stress Chaperones*, **20**: 61-72. doi: 10.1007/s12192-014-0526-3.

Marti, M., Good, R.T., Rug, M., Knue*Pf*er, E., Cowman, A.F. (2004). Targeting malaria virulence and remodeling proteins to the host erythrocyte. *Science*, **306**: 1930-1933. e0152626. doi: 10.1371/journal.pone.0152626.

Mayer, M.P., Bukau, B. (2005). Hsp70 chaperones: Cellular functions and molecular mechanisms. *Cell Mol Life Sci*, **62**: 670-684. doi: 10.1007/s00018-004-4464-6.

Mayer, M.P., Kityk, R. (2015). Insights into the molecular mechanism of allostery in Hsp70s. *Front Mol Biosci*, **2**: 58. doi: 10.3389/fmolb.2015.00058.

Mbengue, A., Yam, X.Y., Braun-Breton, C. (2012). Human erythrocyte remodeling during *Plasmodium falciparum* malaria parasite growth and egress. *Br J Haematol*, **157**: 171-179. doi: 10.1111/j.1365-2141.2012.09044.x.

McHaourab, H.S., Godar, J.A., Stewart, P.L. (2009). Structure and mechanism of protein stability sensors: chaperone activity of small heat shock proteins. *Biochemistry*, **48**: 3828-3837. doi: 10.1021/bi900212j.

Meyer, A.S., Gillespie, J.R., Walther, D., Millet, I.S., Doniach, S., Frydman, J. (2003). Closing the folding chamber of the eukaryotic chaperonin requires the transition state of ATP hydrolysis. *Cell*, **11**: 369-381. doi: 10.1016/S0092-8674(03)00307-6.

Milani, K.J., Schneider, T.G., Taraschi, T.F. (2015). Defining the morphology and mechanism of the hemoglobin transport pathway in *Plasmodium falciparum*-infected erythrocytes. *Eukaryot Cell*, **14**: 415-426. doi: 10.1128/EC.00267-14.

Miller, C.M.D., Smith, N.C., Johnson, A.M. (1999). Cytokines, nitric oxide, heat shock proteins and virulence in *Toxoplasma. Parasitol Today*, **10**: 418-422. doi: 10.1016/S0169-4758(99)01515-X.

Minagawa, S., Kondoh, Y., Sueoka, K., Osada, H., Nakamoto, H. (2012). Cyclic lipopeptide antibiotics bind to the N-terminal domain of the prokaryotic Hsp90 to inhibit the chaperone activity. *Biochem J*, **435**: 237-246. doi: 10.1042/BJ2010074.

Misra, G., Ramachandran, R. (2009). Hsp70-1 from *Plasmodium falciparum*: Protein stability, domain analysis, and chaperone activity. *Biophys Chem*, **142**: 55-64. doi: 10.1016/j.bpc.2009.03.006.

Misselwitz, B., Staeck, O., Rapoport, T. A. (1998). J proteins catalytically activate Hsp70 molecules to trap a wide range of peptide sequences. *Mol Cell*, **2**: 593-603. doi: 10.1016/S1097-2765(00)80158-6.

References

Mohandas, N., An, X. (2012). Malaria and human red blood cells. *Med Microbiol Immunol,* **201**: 593-598. doi: 10.1007/s00430-012-0272-z.

Moll, K., Palmkvist, M., Ch'ng, J., Kiwuwa, M.S., Wahlgren, M. (2015). Evasion of Immunity to *Plasmodium falciparum*: Rosettes of blood group A impair recognition of *Pf*EMP1. *PLoS ONE,* **10**: e0145120. doi: 10.1371/journal.pone.0145120.

Mondal, T., Rasmussen, M., Pandey, G.K., Isaksson, A., Kanduri, C. (2010). Characterization of the RNA content of chromatin. *Genome Res*, **20**: 899-907. doi: 10.1101/gr.103473.109.

Monera, O.D., Sereda, T.J., Zhou, N.E., Kay, C.M., Hodges, R.S. (1995). Relationship of sidechain hydrophobicity and alpha-helical propensity on the stability of the single-stranded amphipathic alpha-helix. *J Pept Sci,* **1**: 319-329. doi: 10.1002/psc.310010507.

Money, T., Barrett, J., Dixon, R., Austin, S. (2001). Protein-protein Interactions in the complex between the enhancer binding protein NIFA and the sensor NIFL from *Azotobacter vinelandii. J Bacteriol*, **183**: 1359-1368. doi: 10.1128/JB.183.4.1359–1368.2001.

Mora´n Luengo, T., Kityk, R., Mayer, M.P., Rudiger, S.D.G. (2018). Hsp90 breaks the deadlock of the Hsp70 chaperone system. *Molecular Cell*, **70**: 1-8. doi: 10.1016/j.molcel.2018.03.028.

Morales, M.A., Watanabe, R., Dacher, M., Chafey, P., Osorio, Y., Fortéa, J., Scott, D.A., Beverley, S.M., Ommen, G., Clos, J., Hem, S., Lenormand, P., Rousselle, J.C., Namane, A., Späth, G.F. (2010). Phosphoproteome dynamics reveal heat-shock protein complexes specific to the *Leishmania donovani* infectious stage. *Proc Natl Acad Sci USA*, **107**: 8381-8386. doi: 10.1073/pnas.0914768107.

Morgan, R.M.L., Hernández-Ramírez, L.C., Trivellin, G., Zhou, L., Roe, S.M., Korbonits, M., Prodromou, C. (2012). Structure of the TPR Domain of AIP: Lack of client protein interaction with the C-Terminal α-7 helix of the TPR Domain of AIP is sufficient for pituitary adenoma predisposition. *PLoS ONE,* **7**: e53339. doi: 10.1371/journal.pone.0053339.

Moudgil, K.D., Thompson, S.J., Geraci, F., Paepe, B.D., Shoenfeld, Y. (2013). Heat-shock proteins in autoimmunity. *Autoimmune Dis*, doi: 10.1155/2013/621417.

Mundwiler-Pachlatko, E., Beck, H.P. (2013). Maurer's clefts, the enigma of *Plasmodium falciparum. Proc Natl Acad Sci USA*, **110**: 19987-19994. doi: 10.1073/pnas.1309247110.

Muralidharan, V., Oksman, A., Pal, P., Lindquist, S., Goldberg, D.E. (2012). *Plasmodium falciparum* heat shock protein 110 stabilizes the asparagine repeat-rich parasite proteome during malarial fevers. *Nat Commun*, **3**: 1310. doi: 10.1038/ncomms2306.

Nakamoto, H., Fujita, K., Ohtaki, A., Watanabe, S., Narumi, S., Maruyama, T., Suenaga, E., Misono, T.S., Kumar, P.K.R., Goloubinoff, P., Yoshikawa, H. (2014). Physical interaction

between bacterial heat shock protein (Hsp) 90 and Hsp70 chaperones mediates their cooperative action to refold denatured proteins. *J Biol Chem*, **289**: 6110-6119. doi: 10.1074/jbc.M113.524801.

Njunge, J.M., Ludewig1, M.H., Boshoff, A., Pesce, E.R., Blatch, G.L. (2013). Hsp70s and J proteins of *Plasmodium* parasites infecting rodents and primates: structure, function, clinical relevance, and drug targets. *Current Pharm Des*, **19**: 387-403. doi: 10.2174/138161213804143734.

Njunge, J.M., Mandal, P., Przyborski, J.M., Boshoff, A., Pesce, E.R., Blatch, G.L. (2015). PFB0595w is a *Plasmodium falciparum* J protein that co-localizes with PfHsp70-1 and can stimulate its in vitro ATP hydrolysis activity. *Int J Biochem Cell Biol*, **62**: 47-53. doi: 10.1016/j.biocel.2015.02.008.

Nocek, B., Kochinyan, S., Proudfoot, M., Brown, G., Evdokimova, E., Osipiuk, J., Edwards, A.M., Savchenko, A., Joachimiak, A., Yakunin, A.F. (2008). Crystal structure of putative polyphosphate kinase 2 from *Pseudomonas aeruginosa* PA01. *Proc Natl Acad Sci USA*, **105**: 17730-17735. doi: 10.1038/sj.embor.7400448.

Nowicki, Ł., Leźnicki, P., Morawiec, E., Litwińczuk, N., Liberek, K. (2012). Role of a conserved aspartic acid in nucleotide binding domain 1 (NBD1) of Hsp100 chaperones in their activities. *Cell Stress Chaperones*, **17**: 361-373. doi: 10.1007/s12192-011-0312-4.

Nyakundi, D.O., Vuko, L.A.M., Bentley, S.J., Hoppe, H., Blatch, G.L., Boshoff, A. (2016). *Plasmodium falciparum* Hep1 is required to prevent the self-aggregation of PfHsp70-3. *PLoS One*, **11**: e0156446. doi: 10.1371/journal.pone.0156446**.**

Nyalwidhe, J., Lingelbach, K. (2006). Proteases and chaperones are the most abundant proteins in the parasitophorous vacuole of *Plasmodium falciparum*-infected erythrocytes. *Proteomics*, **6**: 1563-1573. doi: 10.1002/pmic.200500379.

Odunuga O. O., Longshaw V. M., Blatch G. L. (2004). Hop: more than an Hsp70/Hsp90 adaptor protein. *Bioessays*, **26**: 1058-1068. doi: 10.1002/bies.20107.

Onuoha, S. C., Coulstock, E. T., Grossmann, J. G., Jackson, S. E. (2008). Structural studies on the co-chaperone Hop and its complexes with Hsp90. *J Mol Biol*, **379**: 732-744. doi: 10.1016/j.jmb.2008.02.013.

Ozbabacan, S.E.A., Engin, H.B., Gursoy, A., Keskin, O. (2011). Transient protein-protein interactions. *Protein Eng Des Sel*, **24**: 635-648. doi: 10.1093/protein/gzr025.

Pallarès, I., de Groot, N.S., Iglesias, V., Sant'Anna, R., Biosca, A., Fernàndez-Busquets, X., Ventura, S. (2018). Discoveringputative prion-like proteins in *Plasmodium falciparum*: A computational and experimental analysis. *Front Microbiol*, **9**: 1737. doi: 10.3389/fmicb.2018.01737.

Pallavi, R., Roy N., Nageshan, R.K., Talukdar, P., Pavithra, S.R., Reddy, R., Venketesh, S., Kumar, R., Gupta, A.K., Singh, R.K., Yadav S,C., Tatu U. Heat shock protein 90 as a drug target against protozoan infections: biochemical characterization of HSP90 from *Plasmodium falciparum* and

References

Trypanosoma evansi and evaluation of its inhibitor as a candidate drug. *J Biol Chem*, **285**: 37964-37975. doi: 10.1074/jbc.M110.155317.

Pavithra, S.R., Banumathy, G., Joy, O., Singh, V., Tatu, U. (2004). Recurrent fever promotes *Plasmodium falciparum* development in human erythrocytes. *J Biol Chem*, **279**: 46692-46699. doi: 10.1074/jbc.M409165200.

Pavithra, S.R., Kumar, R., Tatu, U. (2007). Systems analysis of chaperone networks in the malarial parasite *Plasmodium falciparum*. *PLOS Comput Biol*, **3**: e168. doi: 10.1371/journal.pcbi.0030168.

Pei, X., An, X., Guo, X., Tarnawski, M., Coppel, R., Mohandas, N. (2005). Structural and functional studies of interaction between *Plasmodium falciparum* knob-associated histidine-rich protein (KAHRP) and erythrocyte spectrin. *J Biol Chem*, **280**: 31166-31171. doi:10.1074/jbc.M505298200.

Pellegrini, M. (2015). Tandem repeats in proteins: prediction algorithms and biological role. *Front Bioeng Biotechnol*, **3**: 143. doi: 10.3389/fbioe.2015.00143.

Penkler, D.L., Atilgan, C., Bishop, Ö.T. (2018). Allosteric modulation of human Hsp90α conformational dynamics. *J Chem Inf Model,* **58**: 383-404. doi: 10.1021/acs.jcim.7b00630.

Pesce, E.R., Acharya, P., Tatu, U., Nicoll, W.S., Shonhai, A., Hoppe, H.C., Blatch, G.L. (2008). The *Plasmodium falciparum* heat shock protein 40, *Pf*j4, associates with heat shock protein 70 and shows similar heat induction and localization patterns. *Int J Biochem Cell Biol*, **40**: 2914-2926. doi: 10.1016/j.biocel.2008.06.011.

Peter, B., Bosze, S., Horvath, R. (2017). Biophysical characteristics of proteins and living cells exposed to the green tea polyphenol epigallocatechin-3-gallate (EGCg): Review of recent advances from molecular mechanisms to nanomedicine and clinical trials. *Eur Biophys J*, **46**: 1-24. doi: 10.1007/s00249-016-1141-2.

Pettersen, E.F., Goddard, T.D., Huang, C.C., Couch, G.S., Greenblatt, D.M., Meng, E.C., Ferrin, T.E. (2004). UCSF Chimera--a visualization system for exploratory research and analysis. *J Comput Chem*, **25**: 1605-1612. doi: 10.1002/jcc.20084.

Pishchany, G., Skaar, E.P. (2012). Taste for Blood: Hemoglobin as a nutrient source for pathogens *PLoS Pathog*, **8**: e1002535. doi: 10.1371/journal.ppat.1002535.

Pooe, O.J., Köllisch, G., Heine, H., Shonhai, A. (2017). *Plasmodium falciparum* Hsp70 lacks immune modulatory activity. *Protein Pept Lett*, **24**: 503-510. doi: 10.2174/0929866524666170214141909.

Posfai, D., Eubanks, A.L., Keim, A.I., Lu, K-Y., Wang, G.Z., Hughes, P.F., Kato, N., Haystead, T.A., Derbyshire, E.R. (2018). Identification of Hsp90 inhibitors with anti-*Plasmodium* activity. *Antimicrob Agents Chemother,* **62**: e01799-17. doi:10.1128/AAC.01799-17.

Prapapanich, V., Chen, S., Toran, E.J., Rimerman, R.A., Smith, D.F. (1996). Mutational analysis of the hsp70-interacting protein Hip. *Mol Cell Biol*, 6200-6207. doi: 10.1128/mcb.16.11.6200.

References

Prodromou, C., Roe, S.M., O'Brien, R., Ladbury, J.E., Piper, P.W., Pearl, L.H. (1997). Identification and structural characterization of the ATP/ADP-binding site in the Hsp90 molecular chaperone. *Cell*, **90**: 65-75. doi: 10.1016/S0092-8674(00)80314-1.

Przyborski, J.M., Diehl, M., Blatch, G.L. (2015). Plasmodial Hsp70s are functionally adapted to the malaria parasite life cycle. *Front Mol Biosci*, **2**: 34. doi: 10.3389/fmolb.2015.00034.

Przyborski, J.M., Nyboer, B., Lanzer, M. (2016). Ticket to ride: export of proteins to the *Plasmodium falciparum*-infected erythrocyte. *Mol Microbiol*, **101**: 1-11. doi: 10.1111/mmi.13380.

Qi, R., Sarbeng, E.B., Liu, Q., Le, K.Q., Xu, X., Xu, H., Yang, J., Wong, J.L., Vorvis, C., Hendrickson, W.A., Zhou, L., Liu, Q. (203). Allosteric opening of the polypeptide-binding site when an Hsp70 binds ATP. *Nat Struct Mol Biol*, **20**: 900-907. doi: 10.1038/nsmb.2583.

Radons, J. (2016). The human Hsp70 family of chaperones: where do we stand? *Cell Stress Chaperones*, **21**: 379-404. doi: 10.1007/s12192-016-0676-6.

Ramdhave, A.S., Patel, D., Ramya, I., Nandave, M., Kharkar, P.S**.** (2013). Targeting heat shock protein 90 for malaria. *Mini Rev Med Chem*, **13**: 1903-1920. doi: 10.2174/13895575113136660094.

Ramya, T. N., Surolia, N., and Surolia, A. (2006). 15-Deoxyspergualin modulates *Plasmodium falciparum* heat shock protein function. *Biochem Biophys Res Commun*, **348**: 585-592. doi: 10.1016/j.bbrc.2006.07.082.

Raska, M., Weigl, E. (2005). Heat shock proteins in autoimmune diseases. *Biomed Pap*, **149**: 243-9. doi: 10.5507/bp.2005.033.

Raviol, H., Sadlish, H., Rodriguez, F., Mayer, M.P., Bukau, B. (2006). Chaperone network in the yeast cytosol: Hsp110 is revealed as an Hsp70 nucleotide exchange factor. *EMBO J*, **25**: 2510-2518. doi: 10.1038/sj.emboj.7601139.

Reidy, M., Kumar, S., Anderson, D.E., Masison, D.C. (2018). Dual roles for yeast Sti1/Hop in regulating the Hsp90 chaperone cycle. *Genetics*, **209**: 1139-1154. doi: 10.1534/genetics.118.301178.

Renwrantz, L., Marquart, A., Möck, A., Richards, E. (2008). Molecular properties of the partially SDS-resistant lectin from the albumen gland of *Helix pomatia* and demonstration of lectin-related molecules on the surface of *H. pomatia* hemocytes. *J Molluscan Stud*, **75**: 41-49. doi: 10.1093/mollus/eyn037.

Rhiel, M., Bittl, V., Tribensky, A., Charnaud, S.C., Strecker, M., Müller, S., Lanzer, M., Sanchez, C., Schaeffer-Reiss, C., Westermann, B., Crabb, B.S., Gilson, P.R., Külzer, S., Przyborski, J.M.

References

(2016). Trafficking of the exported *P. falciparum* chaperone PfHsp70x. *Sci Rep*, **6**: 36174. doi: 10.1038/srep36174.

Rinehart, M.T., Park, H.S., Walzer, K.A., Chi, J-T.A., Wax, A. (2016). Hemoglobin consumption by *P. falciparum* in individual erythrocytes imaged via quantitative phase spectroscopy. *Sci Rep,* **6**: 24461. doi: 10.1038/srep24461.

Rocamora, F., Zhu, L., Liong, K.Y., Dondorp, A., Miotto, O., Mok, S., et al. (2018). Oxidative stress and protein damage responses mediate artemisinin resistance in malaria parasites. *PLoS Pathog,* **14**: e1006930. doi: 10.1371/journal. ppat.1006930.

Röhl, A., Tippel, F., Bender, E., Schmid, A.B., Richter, K., Madl, T., Buchner, J. (2015a). Hop/Sti1 phosphorylation inhibits its co-chaperone function. *EMBO Reports*, **16**: 240-249. doi. 10.15252/embr.201439198.

Röhl, A., Wengler, D., Madl, T., Lagleder, S., Tippel, F., Herrmann, M., Hendrix, J., Richter, K., Hack, G., Schmid, A.B., Kessler, H., Lamb, D.C., Buchner, J. (2015b). Hsp90 regulates the dynamics of its cochaperone Sti1 and the transfer of Hsp70 between modules. *Nat Commun*, **6**: 6655. doi: 10.1038/ncomms7655.

Rowe, J.A., Claessens, A., Ruth, A. Corrigan and Monica Arman (2009). Adhesion of *Plasmodium falciparum*-infected erythrocytes to human cells: molecular mechanisms and therapeutic implications. *Expert Rev Mol Med*, **11**: e16. doi: 10.1017/S1462399409001082.

Ruskamo, S. Chukhlieb, M., Vahokoski, J., Bhargav, S.P., Liang, F., Kursula, I., Kursula, P. (2012). Juxtanodin is an intrinsically disordered F-actin-binding protein. *Sci Rep*, **2**: 899. doi: 10.1038/srep00899.

Sargeant T.J., Marti, M., Caler, E., Carlton, J.M., Simpson, K., Speed, T.P., Cowman, A.F. (2006). Lineage-specific expansion of proteins exported to erythrocytes in malaria parasites. *Genome Biol*, **7**: R12. doi: 10.1186/gb-2006-7-2-r12.

Sato, S., Wilson, R.J. (2004). The use of DsRED in single- and dual-color fluorescence labeling of mitochondrial and plastid organelles in *Plasmodium falciparum*. *Mol Biochem Parasitol*, **134**: 175-179. doi: 10.1016/j.molbiopara.2003.11.015.

Scherf, A., Lopez-Rubio, J.J., Riviere, L. (2008). Antigenic variation in *Plasmodium falciparum*. *Annu Rev Microbiol*, **62**: 445-470. doi: 10.1146/annurev.micro.61.080706.093134.

Scheufler C., Brinker A., Bourenkov G., Pegoraro S., Moroder L., Bartunik H., Hartl F. U., Moarefi I. (2000). Structure of TPR domain-peptide complexes: critical elements in the assembly of the Hsp70-Hsp90 multi-chaperone machine. *Cell*, **101**: 199-210. doi: 10.1016/S0092-8674(00)80830-2.

References

Schmid A. B., Lagleder S., Grawert M. A., Rohl A., Hagn F., Wandinger S. K., Cox M. B., Demmer O., Richter K., Groll M., Kessler H., Buchner J. (2012). The architecture of functional modules in the Hsp90 co-chaperone Sti1/Hop. *EMBO J*, **31**: 1506-1517. doi: 10.1038/emboj.2011.472.

Schmidt, J.C., Manhães, L., Fragoso, S.P., Pavoni, D.P., Krieger, M.A. (2018). Involvement of STI1 protein in the differentiation process of *Trypanosoma cruzi*. *Parasit Int*. **67**: 131-139. doi: 10.1016/j.parint.2017.10.009.

Schuster, F.L. (2002). Cultivation of *Plasmodium* spp. *Clin Microbiol Rev*, **15**: 355-364. doi: 10.1128/CMR.15.3.355-364.2002.

Seo, Y.H. (2015). Small molecule inhibitors to disrupt protein-protein interactions of heat shock protein 90 chaperone machinery. *J Cancer Prev*, **20**: 5-11. doi: 10.15430/JCP.2015.20.1.5.

Shahinas, D., Folefoc, A., Pillai, D.A. (2013). Targeting *Plasmodium falciparum* Hsp90: Towards reversing antimalarial resistance. *Pathogens*, **2**: 33-54. doi: 10.3390/pathogens2010033.

Sharma, S.K, Parasuraman, P., Kumar, G., Surolia, N., Surolia, A. (2007). Green tea catechins potentiate triclosan binding to enoyl-ACP reductase from *Plasmodium falciparum* (*Pf*ENR). *J Med Chem*, **50**: 765-775. doi: 10.1021/jm061154d.

Sharma, Y.D. (1992). Structure and possible function of heat-shock proteins in *Plasmodium falciparum*. *Comp Biochem Physiol*, **102**: 437-444. doi: 10.1016/0305-0491(92)90033-N.

Shomura, Y., Dragovic, Z., Chang, H.C., Tzvetkov, N., Young, J.C. *et al*. (2005). Regulation of Hsp70 function by HspBP1: structural analysis reveals an alternate mechanism for Hsp70 nucleotide exchange 2665. *Mol Cell*, **17**: 367-379. doi: 10.1016/j.molcel.2004.12.023.

Shonhai, A. (2010). Plasmodial heat shock proteins: targets for chemotherapy. *FEMS Immunol Med Microbiol*, **58**: 61-74. doi: 10.1111/j.1574-695X.2009.00639.x.

Shonhai, A. (2014). Role of Hsp70s in development and pathogenicity of *Plasmodium* species. In Heat Shock Proteins of Malaria; Shonhai, A., Blatch, G., Eds.; Springer: New York, NY, USA, pp. 47-70.

Shonhai, A., Boshoff, A., Blatch, G.L. (2005). *Plasmodium falciparum* heat shock protein70 is able to suppress the thermosensitivity of an *Escherichia coli* DnaK mutant strain. *Biol Gen Genomics*, **274**: 70-78. doi: 10.1007/s00438-005-1150-9.

Shonhai, A., Boshoff, A., Blatch, G.L. (2007). The structural and functional diversity of Hsp70 proteins from *Plasmodium falciparum*. *Protein Sci*, **16**: 1803-1818. doi: 10.1110/ps.072918107.

Shonhai, A., Botha, M., de Beer, T.A.P., Boshoff, A., Blatch, G.L. (2008). Structure-function study of *Plasmodium falciparum* Hsp70 using three-dimensional modeling and *in vitro* analyses. *Protein Pept Lett*, **15**: 1117-1125. doi: 10.1110/ps.072918107.

References

Shonhai, A., Maier, A.G., Przyborski, J., and Blatch, G.L. (2011). Intracellular protozoan parasites of humans: the role of molecular chaperones in development and pathogenesis. *Protein Pept Lett*, **18**: 143-157 doi: 10.2174/092986611794475002.

Siddiqi, M. K., Alam, P., Chaturvedi, S. K., Nusrat, S., Shahein, Y. E., Khan, R. H. (2017). Attenuation of amyloid fibrillation in the presence of warfarin: a biophysical investigation. *Int J Biol Macromol*, **95**: 713-718. doi: 10.1016/j.ijbiomac.2016.11.110.

Silberg J. J., Vickery L. E. (2000). Kinetic characterization of the ATPase cycle of the molecular chaperone Hsc66 from *Escherichia coli*. *J Biol Chem*, **275**: 7779-7786. doi: 10.1074/jbc.275.11.7779.

Silberg, J. J., Tapley, T. L., Hoff, K. G., Vickery, L. E. (2004). Regulation of the HscA ATPase reaction cycle by the co-chaperone HscB and the iron-sulfur cluster assembly protein IscU. *J Biol Chem*, **279**: 53924-53931. doi: 10.1074/jbc.M410117200.

Smock, R.G., Blackburn, M.E., Gierasch, L.M. (2011). Conserved, disordered C terminus of DnaK enhances cellular survival upon stress and DnaK in vitro chaperone activity. *J Biol Chem*, **286**: 31821-31829. doi: 10.1074/jbc.M111.265835.

Soni, R., Sharma, D., Bhatt, T.K. (2016). *Plasmodium falciparum* secretome in erythrocyte and beyond. *Front Microbiol*, **7**: 194. doi: 10.3389/fmicb.2016.00194.

Southworth, D.R., Agard, D.A. (2011). Client-loading conformation of the Hsp90 molecular chaperone revealed in the Cryo-EM structure of the human Hsp90: Hop complex. *Molecular Cel*, **42**: 771-781. doi: 10.1016/j.molcel.2011.04.023.

Spielmann, T., Gilberger, T.W. (2015). Critical steps in protein export of *Plasmodium falciparum* blood stages. *Trends Parasitol*, **31**: 514-525. doi: 10.1016/j.pt.2015.06.010.

Sreerama, N., Venyaminov, S.Y., Woody, R.W. (1999). Estimation of the number of alpha-helical and beta-strand segments in proteins using circular dichroism spectroscopy. *Protein Sci*, **8**: 370. doi: 10.1110/ps.8.2.370.

Stephens, L.L., Shonhai, A., Blatch, G.L. (2011). Co-expression of the *Plasmodium falciparum* molecular chaperone, PfHsp70, improves the heterologous production of the antimalarial drug target GTP cyclohydrolaseI, PfGCHI. *Protein Expr Purif*, **77**: 159-165. doi: 10.1016/j.pep. 2011.01.005.

Stetz, G., Verkhivker, G.M. (2015). Dancing through Life: Molecular dynamics simulations and network-centric modeling of allosteric mechanisms in Hsp70 and Hsp110 chaperone proteins. *PLoS ONE*, **10**: e0143752. doi: 10.1371/journal.pone.0143752.

References

Surtees, R., Ariza, A., Punch, E.K., Chi, T., Dowall, S., Hewson, R., Hiscox, J., Barr, J.N., Edwards, T. (2015). The crystal structure of the Hazara virus nucleocapsid protein. *BMC Struct Biol*, **15**: 24. doi: 10.1186/s12900-015-0051-3.

Sussmann, R.A.C., Fotoran, W.L., Kimura, E.A., Katzin, A.M. (2017). *Plasmodium falciparum* uses vitamin E to avoid oxidative stress. *Parasit Vectors*, **10**: 461. doi: 10.1186/s13071-017-2402-3.

Suzuki, H., Noguchi, S., Arakawa, H., et al. (2010). Peptide-binding sites as revealed by the crystal structures of the human Hsp40 Hdj1 C-terminal domain in complex with the octapeptide from human Hsp70. *Biochemistry*, **49**: 8577-8584. doi: 10.1021/bi100876n.

Szklarczyk, D., Morris, J.H., Cook, H., Kuhn, M., Wyder, S., Simonovic, M., Santos, A., Doncheva, N.T., Roth, A., Bork, P., Jensen, L.J., von Mering, C. (2017). The STRING database in 2017: quality-controlled protein-protein association networks, made broadly accessible. *Nucleic Acids Res*, **45**: 362-368. doi: 10.1093/nar/gkw937.

Taipale, M., Tucker, G., Peng, J., Krykbaeva, I., Lin, Z-Y., Larsen, B., Choi, H., Berger, B., Gingras, A-C., Lindquist, S. (2014). A quantitative chaperone interaction network reveals the architecture of cellular protein homeostasis pathways. *Cell*, **158**: 434-448. doi: 10.1016/j.cell.2014.05.039.

Takayama, S., Sato, T., Krajewski, S., Kochel, K., Irie, S., Millan, J.A., Reed, J.C. (1995). Cloning and functional analysis of BAG-1: a novel Bcl-2-binding protein with anti-cell death activity. *Cell*, **80**: 279-84. doi: 10.1016/0092-8674(95)90410-7.

Tang, Y.C., Chang, H.C., Roeben, A., Wischnewski, D., Wischnewski, N., Kerner, M.J., Hartl, F.U., Hayer-Hartl, M. (2006). Structural features of the GroEL-GroES nano-cage required for rapid folding of encapsulated protein. *Cell*, **125**: 903-914. doi: 10.1016/j.cell.2006.04.027.

Terasawa, K., Minami, M., Minami, Y. (2005). Constantly updated knowledge of Hsp90. *J Biochem*, **137**: 443-447. doi**:** 10.1093/jb/mvi056.

Tilley, L., Matthew, W.A., Dixon, K.K. (2011). The *Plasmodium falciparum*-infected red blood cell. *Int J Biochem Cell Biol*, **43**: 839-842. doi: 10.1016/j.biocel.2011.03.012.

Tilly, K., McKittrick, N., Zylicz, M., Georgopoulos, C. (1983). The DnaK protein modulates the heat-shock response of *Escherichia coli*. *Cell*, **34**: 641-646. doi: 10.1016/0092-8674(83)90396-3.

Tokmakov, A.A., Kurotani, A., Takagi, T., Toyama, M., Shirouzu, M., Fukami, Y., Yokoyama, S. (2012). Multiple post-translational modifications affect heterologous protein synthesis. *J Biol Chem*, **287**: 27106-27116. doi: 10.1074/jbc.M112.366351.

Toll-Riera, M., Radó-Trilla, N., Martys, F., Albà, M.M. (2012). Role of low-complexity sequences in the formation of novel protein coding sequences. *Mol Biol Evo*, **29**: 883-886. doi:10.1093/molbev/msr263.

References

Torrente, M.P., Shorter, J. (2013). The metazoan protein disaggregase and amyloid depolymerase system: Hsp110, Hsp70, Hsp40, and small heat shock proteins. *Prion,* **7**: 457-463. doi: 10.4161/pri.27531.

Tsan, MF., Gao, B. (2004). Heat shock protein and innate immunity. *Cell Mol Immunol*, **1**: 274-279.

Tsutsumi, S., Mollapour, M., Prodromou, C., Lee, C-T., Panaretou, B., Yoshida, S., Mayer, M.P., Neckers, L.M. (2012). Charged linker sequence modulates eukaryotic heat shock protein 90 (Hsp90) chaperone activity. *Proc Natl Acad Sci USA,* **109**: 2937-2942. doi: 10.1073/pnas.1114414109.

Turturici, G., Sconzo, G., Geraci, F. (2011). Hsp70 and its molecular role in nervous system diseases. *Biochem Res Int*, **2011**: 618127. doi: 10.1155/2011/618127.

Tuteja, R. (2007). Malaria−an overview. *FEBS*, **274**: 4669-4941. doi: 10.1111/j.1742-4658.2007.05997.x.

Tzankov, S., Wong, M.J., Shi, K., Nassif, C., Young, J.C. (2008). Functional divergence between co-chaperones of Hsc70. *J Biol Chem,* **283**: 27100-27109. doi: 10.1074/jbc.M803923200.

Vale, N., Aguiar, L., Gomes, P. (2014). Antimicrobial peptides: a new class of antimalarial drugs? *Front Pharmacol*, **5**:275. doi: 10.3389/fphar.2014.00275.

van Schalkwyk, D.A., Saliba, K.J., Biagini, G.A., Bray, P.G., Kirk, K. (2013). Loss of pH control in *Plasmodium falciparum* parasites subjected to oxidative stress. *PLoS ONE*, **8**: e58933. doi: 10.1371/journal.pone.0058933.

Vos, M.J., Hageman, J., Carra, S., and Kampinga, H.H. (2008). Structural and functional diversities between members of the human HSPB, HSPH, HSPA, and DNAJ chaperone families. *Biochemistry,* **47**: 7001-7011. doi: 10.1021/bi800639z.

Vythilingam, I., Tan, C.H., Asmad, M., Chan, S.T., Lee, K.S., Singh, B. (2006). Natural transmission of *Plasmodium knowlesi* to humans by *Anopheles latens* in Sarawak, Malaysia. *Trans R Soc Trop Med Hyg*, **100**: 1087-1088. doi: 10.1016/j.trstmh.2006.02.006.

Wang, T., Mäser, P., Picard, D. (2016). Inhibition of *Plasmodium falciparum* Hsp90 contributes to the antimalarial activities of aminoalcohol-carbazoles. *J Med Chem*, **59**: 6344-6352. doi: 10.1021/acs.jmedchem.6b00591.

Wanjiang, H., Philipp, C. (2004). cis-Effect of DnaJ on DnaK in ternary complexes with chimeric DnaK/DnaJ-binding peptides. *FEBS lett*, **563**. 146-150. doi: 10.1016/S0014-5793(04)00290-X.

Wayne, N., Bolon D.N. (2007). Dimerization of Hsp90 is required for in vivo function. Design and analysis of monomers and dimers. *J Biol Chem*, **282**: 35386-35395. doi: 10.1074/jbc.M703844200.

References

Weiss, G.E., Gilson, P.R., Taechalertpaisarn, T., Tham, W-H., de Jong, N.W.M., Harvey, K.L., et al. (2015). Revealing the sequence and resulting cellular morphology of receptor-ligand interactions during *Plasmodium falciparum* invasion of erythrocytes. *PLoS Pathog*, **11**: e1004670. doi: 10.1371/journal. ppat.1004670.

Wendt, C., Rachid, R., Souza, W., Miranda, K. (2016). Electron tomography characterization of hemoglobin uptake in *Plasmodium chabaudi* reveals a stage-dependent mechanism for food vacuole morphogenesis. *J Struct Biol*, **194**: 171-179. doi: 10.1016/j.jsb.2016.02.014.

Weng, H., Guo, X., Papoin, J., Wang, J., Coppel, R., Mohandas, N., An, X. (2014). Interaction of *Plasmodium falciparum* knob-associated histidine-rich protein (KAHRP) with erythrocyte ankyrin R is required for its attachment to the erythrocyte membrane. *Biochim Biophys Acta,* **1838**: 185-192. doi: 10.1016/j.bbamem.2013.09.014.

Whitmore, L., Wallace, B.A. Protein secondary structure analyses from circular dichroism spectroscopy: methods and reference databases. Biopolymers, **89**: 392-400. doi: 10.1002/bip.20853.

WHO 2018. World Health Organization World Malaria Report https://www.who.int/malaria/publications/world-malaria-report-2018/report/en/. ISBN: 978 92 4 156565 3.

Willmer, T., Contu, L., Blatch, G.L., Edkins, A.L. (2013). Knockdown of Hop downregulates RhoC expression and decreases pseudopodia formation and migration in cancer cell lines. *Cancer Lett*, **328**: 252-260. doi: 10.1016/j.canlet.2012.09.021.

Wu, R., Sun, Y., Lei, L.M., Xie, S.T. (2008). Molecular identification and expression of heat shock cognate 70 (HSC70) in the pacific white shrimp *Litopenaeus vannamei*. *Mol Biol*, **42**: 265-274. doi: 10.1134/S002689330802009X.

Wyttenbach, A., Arrigo, A.P. (2009). The role of heat shock proteins during neurodegeneration in Alzheimer's, Parkinson's and Huntington's Disease. In: Heat Shock Proteins in Neural Cells. Neuroscience Intelligence Unit. Springer, New York, NY. doi: 10.1007/978-0-387-39954-6_7.

Yamamoto, S., Subedi, G.P., Hanashima, S., Satoh, T., Otaka, M., Wakui, H., Sawada, K., Yokota, S., Yamaguchi, Y., Kubota, H., Itoh, H. (2014). ATPase activity and ATP-dependent conformational change in the co-chaperone HSP70/HSP90-organizing protein (HOP). *J Biol Chem*, **14**: 9880-9886. doi: 10.1074/jbc.M114.553255.

Yang, J., Nune, M., Zong, Y., Zhou, L., Liu, Q. (2015). Close and allosteric opening of the polypeptide-binding site in a human Hsp70 chaperone BiP. *Structure*, **23**: 2191-2203. doi: 10.1016/j.str.2015.10.012.

References

Yang, Y., Rao, R., Shen, J., Tang, Y., Fiskus, W., Nechtman, J., Atadja, P., Bhalla, K. (2008). Role of acetylation and extracellular location of heat shock protein 90 alpha in tumor cell invasion. *Cancer Res*, **68**: 4833-4842. doi: 10.1158/0008-5472.CAN-08-0644.

Yu, A., Li, P., Tang, T., Wang, J., Chen, Y., Liu, L. (2015). Roles of Hsp70s in stress responses of microorganisms, plants, and animals. *BioMed Research International*, **2015.** doi: 10.1155/2015/510319.

Zeytuni, N., Zarivach, R. (2012). Structural and functional discussion of the tetra-trico-peptide repeat, a protein interaction module. *Structure*, **20**: 397-405. doi: 10.1016/j.str.2012.01.006.

Zhang, J., Schröder, G.F., Douglas, N.R., Reissmann, S., Jakana, J., Dougherty, M., Fu, C.F., Levitt, M., Ludtke, S.J., Frydman, J., Chiu, W. (2010). Mechanism of folding chamber closure in a group II chaperonin. *Nature*, **463**: 379-383. doi: 10.1038/nature08701.

Zhang, P., Leu, JI-J., Murphy, M.E., George, D.L., Marmorstein, R. (2014). Crystal structure of the stress-inducible human heat shock protein 70 substrate-binding domain in complex with peptide substrate. *PLoS ONE*, **9**: e103518. doi: 10.1371/journal.pone.0103518.

Zhao, L., Li, L., Liu, GQ., Liu, X.X., Li, B. (2012). Effect of frozen storage on molecular weight, size distribution and conformation of gluten by SAXS and SEC-MALLS. *Molecules*, **17**: 7169-7182. doi: 10.3390/molecules17067169.

Zhuravleva, A., Lila, M. Gierasch, B. (2015). Substrate-binding domain conformational dynamics mediate Hsp70 allostery. *Proc Natl Acad Sci USA*, **112**: 2865-2873. doi: 10.1073/pnas.1506692112.

Zininga, T., Achilonu, I., Hoppe, H., Prinsloo, E., Dirr, H.W., Shonhai, A. (2015a). Overexpression, purification, and characterization of the *Plasmodium falciparum* Hsp70-z (*Pf*Hsp70-z) protein. *PLoS ONE*, **10**: e0129445. doi: 10.1371/journal.pone.0129445.

Zininga, T., Achilonu, I., Hoppe, H., Prinsloo, E., Dirr, H.W., Shonhai, A. (2016). *Plasmodium falciparum* Hsp70-z, an Hsp110 homolog, exhibits independent chaperone activity and interacts with Hsp70-1 in a nucleotide-dependent fashion. *Cell Stress Chaperones*, **21**: 499-513. doi: 10.1007/s12192-016-0678-4.

Zininga, T., Anokwuru, C.P., Sigidi, M.T., Tshisikhawe, M.P, Ramaite, I.I.D., Traoré, A.N., Hoppe, H., Shonhai, A., Potgieter, N. (2017b). Extracts obtained from *Pterocarpus angolensis* DC and *Ziziphus mucronata* exhibit antiplasmodial activity and inhibit heat shock protein 70 (Hsp70) function. *Molecules*, **22**: 1224. doi: 10.3390/molecules22081224.

Zininga, T., Makumire, S., Gitau, G.W., Njunge, J.M., Pooe, O.J., Klimek, H., et al. (2015b) *Plasmodium falciparum* Hop (*Pf*Hop) interacts with the Hsp70 chaperone in a nucleotide-dependent fashion and exhibits ligand selectivity. *PLoS ONE*, **10**: e0135326. doi: 10.1371/journal.pone.0135326.

References

Zininga, T., Pooe, O.J., Makhado, P.B., Ramatsui, L., Prinsloo, E., Achilonu, I., Dirr, H., Shonhai, A. (2017a). Polymyxin B inhibits the chaperone activity of *Plasmodium falciparum* Hsp70. *Cell Stress Chaperones*, **22**: 707-715. doi: 10.1007/s12192-017-0797-6.

Zininga, T., Ramatsui, L., Makhado, P.B., Makumire, S., Achilinou, I., Hoppe, H., Dirr, H.W., Shonhai, A. (2017c). (-)-Epigallocatechin-3-Gallate inhibits the chaperone activity of *Plasmodium falciparum* Hsp70 chaperones and abrogates their association with functional partners. *Molecules*, **22**: 2139. doi: 10.3390/molecules22122139.

Zininga, T., Ramatsui, L., Shonhai, A. (2018). Heat shock proteins as immunomodulants. *Molecules*, **23**: 2846. doi: 10.3390/molecules23112846.

Zininga, T., Shonhai, A. (2014). Are heat shock proteins druggable candidates? *Am J Biochem Biotechnol*, **10**: 209-210. doi: 10.3844/ajbbsp.2014.209.210.

Zuiderweg, E.R.P., Bertelsen, E.B., Rousaki, A., Mayer, M.P., Gestwicki, J.E., Ahmad, A. (2012). Allostery in the Hsp70 chaperone proteins. *Top Curr Chem*, **328**: 99-154. doi: 10.1007/128_2012_323.

Zuiderweg, E.R.P., Hightower, L.E., Gestwicki, J.E. (2017). The remarkable multivalency of the Hsp70 chaperones. *Cell Stress Chaperones*, **22**: 173-189. doi: 10.1007/s12192-017-0776-y.

Zwirowski, S., Kłosowska, A., Obuchowski, I., Nillegoda, N.B., Piróg, A., Zieztkiewicz, S., Bukau, B., Mogk, A., Liberek, K. (2017). Hsp70 displaces small heat shock proteins from aggregates to initiate protein refolding. *EMBO J*, **36**: 783-796. doi: 10.15252/embj.201593378.

Zylicz, M., Wawrzynow, A. (2001). Insights into the function of Hsp70 chaperones. *IUBMB Life,* **51**: 283-287. doi: 10.1080/152165401317190770.

Appendix A: General experimental procedures

Appendix A: General experimental procedures

A1 Plasmid DNA extraction

Plasmid DNA was extracted using Zyppy™ Plasmid Miniprep Kit according to the manufacturer's Protocol.

A2 Restriction digest analysis

Plasmid DNA was digested using the desired diagnostic restriction enzymes following the method described below. The reagents were set up as follows: Sterile deionized water (16 µl), 10x restriction buffer (2 µl) and DNA (100-200 ng) 2 µl. The reaction was initiated by addition of two units (2 µl) of restriction enzymes. The restriction was allowed to proceed for 2-3 hours at 37 °C. The reaction was stopped by addition of 4 µl of 10x DNA loading buffer (0.25 %) bromophenol blue and 30 % glycerol). The product was then analyzed by agarose gel electrophoresis as described in (Appendix A.3).

A3 Agarose gel electrophoresis

To prepare 0.8 % (w/v) agarose gel, the required amount of agarose was completely dissolved in 1x TAE buffer (40 mM, 20 mM acetic acid and 1 mM EDTA) by heating with frequent agitation. The agarose was then cooled to 55ºC prior to addition of ethidium bromide (0.5 µg/ml). The agarose gel was allowed to polymerize for 15-30 minutes at room temperature. The gel was placed in the electrophoresis chamber and covered with 1x TAE buffer. A volume of 4 µl of 10x DNA loading buffer (0.25% bromophenol blue + 30% glycerol) was added to 20 µl of the sample followed by loading of the samples into the wells. Electrophoresis was conducted at 100 volts for one hour. The gel was then visualized using UV light (GeneGenius Bioimaging System (Syngene), USA).

Appendix A.4 Transformation

A volume of 2 µl (equivalent to about 10 ng) of plasmid DNA was added into an aliquot of 100 µl of competent cells. The cells were then incubated on ice for 30 minutes followed by heat shock

at 42 °C for 45 seconds and immediately placed on ice for 10 minutes. A volume of 900 µl of 2YT broth was added and then incubated at 37 °C for one hour with gentle agitation. The cells were transferred on 2YT plates containing the desired antibiotics followed by incubation at 37 °C overnight.

A5 DNA sequencing

The PfHsp70-1 and variant plasmid DNA was sequenced using forward primers (5'CAGCTGCTATTGCATATGGTTT-3'; binds at position 718-740); (5'-CAAGAATTCCAAAAATCCAAACT-3'; binds at positions 1211-1233) and reverse primer (5'GAGTTCTGAGGTCATTACTGG-3'; binds at position 2243 to 2223 in the reverse direction).

Reagent	Volume (µl)
Big dye 3.1	1
Sequencing buffer	1
Primer (3.2 pmol)	1
Plasmid (100ng)	X
Water (ultrapure)	10 –(3+x)

A6 SDS PAGE analysis

Proteins were treated by boiling in SDS sample buffer (0.25% Bromophenol blue (R250), 2% SDS, 10 % glycerol (v/v), 100 mM Tris, and 1 % β-mercaptoethanol) in a ratio of 4:1 for 5 mins at 95 °C and resolved using 12 % acrylamide resolving gel prepared as shown below (Table A.1). The gel is then transferred into the electrophoresis tank and electrophoresis buffer (25 mM Tris, pH 8.3 250 mM glycine and 0.1% (w/v) SDS) was added. The boiled samples were loaded in the respective wells and pre-stained protein molecular weight markers (ThermoFisher Scientific, USA) were also loaded. The electrophoresis was performed at 150 volts for one hour using the Bio-Rad Mini protein electrophoresis system (Biorad, U.S.A).

Coomassie Staining

The gel was removed from the electrophoresis chamber and placed in enough 0.5% Coomassie Blue G-250 (prepared in 50% methanol/ 10% acetic acid) to cover the gel. Staining continued for

about 30 m. The stain was discarded and the gel rinsed briefly with MilliQ water to remove most of the residual stain in the glassware. Destain was carried out with 40% HPLC grade methanol/ 10% acetic acid, replacing the solution every 10-20 minutes until faint bands were observed. Continue washing with MilliQ water until bands were very clean.

Table A1 Preparation of SDS-PAGE

Reagent (ml)	5 % Stacking Gel	12 % Separating Gel
30 % Bis/acrylamide	0.235	2.08
1.5 M Tris (pH 8.8)	-	1.25
1.0 M Tris (pH 6.8)	0.437	-
10 % SDS	0.0175	0.05
10 % Ammonium persulphate	0.00875	0.025
Distilled water	1.05	1.58
TEMED	0.020	0.020

A7 Western blot analysis

Proteins were resolved in 12% acrylamide gel as described above (Appendix A.7). Removal of SDS-PAGE gel from the glass plates after completion of electrophoresis process and cutting off of the stacking gel was done. The Whatman filter papers, gel, two scotchbrite fiber pads, and nitrocellulose were immersed in the buffer and left to equilibrate at 8 °C for 30 minutes. Preparation of the gel for transfer was done as follows: filter paper was placed on a scotch brite pad; Gel was placed on the filter paper ensuring no air bubbles are trapped; nitrocellulose was placed over the gel; another filter paper was laid on top of the nitrocellulose, followed by another scotch brite pad. The transfer of the protein on the nitrocellulose membrane was performed by running at 100 volts for one hour. The membrane was removed from the sandwich and rinsed using transfer buffer as well as the removal of adhering gel on the nitrocellulose membrane using a cotton swab. The blot was stained with Ponceau S stain to determine the success of the transfer.

Appendix A: General experimental procedures

The membrane was blocked in 10 ml of (5 % non-fat milk in TBS) for one hour on a rotary shaker set at 1 rpm. The membrane was washed three times in TBS-Tween (0.1 % Tween-20) for 10 minutes followed by incubation of the membrane with primary antibody for one hour. Unbound primary antibody was removed by washing of the membrane three times using TBS-Tween for 10 minutes each wash. The membrane was incubated with secondary antibody for one hour followed by washing of the membrane three times using TBS-Tween.

Ponceau Stain procedure

Subsequent to the SDS-PAGE run, the membrane was transferred to 5ml Ponceau S Stain solution. This was shaken for 5 min at room temperature. The membrane was rinsed with deionized water to achieve the desired staining. To destain, the membrane was washed with TBS for 5 min. The membrane was then washed 2-3 times with deionized water for 5 min prior to continuing with the Western blot.

A8 Chemiluminescent detection

The Thermo Scientific Pierce ECL Western Blotting Substrate is a highly sensitive nonradioactive, enhanced luminol-based chemiluminescent substrate for the detection of horseradish peroxidase (HRP) on immunoblots.

1. Remove blot from the transfer apparatus and block nonspecific sites with Blocking Reagent for 60 minutes at room temperature (RT) with shaking. If desired, block overnight at 2-8 °C without shaking.
2. Remove the Blocking Reagent and add the primary antibody working dilution. Incubate blot for 1 hour at RT with shaking or overnight at 2-8 °C without shaking.
3. Briefly rinse membrane in Wash Buffer two times.
4. Wash membrane by suspending it in Wash Buffer and agitating for ≥ 5 minutes. Replace Wash Buffer at least 4-6 times. Increasing the Wash Buffer volume, the number of washes and wash duration may help minimize background signal.
5. Incubate blot with the HRP-conjugate working dilution for one hour at RT with shaking.

Appendix A: General experimental procedures

6. Repeat Steps 3 and 4 to remove non-bound HRP-conjugate. Note: Membrane MUST be thoroughly washed after incubation with the HRP-conjugate.

7. Prepare the substrate working solution by mixing equal parts of Detection Reagents 1 and 2. Use 0.125 mL Working Solution per cm^2 of the membrane. Note: For best results prepare working solution immediately before use. The working solution is stable for one hour at RT.

8. Incubate blot with a working solution for one minute at RT.

9. Remove blot from working solution and place it in a plastic sheet protector or clear plastic wrap. Use an absorbent tissue to remove excess liquid and to carefully press out any bubbles from between the blot and the membrane protector.

A9 Determination of protein concentration using Bradford assay

Protein concentration was determined by Bradford's method (Bradford, 1976). Bovine serum albumin (BSA) standards were prepared using concentration ranging from 0 to 1 mg/ml in 0.15 M NaCl. Bradfords reagent 200 µl (Sigma Aldrich, USA) was added to 10 µl of protein and the reaction incubated in the dark at room temperature for five minutes. Absorbance was read at 595 nm using a SpectraMax M3 (Molecular devices, USA). The recombinant protein was similarly treated and the protein concentration determined by extrapolation from the standard curve as indicated in (Figure A1). The readings were prepared in triplicate and the average obtained.

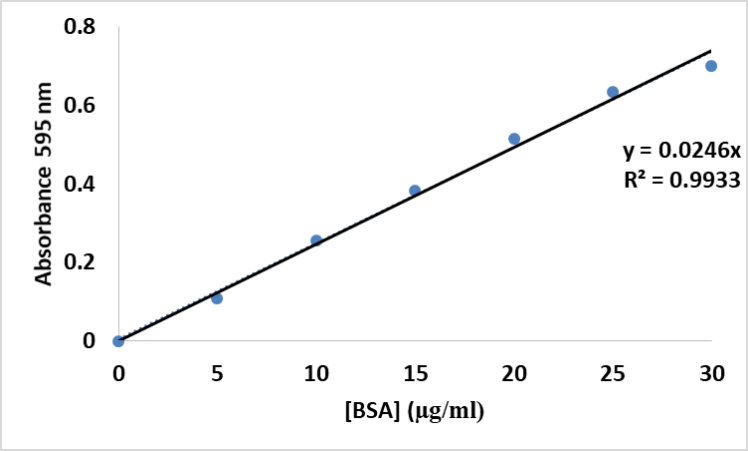

Figure A1. Bradford protein standard curve.

Appendix A: General experimental procedures

A10 Determination of protein concentration using Christoph-Leidig webtool assay

Protein concentration was determined using the Christoph-leidig webtool (http://christophleidig.de/tprot.html) using the following formula

$$A = c \times d \times \varepsilon \quad \text{Equation 1}$$

$$m = n \times M \quad \text{Equation 2}$$

where A: Absorbance at 280 nm

c: concentration (mol/l)

d: cuvette length (cm)

ε: extinction coefficient (L/mol x cm)

m: mass (g)

n: quantity (mol)

M: molecular unit (g/mol)

A11 determination of CD molar residue ellipticity

The analysis of the CD spectrum was conducted by conversion of ellipticity units from the CD spectrometer to molar residue ellipticity. This was achieved using the following formula

$$[\theta] = (100 \times \theta) / CMR \times l \quad \text{Equation 3}$$

Where [θ]: molar residue ellipticity ($deg.cm^2.dmol^{-1}$)

100: constant converting path length in meters

θ: ellipticity (mdeg)

l: cuvette path length

CMR: mean residue concentration

$$CMR = c \times N \quad \text{Equation 4}$$

Where c: Protein concentration (mol)

N: number of amino acids on the protein

Appendix A: General experimental procedures

A12 BioRad GLC chip activation and regeneration protocol

The GLC sensor chip was conditioned (Appendix B4), Pre-concentration of ligand (Appendix B5); immobilization of ligand (Appendix B6) and stabilized following the manufacturer's protocol BioRad bulletin 6414.

Appendix B: Supplementary data

B1: Templates used to model SBDs of the Hsp70s

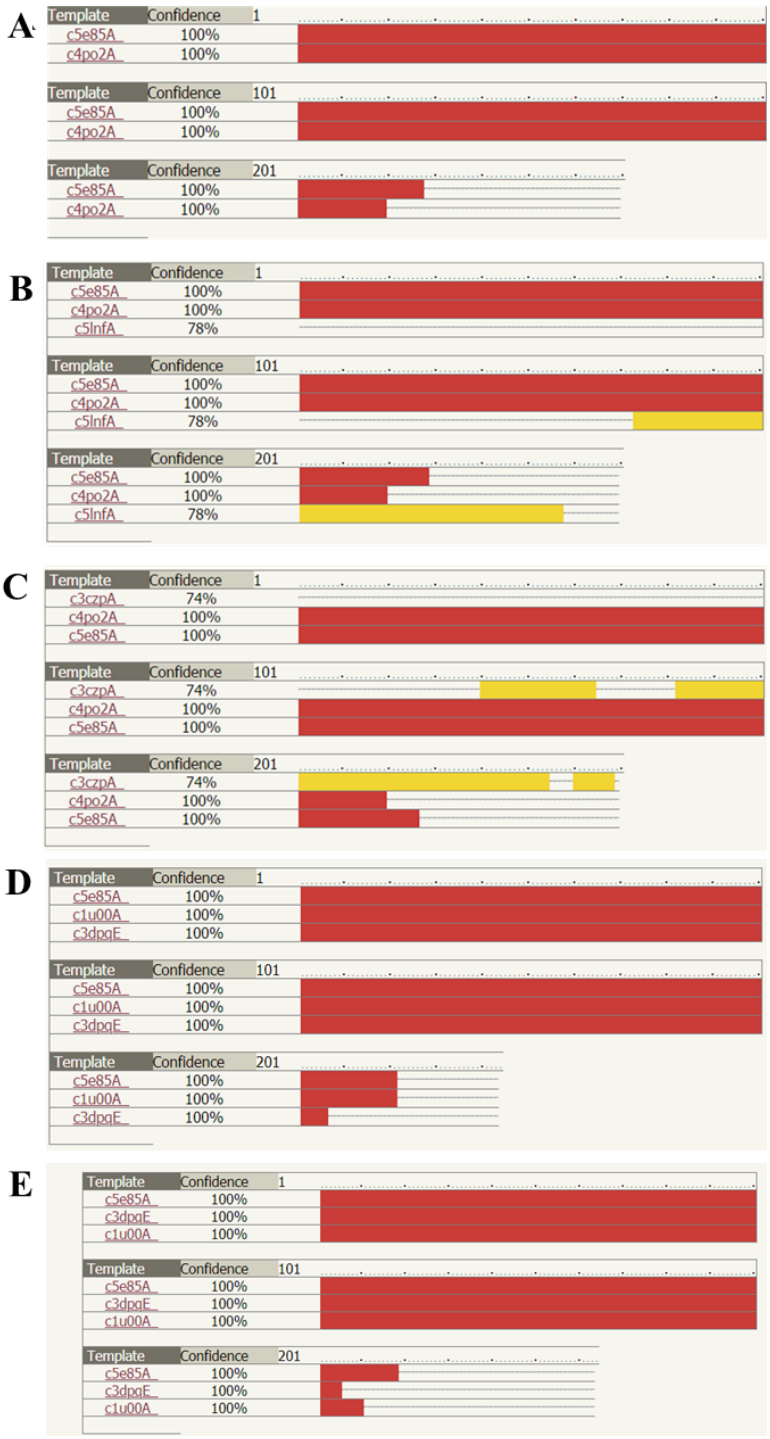

Figure B1: **Sequence coverage by each template**.
Template coverage for the modeling of (**A**) PfHsp70-1 (wt); (**B**) PfHsp70-G632; (**C**) PfHsp70-G648; (**D**) DnaK and DnaK-G. These are color-coded by the confidence of the match to that template overall. Templates were selected based on sequence identity and coverage on the query sequence.

Appendix B: Supplementary data

Table B1: List of templates used for Homology modeling

Template name	PDB	Reference
isolated SBD of Human Hsp70 chaperone binding immunoglobulin protein (BiP)	5e85.pdb	Yang *et al*., 2015
Stress-inducible human Hsp70 SBD in complex with peptide substrate	4po2A.pdb	Zhang *et al*., 2014
putative polyphosphate kinase 2 from *Pseudomonas aeruginosa*	3czp.pdb	Nocek *et al*., 2008
C-terminal domain of Peroxisomal biogenesis factor 19	5lnf.pdb	Schutz et al., 2017
Molecular Chaperone HscA Substrate Binding Domain Complexed with the IscU Recognition Peptide ELPPVKIHC	1u00.pdb	Cupp-Vickery et al., 2004
substrate binding domain of E. coli DnaK in complex with a long pyrrhocoricin-derived inhibitor peptide (form B)	3dpq.pdb	Roujeinikova, 2009

B2: Validation of the generated SBD 3D models

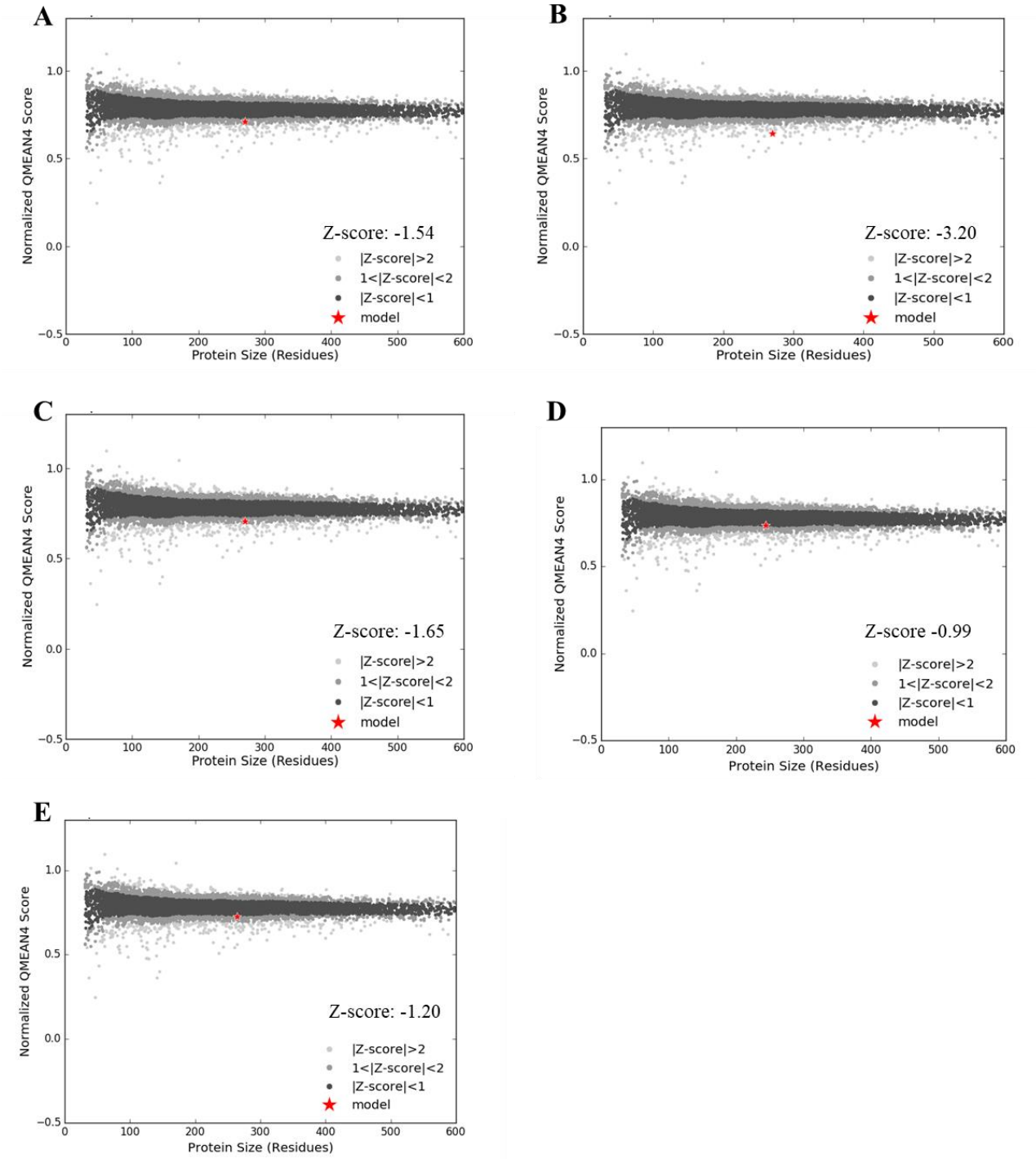

Figure B2: Validation of the 3D SBD models for Hsp70s
Qmean scores were calculated for SBD models for (A) PfHsp70-1 (wt); (B) PfHsp70-G632; (C) PfHsp70-G648; (D) DnaK and (E) DnaK-G. The red star represents the 3D model in each case.

B3: PfHsp70-1 interacting partners

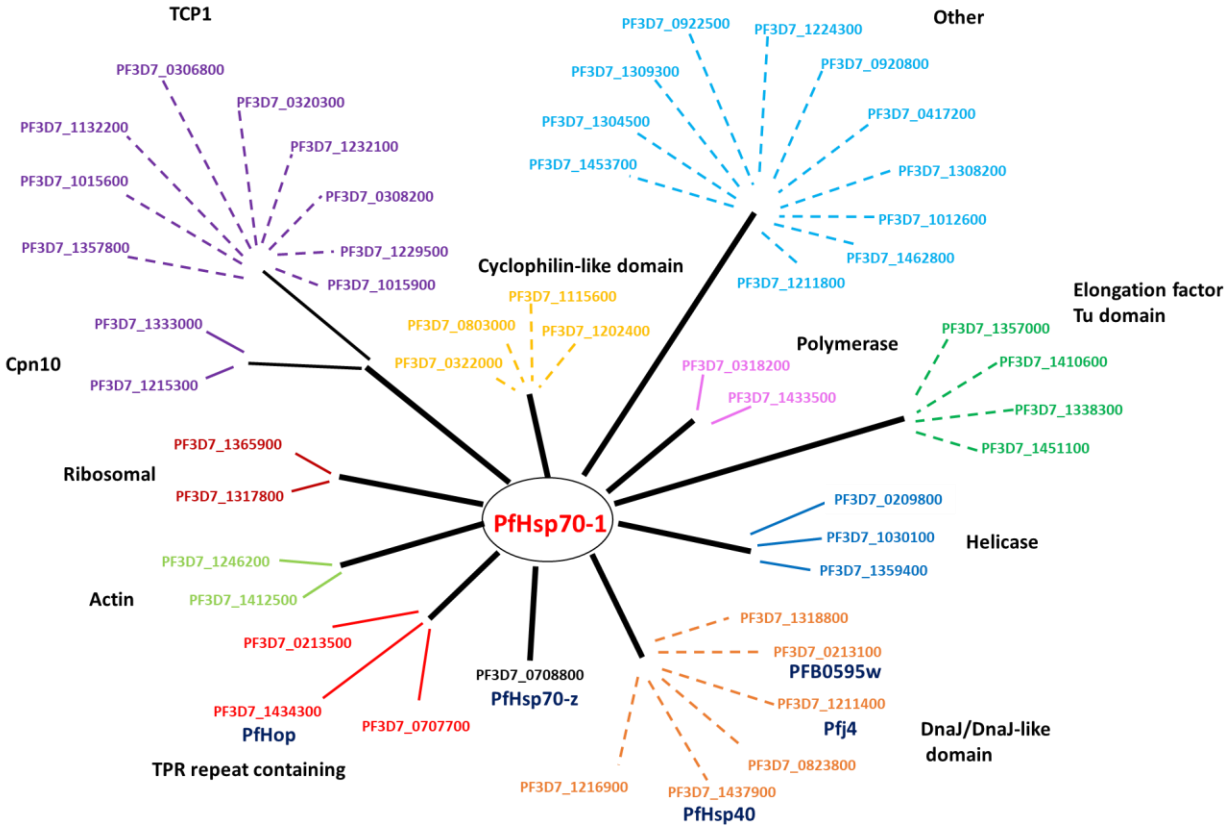

Figure B3: Predicted PfHsp70-1 interaction partners

Potential interactors of PfHsp70-1 are represented. The various chaperones and protein partners are represented by the lines and colors indicating the different groups. Line (edge) length or thickness is not of importance in this case. The nodes written in red represent some of the experimentally validated interactions. Prediction and analysis of the network was carried out using STRING (Jensen *et al.*, 2009).

Table B2: Predicted interactome for PfHsp70-1

Family (Domain Group)	Protein	Description	Localization	Score
Chaperonin Cpn10	PF3D7_1333000	Plastidic co-chaperonin	Cytoplasm, apicoplast	0.997
	PF3D7_1215300	Mitochondrial co-chaperonin	Cytoplasm, mitochondria	0.833
DnaJ	PF3D7_1437900	HSP40, subfamily A, putative	Cytosol	0.754
	PF3D7_0213100	Heat shock 40 kDa protein, putative (SIS1)	Cytosol	0.964
	PF3D7_1211400	Heat shock protein DNAJ homolog Pfj4	cytoplasm, nucleus	0.867
	PF3D7_0823800	DNAJ protein, putative	nucleus, cytosol	0.85
	PF3D7_1318800	DnaJ/SEC63 protein, putative	cytoplasm (Sec62/Sec63 complex)	0.73
	PF3D7_1216900	DNA-binding chaperone, putative	Nucleus	0.824
Chaperonin Cpn60/TCP-1	PF3D7_1357800	T-complex protein 1 subunit delta	Cytosol	0.999
	PF3D7_1015600	Heat shock protein 60	Cytoplasm and mitochondria	0.776
	PF3D7_1132200	T-complex protein 1 subunit alpha;	Cytosol	0.748
	PF3D7_0306800	T-complex protein beta subunit, putative	Cytosol	0.889
	PF3D7_0320300	T-complex protein 1 epsilon subunit, putative	Cytosol	0.797
	PF3D7_1232100	Chaperonin, cpn60	Cytoplasm	0.806
	PF3D7_0308200	T-complex protein 1 subunit eta	cytosol, chaperonin-containing T-complex	0.893
	PF3D7_1229500	T-complex protein 1, gamma subunit, putative	Cytosol, chaperonin-containing T-complex,	0.811
	PF3D7_1015900	Enolase	cytoplasm, nucleus	0.764
TPR repeat-containing	PF3D7_0213500	Conserved Plasmodium protein, tetratricopeptide repeat protein, putative	Cytoplasm	0.908

	PF3D7_1434300	STI1-like protein	cytosol, nucleus	0.761
	PF3D7_0707700	Ubiquitin-protein ligase E3, putative	Cytosol	0.906
Hsp70	PF3D7_0708800	Cg4 protein/heat shock protein 110	Cytoplasm	0.904
Cyclophilin-like domain	PF3D7_0322000	Peptidyl-prolyl cis-trans isomerase	Cytosol	0.794
	PF3D7_1202400	Cyclophilin, putative	Unknown	0.875
	PF3D7_1115600	Peptidyl-prolyl cis-trans isomerase	cytosol and E.R	0.749
	PF3D7_0803000	SYF2 splicing factor, putative	Nucleus	0.806
Ribosomal protein	PF3D7_1365900	60S ribosomal protein L40/UBI, putative	cytosolic large ribosomal subunit	0.794
	PF3D7_1317800	40S ribosomal protein S15/S19, putative	Cytosol, structural constituent of ribosome,	0.948
Elongation factor Tu Domain	PF3D7_1357000	Elongation factor 1-alpha	Cytoplasm	0.996
	PF3D7_1410600	Eukaryotic translation initiation factor 2 gamma subunit, putative	Cytoplasm	0.777
	PF3D7_1338300	Elongation factor 1-gamma, putative	cytoplasm	0.996
	PF3D7_1451100	Elongation factor 2	Cytosol	0.746
Actins	PF3D7_1246200	Actin-1	cytoplasm and cell surface, cytoskeleton	0.8
	PF3D7_1412500	Actin-2	cytoplasm, cytoskeleton	0.764
Helicases	PF3D7_1359400	RNA binding protein, putative	Cytoplasm	0.797
	PF3D7_0209800	DEAD-box helicase 1	cytoplasm, nucleus	0.783
	PF3D7_1030100	RNA helicase, putative	Cytoplasm	0.763
Ubiquitin conserved site	PF3D7_1211800	Polyubiquitin	cytoplasm, ubiquitin ligase complex	0.86

Polymerases	PF3D7_1433500	DNA topoisomerase 2	Nucleus	0.764
	PF3D7_0318200	DNA-directed RNA polymerase;	nucleus, DNA-directed RNA polymerase II core complex	0.807
Other	PF3D7_1462800	Glyceraldehyde-3-phosphate dehydrogenase	Cytosol, cell surface	0.713
	PF3D7_1012600	GMP synthetase	Nucleus	0.78
	PF3D7_1308200	Carbamoyl phosphate synthetase	Cytoplasm	0.999
	PF3D7_0417200	Bifunctional dihydrofolate reductase-thymidylate synthase	Cytoplasm	0.891
	PF3D7_0920800	Inosine-5'-monophosphate dehydrogenase	Cytoplasm	0.883
	PF3D7_1224300	Polyadenylate-binding protein	cytoplasm, P granule	0.822
	PF3D7_0922500	Phosphoglycerate kinase	Unknown	0.878
	PF3D7_1309300	U4/U6 small nuclear ribonucleoprotein, putative	Nucleus	0.989
	PF3D7_1304500	Small heat shock protein, putative	Cytosol	0.743
	PF3D7_1453700	P23 co-chaperone, putative	Cytosol	0.724

B4: Confirmation of pQE30/PfHsp70-1 DNA construct

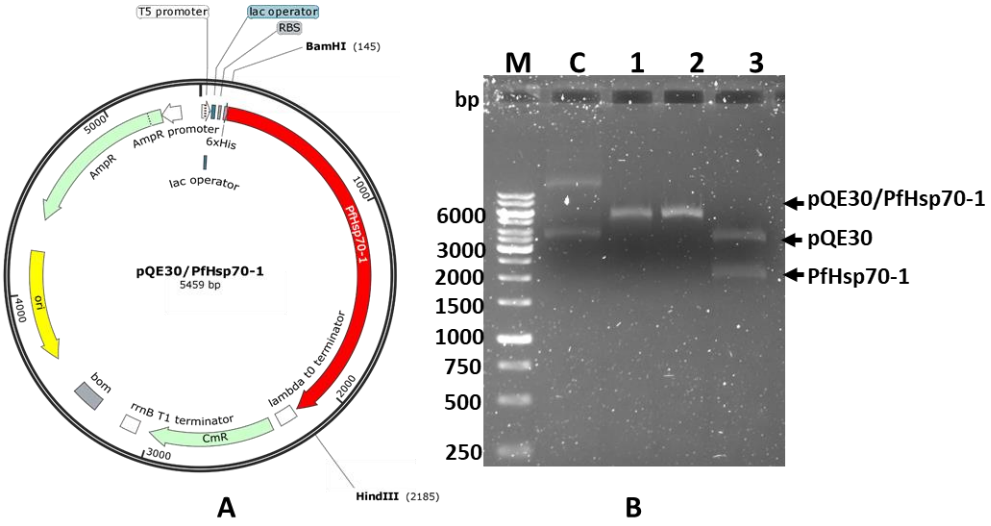

Figure B4. pQE30/PfHsp70-1 plasmid map and restriction agarose gel
Restriction analysis of pQE30/PfHsp70-1 DNA plasmid (**A**) Plasmid map of pQE30/PfHsp70-1 showing the *Bam*HI and *Hind*III restriction sites. (**B**) Agarose gel electrophoresis of pQE30/PfHsp70-1: lane M: DNA molecular weight marker in base pairs (bp); lane C: undigested pQE30/PfHsp70-1 plasmid; lane 1: pQE30/*Pf*Hsp70-1 digested with *Bam*HI; lane 2: pQE30/*Pf*Hsp70-1 digested with *Hind*III; lane 3: pQE30/*Pf*Hsp70-1 digested with both *Bam*HI and *Hind*III.

B5: Confirmation of pQE30/PfHsp70-G632 DNA construct

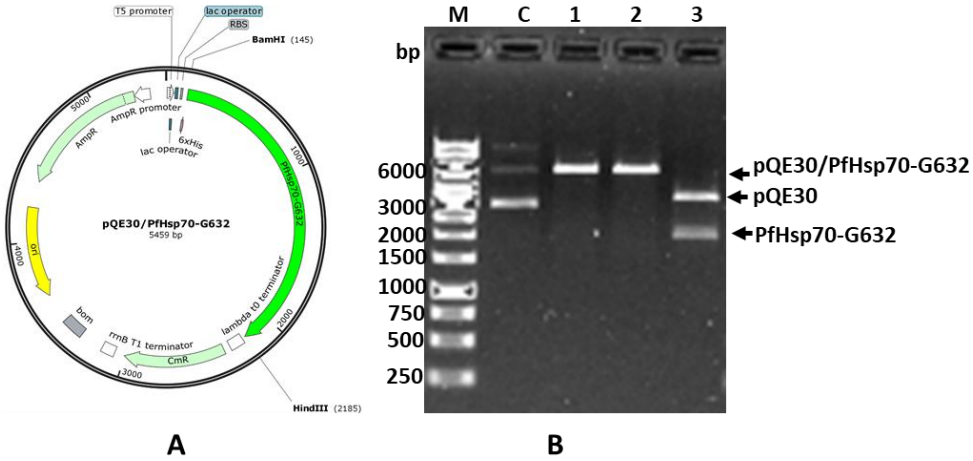

Figure B5. pQE30/PfHsp70-G632 plasmid map and restriction agarose gel
Restriction analysis of pQE30/PfHsp70-G632 DNA plasmid. (**A**) Plasmid map of pQE30/PfHsp70-G632 showing the *Bam*HI and *Hind*III restriction sites. (**B**) Agarose gel electrophoresis of pQE30/PfHsp70-G632: lane M, DNA molecular weight marker; lane 1, undigested pQE30/PfHsp70-G632 plasmid; lane 2, pQE30/PfHsp70-G632 digested with *Bam*HI; lane 3, pQE30/PfHsp70-G632 digested with *Hind*III; lane 4, pQE30/PfHsp70-G632 digested with *Bam*HI and *Hind*III.

B6: Confirmation of pQE30/PfHsp70-G648 DNA construct

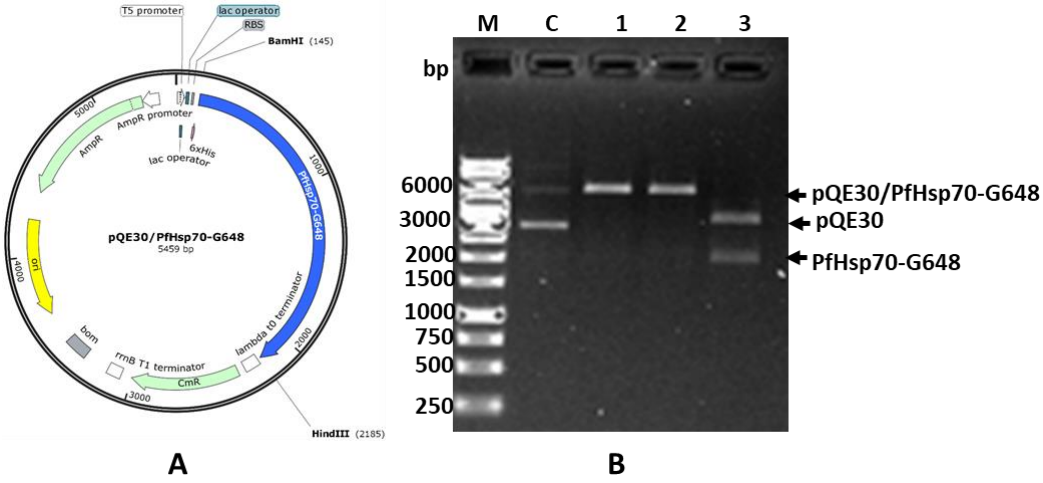

Figure B6. pQE30/PfHsp70-G648 plasmid map and restriction agarose gel

Restriction analysis of pQE30/PfHsp70-G648 DNA plasmid. (**A**) Plasmid map of pQE30/PfHsp70-G648 showing the *Bam*HI and *Hind*III restriction sites. (**B**) Agarose gel electrophoresis of pQE30/PfHsp70-G648: lane M: DNA molecular weight marker; lane C: undigested pQE30/PfHsp70-G648 plasmid; lane 1: pQE30/PfHsp70-G648 digested with *Bam*HI; lane 2: pQE30/PfHsp70-G648 digested with *Hind*III; lane 3: pQE30/PfHsp70-G648 digested with *Bam*HI and *Hind*III.

B7: Confirmation of pQE30/DnaK and pQE30/DnaK-G DNA constructs

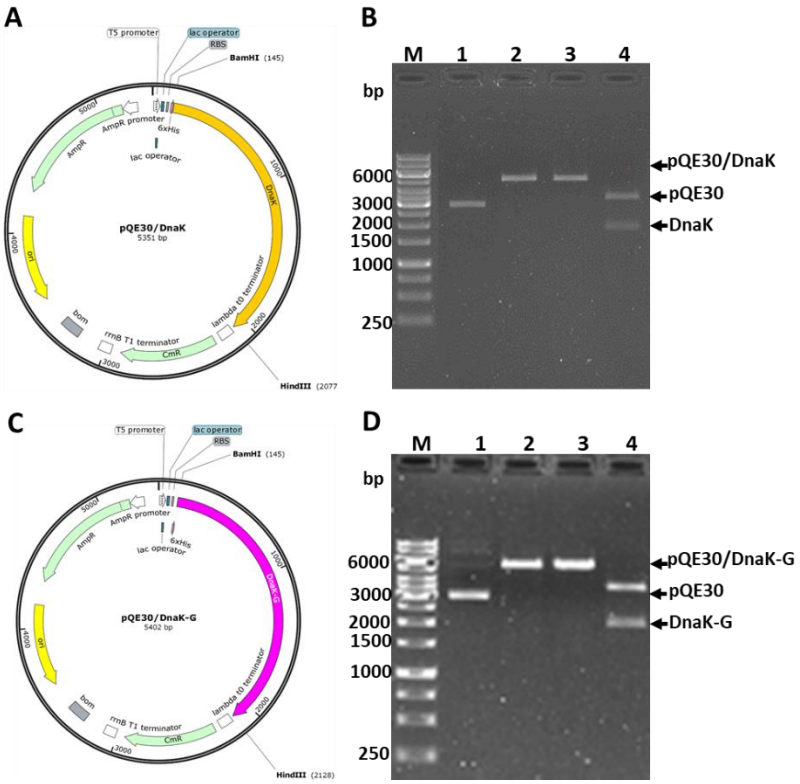

Figure B7. Restriction analyses of pQE30/DnaK and pQE30/DnaK-G constructs

Restriction analysis of pQE30/DnaK and pQE30/DnaK-G plasmid constructs. (**A**) and (**C**) Plasmid maps of pQE30/DnaK and pQE30/DnaK-G showing the *Bam*HI and *Hind*III restriction sites. (**B** and **D**) Agarose gel electrophoresis of pQE30/DnaK and pQE30/DnaK-G respectively: lane M: DNA molecular weight marker; lane 1: undigested plasmid; lane 2: plasmid digested with *Bam*HI; lane 3: plasmid digested with *Hind*III; lane 4: plasmid digested with *Bam*HI and *Hind*III.

B8: Sequencing data for the pQE30/PfHsp70-G632 plasmid construct

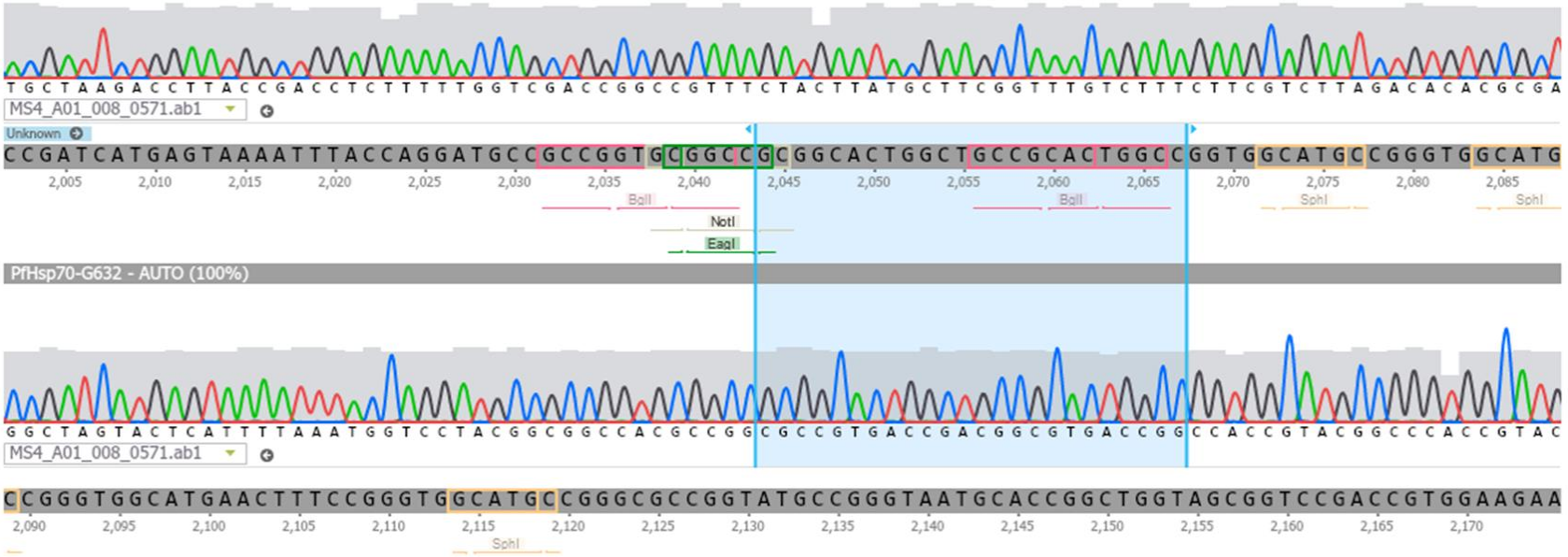

Figure B8: Confirmation of pQE30/PfHsp70-G632plasmid construct using DNA sequencing

Sequencing was performed using the Big Dye method. A T5 (pQE30) reverse primer was used resulting in a reverse sequence MS4_A01_008_0571.ab1. The region highlighted in blue represents the region in which the G632 mutation was introduced. The sequencing confirmed that the highlighted codons code for the mutated amino acids.

Appendix B: Supplementary data

B9: Sequencing data for the pQE30/PfHsp70-G648 plasmid construct

Figure B9: Confirmation of pQE30/PfHsp70-G648 plasmid construct using DNA sequencing

Sequencing was performed using the Big Dye method. A T5 (pQE30) reverse primer was used resulting in a reverse sequence MS5_A01_008_0571.ab1. The region highlighted in blue represents the region in which the G648 mutation was introduced.

B10: Mass Spectrometry sequencing data for PfHsp70-1

Intensity Coverage: 69.2 % (1040088 cnts) Sequence Coverage MS: 45.3%

Sequence Coverage MS/MS: 12.9% pI (isoelectric point): 5.8

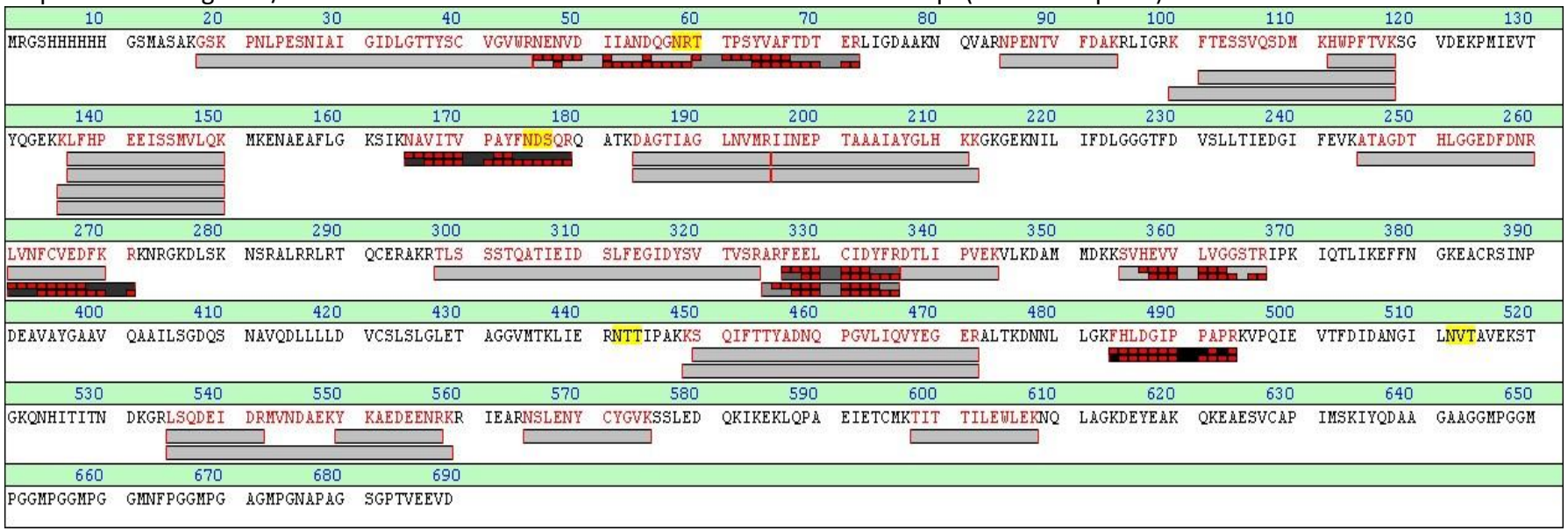

Figure B10: Confirmation of PfHsp70-1 by mass spectrometry

Trypsin digested fragments were sequenced using MALDI-TOFF.

B11: Mass Spectrometry sequencing data for PfHsp70-G632

Intensity Coverage:	64.8 % (1147563 cnts)	Sequence Coverage MS:	38.6%
Sequence Coverage MS/MS:	8.7%	pI (isoelectric point):	5.8

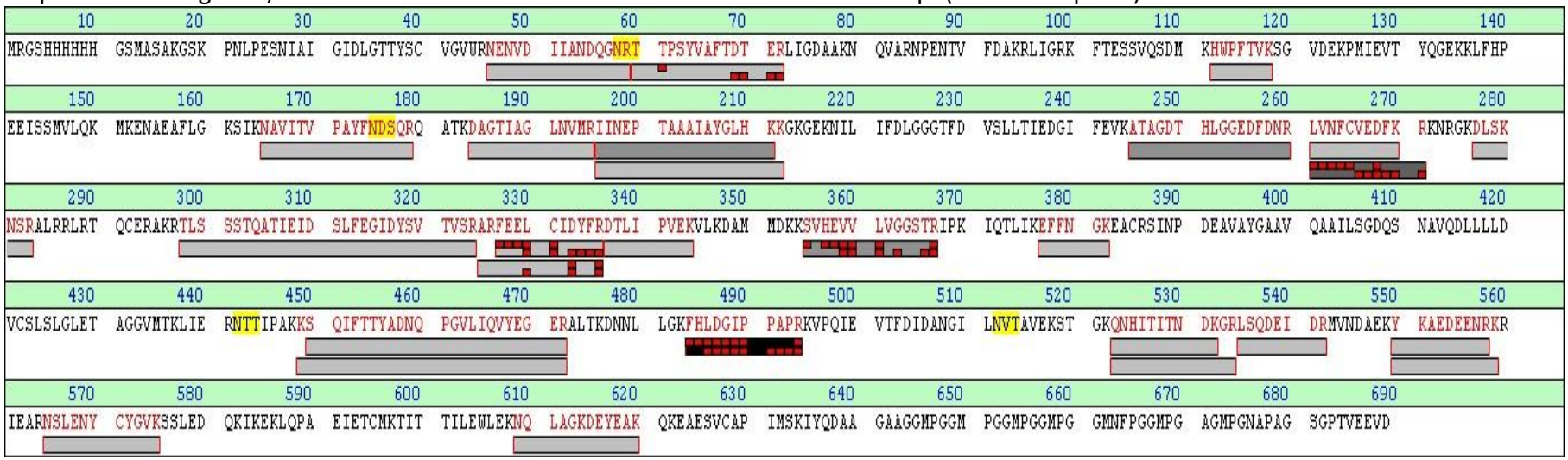

Figure B11: Confirmation of PfHsp70-G632 by mass spectrometry
Trypsin digested fragments were sequenced using MALDI-TOFF.

B12: Mass Spectrometry sequencing data for PfHsp70-G648

Intensity Coverage:	60.6 % (917451 cnts)	Sequence Coverage MS:	39.5%
Sequence Coverage MS/MS:	11.6%	pI (isoelectric point):	5.8

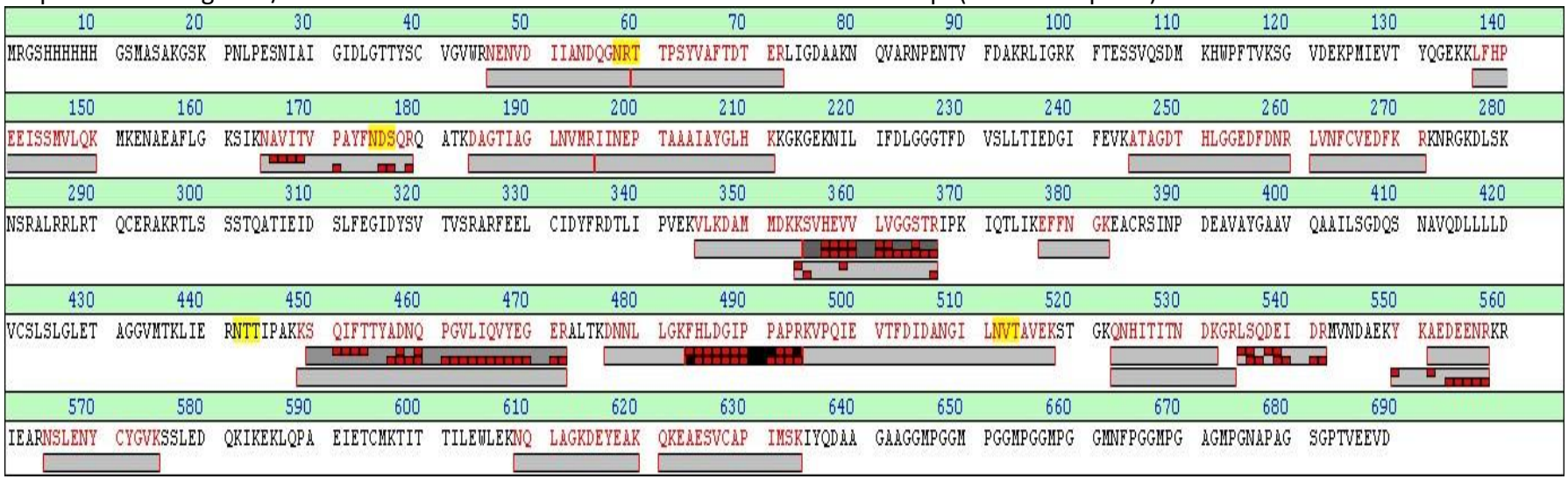

Figure B12: Confirmation of PfHsp70-G648 by mass spectrometry

Trypsin digested fragments were sequenced using MALDI-TOFF.

B13: Mass Spectrometry sequencing data for PfHop

Intensity Coverage:622	80.0 % (493614 cnts)	Sequence Coverage MS:	58.0%
Sequence Coverage MS/MS:	15.6%	pI (isoelectric point):	7.2

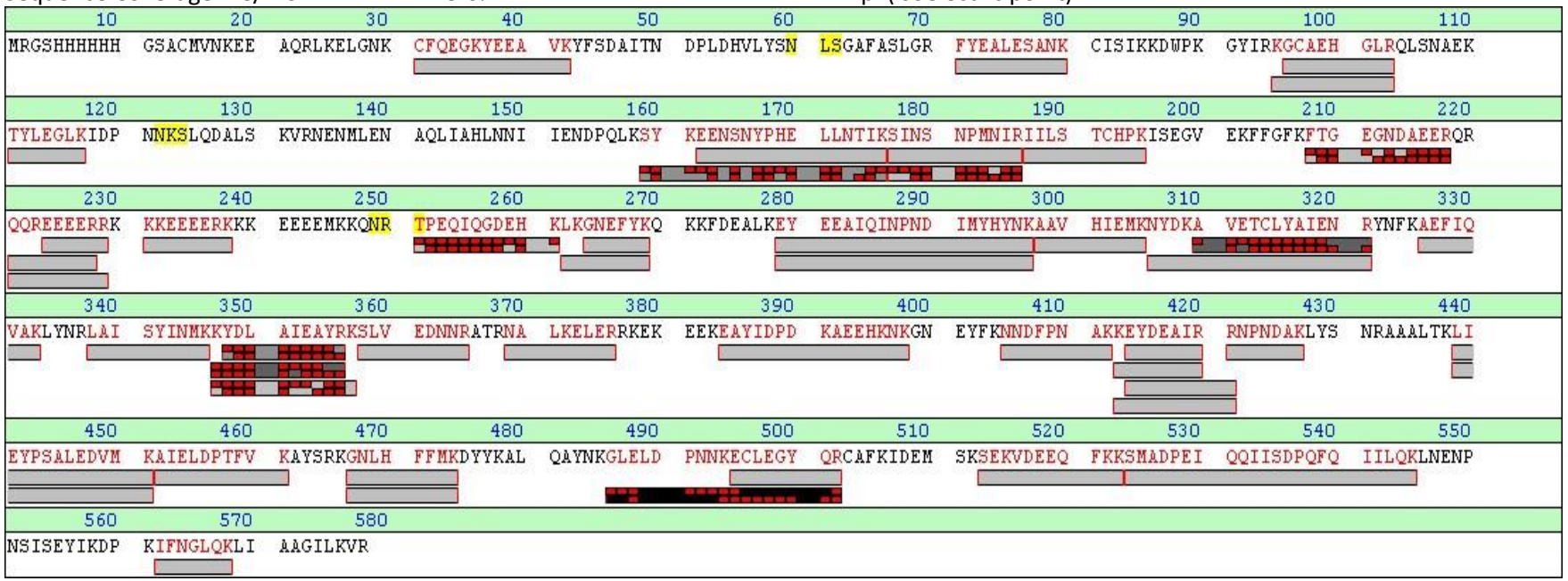

Figure B13. Confirmation of PfHop by mass spectrometry
Trypsin digested fragments were sequenced using MALDI-TOFF.

B14: Circular dichroism data before and after heat stress

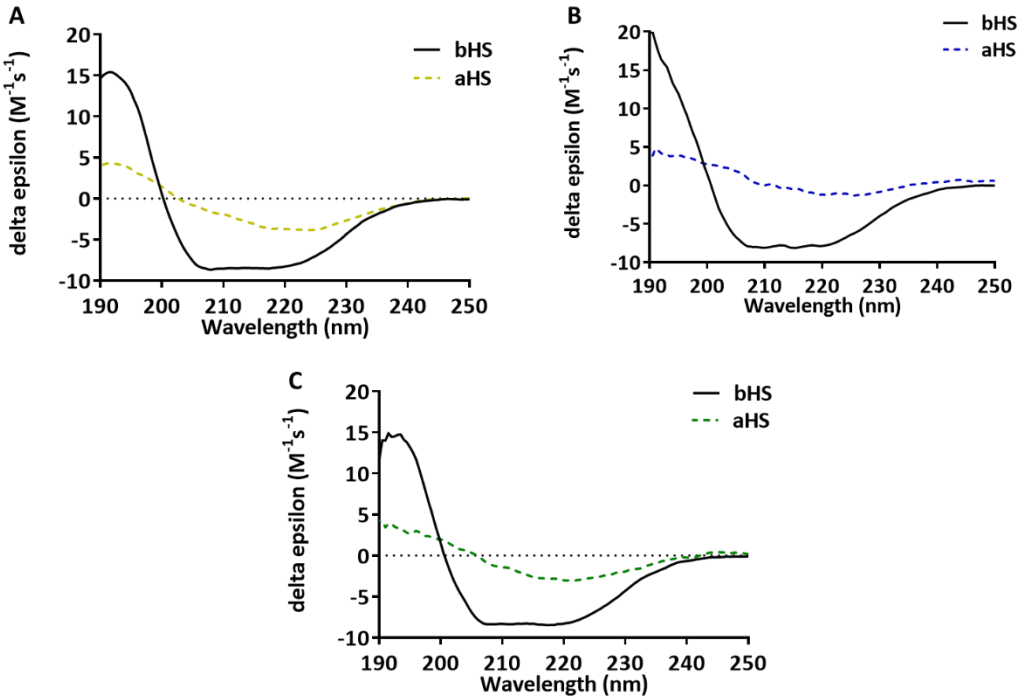

Figure B14. Thermal unfolding of PfHsp70-1 and its GGMP variants

The CD spectrum was presented as delta epsilon ($M^{-1}s^{-1}$). The temperature was raised from 19 °C to 90 °C and ellipticity measured at 222 nm. The data represents the CD spectrum of native (bHs) and heat-stressed (aHS) (**A**) PfHsp70-1; (**B**) PfHsp70-G632 and (**C**) PfHs70-G648.

B15: Intrinsic tryptophan fluorescence spectra for PfHsp70-1 and its GGMP variants

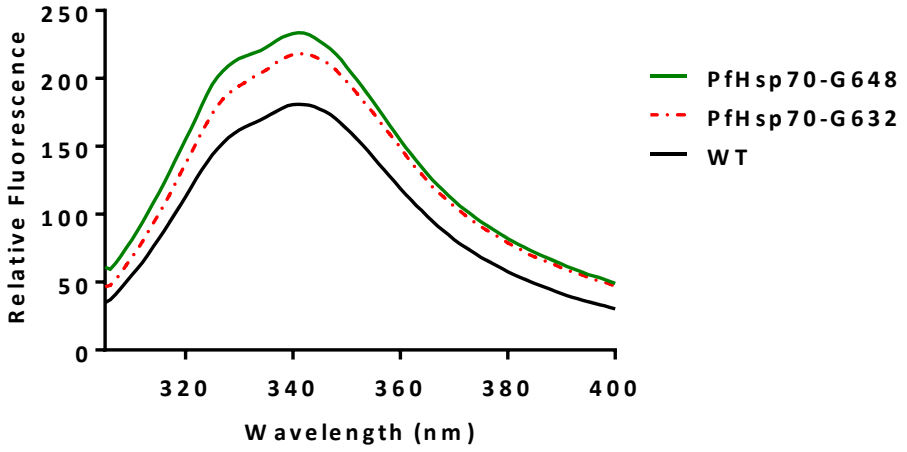

Figure B15. Intrinsic tryptophan fluorescence spectra for PfHsp70-1 and variants.

Recombinant proteins at 2 µM were excited at 295 and emission measured from 300-400 nm.

B16: GdHCl induced changes in protein structure

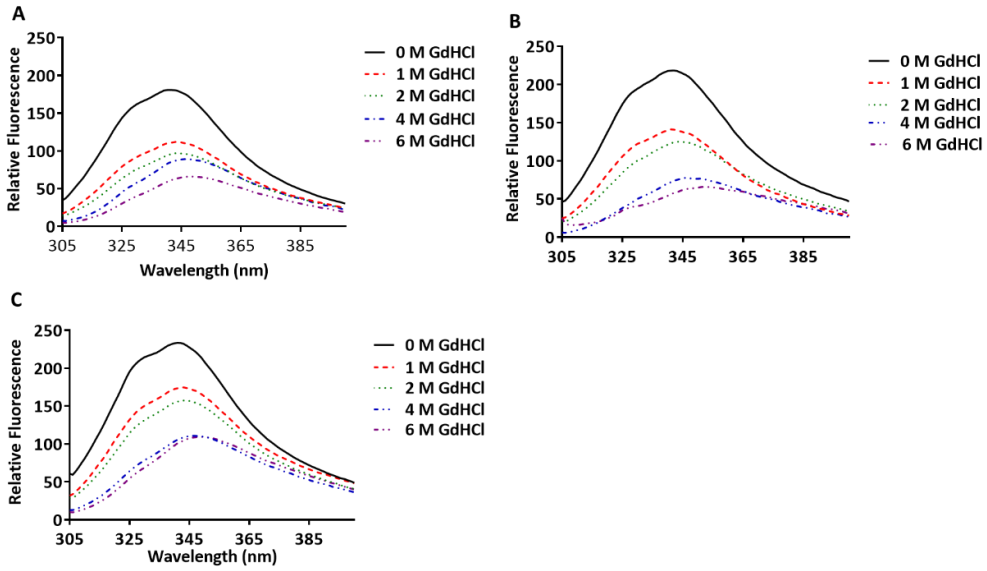

Figure B16. GdHCl induced changes in protein structure in the various recombinant proteins. (**A**), (**B**) and (**C**) changes in fluorescence intensity for PfHsp70-1, PfHsp70-G632 and PfHsp70-G648 incubated with 0-6M GdHCl.

B17: Peptide binding to PfHs70-1 and its GGMP variants

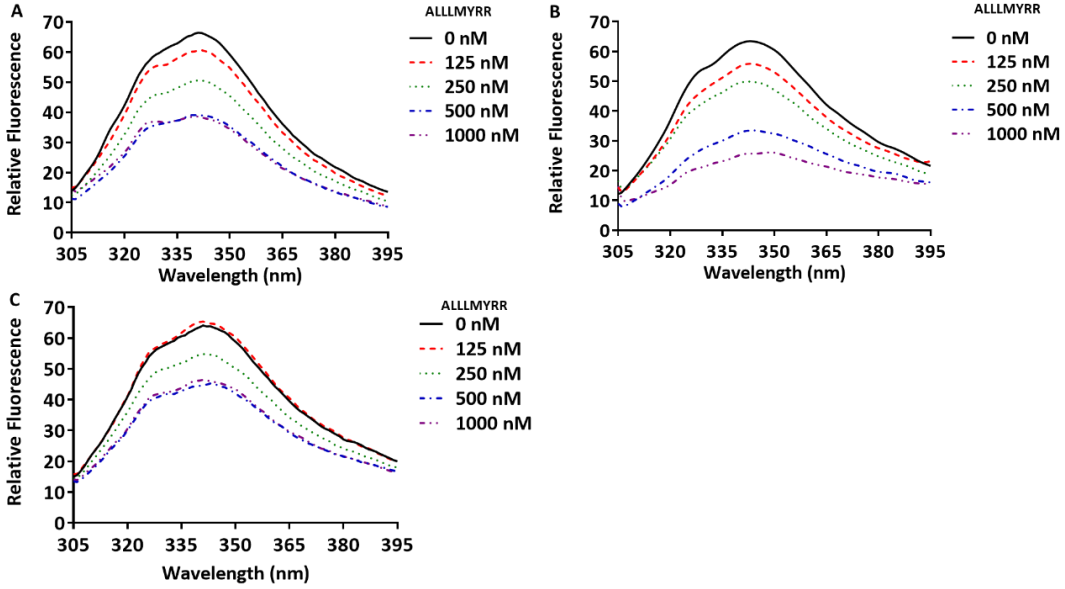

B17. Representative fluorescence spectra for PfHsp70-1 and GGMP mutants.
Excitation was at 295 nm with the emission measured from 300-400 nm. Peptide ALLLMYRR at varying concentrations (0-100 nM) was incubated with recombinant proteins and the effect on the intrinsic protein tryptophan fluorescence was measured. (**A**) PfHsp70-1 (**B**) PfHsp70-G632 and (**C**) PfHsp70-G648.

B18: ADP binding to PfHs70-1 and its GGMP variants

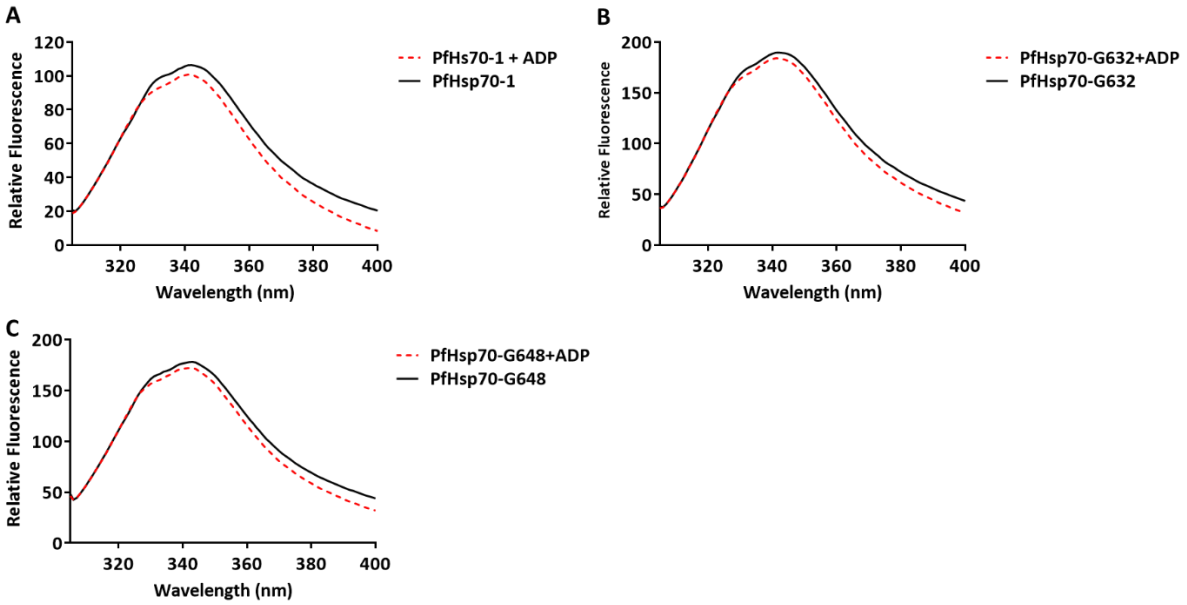

Figure B18: The conformation of PfHsp70-1 and variants is regulated by nucleotides
Tryptophan fluorescence signals for nucleotide-free PfHsp70s or upon incubation with 5mM ADP. (**A**) PfHsp70-1, (**B**) PfHsp70-G632 and (**C**) PfHsp70-G648.

B19: Confirmation of the variant KPf plasmid constructs

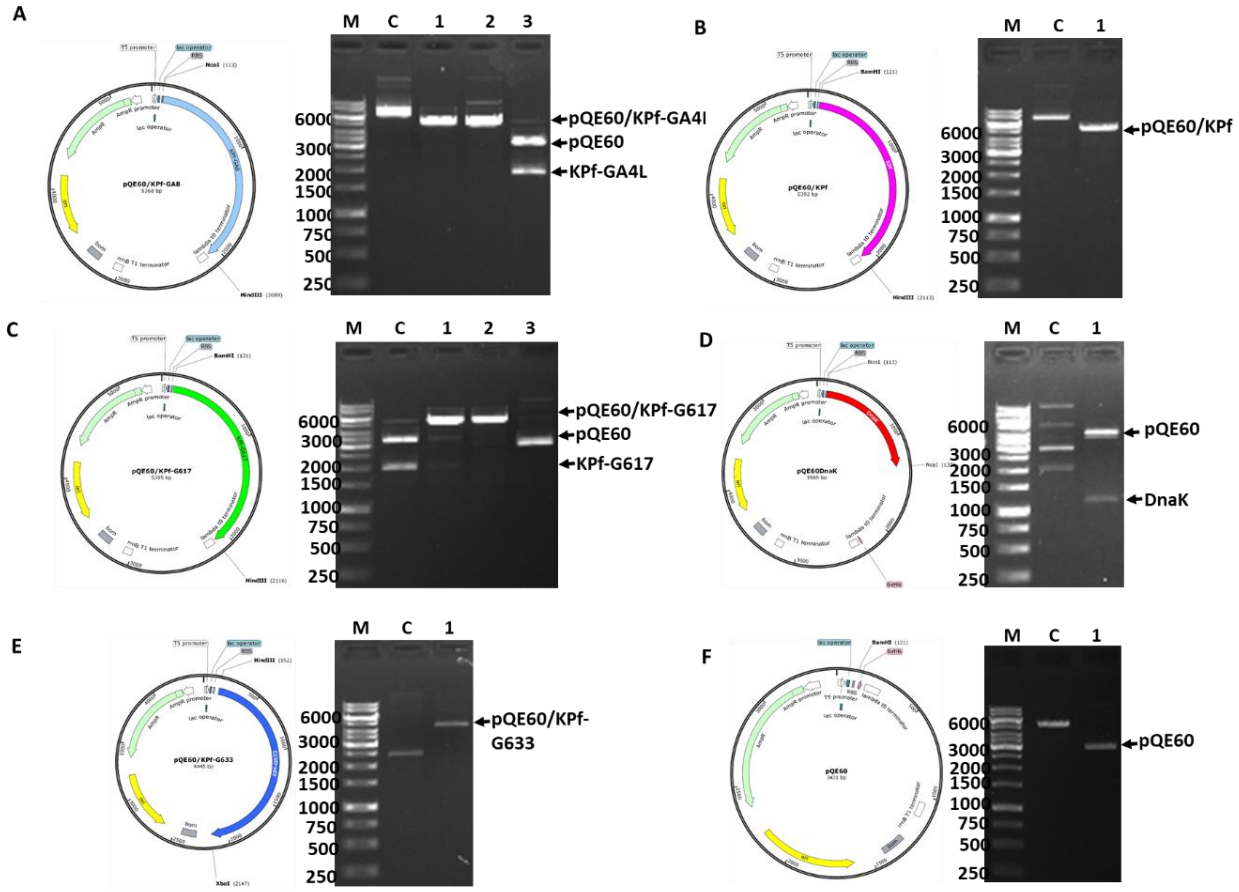

Figure B19. Plasmid maps and restriction agarose gel for KPf plasmid constructs
Restriction analysis of DNA plasmids. (**A**) Plasmid map and agarose gel electrophoresis of pQE60/KPf showing the *Bam*HI and *Hind*III restriction sites. (**B**) Plasmid map and agarose gel electrophoresis of pQE60/KPf-G617 showing the *Bam*HI and *Hind*III restriction sites. (**C**) Plasmid map and agarose gel electrophoresis of pQE60/DnaK showing the *Nco*I restriction sites. (**D**) Plasmid map and agarose gel electrophoresis of pQE60/K*Pf*-G633 showing the *Bam*HI and *Xba*I restriction sites. (**E**) Plasmid map and agarose gel electrophoresis of pQE60 showing the *Bam*HI and *Hind*III restriction site. lane M, DNA molecular weight marker; lane C, undigested plasmid; lane 1, a single digest of each respective with one of the enzymes; lane 3, a single digest of each respective with the second enzyme; lane 4, double digest with both enzymes for each respective plasmid.

B20: Phosphate standard curve

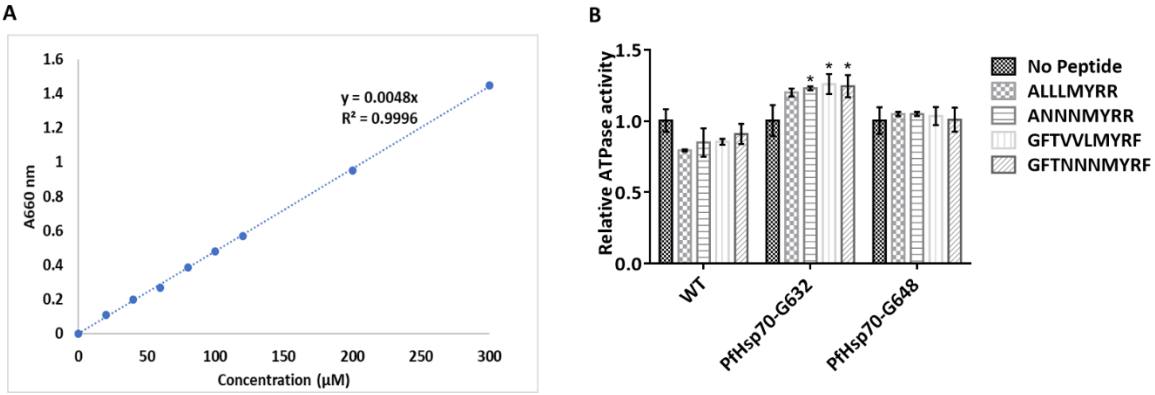

Figure B20. Phosphate standard curve for ATP hydrolysis analysis

(**A**) Phosphate standards of concentration ranging from 0 to 300 µM were prepared and absorbance was read at 660 nm using (SpectraMax M3, Molecular Devices, U.S.A). The linear equation: y = 0.0048x; R^2 = 0.9996 was used to calculate inorganic phosphate released during ATP hydrolysis. (**B**) The effect of peptides on the basal ATPase activities of PfHsp70-1 and variants. The experiment was repeated in the presence of varying concentration (0-2000 nM) of peptides: ALLLMYRR, ANNNMYRR, GFTVVLMYRF, and GFTNNNMYRF. Statistical analysis was carried out using two-way ANOVA (p<0.001). The stars showed that there were statistically significant differences in the relative ATPase activity.

B21: Assessment of the thermal stability for PfHsp70-1 and variants

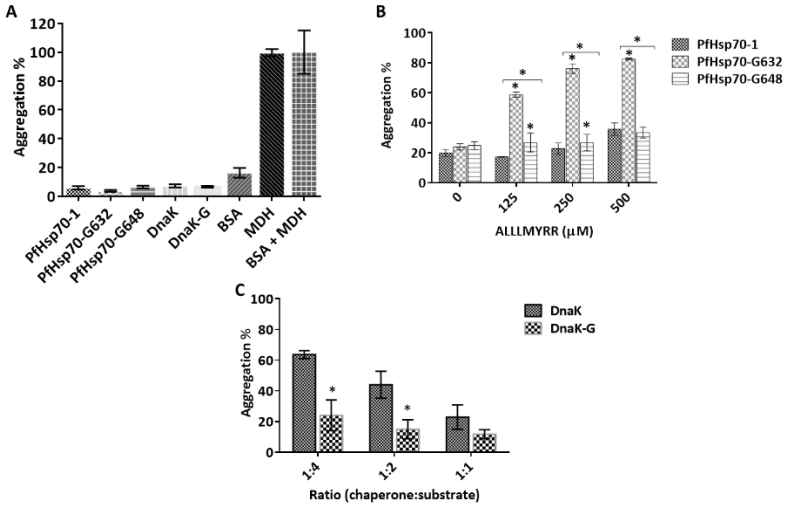

Figure B21. Assessment of the thermal stability of Hsp70 chaperones and their GGMP derivatives

(**A**) Heat stability of the recombinant proteins was assessed by the presence of heat-induced aggregates measured by an increase in turbidity at 340 nm for MDH using the Spectramax M3 (Molecular Devices). Recombinant proteins PfHsp70-1, PfHsp70-G632, PfHsp70-G648 and substrate MDH, BSA and the peptide (ALLLMYRR) as controls. Three independent assays were performed, and results are plotted as mean with standard deviations shown. (**C**) The heat-induced aggregation of malate dehydrogenase was assessed *in vitro* at 51 °C. The assay was initiated by adding MDH and varying concentration of recombinant DnaK and DnaK-G. Aggregation was measured as turbidity at 340 nm. Statistical analysis was carried out using two-way ANOVA (p<0.001).

B22: Confirmation of pQE30/PfHop DNA construct

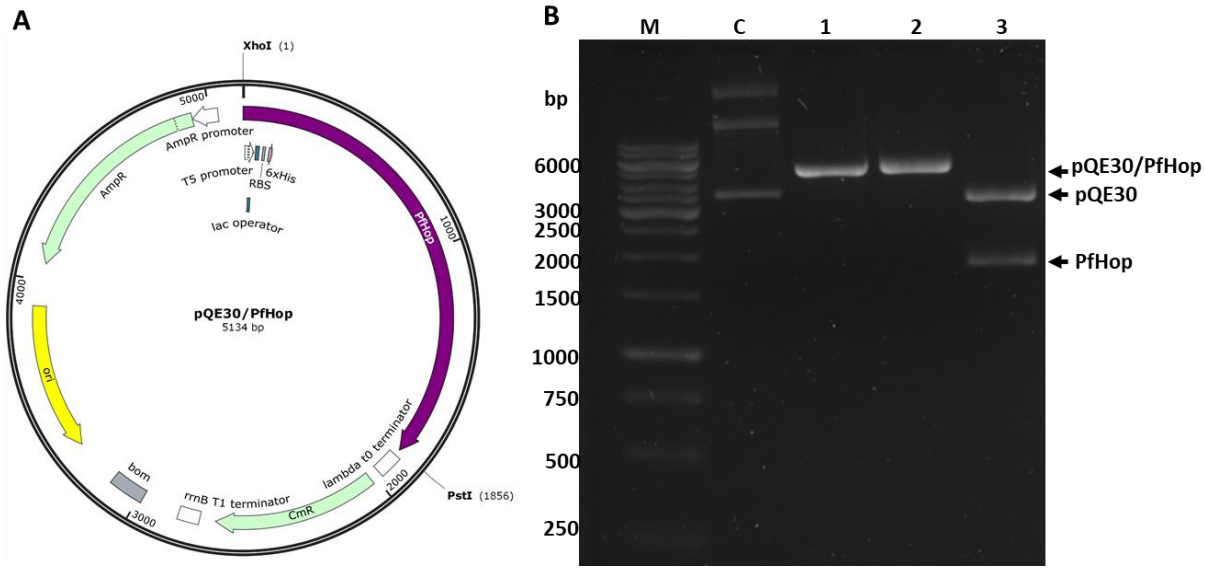

Figure B22. pQE30/PfHop plasmid map and restriction agarose gel

Restriction analysis of pQE30/PfHop DNA plasmid (**A**) Plasmid map of pQE30/PfHop showing the *Xho*I and *Pst*I restriction sites. (**B**) Agarose gel electrophoresis of pQE30/PfHop: lane M: DNA molecular weight marker in bp; lane C: undigested pQE30/PfHop plasmid; lane 1: pQE30/PfHop digested with *Xho*I; lane 2: pQE30/PfHop digested with *Pst*I; lane 3: pQE30/PfHop digested with both *Xho*I and *Pst*I.

B23: Secondary structure determination using conventional circular dichroism

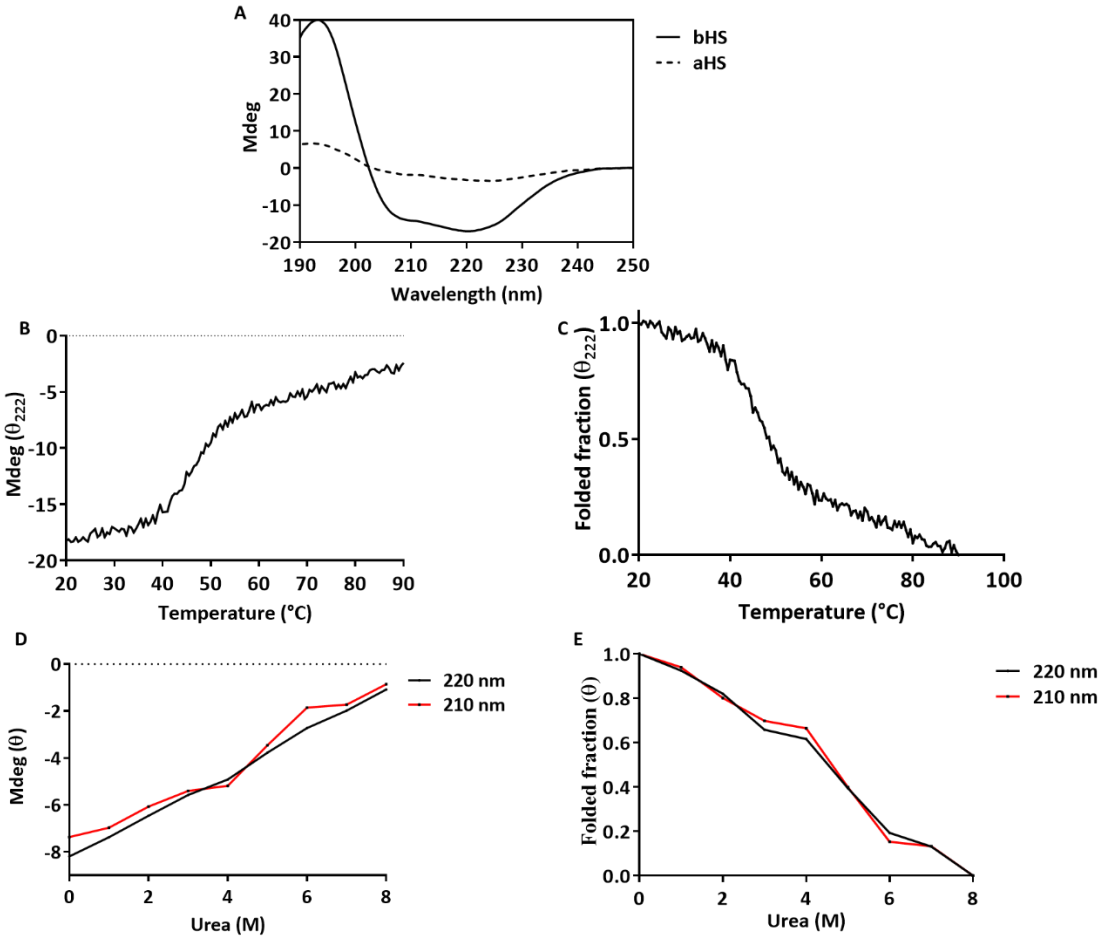

Figure B23. PfHop secondary structure determination using conventional CD spectroscopy
(**A**) Far-UV spectra for PfHop protein before (bHS) and after (aHS) heat denaturation. (**B**) Changes in CD ellipticity at 220 nm measured for PfHop. (**C**) The folded fraction of the proteins under varying temperatures. Data were fit into Eq. (1). (**D**) Urea unfolding of PfHop secondary structure. (**E**) The folded fraction of urea exposed PfHop as calculated using Equation 1.

B24: Demonstration of antibody specificity

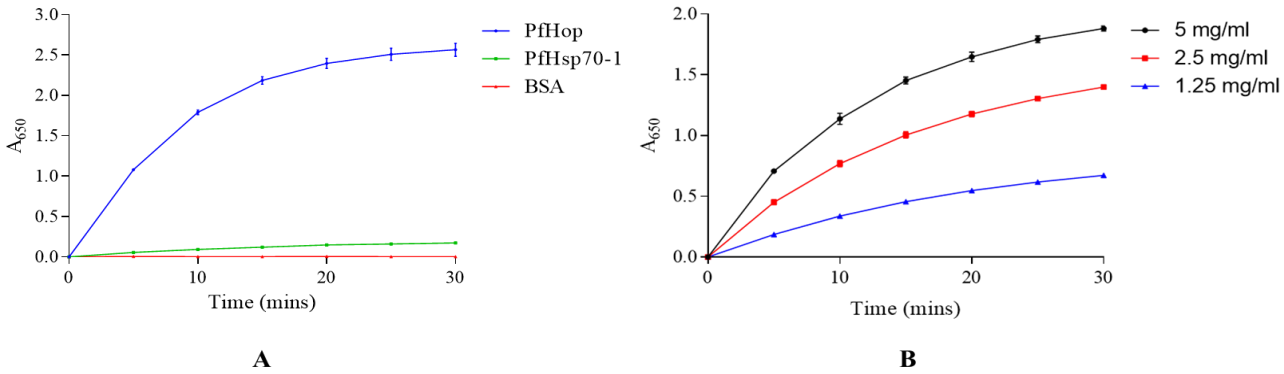

Figure B24 Specificity of the anti-PfHop antibody

(**A**) Immobilized PfHop, PfHsp70-1 and BSA proteins were probed by primary α-PfHop antibody and (**B**) PfHsp70-1 immobilized at varying concentrations was probed with α-PfHsp70-1. To quantify the bound protein, the secondary HRP conjugated goat raised α-Rabbit antibody was used and detection was started by addition of TMB substrate solution and color changes recorded photometrically at 650 nm.

B25: Slot bot analysis of the PfHsp70-1/PfHop interaction

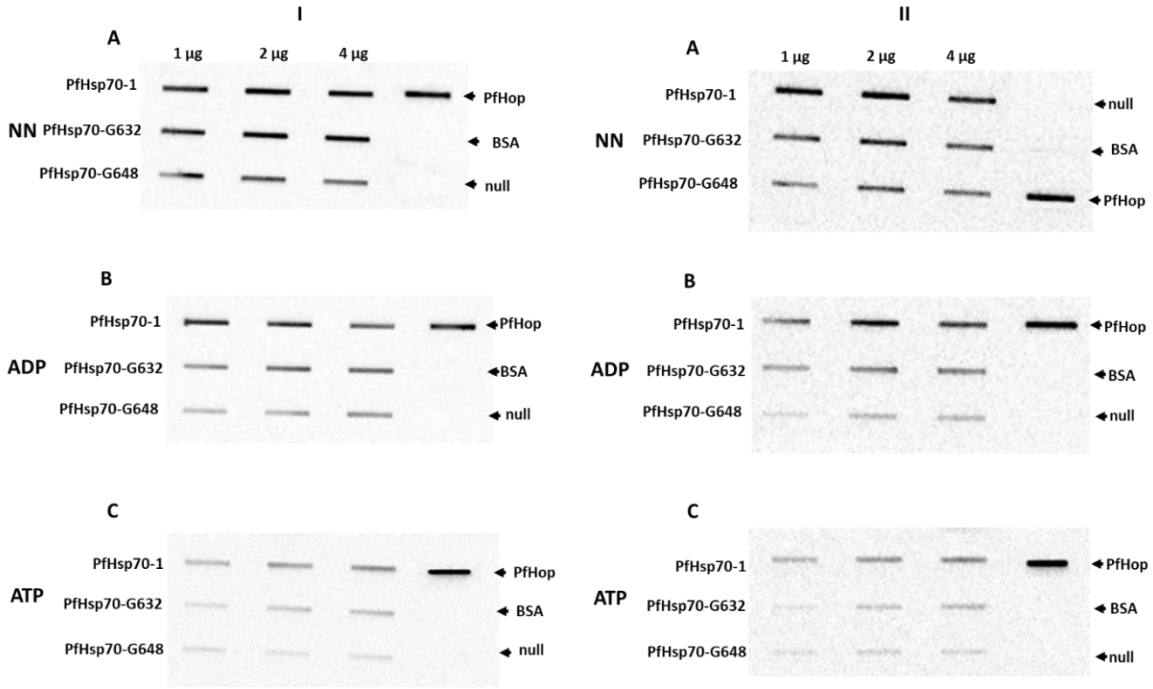

Figure B25. The GGMP motif is important for the interaction between PfHsp70-1 and PfHop

Various concentrations of PfHsp70s (1 µg, 2 µg, and 4 µg) were spotted onto nitrocellulose membrane as the prey protein. BSA (4 µg) was used as a negative control, PfHop was used as antibody control and null represents buffer without ligand. Each respective protein concentration was spotted using a vacuum and overlaid with 4 µg of purified PfHop protein (**A**). The assay was also conducted in the presence of ADP and ATP (**B** and **C**) and α- PfHop antibody was used to detect the presence of PfHop protein. The data represents 2 of 3 independent assays (I and II).

B26. Slot blot analysis of the interaction of PfHop versus DnaK and DnaK-G

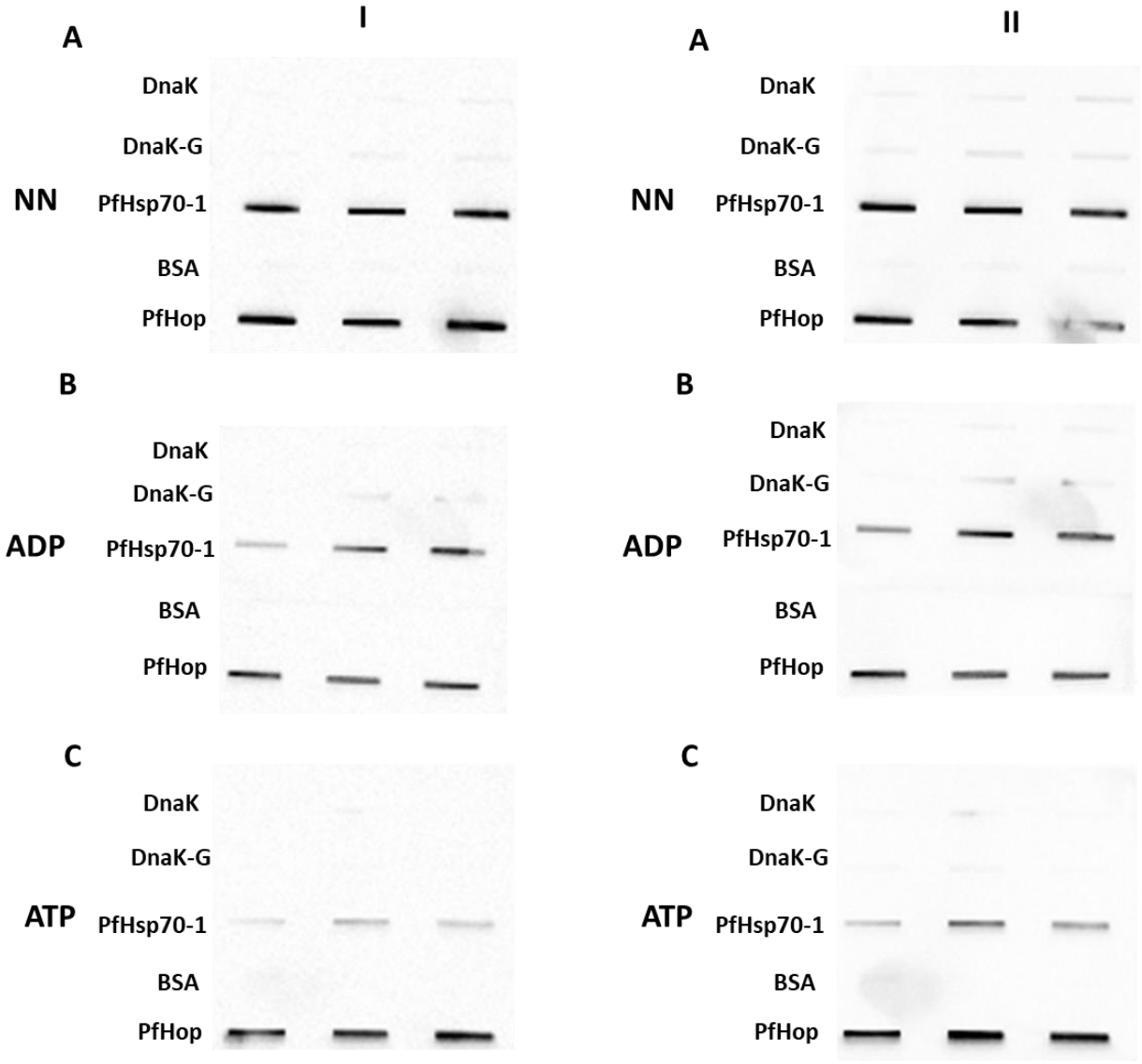

Figure B.26. Introduction of the GGMP motif of PfHsp70 into DnaK did not facilitate its association with PfHop

Slot blots for the association between DnaK-PfHop and DnaK-G-PfHop. Various concentrations of DnaK and DnaK-G (1 µg, 2 µg, and 4 µg) were spotted onto nitrocellulose membrane as the prey protein. BSA (4 µg) was used as a negative control. PfHop was used as an antibody control. Each respective protein concentration was spotted using a vacuum and overlaid with 4 µg of purified PfHop protein. The assay was repeated in presence of 5 mM ADP and ATP (B and C). The data represents 2 of 3 independent assays (I and II).

Appendix C: List of Reagents

REAGENT	SUPPLIER
Acetic acid	Merck, Germany
Adenosine triphosphate	Sigma, U.S.A
Agarose	Whitehead scientific, South Africa
Ammonium molybdate	Merck, Germany
Ammonium persulphate	Merck, Germany
Ampicillin	Sigma, U.S.A
Bovine serum albumin	Sigma, U.S.A
Bromophenol blue	Sigma, U.S.A
Calcium chloride	Merck, Germany
Chloramphenicol	Sigma, U.S.A
Coomasie brilliant blue R250	Merck, Germany
Diethiothreitol	Sigma, U.S.A
DreamTaq master mix	Thermo Scientific, U.S.A
Ethidium bromide	Sigma, U.S.A
Glacial acetic acid	Merck, Germany
Glycerol	Merck,
Glycine	Merck, Germany
Imidazole	Sigma, U.S.A
Isopropyl-1-thio-D-galacopyranoside	Sigma, U.S.A
Lysozyme	Merck, Germany
Magnesium chloride	Merck, Germany
Methanol	Merck, Germany
Monoclonal anti-His6-HRP antibodies	Sigma, U.S.A
Ni-NTA resin	Thermo Scientific, U.S.A
Nitrocellulose membrane	Pierce, U.S.A

Appendix C: List of Reagents

PagerRuler Prestained Protein Ladder	Thermo Scientific, U.S.A
Peptone	Merck, Germany
Phenylmethylsufonyl fluoride	Sigma, U.S.A
Polyacrylamide	Merck, Germany
Polyethylene glycol 2000	Sigma, U.S.A
Polyethylenimine	Sigma, U.S.A
Ponceau S	Sigma, U.S.A
Potassium chloride	Merck, Germany
Potassium dihydrogen phosphate	Merck, Germany
Proteinase-K	Sigma, U.S.A
Rapid ligation buffer	Promega, Germany
Restriction enzymes	Thermo Scientific, U.S.A
Snakeskin™ pleated dialysis tubing	Pierce, U.S.A
Sodium chloride	Merck, Germany
Sodium dodecyl sulphate	Merck, Germany
Sodium hydroxide	Merck, Germany
TEMED	Sigma, U.S.A
Tris	Merck, Germany
Tryptone	Merck, Germany
Tween 20	Merck, Germany
Urea	Melford, UK
Yeast extract powder	Merck, Germany
β-mercaptoethanol	Sigma, U.S.A